

Topics in Current Chemistry 323

Luigi Fabbrizzi *Editor*

# Beauty in Chemistry

Artistry in the Creation of New Molecules

 Springer

## Topics in Current Chemistry

**Editorial Board:**

**K.N. Houk • C.A. Hunter • M.J. Krische • J.-M. Lehn**

**S.V. Ley • M. Olivucci • J. Thiem • M. Venturi • P. Vogel**

**C.-H. Wong • H. Wong • H. Yamamoto**

# Topics in Current Chemistry

## Recently Published and Forthcoming Volumes

### **Beauty in Chemistry**

Volume Editor: Luigi Fabbrizzi  
Vol. 323, 2012

### **Constitutional Dynamic Chemistry**

Volume Editor: Mihail Barboiu  
Vol. 322, 2012

### **EPR Spectroscopy**

Volume Editors: Malte Drescher,  
Gunnar Jeschke  
Vol. 321, 2012

### **Radicals in Synthesis III**

Volume Editors: Markus R. Heinrich,  
Andreas Gansäuer  
Vol. 320, 2012

### **Chemistry of Nanocontainers**

Volume Editors: Markus Albrecht,  
F. Ekkehardt Hahn  
Vol. 319, 2012

### **Liquid Crystals: Materials Design and Self-Assembly**

Volume Editor: Carsten Tschierske  
Vol. 318, 2012

### **Fragment-Based Drug Discovery and X-Ray Crystallography**

Volume Editors: Thomas G. Davies,  
Marko Hyvönen  
Vol. 317, 2012

### **Novel Sampling Approaches in Higher Dimensional NMR**

Volume Editors: Martin Billeter,  
Vladislav Orekhov  
Vol. 316, 2012

### **Advanced X-Ray Crystallography**

Volume Editor: Kari Rissanen  
Vol. 315, 2012

### **Pyrethroids: From Chrysanthemum to Modern Industrial Insecticide**

Volume Editors: Noritada Matsuo, Tatsuya Mori  
Vol. 314, 2012

### **Unimolecular and Supramolecular Electronics II**

Volume Editor: Robert M. Metzger  
Vol. 313, 2012

### **Unimolecular and Supramolecular Electronics I**

Volume Editor: Robert M. Metzger  
Vol. 312, 2012

### **Bismuth-Mediated Organic Reactions**

Volume Editor: Thierry Ollevier  
Vol. 311, 2012

### **Peptide-Based Materials**

Volume Editor: Timothy Deming  
Vol. 310, 2012

### **Alkaloid Synthesis**

Volume Editor: Hans-Joachim Knölker  
Vol. 309, 2012

### **Fluorous Chemistry**

Volume Editor: István T. Horváth  
Vol. 308, 2012

### **Multiscale Molecular Methods in Applied Chemistry**

Volume Editors: Barbara Kirchner,  
Jadran Vrabec  
Vol. 307, 2012

### **Solid State NMR**

Volume Editor: Jerry C. C. Chan  
Vol. 306, 2012

### **Prion Proteins**

Volume Editor: Jörg Tatzelt  
Vol. 305, 2011

# Beauty in Chemistry

Artistry in the Creation of New Molecules

Volume Editor: Luigi Fabbrizzi

With Contributions by

D.B. Amabilino · V. Balzani · C.J. Brown · C.J. Bruns ·  
L. Fabbrizzi · E. Marchi · K.N. Raymond · J.F. Stoddart ·  
M. Venturi · J.-P. Sauvage

 Springer

*Editor*

Prof. Dr. Luigi Fabbrizzi  
Dipartimento di Chimica  
via Taramelli 12  
Pavia  
Italy

ISSN 0340-1022

e-ISSN 1436-5049

ISBN 978-3-642-28340-6

e-ISBN 978-3-642-28341-3

DOI 10.1007/978-3-642-28341-3

Springer Heidelberg Dordrecht London New York

Library of Congress Control Number: 2012932057

© Springer-Verlag Berlin Heidelberg 2012

This work is subject to copyright. All rights are reserved, whether the whole or part of the material is concerned, specifically the rights of translation, reprinting, reuse of illustrations, recitation, broadcasting, reproduction on microfilm or in any other way, and storage in data banks. Duplication of this publication or parts thereof is permitted only under the provisions of the German Copyright Law of September 9, 1965, in its current version, and permission for use must always be obtained from Springer. Violations are liable to prosecution under the German Copyright Law.

The use of general descriptive names, registered names, trademarks, etc. in this publication does not imply, even in the absence of a specific statement, that such names are exempt from the relevant protective laws and regulations and therefore free for general use.

Printed on acid-free paper

Springer is part of Springer Science+Business Media ([www.springer.com](http://www.springer.com))

---

## Volume Editor

Prof. Dr. Luigi Fabbrizzi

Dipartimento di Chimica  
via Taramelli 12  
Pavia  
Italy

## Editorial Board

Prof. Dr. Kendall N. Houk

University of California  
Department of Chemistry and Biochemistry  
405 Hilgard Avenue  
Los Angeles, CA 90024-1589, USA  
*houk@chem.ucla.edu*

Prof. Dr. Christopher A. Hunter

Department of Chemistry  
University of Sheffield  
Sheffield S3 7HF, United Kingdom  
*c.hunter@sheffield.ac.uk*

Prof. Michael J. Krische

University of Texas at Austin  
Chemistry & Biochemistry Department  
1 University Station A5300  
Austin TX, 78712-0165, USA  
*mkrische@mail.utexas.edu*

Prof. Dr. Jean-Marie Lehn

ISIS  
8, allée Gaspard Monge  
BP 70028  
67083 Strasbourg Cedex, France  
*lehn@isis.u-strasbg.fr*

Prof. Dr. Steven V. Ley

University Chemical Laboratory  
Lensfield Road  
Cambridge CB2 1EW  
Great Britain  
*Svl1000@cus.cam.ac.uk*

Prof. Dr. Massimo Olivucci

Università di Siena  
Dipartimento di Chimica  
Via A De Gasperi 2  
53100 Siena, Italy  
*olivucci@unisi.it*

Prof. Dr. Joachim Thiem

Institut für Organische Chemie  
Universität Hamburg  
Martin-Luther-King-Platz 6  
20146 Hamburg, Germany  
*thiem@chemie.uni-hamburg.de*

Prof. Dr. Margherita Venturi

Dipartimento di Chimica  
Università di Bologna  
via Selmi 2  
40126 Bologna, Italy  
*margherita.venturi@unibo.it*

**Prof. Dr. Pierre Vogel**

Laboratory of Glycochemistry  
and Asymmetric Synthesis  
EPFL – Ecole polytechnique fédérale  
de Lausanne  
EPFL SB ISIC LGSA  
BCH 5307 (Bat.BCH)  
1015 Lausanne, Switzerland  
*pierre.vogel@epfl.ch*

**Prof. Dr. Chi-Huey Wong**

Professor of Chemistry, Scripps Research  
Institute  
President of Academia Sinica  
Academia Sinica  
128 Academia Road  
Section 2, Nankang  
Taipei 115  
Taiwan  
*chwong@gate.sinica.edu.tw*

**Prof. Dr. Henry Wong**

The Chinese University of Hong Kong  
University Science Centre  
Department of Chemistry  
Shatin, New Territories  
*hncwong@cuhk.edu.hk*

**Prof. Dr. Hisashi Yamamoto**

Arthur Holly Compton Distinguished  
Professor  
Department of Chemistry  
The University of Chicago  
5735 South Ellis Avenue  
Chicago, IL 60637  
773-702-5059  
USA  
*yamamoto@uchicago.edu*

# Topics in Current Chemistry Also Available Electronically

*Topics in Current Chemistry* is included in Springer's eBook package *Chemistry and Materials Science*. If a library does not opt for the whole package the book series may be bought on a subscription basis. Also, all back volumes are available electronically.

For all customers with a print standing order we offer free access to the electronic volumes of the series published in the current year.

If you do not have access, you can still view the table of contents of each volume and the abstract of each article by going to the SpringerLink homepage, clicking on "Chemistry and Materials Science," under Subject Collection, then "Book Series," under Content Type and finally by selecting *Topics in Current Chemistry*.

You will find information about the

- Editorial Board
- Aims and Scope
- Instructions for Authors
- Sample Contribution

at [springer.com](http://springer.com) using the search function by typing in *Topics in Current Chemistry*.

*Color figures* are published in full color in the electronic version on SpringerLink.

## Aims and Scope

The series *Topics in Current Chemistry* presents critical reviews of the present and future trends in modern chemical research. The scope includes all areas of chemical science, including the interfaces with related disciplines such as biology, medicine, and materials science.

The objective of each thematic volume is to give the non-specialist reader, whether at the university or in industry, a comprehensive overview of an area where new insights of interest to a larger scientific audience are emerging.



Thus each review within the volume critically surveys one aspect of that topic and places it within the context of the volume as a whole. The most significant developments of the last 5–10 years are presented, using selected examples to illustrate the principles discussed. A description of the laboratory procedures involved is often useful to the reader. The coverage is not exhaustive in data, but rather conceptual, concentrating on the methodological thinking that will allow the non-specialist reader to understand the information presented.

Discussion of possible future research directions in the area is welcome.

Review articles for the individual volumes are invited by the volume editors.

In references *Topics in Current Chemistry* is abbreviated *Top Curr Chem* and is cited as a journal.

Impact Factor 2010: 2.067; Section “Chemistry, Multidisciplinary”: Rank 44 of 144

# Preface

Don't ask a joiner which is the most beautiful trade. He will answer his own. For two main reasons: the pleasure of doing his professional activity with conscious skillfulness, the intrinsic beauty (if any) of the products of his work (a chair, a table, a door). If an alchemist had been asked the same question, say five hundred years ago, he would have probably given the same answer, proud of his capability of mastering fine and sophisticated techniques and fascinated by the new substances he was able to create. The successors of alchemists – chemists – have a further reason for enjoying the products of their activity; formulae. First, each substance can be fully described and identified by its formula, an achievement dating back to the first half of the 19<sup>th</sup> century, when techniques of chemical analysis developed. Second, and most importantly, when in the second half of the same century the first ideas on chemical bonding were outlined, formulae took a spatial character (structural formulae), which enriched the chemical thinking of new fascinating concepts: molecular shape, geometry, symmetry. Since then, chemists have acquired the consciousness of being able, on the macroscopic side, to produce new substances displaying useful properties and, on the microscopic side, to create new molecular structures of designed size and shape, exactly like a joiner making a wood object or a sculptor giving a desired shape to a block of marble.

Nevertheless, chemistry is a utilitarian discipline and any synthetic design is driven by a definite functional interest (e.g. making a catalyst, a drug, a reagent for analysis) and is rarely addressed for deliberate aesthetic purposes. Based on this assumption, chemical products should not be associated with beauty and chemistry should not be considered an artistic discipline. However, cathedrals of the Middle Ages (just to mention something considered beautiful by almost everyone in every time period) were not built for generating an aesthetic pleasure in the viewers, but with the practical purpose of creating a place where the believers could gather for praying and honouring God. Frescos decorating the walls of churches, after Giotto and his followers, were painted not for inducing aesthetical emotions, but for helping priests to illustrate the lives of the Saints, like the slides of today's PowerPoint presentations. In this respect, chemists can be considered artists,

because they create molecular objects for displaying a practical function, but their structure may also cause emotion, pleasure and ultimately a sense of beauty.

This volume contains essays on beauty and chemistry by some renowned molecular artists (with the notable exception of the guest editor), who have created over the past three decades beautiful molecular objects (vessels, knots, mechanically bound supramolecules *et cetera*). In their individual chapters, each author has illustrated and commented on the development of their ideas and on the significance of their findings. Thus, this volume could be compared to having access to old manuscripts in which Michelangelo himself describes and comments on the steps of his frescoing the 1,100 m<sup>2</sup> of the ceiling of the Sistine Chapel, or Sandro Botticelli kindly reveals the secret allegory of 'Primavera'.

Luigi Fabbrizzi

# Contents

<b>Inner and Outer Beauty</b> .....	1
Kenneth N. Raymond and Casey J. Brown	
<b>The Mechanical Bond: A Work of Art</b> .....	19
Carson J. Bruns and J. Fraser Stoddart	
<b>The Beauty of Chemistry in the Words of Writers and in the Hands of Scientists</b> .....	73
Margherita Venturi, Enrico Marchi, and Vincenzo Balzani	
<b>The Beauty of Knots at the Molecular Level</b> .....	107
Jean-Pierre Sauvage and David B. Amabilino	
<b>Living in a Cage Is a Restricted Privilege</b> .....	127
Luigi Fabbrizzi	
<b>Index</b> .....	167



# Inner and Outer Beauty

**Kenneth N. Raymond and Casey J. Brown**

**Abstract** Symmetry and pattern are precious forms of beauty that can be appreciated on both the macroscopic and molecular scales. Crystallographers have long appreciated the intimate connections between symmetry and molecular structure, reflected in their appreciation for the artwork of Escher. This admiration has been applied in the design of highly symmetrical coordination compounds. Two classes of materials are discussed: extended coordination arrays and discrete supramolecular assemblies. Extended coordination polymers have been implemented in gas separation and storage due to the remarkably porosity of these materials, aided by the ability to design ever-larger inner spaces within these frameworks. In the case of discrete symmetrical structures, defined inner and outer space present a unique aesthetic and chemical environment. The consequent host–guest chemistry and applications in catalysis are discussed.

**Keywords** Catalysis · Host–guest chemistry · Metal–organic frameworks · Rational design · Supramolecular chemistry

## Contents

1	Symmetrical Extended Arrays .....	4
2	Discrete, Symmetric Assemblies .....	7
3	Nanoscale, Symmetrical Flasks: Inner and Outer Space .....	9
4	How the Electronic Structure Affects Guest Chemistry .....	12
5	Closing Remarks on Inner and Outer Beauty .....	16
	References .....	17

What is beauty? There are certainly as many answers to be found within this book as there are authors, and perhaps there are as many answers in the world as there are people. However, the thesis of this book, and shared by this chapter, is that there are generalizations that can be made about beauty: what it is, and its relevance to the natural sciences in general and chemistry in particular. As defined by *Merriam-Webster's Dictionary* [1] beauty is: “the quality or aggregate of qualities in a person or thing that gives pleasure to the senses or pleasurably exalts the mind or spirit.” Aristotle asserted that symmetry holds a special place amongst these qualities, arguing that “the chief forms of beauty are order and symmetry and definiteness, which the mathematical sciences demonstrate in a special degree.” [2].

We frequently see beauty in the natural world. A quote from John Muir [3] expresses this well:

Fresh beauty opens one's eyes wherever it is really seen, but the very abundance and completeness of the common beauty that besets our steps prevents its being absorbed and appreciated. It is a good thing, therefore, to make short excursions now and then to the bottom of the sea among dulce and coral, or up among the clouds on mountain-tops, or in balloons, or even to creep like worms into dark holes and caverns underground, not only to learn something of what is going on in those out-of-the-way places, but to see better what the sun sees on our return to common everyday beauty.

Ironically, the thesis of this chapter is about symmetry (a kind of simplicity) and chemistry. Muir's quotation points out that for most of us there is a beauty in the natural world that can be quite complex. An example is the figure of Yosemite and the rising moon (Fig. 1). In a way, this represents the yin and yang of beauty. On one hand is the complexity of the natural world and our perception of its beauty



**Fig. 1** *Moon and Half Dome, Yosemite National Park* (December 28, 1960). The overwhelming beauty of this natural landscape fills us with a sense of awe and admiration. This is a stark contrast to our aesthetic appreciation of the simple elegance of patterns and symmetry. Photograph by Ansel Adams. Copyright 2011 The Ansel Adams Publishing Rights Trust

**Fig. 2** Subjects were asked to rate the attractiveness of (a) actual facial photographs and (b) remapped photographs that symmetrize the facial features of those photographs. Viewers strongly favored the symmetrical photographs. Reprinted from [5], Copyright (1999), with permission from Elsevier



(and this also can apply to chemistry) and on the other is the beauty that we see in crystals, or patterns, or even theories, that has to do with symmetry or the beautiful structure of simplicity.

In the field of psychology, it is established that human perception of beauty among other humans has an important component of symmetry. For example, the study of human subjects and how they perceived the beauty of subjects presented to them in photographs [4] showed that the more symmetrical faces, as illustrated in Fig. 2, were found to be more beautiful on average.

The observation that we find symmetrical faces to be more attractive is impossible to attribute to any one cause. It has been suggested that facial symmetry is an indication of genetic health and helps to attract us to desirable partners. But our appreciation of symmetry extends beyond choosing mates – we find symmetry beautiful not only in other people, but also in both the natural world and in all forms of art.

Many chemists and crystallographers are highly appreciative of the work of the Dutch artist Escher. Although Escher had no advanced training in mathematics, the tessellation drawings that he generated are excellent illustrations of two-dimensional space groups. The importance of space group theory in crystallography and the possible arrangements of ordered, extended domains in either two or three dimensions is of fundamental importance in many areas of chemistry. The wonderful book *Symmetry Aspects of Escher's Periodic Drawings* by Caroline MacGillavry [6] was published by the International Union of Crystallography in 1965. It effectively employed the Escher diagrams to teach the principles of chemical symmetry and space group theory to students. This book has a charming introduction by Escher, in which he wrote: "Though the text of scientific publications is mostly beyond my means of comprehension, the figures with which they are illustrated bring me occasionally on the track of new possibilities for my work. It was in this way that a fruitful contact could be established between mathematicians and myself." One notable example of these illustrations is his work *Study of Regular Division of the Plane with Human Figures* (1944) [6], shown as Fig. 3. Consider as a single operation (termed glide) the vertical movement of one figure (e.g., with the left hand raised) to bring it into register with the next figure up (with the right hand extended) through reflection of the right handed figure from left to right across the line that bisects the vertical rows.



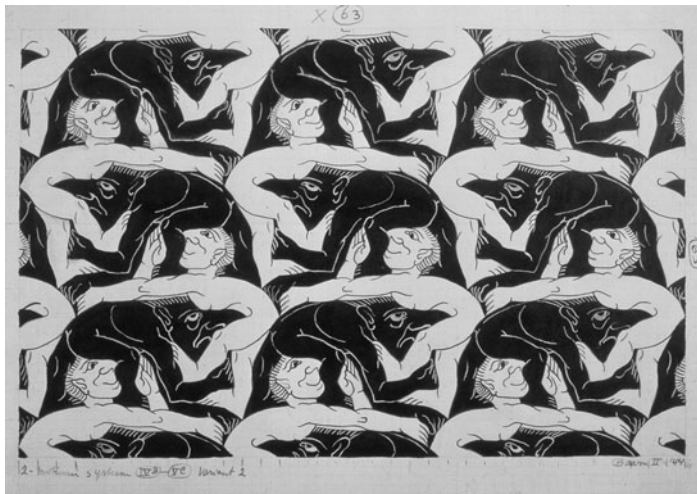


**Fig. 3** M.C. Escher's *Study of Regular Division of the Plane with Human Figures* (1944). As in Escher's other tessellation diagrams, translational and point symmetry operations are used to completely fill the plane with repeated, ordered objects. Copyright 2011 The M.C. Escher Company – Holland. All rights reserved. [www.mcescher.com](http://www.mcescher.com)

This illustrates a type of symmetry only seen in crystals and other extended arrays. That is, the symmetry operation combines both elements of point symmetry (as seen in molecules) and translation (which generates arrays). Here you can see that the repeat of this operation yields a vertical translation of one unit. The two- and three-dimensional space groups are realizations of the more general topic of group theory, which has been one of the tremendous scientific achievements in the last two centuries in the field of pure mathematics.

## 1 Symmetrical Extended Arrays

*Cubic Space Division* (1952) [7] (Fig. 4) anticipates a current chemical interest in open arrays as storage materials.

While this general topic has an ancient lineage, it is an area of intense current research. What is now described as the Hofmann clathrate was first reported in 1897 [8]. However, the structure was not known until 50 years later when reported by Powell and coworkers [9]. Single crystal X-ray diffraction showed the structure in Fig. 5, in which a two-dimensional array of nickel cyanide encapsulates trapped benzene molecules.

A general review of the principles and structures of metal coordination chemistry arrays was published in 1964 by Bailar, one of the founders of modern inorganic chemistry [10]. The chapter "Coordination polymers" included both inorganic and organic bridging ligands. The extension of this chemistry into something more like Escher's vision in Fig. 4 was described by Hoskins and Robson [11], stating in their

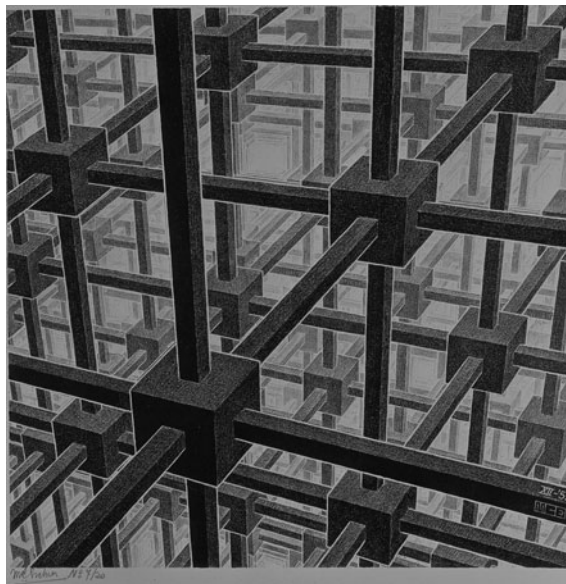


**Fig. 4** M.C. Escher's *Cubic Space Division* (1952) by Escher. In this three-dimensional array of cubic symmetry, we can see that sites of octahedral symmetry are connected by linear spacers in an infinite array. Copyright 2011 The M.C. Escher Company – Holland. All rights reserved. [www.mcescher.com](http://www.mcescher.com)

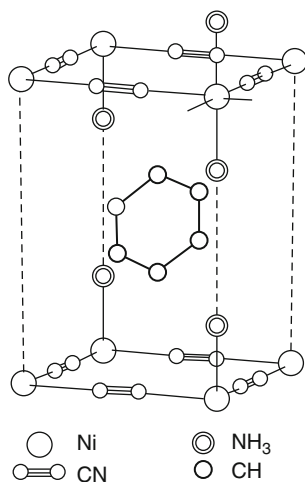


**Fig. 5** The Hoffman clathrate, structurally characterized by X-ray crystallography. Nickel centers separated by cyanide linkers form extended two-dimensional frameworks. These layers are linked together by hydrogen-bonded ammonia ligands, trapping benzene molecules within the three-dimensional framework. Reprinted from [9] by permission from Macmillan, copyright (1949)

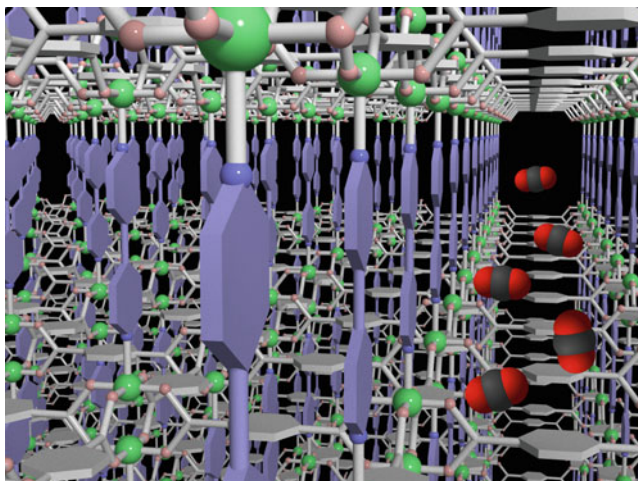


**Fig. 6** Porous coordination polymer (PCP) developed by Kitagawa and coworkers. The pores, which extend throughout the array, can be filled by CO<sub>2</sub> molecules (*grey and red*), allowing these materials to employ their high internal surface area as gas adsorbents [13]. Reprinted with permission

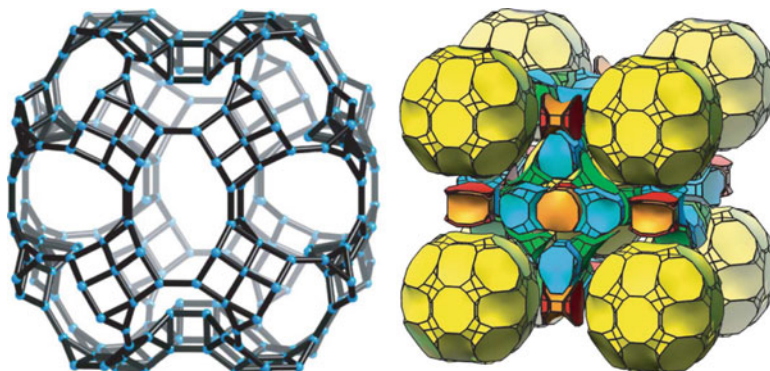


**Fig. 7** *Left*: The metal–organic framework ZIF-100; Zn atoms are shown as *blue*, while the imidazolate ligands are represented simply as *black rods*. The defined inner space of the framework is 35.6 by 67.2 Å, with a surface area of 595 m<sup>2</sup> g<sup>-1</sup>. *Right*: These giant cages are part of a larger (but equally symmetric) superstructure [15]. Reprinted by permission from Macmillan Publishers

abstract that: “It is proposed that a new and potentially extensive class of scaffolding-like materials may be afforded by linking together centers with either a tetrahedral or an octahedral array of valences by rodlike connecting units.”

The current focus on highly porous materials has led to a great deal of activity in this field. Kitagawa and coworkers developed what they called porous coordination polymers that were rigid enough to survive loss of the encapsulated solvent from

synthesis and generate materials with high gas absorptivity [12]. One image of  $\text{CO}_2$  trapped inside such an array is shown in Fig. 6 [5], and has a remarkable similarity to the Escher image in Fig. 4 [6].

The record holders for surface area per gram and for gas storage are materials prepared by Yaghi and coworkers that they call metal–organic frameworks (MOFs). The first of these MOFs [14] looked much like the Robsen design. Increasingly, these beautiful structures, with dramatically increased porosity, look like a vision of Escher’s (Fig. 7).

## 2 Discrete, Symmetric Assemblies

The spontaneous assembly of small molecular fragments into larger, high-symmetry clusters has been accomplished in Nature for more than a billion years. Examples in the natural world include the protein ferritin. This very ancient protein is found in bacteria, plants, and animals. Mammalian ferritin is a 24-mer with octahedral symmetry (such that each of the asymmetric subunits is related to the other 23 by one of the symmetry operations of the pure rotation group  $O$  and its 24 symmetry elements), but there is a microbial ferritin with 12 subunits and  $T$  symmetry. An illustration of this structure is shown in Fig. 8.

Assemblies with a segregated inner space are generally found in the natural world as protective containers. In the case of the ferritins, a valuable piece of iron hydroxyoxide is maintained in soluble form by preventing the aggregation of these particles beyond the nanoscale. The discrete inner environment of such assemblies can also be used to protect reactive species that cannot be isolated without a suitably

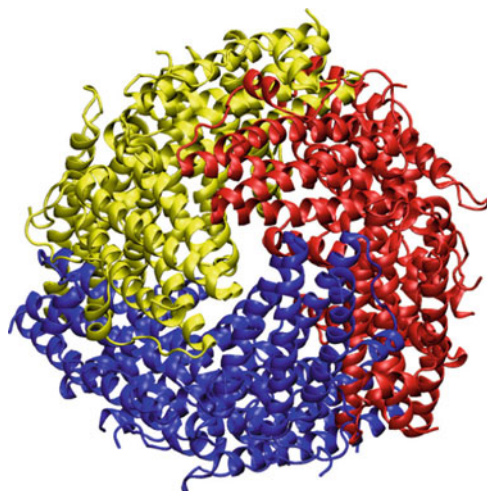


**Fig. 8** View of microbial ferritin down the threefold axis of symmetry, with each of the three symmetry-related portions colored differently

tailored microenvironment. An early example of the application of this general principle in synthetic chemistry was the encapsulating vessel produced by Cram and coworkers (Fig. 9) that encapsulated cyclobutadiene and stabilized this otherwise highly unstable molecule [16]. Encapsulation blocks the contact of one guest with another and prevents reaction, just as encapsulation of the iron cluster blocks the contact with other iron clusters that would lead to a larger particle and eventually precipitation. This general principle is extremely powerful, but is limited by the synthetic complexity of large, covalent structures like the one shown in Fig. 9.

A powerful approach for circumventing the difficulty of the synthesis of large hosts through conventional organic chemistry is the use of spontaneous self-assembly. This can generate large, symmetrical structures with a defined inner and outer space. Jean-Marie Lehn provided early examples of spontaneous assembly of small subunits into larger ones with long-range order [17] and coined the term “supramolecular assemblies” to describe these compounds.

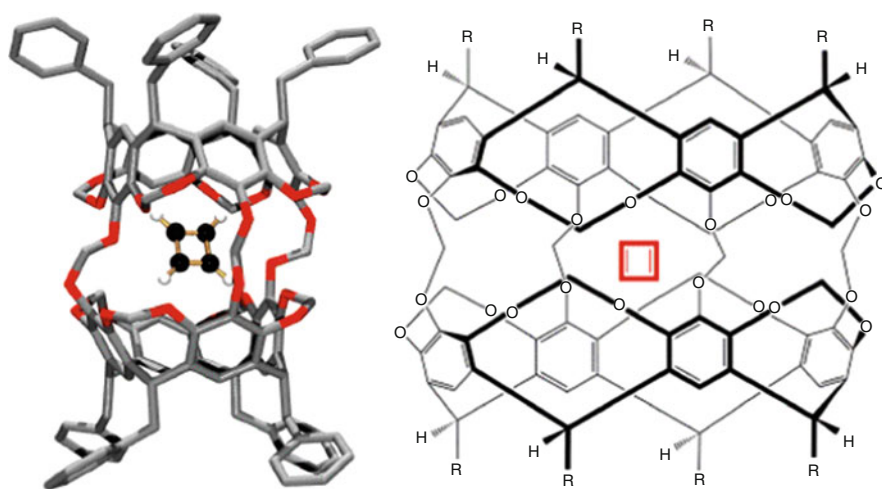


**Fig. 9** Encapsulation within a hemicarcerand allows cyclobutadiene, an anti-aromatic, highly strained and reactive molecule, to be isolated

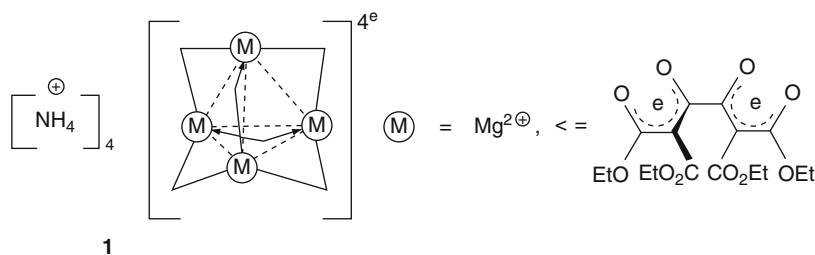


**Fig. 10** Ligand L and tetrahedral  $M_4L_6$  assembly first isolated by Saalfrank and coworkers and reported in 1988. Taken from the table of contents illustration in [18]. Copyright Wiley-VCH. Reproduced with permission

A tetrahedral discrete supramolecular assembly formed by magnesium–ligand coordination was reported by Saalfrank (Fig. 10) as a consequence of serendipity [18]. The same ligand was subsequently incorporated in several clusters formed from transition metals. A number of similar tetrahedral metal–ligand structures have been prepared using a variety of approaches and components [19]. The elegance of these supramolecular clusters and their potential for isolating guest molecules in their sheltered interiors has become a driving force for the development of new, symmetrical materials that can alter or catalyze the reactivity of the guest. The discussion of this transition from serendipity to rational design is the core of the artistry in the preparation of supramolecular coordination compounds.

### 3 Nanoscale, Symmetrical Flasks: Inner and Outer Space

Our approach to the design and synthesis of new supramolecular clusters was first described in two review articles [20, 21]. An illustration of the explicit symmetry-design of these clusters is shown in Fig. 11.

The key here is the rigidity of the subunit and the symmetry and orientation of the components. The twofold symmetry of the naphthalene ligand is consistent with the formation of a tetrahedral structure, whose symmetry numbers are 2 and 3. The trigonal symmetry results from the tris (bidentate) complex of the metal coordinated by the catechol groups. What is essential is to make sure that the angle between these two axes of symmetry is  $54^\circ$ , the angle between the twofold and threefold symmetry axes of the tetrahedron. The rigidity of the linker ensures that only this cluster can form, since distortion of the assembly by bending

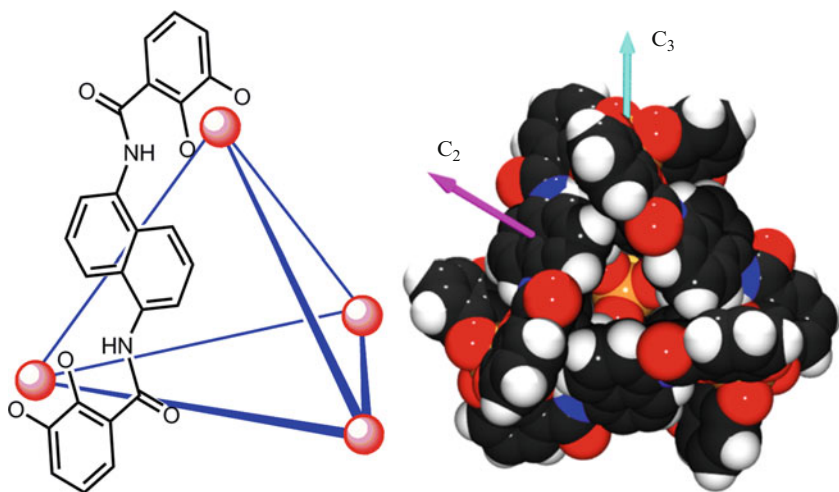


**Fig. 11** Schematic (*left*) and space-filling model (*right*) of the tetrahedral  $M_4L_6$  assemblies developed by Raymond and coworkers

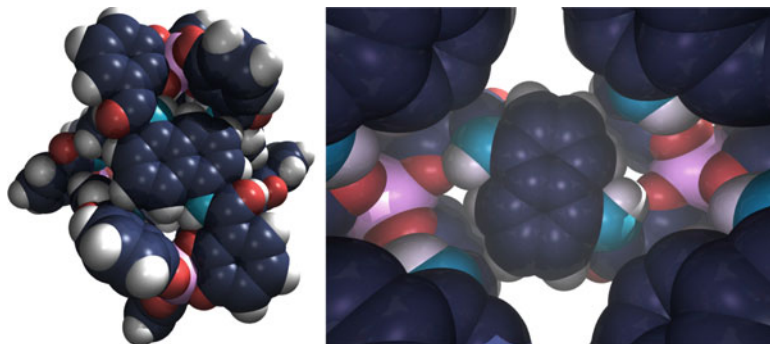


**Fig. 12** Views of the exterior (*left*) and interior (*right*) environments of the  $M_4L_6$  assembly. The assembly exterior has four vertices bearing a  $3^-$  charge, and is highly solvated in water. In contrast, the interior environment is defined primarily by the naphthalene walls, with limited access to the vertices and very limited exposure to the bulk aqueous solvent

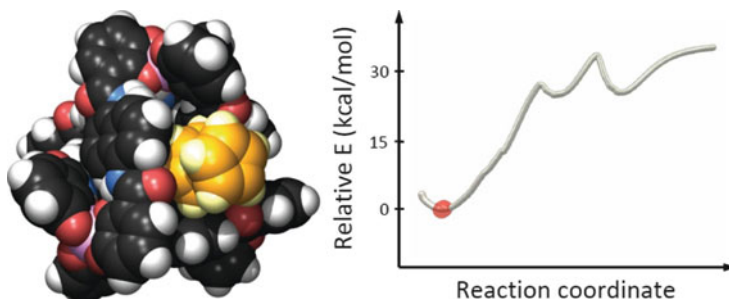


**Fig. 13** *Left*: Ruthenium sandwich complex exits the assembly cavity through distortion of the aperture. *Right*: Energy profile of this distortion

the linking components cannot occur. Because the resultant complex is highly negatively charged it is very strongly solvated in water and is highly soluble. However, the interior of the cluster is surrounded primarily by a shell of naphthalene rings and is highly hydrophobic. Hence, the inner and outer spaces of this molecule (and their beauty!) are very different (Fig. 12).

In looking at the structure on the left in Fig. 12 one sees there are only small apertures, on the order of 3 Å diameter, for ingress and egress to and from the interior of the cavity. How then does guest exchange occur? The answer to this is illustrated in Fig. 13, which shows the distortion of the stretching of the aperture as the molecule leaves or enters the cavity, much like the pores of many proteins involved in transport or used as gates [22].

The electronic environment of the interior is strongly affected by the ring currents of the naphthalene groups. A consequence of this is that the NMR signals of encapsulated guests are strongly shifted due to ring currents. A mapping of the magnetic field as a function of position within the cluster demonstrates clearly that

**Fig. 14** Calculated  $^1\text{H}$  NMR shifts as a consequence of location within the inner space of the  $\text{M}_4\text{L}_6$  assembly [24]

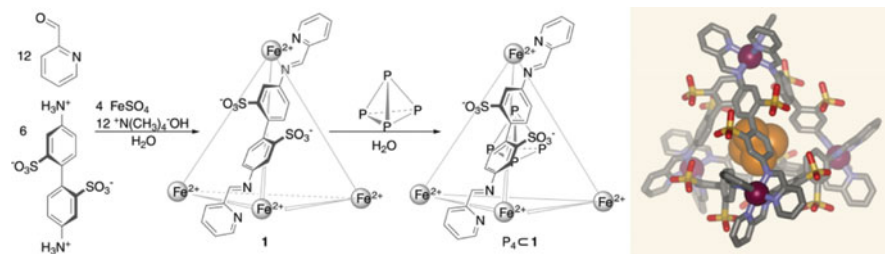
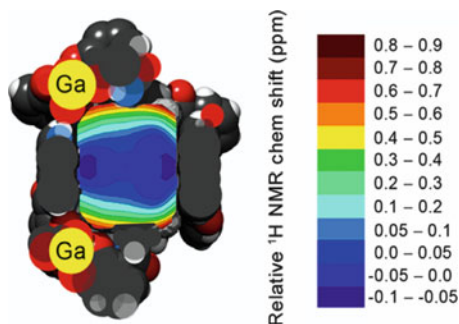


**Fig. 15** Three-dimensional view of Nitschke's tetrahedral assembly for the protective encapsulation of  $\text{P}_4$ . Iron atoms are drawn in *purple*, carbon atoms *gray*, nitrogen atoms *blue*, and phosphorous atoms are *orange*. The sulfonate groups, which help solubilize the assembly in water, are *yellow* and *red* [24]. Reprinted with permission from AAAS

the interior of the cluster is strongly de-shielding, while the spaces close to the walls and apertures instead shield guests. The result is that encapsulated species have diagnostic shifts, which provide information about the guest orientation within the cavity of the  $\text{M}_4\text{L}_6$  assembly [23] (Fig. 14).

Another example, which combines both the self-assembly type of cluster and the intention illustrated by Cram of stabilizing otherwise unstable guests, is the work by Nitschke in which the tetrahedral and highly elemental form of phosphorous,  $\text{P}_4$ , is stabilized [24]. This structure is shown in Fig. 15. The importance of this was highlighted in a Nature Commentary [25]:

White phosphorus reacts with oxygen to produce an oxide ( $\text{P}_2\text{O}_5$ ). This oxide then reacts with any water that is around to form phosphoric acid. The phosphorus–phosphorus bonds of  $\text{P}_4$  are weak compared with the stronger phosphorus–oxygen bonds of  $\text{P}_2\text{O}_5$ ; in other words, the oxide is thermodynamically much more stable than white phosphorus, and this drives the reaction to such an extent that white phosphorus spontaneously combusts in air.

One might therefore assume that Mal and colleagues' nanoflasks simply isolate  $\text{P}_4$  molecules from oxygen. But this isn't the case: oxygen molecules are smaller than  $\text{P}_4$  molecules, and must therefore also be able to gain access to the flasks' interiors. Instead, the tight confinement of  $\text{P}_4$  molecules prevents the formation of phosphorus–oxygen bonds during the first steps of phosphorus oxidation – there simply isn't room for the reaction intermediates to form. This is the first time that a reactive species has been stabilized by such an effect, and represents a fundamental advance for the field.



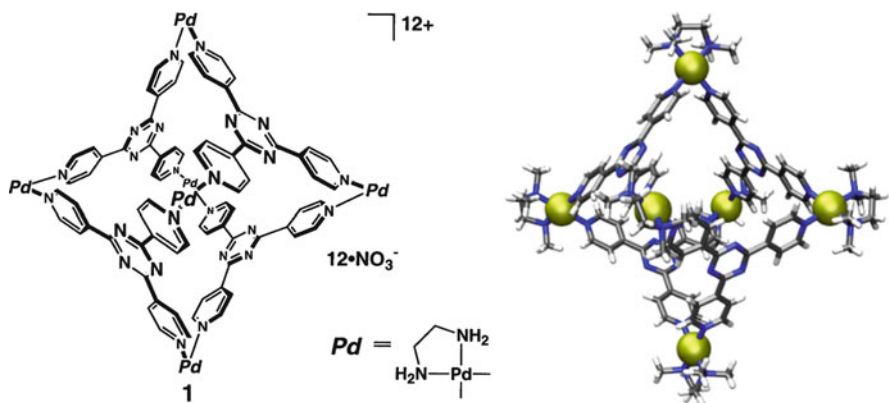


**Fig. 16** Fujita's highly charged octahedra. Although these assemblies have precisely the same elements of symmetry as the  $M_4L_6$  assemblies of Raymond and coworkers they differ in that the ligands are the threefold symmetrical unit, while the metals provide the twofold axis. Reprinted with permission

## 4 How the Electronic Structure Affects Guest Chemistry

At the outset of this chapter, we noted that the beauty of symmetry and pattern is ultimately the beauty of simplicity. The elegance of the chemistry of these supramolecular capsules, too, lies in the profound chemical consequences of simple changes wrought by the defined microenvironments within these assemblies. The earliest examples of altered chemical activity within supramolecular coordination compounds come from Fujita and coworkers, in which they employed their palladium-vertexed octahedra (Fig. 16) in the Diels–Alder cycloaddition of isoprene with naphthoquinone [26], accelerating this bimolecular addition 113-fold.

The basis of the rate acceleration by this host is an increased effective molarity within the assembly cavity. This principle has been demonstrated with other supramolecular compounds that possess a defined inner space [27, 28]. This is a powerful but narrow capability of these assemblies, employing size- and shape-complementarity to bring molecules together in the promotion of bimolecular reactions. Importantly, this phenomenon does not depend on perturbation of the potential energy surface to effect the rate accelerations.

This is not to say, however, that supramolecular assemblies can only affect reactivity kinetically (i.e., by bringing reagents into proximity or providing a spatial barrier between them, as in the  $P_4$  example earlier). An important example of the perturbation of a thermodynamic equilibrium by a supramolecular coordination cage is the increased acidity of encapsulated amines within the  $M_4L_6$  assembly shown in Fig. 17 [29]. A wide variety of amines can be encapsulated within the supramolecular framework, bound as the protonated ammonium species.

In basic aqueous solution, the equilibrium between free amines and their conjugate ammonium ions strongly favors the free amine. In the presence of the  $M_4L_6$

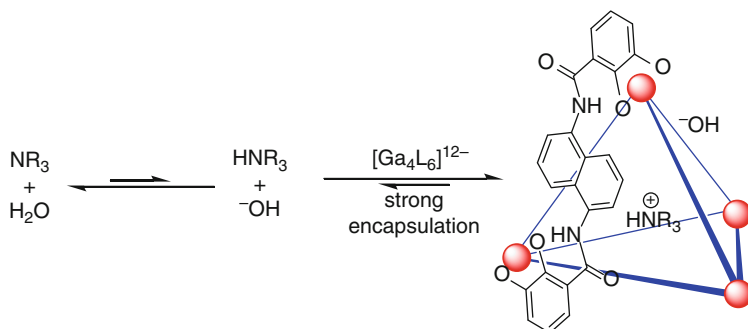


**Fig. 17** The equilibrium between free amine  $\text{NR}_3$  and protonated ammonium cation  $\text{HNR}_3^+$  as promoted by encapsulation within the  $\text{M}_4\text{L}_6$  assembly. Strong binding by the  $\text{M}_4\text{L}_6$  assembly drives formation of the ammonium cation

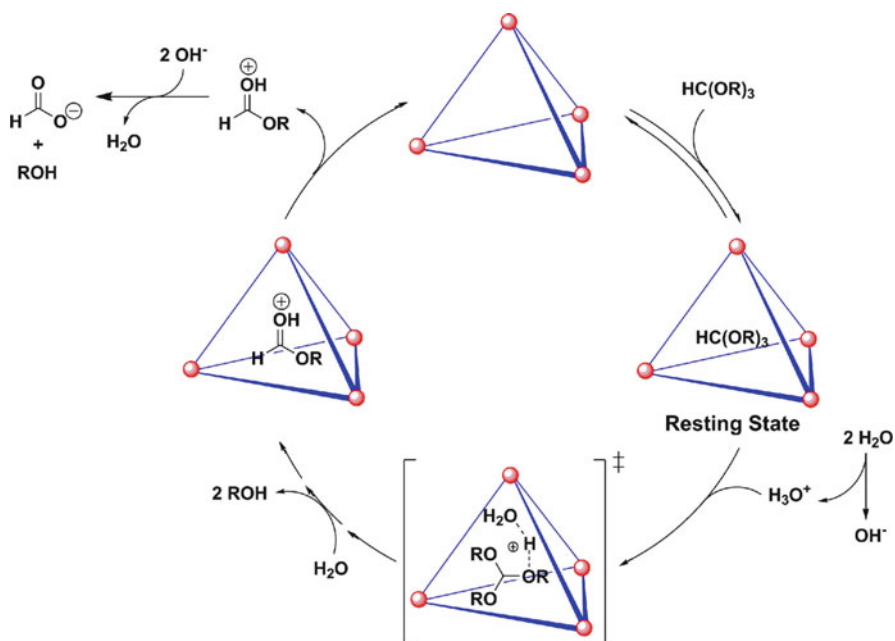


**Fig. 18** Catalysis of the hydrolysis of orthoformates as promoted by encapsulation within the  $\text{M}_4\text{L}_6$  assembly. Binding of the protonated intermediate allows catalytic turnover even in basic aqueous solution, which would normally preclude the formation of acidic intermediates

assembly, the ammonium species is tightly bound and the equilibrium is shifted in favor of the protonated species. The  $\text{M}_4\text{L}_6$  host is highly negatively charged and has a strong affinity for monocationic guests, tightly binding the protonated amine. This strongly perturbs the equilibrium in favor of the bound cation, increasing the basicity of these amines by up to 4.5 orders of magnitude!

Recognizing that this principle could be applied not only to perturbing the equilibrium of unreactive species such as ammonium ions, the  $\text{M}_4\text{L}_6$  assembly

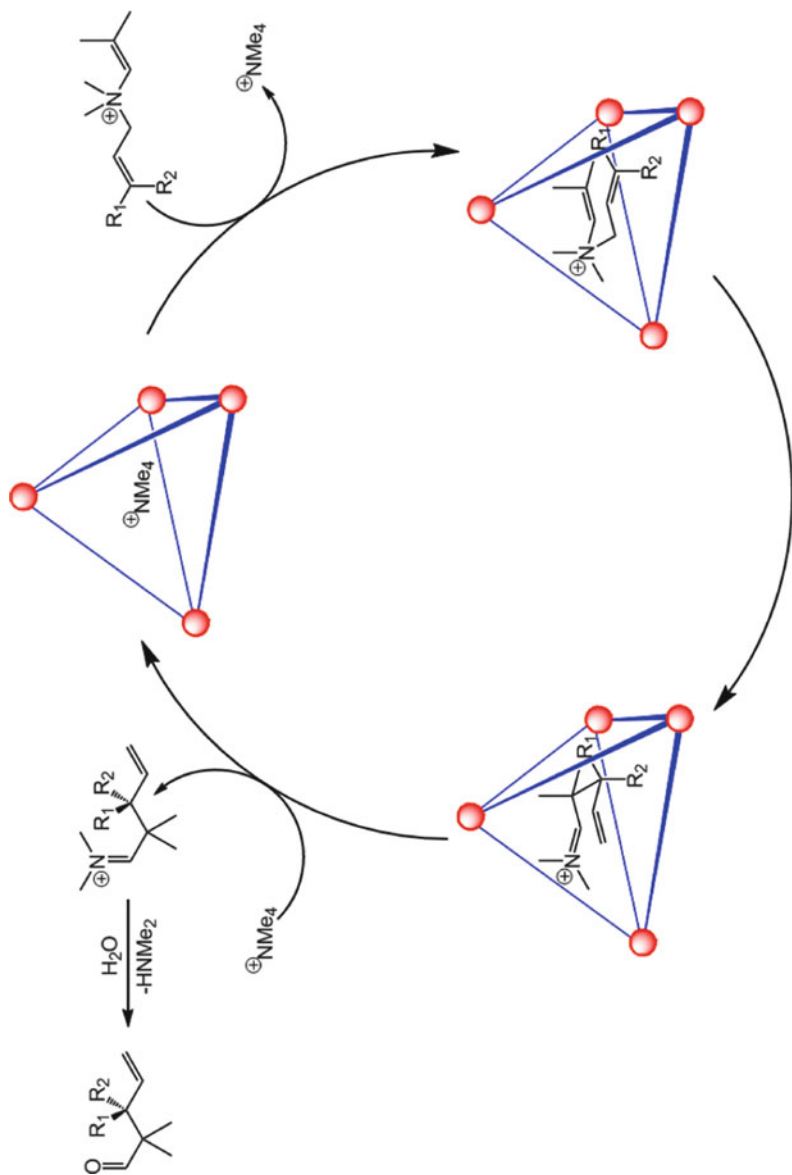


**Fig. 19** Allyl enammonium salts are encapsulated within the supramolecular assembly, promoting electrocyclicization to the corresponding iminium cation. This cation is subject to hydrolysis in basic solution, yielding the aldehyde products while promoting catalytic turnover

was employed in acid-catalyzed reactions, which could be conducted in strongly basic solutions [21]. The catalysis of the hydrolysis of orthoformates and acetals was enhanced by 1,000-fold in basic solution using this principle (Fig. 18).

Complementary to this strategy, the inner space of these supramolecular assemblies has been employed to enforce the reactive conformations of substrates. Unlike the previous example, instead of promoting an otherwise unstable chemical intermediate, the spatial restrictions of the supramolecular coordination cage promote the formation of reactive intermediates, as in the aza-Cope electrocyclozation in Fig. 19. Furthermore, the enantiopure form of the assembly could be used to make

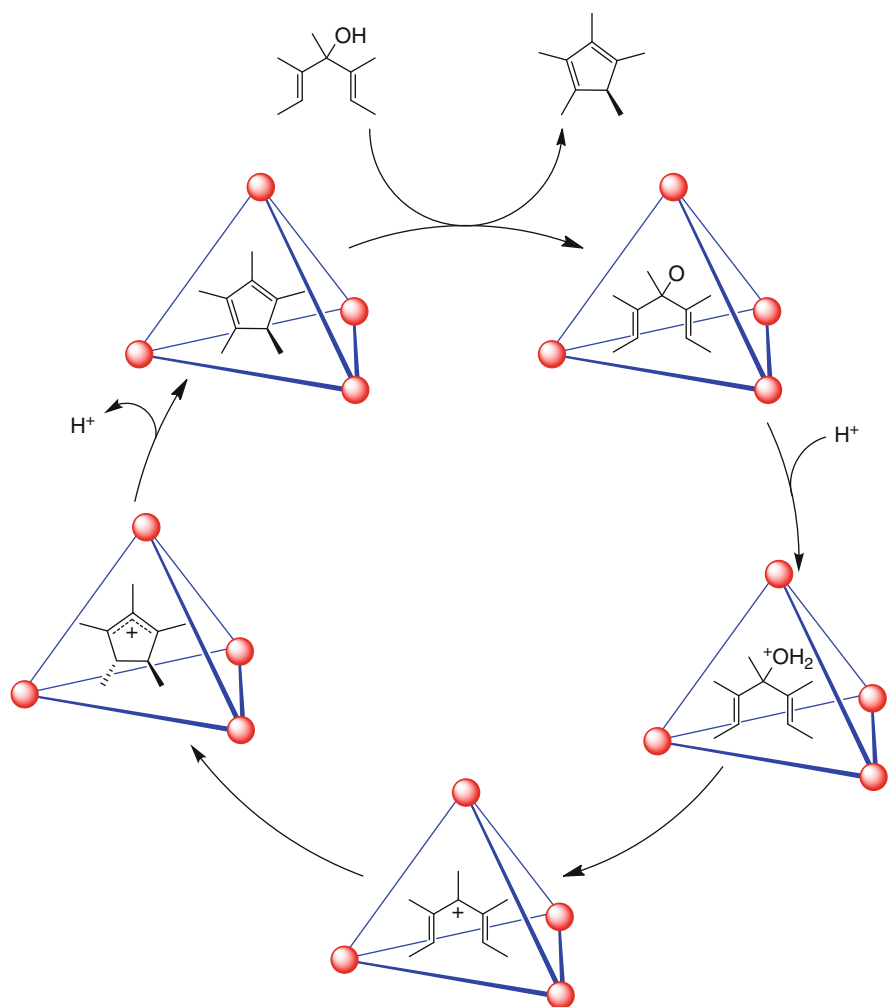


**Fig. 20** The Nazarov cyclization as catalyzed by the  $M_4L_6$  assembly

this rearrangement asymmetrically [30], normally a very challenging task for electrocyclizations.

The most recent and powerful example of supramolecular catalysis comes from an elegant combination of the principles delineated above. The Nazarov cyclization can be used to prepare Cp\*(pentamethylcyclopentadiene) from a mixture of pentanediols, as in Fig. 20. This reaction requires formation of a carbocation by dehydration of the protonated alcohol, and then electrocyclization of the corresponding bis-allylic carbocation.

The rate accelerations observed in the presence of the  $M_4L_6$  assembly are spectacular – the encapsulated substrate cyclizes over two million times faster than the unencapsulated alcohol [31]. This very high level of catalytic activity and the observed kinetics emulate the remarkable activity of enzymes. The observed rate acceleration is too large to be explained by an equilibrium perturbation such as the increased basicity of the substrate, leading to a 1,000-fold rate acceleration in the hydrolysis of orthoformates [21], the idea is that the act of binding the guest in the cavity can only be responsible for four to five of the orders of magnitude of rate acceleration. Thus, the million-fold rate enhancement in this system is due at least in part to binding of the transition state.

## 5 Closing Remarks on Inner and Outer Beauty

The clusters whose chemistry our research group has explored in recent years have been remarkable in continuing to show new and unusual properties. Like enzymes, in which the inner space is controlled by protein folding and hence micro-environments are created that differ dramatically from the surrounding bulk solvent, these clusters are highly water-soluble and yet carry out chemistry normally seen only in nonaqueous solvents. Also like enzymes, stabilization of the transition state upon guest binding can dramatically alter the reactivity, and even change the product distribution, for the reactions of guest molecules. Although this beauty may be particularly appreciated in the eyes of these authors, we offer these examples – and related chemical examples for which we express both aesthetic and scientific admiration – to our readers, with the hope that they will also appreciate them.

Having started with a quote from the famous naturalist John Muir we will end with a quote from an artist who had the same appreciation for the natural beauty that Muir described. As Ansel Adams expressed in a letter to his friend Cedric Wright [32]:

Art is both love and friendship and understanding: the desire to give. It is not charity, which is the giving of things. It is more than kindness, which is the giving of self. It is both the taking and giving of beauty, the turning out to the light of the inner folds of the awareness of the spirit. It is a recreation on another plane of the realities of the world; the tragic and wonderful realities of earth and men, and of all the interrelations of these.

## References

1. Merriam-Webster (2003) Merriam-Webster's Collegiate Dictionary. Merriam-Webster, Springfield. <http://www.merriam-webster.com/dictionary/beauty>. Accessed 14 Sep 2011
2. Aristotle (1984) Complete works of Aristotle, vol. 1. Princeton University Press, Princeton
3. Muir J (1894) The mountains of California. The Century Company, New York
4. Perrett DI, Burt DM, Penton-Voak IS et al (1999) Symmetry and human facial attractiveness. *Evol Hum Behav* 20:295–307
5. Kitagawa S, Uemura K (2005) Dynamic porous properties of coordination polymers inspired by hydrogen bonds. *Chem Soc Rev* 34:109
6. MacGillavry CH (1965) Symmetry aspects of M.C. Escher's periodic drawings, published for International Union of Crystallography. A. Oosthoek's Uitgeversmaatschappij, Utrecht
7. Escher MC, Locher JL (1984) The infinite world of M C Escher. Abradale/Abrams, New York
8. Hofmann KA, Küspert F (1897) Verbindungen von Kohlenwasserstoffen mit Metallsalzen. *Z Anorg Chem* 15:204–207
9. Powell HM, Rayner JH (1949) Clathrate compound formed by benzene with an ammonia–nickel cyanide complex. *Nature* 163:566–567
10. Bailar JC Jr (1964) Coordination polymers. *Prep Inorg React* 1:1–27
11. Hoskins BF, Robson R (1990) Design and construction of a new class of scaffolding-like materials comprising infinite polymeric frameworks of 3D-linked molecular rods. A reappraisal of the zinc cyanide and cadmium cyanide structures and the synthesis and structure of the diamond-related frameworks  $[N(CH_3)_4][CuIZnII(CN)_4]$  and  $CuI[4,4',4'',4''']$ -tetracyanotetraphenylmethane]BF<sub>4</sub>·xH<sub>2</sub>O. *J Am Chem Soc* 112:1546–1554
12. Kondo M, Yoshitomi T, Matsuzaka H et al (1997) Three-dimensional framework with channeling cavities for small molecules:  $\{[M_2(4, 4'\text{-bpy})_3(NO_3)_4] \cdot xH_2O\}_n$  (M = Co, Ni, Zn). *Angew Chem Int Ed Engl* 36:1725–1727. doi:10.1002/anie.199717251
13. Higuchi M, Kitagawa S (2011) Spatial science that does the trick for coordination chemistry. *Chem Chem Ind* 64:397–399
14. Yaghi OM, Li H (1995) Hydrothermal synthesis of a metal-organic framework containing large rectangular channels. *J Am Chem Soc* 117:10401–10402
15. Wang B, Côte AP, Furukawa H, O'Keeffe M, Yaghi OM (2008) *Nature* 453, 207. <http://www.nature.com/nature/index.html>. Reprinted by permission from Macmillan Publishers Ltd.
16. Cram DJ, Tanner ME, Thomas R (1991) The taming of cyclobutadiene. *Angew Chem Int Ed Engl* 30:1024–1027
17. Lehn J-M, Mascal M, Decian A, Fischer J (1990) Molecular recognition directed self-assembly of ordered supramolecular strands by cocrystallization of complementary molecular components. *J Chem Soc Chem Commun* 1990:479
18. Saalfrank RW, Stark A, Peters K, von Schnering HG (1988) The first “adamantoid” alkaline earth metal chelate complex: synthesis, structure, and reactivity. *Angew Chem Int Ed Engl* 27:851–853
19. Saalfrank RW, Glaser H, Demleitner B et al (2002) Self-assembly of tetrahedral and trigonal antiprismatic clusters  $[Fe_4(L_4)_4]$  and  $[Fe_6(L_5)_6]$  on the basis of trigonal tris-bidentate chelators. *Chem Eur J* 8:493–497
20. Caulder DL, Raymond KN (1999) Supramolecules by design. *Acc Chem Res* 32:975–982
21. Pluth MD, Bergman RG, Raymond KN (2009) Proton-mediated chemistry and catalysis in a self-assembled supramolecular host. *Acc Chem Res* 42:1650–1659
22. Mugridge JS, Bergman RG, Raymond KN (2010) The steric isotope effect in a supramolecular host-guest exchange reaction. *Angew Chem Int Ed Engl* 49(21):3635–3637
23. Mugridge JS, Bergman RG, Raymond KN (2011) <sup>1</sup>H NMR chemical shift calculations as a probe of supramolecular host-guest geometry. *J Am Chem Soc* 133(29):11205–11212
24. Mal P, Breiner B, Rissanen K, Nitschke JR (2009) White phosphorus is air-stable within a self-assembled tetrahedral capsule. *Science* 324:1697–1699
25. Raymond KN (2009) Supramolecular chemistry: phosphorus caged. *Nature* 460:585–586
26. Kusakawa T, Nakai T, Okano T, Fujita M (2003) *Chem Lett* 32:284–285

27. Kang J, Rebek J (1997) Acceleration of a Diels-Alder reaction by a self-assembled molecular capsule. *Nature* 385:50–52
28. Mock WL, Irra TA, Wepsiec JP, Manimaran TL (1983) Cycloaddition induced by cucurbituril: a case of Pauling principle catalysis. *J Org Chem* 48:3619–3620
29. Pluth MD, Bergman RG, Raymond KN (2007) Making amines strong bases: thermodynamic stabilization of protonated guests in a highly-charged supramolecular host. *J Am Chem Soc* 129:11459–11467
30. Brown CJ, Bergman RG, Raymond KN (2009) Enantioselective catalysis of the aza-cope rearrangement by a chiral supramolecular assembly. *J Am Chem Soc* 131:17530–17531
31. Hastings CJ, Pluth MD, Bergman RG, Raymond KN (2010) Enzymelike catalysis of the Nazarov cyclization by supramolecular encapsulation. *J Am Chem Soc* 132:6938–6940
32. Adams A, Alinder MS, Stillman AG (1988) *Ansel Adams: letters and images, 1916–1984*. Little, Brown, Boston

# The Mechanical Bond: A Work of Art

Carson J. Bruns and J. Fraser Stoddart

**Abstract** Mechanically interlocked objects are ubiquitous in our world. They can be spotted on almost every scale of matter and in virtually every sector of society, spanning cultural, temporal, and physical boundaries the world over. From art to machinery, to biological entities and chemical compounds, mechanical interlocking is being used and admired every day, inspiring creativity and ingenuity in art and technology alike. The tiny world of mechanically interlocked molecules (MIMs), which has been established and cultivated over the past few decades, has connected the ordinary and molecular worlds symbolically with creative research and artwork that subsumes the molecular world as a miniaturization of the ordinary one. In this review, we highlight how graphical representations of MIMs have evolved to this end, and discuss various other aspects of their beauty as chemists see them today. We argue that the many aspects of beauty in MIMs are relevant, not only to the pleasure chemists derive from their research, but also to the progress of the research itself.

**Keywords** Beauty · Catenanes · Chemical Topology · Elegance · Knots · Rotaxane

## Contents

1	Introduction .....	20
2	The Beauty of the Mechanical Bond .....	23
	2.1 In Nature .....	23
	2.2 In Art .....	25
	2.3 In Society .....	28

---

C.J. Bruns and J.F. Stoddart (✉)

Department of Chemistry, Northwestern University, 2145 Sheridan Road, Evanston, IL 60208, USA  
e-mail: [stoddart@northwestern.edu](mailto:stoddart@northwestern.edu)



3	The Evolution of MIM Representation .....	30
3.1	A Historical Look at MIMs .....	31
3.2	The Use of Color .....	34
3.3	Crystal Structures .....	37
3.4	The Transition to Cartoons .....	40
3.5	Technomorphism .....	43
4	The Beauty of MIMs .....	44
4.1	Topological Beauty .....	45
4.2	Architectural Beauty .....	47
4.3	Simplicity and Elegance .....	49
4.4	Complexity and Emergence .....	54
4.5	Beautiful Mechanically Interlocked Molecular Machines and Switches .....	56
4.6	The Artwork of MIMs .....	62
5	Conclusions and Perspectives .....	65
	References .....	65

## 1 Introduction

The unique bond, which is shared between chemistry and art, has been recognized since at least 1860, when French chemist Marcellin Berthelot wrote: “La Chimie crée son objet. Cette faculté créatrice semblable à celle de l’art lui-même, a distingue essentiellement des sciences naturelles et historiques,” which translates in English to:

Chemistry creates its own object. This creative quality, resembling that of art itself, distinguishes it essentially from natural and historical sciences.

Berthelot recognized that creativity not only distinguishes chemistry from other sciences, but also assimilates it with art. But what is art? To attempt to define it is to enter a realm that chemists, naïve as we are in these matters, had best avoid. We note, nevertheless, that the Wikipedia [1] definition of art, “the process or product of deliberately arranging elements in a way to affect the senses or emotions,” can be truncated into a reasonably suitable definition for chemistry, “the process or product of deliberately arranging elements.” The essence of creativity is indeed inherent to both disciplines.

The similarities and differences between art and science have been long-deliberated [2, 3]. Foremost among these deliberations is the issue of beauty. Rather than attempting to summarize or evaluate the numerous angles on the relationship between science and art, let us simply draw attention to the philosophy that has profoundly shaped modern notions on the subject of beauty in science, which stems from the notion that science and art are different forms of symbolic activities. Werner Heisenberg, a Nobel Prize winner in physics and proponent of this perspective, defined [4] beauty as “the proper conformity of the parts to one another and to the whole.” He crowned mathematical beauty – unification through abstraction – as the prevailing flavor of beauty in science. This ideal is noble but it is unfortunate that it has reigned so exclusively; others have noted [5] the irony that chemistry, for all its sensory content – its colors, odors, textures – is much less associated with

beauty than mathematical physics. Whence the beauty of empirical science? As Roald Hoffman and Pierre Laszlo [6] have said, “our discipline is a curious mix of empirical observation *and* abstract reasoning. This is not unlike music, but it parts chemistry from the pure rigor of mathematics.” We hope this chapter will contribute support to the growing initiative [7–10] to widen aesthetic considerations in chemistry, even as a basis for research [11].

A discussion of beauty in chemistry might concern the beauty of materials [12] – the color and texture of a pigment, or the shape and clarity of a crystal, for example – or refer to the molecules themselves. Both have an obvious connection with the visual arts; chemistry is largely responsible for the ever-growing diversity of materials that artists manipulate, but there is beauty in the *structures* of molecules as well. In this chapter, we will leave materials aside and focus on the beauty of molecular structures, or more accurately their representations with which chemists engage. The topic of molecular beauty is largely eschewed from the literature, residing instead primarily in the informal discussions, meetings, and conferences between colleagues. Nobel laureate Roald Hoffman, who recognized that chemistry’s rich and visual symbolic language is an important contributor to beauty in science, spearheaded [13–16] a more formal discussion in 1988.

The roots of molecular beauty can be traced back to the Platonic tradition. To Plato, “the most beautiful bodies in the whole realm of bodies” were the tiny polyhedra, now deemed the Platonic solids, which he proposed comprise the universe: the four elements – earth (cube), fire (tetrahedron), air (octahedron), water (icosahedron) – and the ether (dodecahedron) (Fig. 1). Joachim Schummer, who has written [9] extensively on chemical aesthetics, writes:

Modern chemistry is exactly the art that provides creative access to what Plato considered the realm of the most beautiful bodies. Therefore, it is no surprise that chemists put their creative activity also in the service of beauty.

Of course, the “realm of the most beautiful bodies” is too small to see. But there is something romantic about the way a molecule is physically crafted, like sculpture, through diligent labor, yet is only perceived mentally, like poetical imagery, with the aid of symbols. Here, we engage these symbols – our imperfect and incomplete representations of molecules – as artwork. We will not hazard straying into the complex territory of contention on this issue, which has been discussed [9] superbly elsewhere, for we understand beauty as that which provides one with a sense of

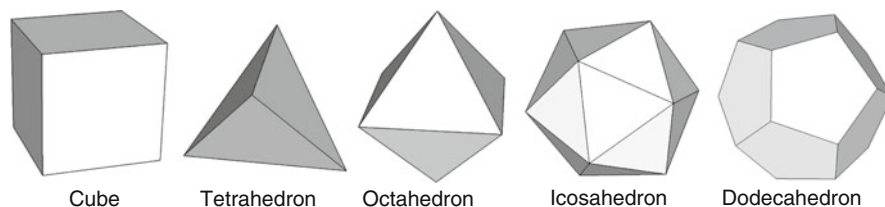


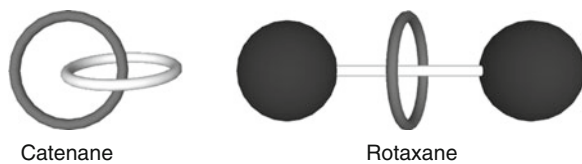
**Fig. 1** The Platonic solids are the most beautiful bodies according to Plato. Like molecules, these imperceptibly small objects were thought to compose the physical world

personal pleasure rather than in the context of rigorous aesthetic formalisms. We take for granted that beauty has a place in chemistry because we know, as chemists, that chemists are passionate in their vocation and take great pleasure in their work. Moreover, despite a lack of formal aesthetic training among most chemists – and the longstanding stigma associated with discussing beauty in the scientific literature – at least 2% of chemistry papers mention [17] aesthetic values as a justification for studying a molecule. Classic examples include a variety of synthetic Platonic and Archimedean objects [18], such as cubane [19], dodecahedrane [20], buckminsterfullerene [21], and many metal–ligand coordination complexes and cages [22–24] that have been appreciated [10] for their symmetry, simplicity, uniformity, and harmony: “simply beautiful and beautifully simple.” On the other hand, natural products and their corresponding organic transformations have been admired for the beauty in their elegance, complexity, and sophistication [25]. For perspectives on beauty in experimental chemistry, see [26] and [27].

Molecular nanotechnology has uncovered yet another way to address beauty in chemistry: miniaturization. Chemists now frequently “miniaturize” everyday objects by constructing them to varying and sometimes quite liberal degrees of approximation, using molecules as their building blocks. Our affinity for miniaturization is a consequence of two factors: (1) the development of supramolecular chemistry [28], which has made this kind of miniaturization possible; and (2) the emergence of a paradigm shift in molecular representations, in which molecules are portrayed more ambiguously so as to resemble their macroscopic analogs. In other words, the vision of a miniaturized world has been catalyzed in part by the beautiful new ways of representing molecules, which deliberately blur the lines between the molecular world and the macroscopic one. We refer to these graphical representations as cartoons, illustrations, and – in this chapter – art.

In this regard, mechanically interlocked molecules (MIMs) are of particular interest because they have played a central role in molecular nanotechnology and the aforementioned paradigm shift to more artistically disposed figures and schemes in the literature. Moreover, the mechanical bond is ubiquitous in the macroscopic world, but has been, until recently, challenging to introduce into molecules. Simply defined, MIMs are molecules with two or more components that are not covalently connected, but cannot be separated without breaking a covalent bond. The inseparability of the components is what makes them molecules instead of supermolecules. Cartoon representations of two prevalent types of MIMs are shown in Fig. 2. A catenane is a molecule with two or more interlocking rings,

**Fig. 2** Graphical representations of the structures of mechanically interlocked molecules (MIMs): a catenane (*left*) and a rotaxane (*right*)



derived from the Latin word *catena*, meaning “chain.” A rotaxane – derived from the Latin words *rota* (wheel) and *axis* (axle) – has a dumbbell-shaped component wherein a rod is threaded through a ring, with ends (stoppers) that are too bulky for the ring to bypass.

We will use images to highlight, support, and substantiate our claims of beauty in MIMs, but first we turn to the mechanical bonds in the ordinary world that inspire this creative subdiscipline in chemistry.

## 2 The Beauty of the Mechanical Bond

Insofar as beauty is derived from that which surrounds us, the mechanical bond cannot be ignored. It is applied and admired in society, art, and nature alike, and its beauty is held as both an ancient and modern sentiment. The development of modern tools and machinery, many of which we consider beautiful today (think of a sporty car or a delicate “Rube Goldberg” or “Heath Robinson” machine) could not have been accomplished without the mechanical bond. Likewise, interlocked rings can be found in thousands of works of art dating through antiquity. Perhaps most surprising to the casual reader will be the predominance of mesoscopic mechanical interlockings in Nature, even within the cells of our own bodies.

### 2.1 In Nature

Perhaps the most incontrovertible source from which we derive beauty is Nature. In terms of molecular beauty, Nature has perfected its brand of chemistry over billions of years and is an endless source of inspiration for chemists. For all our efforts, the number of chemicals and reactions we have discovered and created seem diminished by the bewildering complexity and sheer abundance of those in Nature. In particular, the diversity and intricacy of systems and cycles in the chemistry of life processes are still far beyond our total comprehension. Even so, in a world where structure and function are so intrinsically and intimately linked, it should come as no surprise that Nature started dabbling with mechanical bonds long before humans came to the scene.

In contrast to modern industry, where technology utilizes the mechanical bond far more ubiquitously on the macroscale than on the nanoscale, Nature depends more vitally on mechanical interlocking at the molecular level. To be certain, a few mechanical bonds can be identified in Nature’s macroscale designs, such as the rotaxane-like mammalian spine (Fig. 3a) or a turtle’s shell – a suitane in the molecular world [33] (Fig. 3b). But, mechanical bonds are being made and broken incessantly within the mesoscopic world of cells. DNA is foremost among the players in biological MIMs. DNA catenanes [34] and knots [35] are intermediate

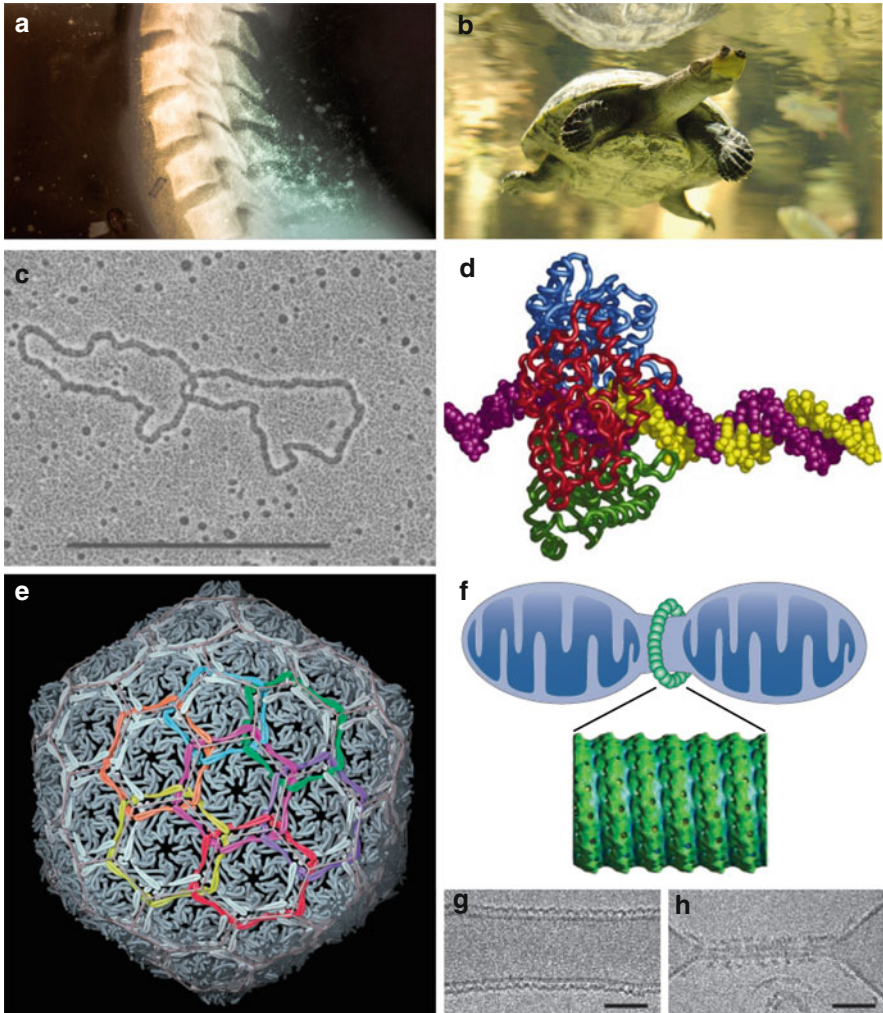


**Fig. 3** Examples of mechanical bonds in nature. (a) X-ray image of human vertebrae, which protect the spinal cord with mechanical bonds. (b) A turtle’s shell has a similar function to the spine, but protects more organs. (c) Electron micrograph of a DNA catenane [29]; scale bar: 1  $\mu\text{m}$ . (d) The crystal structure of  $\lambda$ -exonuclease, paired with a model depicting how it encircles DNA while catalyzing its hydrolysis [30]. (e) “Protein chainmail”: the crystal structure of the bacteriophage HK97 capsid, highlighting catenated protein macrocycles [31]. (f) Cartoon and model of nanotubes that participate in mitochondrial scission [32]. TEM images show mitochondria before (g) and after (h) constriction of the mechanically bound protein nanotubes; scale bars: 50 nm. Reproduced with permission from [29] (copyright 1980 Elsevier), [30] (copyright 2003 Oxford University Press), [31] (copyright 2000 AAAS), [32] (copyright 2011 Nature Publishing Group)

structures in basic biological processes such as DNA recombination and replication as mediated by various enzymes [36]. Many topological DNA structures have now been imaged [29] quite beautifully by electron microscopy (Fig. 3c).

Not only does DNA form itself into catenated and knotted structures, it also rotaxanates itself with macrocyclic enzymes.  $\lambda$ -Exonuclease [30, 37] is an enzyme that participates in DNA replication and repair by fully encircling DNA as it sequentially hydrolyzes nucleotides – a biomolecular rotaxane! The structure of the enzyme is shown in Fig. 3d. T4 DNA polymerase holoenzyme [38] is an analogous example; its protein subunits “clamp” around a DNA strand to form a toroid in what chemists of the mechanical bond would call a “clipping” process. It should be noted that chemists have been able to mimic this concept of a topologically linked catalyst on a polymer [39] using traditional organic catalytic reactions.

DNA is not the only entity that can serve as component of biological MIMs. A recent discovery was the extraordinary interlocked structure of the bacteriophage HK97 capsid. The icosohedral shell of the phage is composed of topologically linked protein macrocycles (Fig. 3e) [31]. This “molecular chainmail” is no less beautiful than it is far beyond the reaches of our current artificial mimicry at the molecular and supramolecular level. It is also known that mitochondria recruit various proteins to encircle them in the form of a nanotube (Fig. 3f) that participates in mitochondrial fission by applying a contractile force [32, 40], as shown by microscopy in Fig. 3g, h. The phenomenon of a ring contracting as it encircles a rod in order to sever it is not unlike certain digestive processes or a common method of bovine castration; it is intriguing that this mechanical “pinching” process happens at the intracellular level as well.

It is apparent that our efforts in the chemistry of the mechanical bond have been surpassed by Nature as usual. Nature executes this chemistry with a level of elegance, complexity, and beauty that we can only strive for, yet will surely use as a source of inspiration for centuries to come.

## 2.2 *In Art*

Nowhere is the beauty of the mechanical bond more validated than in the world of art. If anything can speak to the beauty of the mechanical bond, it is the art that portrays it, and it so happens that artists have been drawing, painting, carving, and sculpting mechanical bonds for thousands of years!

Borromean Rings are a mechanically interlocked species that deserve special attention, for despite being largely absent in the natural world, they are among the most prevalent topologies found in art, spanning many cultures and thousands of years. Their name originates from the Borromeo family of northern Italy, on whose crest (Fig. 4b) and estates the rings frequently appear. The rings have been associated with the Borromeo family from at least the fifteenth century, though recorded use of the symbols date back to the thirteenth century in Christian iconography (Fig. 4c), the twelfth century in Japanese emblems, and the ninth century in Viking symbols (Fig. 4d), making them a remarkably universal icon (for many images of ancient and modern artwork of Borromean Rings, see [41]). Topologically speaking, the three rings are interlocked in such a way that breaking

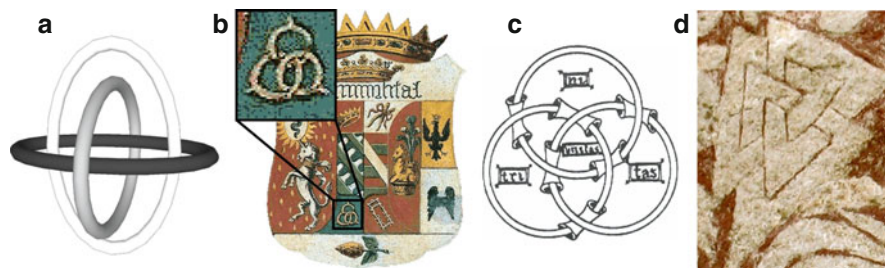


**Fig. 4** The Borromean Rings (BRs). (a) The orthogonal perspective of BRs visualizes the three inseparable rings, where breaking one ring would unlink the other two. (b) BRs appear on the Borromeo family crest. (c) The use of BRs to symbolize the Holy Trinity date back to the thirteenth century. (d) The Valknut is a Borromean Viking symbol found on ancient stone carvings

one ring results in the dissociation of all three components (Fig. 4a). This mutual dependence is what has made the rings such a powerful symbol for threefold unification, having been adopted to symbolize triads ranging from Christianity's Holy Trinity (Fig. 4c) to Ballantine Brewery's "Purity, Body, Flavor." The richness of symbolism, as well as the accompanying centuries of artwork associated with Borromean Rings, leaves little question as to their beauty.

Solomon Knots have a similar record of predominance in art and history. The Solomon Knot is not actually a knot but a link; it has two rings that are doubly interlocked. The structure of the link, which has no obvious beginning or end, has made it a remarkably adaptable icon. It has been an important symbol in many cultures throughout history, including parts of Judaism, Christianity, and Islam, as well as with the Yoruba, Akan, and Kuba people of Africa [42]. Fig. 5a is one ancient example from the Byzantine Basilica beneath the Church of the Nativity in Bethlehem, Israel. As the seal of the Biblical King Solomon, it has represented wisdom and knowledge. In other contexts, it has symbolized eternity, beauty, and royalty. From ancient Roman mosaics to Celtic carvings to African headdresses to Middle Eastern relics and stained glass churches, the Solomon Knot is a powerful symbol of beauty in art, religion, and culture. *Seeing Solomon's Knot* [43] by Lois Rose Rose is a recent and well-crafted exploration of the artwork of Solomon's Knot across time and cultures. We will return later to the appearance of Borromean Rings [44] and Solomon Knots in chemistry.

Though we have given special attention to ancient art, there is no recent lack of artistic interest in mechanical bonds. Symbolizing, as they do, unification and bringing together, many artists are still carrying the banner for all things interlocked, from architecture to textiles to sculpture and origami. Particularly classic examples are the "Bonds of Friendship" statues (Fig. 6) by John Robinson in the sister cities of Sydney, Australia and Portsmouth, England depicting two linked rings [45]. The remaining examples in Fig. 5 are other modern works. Louise Mabbs' *Borro-vari* textile art in Fig. 5b depicts the distinct ways to arrange three rings [46] (top row: separate rings, second row: two linked and one separate, third row: three-link chain, fourth row: Borromean variations, with the bottom corners

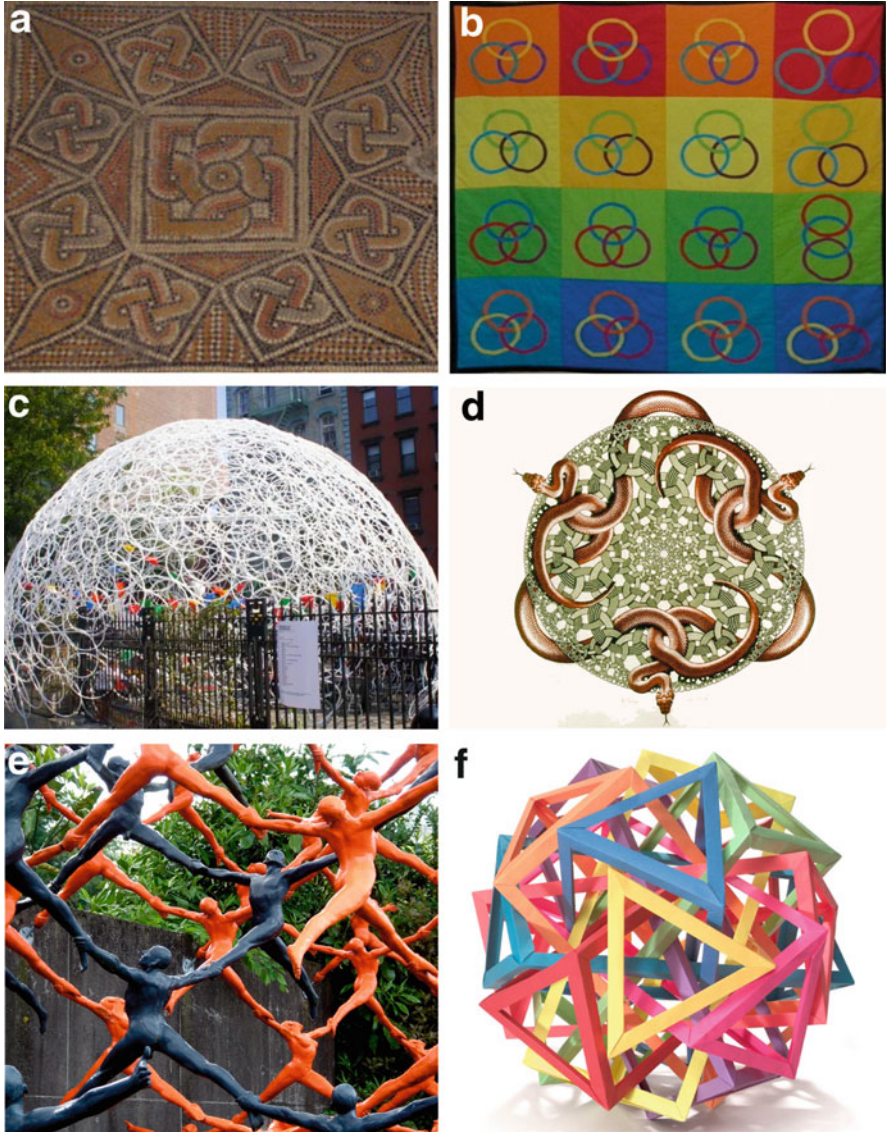


**Fig. 5** Examples of interlocked art: (a) ancient mosaic of Solomon Knots in the Byzantine Basilica, Israel; (b) *Borro-vari* hanging quilt depicting the various ways to interlock three rings (copyright 2007 Louise Mabbs); (c) *Ring Dome* pavilion by architect Minsuk Cho, composed entirely of large and small interlocked rings (Photo: Rory Hyde); (d) *Snakes* woodblock print by M. C. Escher shows a net of multiply interlocked rings extending infinitely inwards; (e) *Intersecting Space Construction* statue at Hakone Open-Air Museum, Japan by Ryoji Goto presents an interlocked network of connected bodies; and (f) *Ten Interlocking Triangular Prisms* origami by Daniel Kwan (Photo: Lynton Gardiner, copyright OrigamiUSA)





**Fig. 6** The identical “Bonds of Friendship” sculptures by John Robinson, located in Portsmouth, England (*left*) and Sydney Cove, Australia (*right*). The statues commemorate the centuries-old relationship between the two sister cities

being true Borromean Rings). Minsuk Cho’s temporary pavilion *Ring Dome* in Fig. 5c marks what must be one of the largest (and perhaps only) architectural structures composed only of mechanically interlocked rings.

One of the most famous artists to glorify the mechanical bond was M. C. Escher, whose mathematics and science-based art has long encouraged the sorts of discourse that can be found in this volume. His final print, *Snakes* (Fig. 5d), was an array of interlocking rings inhabited by a few serpents that extended infinitely inwards. We find this piece beautiful not only for its rotational symmetry and mechanical bonds, but also because it points to the concept of infinitesimal smallness – foreshadowing the days when multiply interlocked rings too small to imagine properly are reality. In another example that points to infinite interlocking, Ryoji Goto’s 1978 *Intersecting Space Construction* sculpture symbolizes the beauty of human connections (Fig. 5e). Finally, the attractive structure of Daniel Kwan’s *Ten Interlocking Triangular Prisms* origami (Fig. 5f) highlights the challenging complexity that can be attained in objects with mechanical bonds.

### 2.3 *In Society*

One cannot navigate the modern world without regularly encountering the mechanical bond (Fig. 7). We typically take it for granted. So pervasive are interlocked structures in all things man-made, if we consciously acknowledged every mechanical bond we encountered, we would scarcely be able to accommodate any other mental processes! Here, we simply point to fashion and technology as illustrative reminders of its omnipresence in society.

We all wear the mechanical bond day in and day out; those with body piercings even use it as a permanent decoration. This practice is not exclusive to Western society; note the mechanically bound objects around the headdress, ears, mouth, and neck of the Mursi woman of southern Ethiopia in Fig. 7a, and the neck-extending



**Fig. 7** Examples of mechanical bonds in society: (a) decorative mechanical bonds of a Mursi woman, (b) portrait of a Khayan Lahwi woman, (c) shower curtain, (d) wristwatch makes a rotaxane with the hand and body as stoppers, (e) chain link, (f) abacus, (g) children’s bead maze, (h) keychain, (i) lock, (j) pulley on a sailship, (k) chainmail, (l) seatbelt buckle, (m) doorknob has the essence of the “dumbbell” portion of a rotaxane (the door is the ring), (n) the mechanical bond of a carabiner helps climbers cling to rock faces, and (o) hundreds of mechanical bonds exist in the chain, crank, and wheels of a bicycle

rings of Northern Thailand's Kayan Lahwi woman (Fig. 7b). These are perhaps extreme examples, but we all use the mechanical bond to tremendous extent in the decoration of our bodies and clothing, from both a practical standpoint and an aesthetic one. Rings, necklaces, bracelets, belts, and even our shirts and pants (trousers) all form mechanical bonds with our bodies and with themselves. For example, compare a necklace with a rotaxane; the necklace is the ring, while the head, neck, and shoulders comprise the "dumbbell". Meanwhile, the necklace itself is composed of mechanical bonds if it is beaded or has a clasp. Consider getting dressed in the morning: if you tie your shoes, put on a belt, button your shirt, and clasp on a watch or jewelry, you have already formed dozens of mechanical bonds around your body before breakfast!

The mechanical bond and technology have gone hand-in-hand since the advent of machinery. Indeed, many of the world's simplest and oldest machines, a wheel on an axle or a pulley (Fig. 7i), for example, are based on the mechanical bond. It has been especially important in transportation; imagine trying to sail without knots and pulleys or drive without wheels! It also appeared as early as 2,700 B.C. in the world's first calculator: the abacus (Fig. 7f). And, just as we find it near the beginning of human history, most of us meet the mechanical bond near the beginning of our lives; it is still among the most common features in children's toys, such as the timeless rattle or the bead maze in Fig. 7g.

Perhaps by now it could go without saying that few modern machines would be capable of existing without some kind of mechanical bond, whether it is the washer around a screw or the disc in a hard drive. Various examples can be found in Fig. 7. Indeed, with every turn of a doorknob, draw of a curtain, or flip of a switch, the mechanical bond is at your service. Between fashion and technology, societies are irrevocably dependent on the mechanical bond. With mechanical bonds being such a necessary component in machinery, it is only fitting that they also represent a cornerstone of molecular machines (Sect. 4.5).

### 3 The Evolution of MIM Representation

Having established a background of beauty for the mechanical bond in art, nature, and society, we now consider beauty as the mechanical bond is miniaturized beyond our ability to perceive it directly. Since they are not available to our senses, their beauty is more associated with the wide variety of modes we use to represent them – drawings, models, and cartoons. Just as chemical signs and symbols have evolved over the centuries from primitive beginnings in alchemy [47–49], portrayals of MIMs have also evolved and even played a vital role in modern expressions of molecules. As chemical structures have grown bigger and more complex, it has become useful to represent them in ways that eliminate finer details, such as the bond order, atomic composition, and so on, especially when trying to convey a message that has more to do with self-assembly, intermolecular interactions, and secondary structure. Because it represents chemistry "beyond the molecule,"

supramolecular chemistry [28] has played a major role in this transition, but so has the chemistry of MIMs, or as we call it, mechanostereochemistry [50].

All sorts of everyday objects have been reconstructed as molecules via template-directed synthesis of mechanical bonds, from switches and buttons to rotors and elevators. The likeness of MIMs to macroscopic objects and machines has done much to advance molecular nanotechnology and is, as we shall see, another important aspect of their beauty.

### 3.1 A Historical Look at MIMs

It is believed that MIMs were discussed hypothetically [51] prior 1912 by Wilstätter at a conference in Zurich, but the idea of mechanical bonds in chemistry did not appear in print [52] until 1953. A significant publication [51] by Frisch and Wasserman in 1961 was the first to articulate in detail the connection between stereochemistry and topology. In chemistry, topology is concerned with the properties of a molecule that are independent of any spatial rearrangements and bond distortions that can be performed without allowing covalent bonds to break or pass through one another. Topologically speaking, catenanes and rotaxanes are dramatically different. The linked rings of a [2]catenane (the bracketed term represents the number of mechanically bound components in a MIM) are topologically distinct from two rings that are not interlocked (they are topological isomers). On the other hand, a [2]rotaxane is topologically identical to its constituent parts because the ring can be separated from the dumbbell by stretching or compressing the appropriate bonds. The concept of chemical topology (for a recent review of the subject, see [53]) has been masterfully expounded by David Walba [54] and Christopher Hunter [55] and is also highly relevant to the study of molecular knots [56], which we have left untouched in this chapter. We shall discuss topological beauty in Sect. 4.

Following a noteworthy attempt [57] in 1958, the first account [58] of a MIM came in 1960, when Wasserman claimed that cyclization of one compound in the presence of a large cycloalkane gave very low yields of a catenane (Fig. 8a), which was isolated by chromatography two years later [60]. Small improvements in the use of this statistical method were made, most notably Harrison and Harrison's 6% yield of a rotaxane by repeating a statistical threading reaction on a resin-bound macrocycle 70 times [61], and Agam and Zilka's two-step catenane synthesis that converted a statistical rotaxane directly to a catenane in 3% overall yield [62, 63]. Meanwhile, Schill was developing an important approach he called "directed synthesis" [59], in which macrocycles were built around an aromatic core such that severing a few bonds at the core in the final steps affords a catenane (Fig. 8b). This approach was further applied to [3]catenanes [64–66], and [2]rotaxanes [67]. Schill's 1971 book, *Catenanes, Rotaxanes, and Knots* [68] is an indispensable reference on the early works of MIMs. For decades, the statistical and directed approaches were the only known methods to afford a catenane, though a Möbius

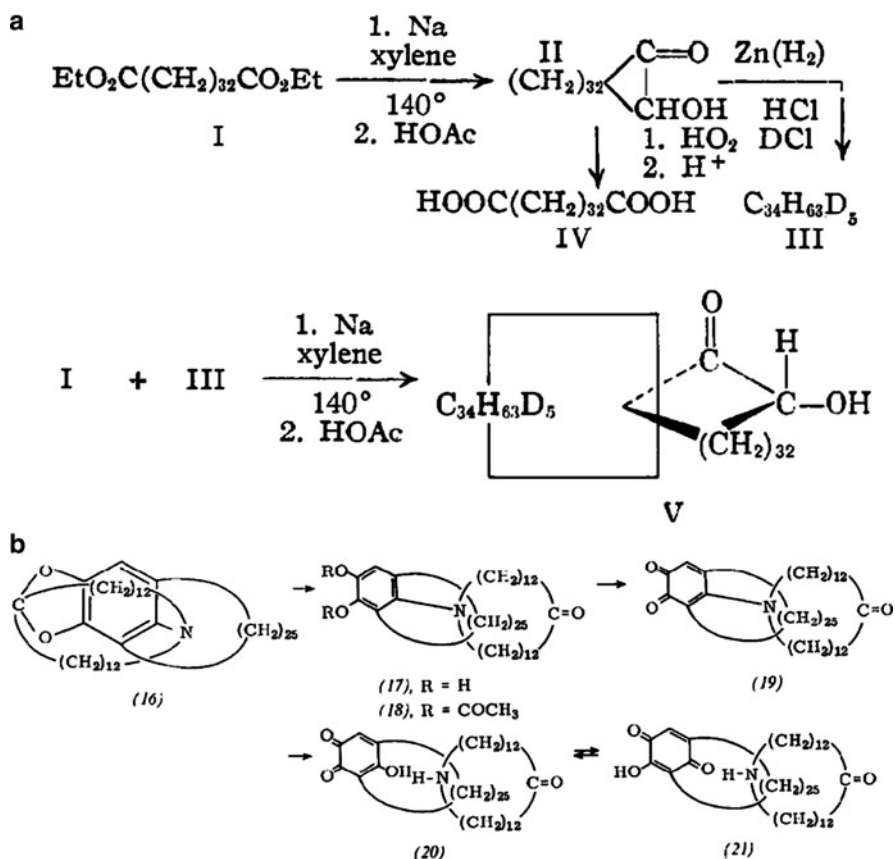
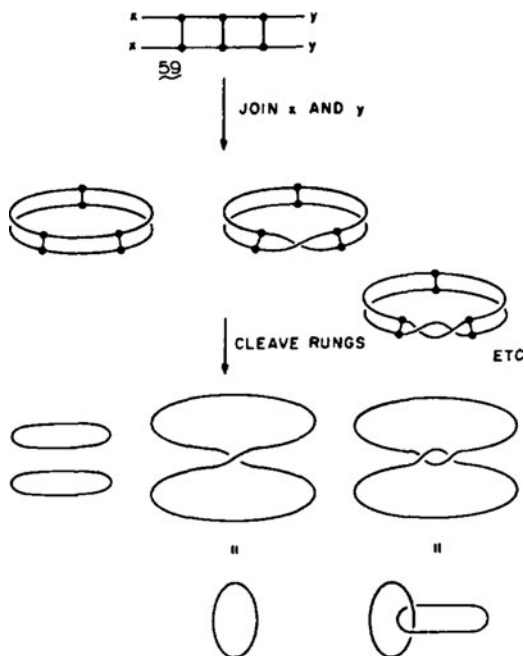


**Fig. 8** The two applied approaches to catenane synthesis prior to 1983. (a) The first statistical synthesis [58] relied upon the macrocyclization of a linear compound (*I*) in the presence of a deuterated cycloalkane (*III*) to achieve small amounts of the catenane *V*. (b) The first example [59] of directed synthesis by covalent templation was a catenane that formed after cleaving the covalent bonds around the aromatic core in compound **16**. Reproduced with permission from [58] (copyright 1960 American Chemical Society), [59] (copyright 1964 Wiley-VCH)

strip approach had been proposed in the late 1950s independently by both Wasserman [51] and van Gulick [69] in an article that was denied publication in *Tetrahedron* at the time (ca. 1961) only to be given the light of day much later on in a special issue of the *New Journal of Chemistry* published in 1993 under the editorship of David Walba. A more detailed history of the Möbius strip approach was discussed by Walba [54]. In 1981, Walba [70] made this approach look more realistic through the use of tetra-hydroxymethylethylene (THYME) polyethers. The bis-macrocyclization of a THYME-based molecule resembling a three-rung ladder can result in a mixture of wreath-like macrocycles with some number of half-twists (Fig. 9). Isolation of the wreath with two half-twists and severing the three ladder rungs would yield a [2]catenane. Walba isolated the zero-twist cylinder and

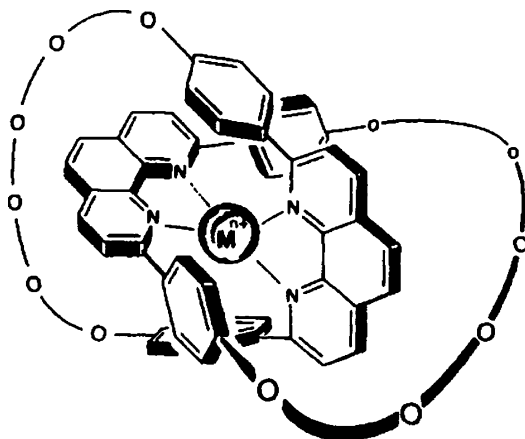
**Fig. 9** The Möbius strip approach to catenane synthesis. The number of half-twists in the strip determine the topology of the product after it is cut down the middle. Two half-twists would afford a [2]catenane. Reproduced with permission from [54] (copyright 1985 Elsevier)



subsequently also synthesized the one half-twist molecular Möbius strip. He verified experimentally that two macrocycles are obtained by cutting the cylinder in half by ozonolysis of the THYME double bonds, while the same action on the Möbius strip leaves it in one piece as a larger macrocycle [71]. However, no double half-twist Möbius strip that would lead to the [2]catenane has been reported to date.

Sauvage's game-changing publication [72] in 1983, which describes the use of a copper(I) ion to template the formation of mechanically interlocked rings (catenands), breathed new life into the field of MIMs in relation to their accessibility, applicability, and even their structural portrayals. The early catenanes were represented conceptually by basic line drawings like those in Fig. 9, and their structures were portrayed in condensed structural formulas, where hydrocarbons assumed the  $C_xH_y$  constitutions and were connected with lines to other functional groups (Fig. 8). The result was a picture that sufficiently communicated atomic and topological content, but bore little resemblance to what the actual structure might look like. When Sauvage [72] revealed a skeletal diagram of his catenane (Fig. 10), the result was a structural drawing that was rich in beauty as well as topological and molecular information. This diagram – hand-drawn in Indian ink – expressed most elegantly the right information while still hinting at the three-dimensional nature of the molecule. It has appeared many times over the years in the literature from Sauvage's group and is a landmark picture of a catenane [73]. It is the gold standard of a MIM drawing, saturated with information and easy to digest.

**Fig. 10** Sauvage's skeletal diagram of a catenand, a major breakthrough in 1983. Reprinted with permission from [73] (copyright 1986 American Chemical Society)



Sauvage's metal coordination template marked the beginning of the modern era of MIMs: template-directed synthesis. Advances in this modern era have been associated with building new interlocked topologies and architectures (Sects. 4.1 and 4.2), discovering new template-directed methods (Sect. 4.3) and emergent properties (Sect. 4.4), and creating molecular switches and machines (Sect. 4.5). In Sects. 3.2–3.5, we examine how depictions of MIMs have changed alongside these many new developments of an evolutionary nature. With simple two- and three-component MIMs, it was possible to achieve Sauvage's gold standard of drawings, but as complexity and diversity grew in the field, it quickly became useful to turn to new tools that aided and abetted the depiction of MIMs in an eye-catching, easily discernable way – namely with the use of color, crystal structures, and cartoons.

### 3.2 *The Use of Color*

Color and MIMs go together like bread and butter. When journals began printing color in the mid-1980s, the mechanical bond made the perfect poster child because color dramatically clarified mechanically interlocked structures, which cannot be drawn without bonds crossing over and under one another. The first example in a primary publication [74] came from the crystal structure of a [3]catenane synthesized in the Sauvage group (Fig. 11). The carbon atoms in each macrocycle were uniquely colored, making each of the three components immediately and effortlessly discernable. This creative act represented a veritable leap forward in MIM portrayal and heralded the changes in chemical depiction that would continue to evolve.

**Fig. 11** Solid-state structure of a [3]catenate from Sauvage's group. The use of color gives unprecedented clarity (and beauty) to the image. Reprinted with permission from [74] (copyright 1987 Wiley-VCH)



Gradually, color made its way past crystal structures and into ordinary structural drawings (Fig. 12). Although we were confronted with heavy criticism, our group was an active participant in this movement, even in the face of what appeared to be extortionate costs imposed by some journal editors. Our first use of color in primary publications came with the initial report of cyclobis(paraquat-*p*-phenylene) (CBPQT<sup>4+</sup>) in two communications [79, 80] in 1988. Since then, both CBPQT<sup>4+</sup> and the use of color have become major workhorses in mechanostereochemistry. From the very beginning we have used royal blue to represent  $\pi$ -acceptors (which is why CBPQT<sup>4+</sup> is known as the little blue box) and pillar-box red to represent  $\pi$ -donors, and have stayed true to this motif to this day (Fig. 12a,b). Though we were among the minority of scientists who chose this approach at the beginning, today the use of color has spread to many research groups and well beyond MIMs; now scientists in most fields of chemistry use color very effectively to enhance clarity and comprehension.

Several examples of colored MIMs are shown in Fig. 12. In particular, these examples [75–78] illustrate that color-coding the constituents of a MIM forms a cohesive link between its various representations, two-dimensional, three-dimensional, graphical, or otherwise. The coherence and readability of these figures is what makes them beautiful, in addition to our natural proclivity for color. We will discuss shortly the use of graphical representations (cartoons) to represent MIMs, a context in which color can be employed to great effect. We conclude that colors communicate molecular information clearly, precisely, and consistently. To the scientifically minded person, the beauty that color gives to an image often has less to do with its aesthetic appeal than with the augmented intelligibility it imparts.



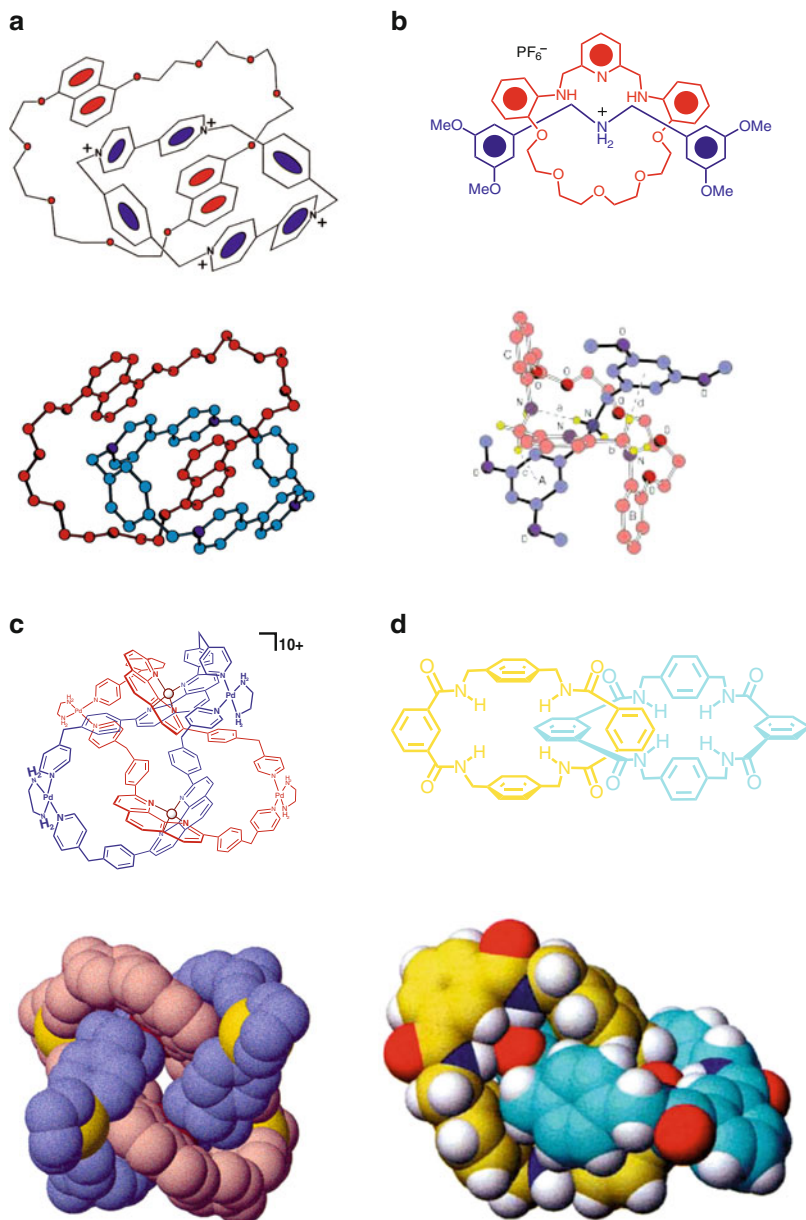


**Fig. 12** Examples of the use of color in depictions of various types of MIMs. Note how the colors and positions of constituent parts in the three-dimensional structures reflect those in the structural drawings to enhance clarity between representations of (a) a donor-acceptor [2]catenane [75] and (b) an ammonium-binding [2]rotaxane [76] from our group, (c) a transition metal-templated Solomon Knot from the Sauvage and Fujita groups [77], and (d) a benzylic amide [2]catenane from the Leigh group [78]. Reproduced with permission from [75] (copyright 1991 Royal Society of Chemistry), [76] (copyright 2000 Wiley-VCH), [77] (copyright 1999 Royal Society of Chemistry), [78] (copyright 1995 Wiley-VCH)

### 3.3 *Crystal Structures*

To many of us, a crystal structure is the most beautiful conceivable representation of a MIM because of its high content of truth; nothing can be more accurate about the way a molecule “looks” – in the solid state at least – than an X-ray crystal structure, save perhaps for some very recent advances in single molecule imaging provided by atomic-resolution microscopy [81]. Although we cannot see the molecule itself, a crystal structure elicits the visualization of the exact positions of every atom and bond in a molecule relative to one another in the solid state. The ability to rotate and examine the structure from any angle in three dimensions supplies a satisfying sense of connection with the molecular world.

Likewise, three-dimensional renderings of MIMs remind us instantly of some of the ordinary objects we encounter in our everyday lives (see Sect. 2.3). Take olympiadane [82], for example (Fig. 13), with its five interlocked rings unmistakably sharing the same topology as the Olympic logo! Most catenanes bear resemblance at least to the links of a chain, as their name implies. Regardless of their resemblance to familiar objects, hundreds of beautiful crystal structures of MIMs have been produced since their debut in 1985, when Sauvage [83] published the first solid-state structure of a [2]catenane (Fig. 14a). It would be impossible to do justice to all of the beauty contained in the databank of solid-state mechanically interlocked structures. In Fig. 14 we simply present a few examples that we find noteworthy [84–88]. See Fig. 23 in Sect. 4.2 for more beautiful crystal structures of some particularly novel MIMs.

David Williams, X-ray crystallographer extraordinaire, erstwhile Professor of Structural Chemistry at Imperial College London, deserves very special recognition when it comes to the portrayal of solid-state superstructures and structures, particularly those involving MIMs. Not only was he the ultimate in creative artisans when it came to handling delicate and sensitive (to volatile solvent loss) single crystals and then mounting them onto state-of-the-art diffractometers before subsequently solving solid-state structures that few in his time could even begin to contemplate tackling, but he also completely revolutionized the presentation of small – and ultimately not so small – superstructures and structures. During the period 1976–2009, he published some 240 articles jointly with the senior author, a number representing less than one quarter of his more than 1,000 publications

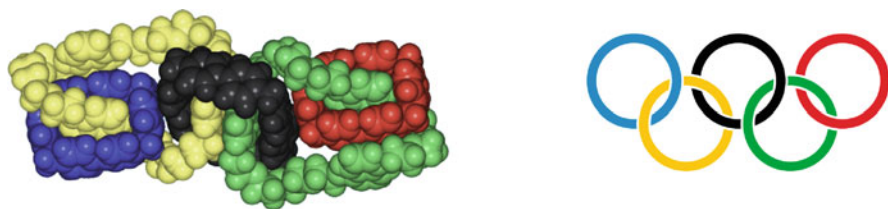


**Fig. 13** Solid-state structure of Olympiadane, [82] which shares its topology with the logo of the Olympic games

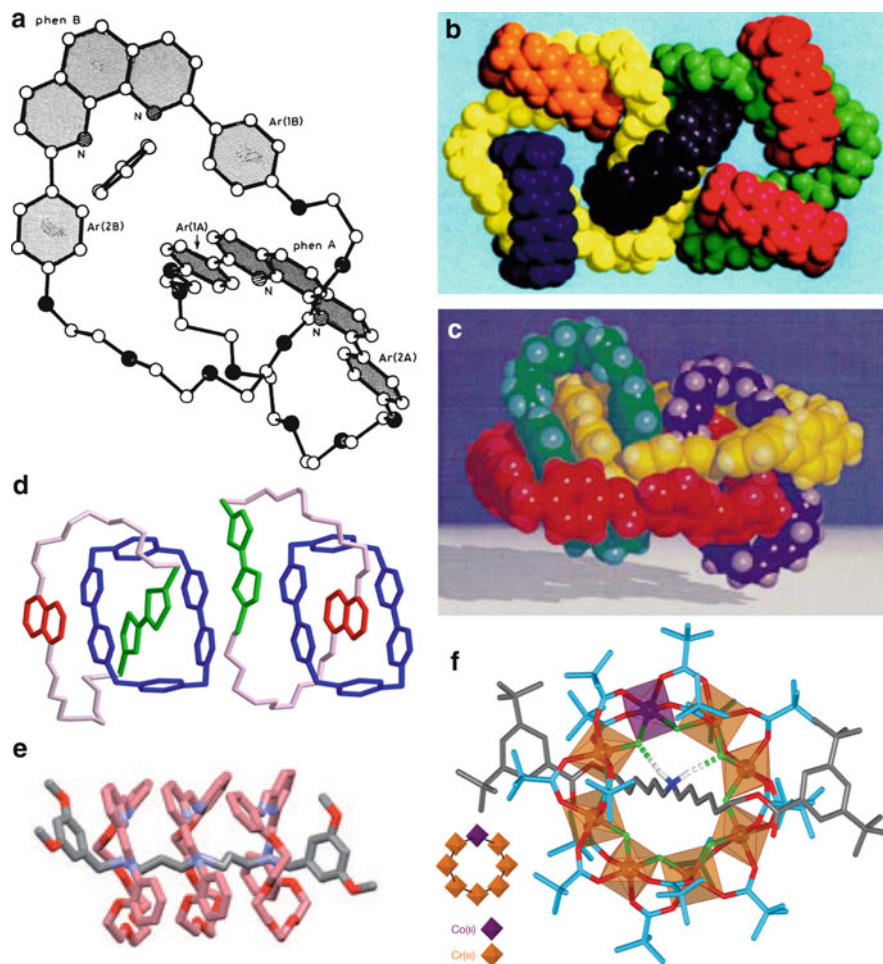


**Fig. 14** Examples of beautiful X-ray crystal structures of MIMs. (a) The first crystal structure of a MIM – Sauvage’s [2]catenane [83]. (b) A branched heptacatenane [84] has a dizzying number of interlocked macrocycles for a discrete molecule, appealing Euclidean shape, and intriguing intermolecular interactions ( $\pi$ - $\pi$ , C-H- $\pi$ , H-bonding). (c) Two identical catenanes in a supramolecular complex – a self-complexing [2]catenane [85]. (d) Two translational isomers of a bistable [2]catenane, which were simultaneously crystallized from the same solution and isolated by hand-picking from the mother liquor [86]. (e) Dynamically assembled [4]rotaxane, forced into a rigid-rod shape by  $\pi$ -stacking interactions [87]. (f) The first inorganic-organic hybrid [2]rotaxane, simple and elegant [88]. Reproduced with permission from [83] (copyright 1985 Royal Society of Chemistry), [84] (copyright 1997 Wiley-VCH), [85] (copyright 2000 Wiley-VCH), [86] (copyright 2010 National Academy of Sciences USA), [87] (copyright 2010 Wiley-VCH), [88] (copyright 2009 Nature Publishing Group)

spanning a prodigiously productive and iconoclastic academic career. This latter-day wizard of chemical crystallography unraveled the solid-state structures of hundreds of MIMs during two decades following the first report [89] of a donor-acceptor [2]catenane in 1989. In addition to the sheer abundance of his

crystallographic investigations on MIMs and their supramolecular precursors, his extraordinary attention to detail in the presentation of ball-and-stick representations of MIMs is a heroic legacy in itself. He was always at pains to ensure that few if any atoms were obscured behind others, that bonds crossed over each other as clearly as possible close to their mid-points, and that the elevation chosen illustrated the most salient aspects of the MIM's geometry. His immense talent in the design arena was matched by his complete command of the graphics programs required to give expression to his artistic genius. Williams' handiwork is featured throughout this chapter, for example in Figs. 12a,b, 13, 14b, c, and 23a, d.

It is important now to discuss a different kind of mechanically interlocked solid-state structure made possible through the development of metal–organic frameworks (MOFs) [90–93]. MOFs are infinite, robust, crystalline networks composed of organic struts coordinated to metals or metal clusters as secondary building units and have very high porosities on account of their rigid reticular architectures. The massive amount of void space in some kinds of MOFs sometimes coaxes them into forming two or more interpenetrated networks (Fig. 15a) in the same crystal, i.e., catenated frameworks [94–96]. Although researchers interested in high surface area and porosity want to avoid catenated MOFs, they are marvelous structures from the perspective of topology: these infinite catenated networks are the molecular cousins of the sculpture in Fig. 6e. Recently, MIMs have also been introduced into MOFs [97–100]. The example in Fig. 15 from the Yaghi and Stoddart groups incorporates a molecular catenane into a catenated MOF [99]. The beauty of this framework lies in the unprecedented complexity, linker size, and

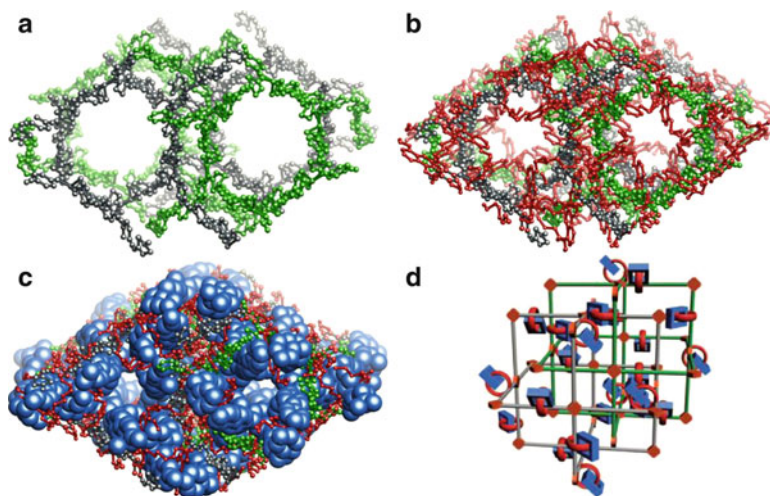


**Fig. 15** Catenated MOF with catenated linkers [99]. (a) Ball-and-stick representation of the X-ray crystal structure of the MOF with the pendent catenanes omitted in order to permit the visualization of the interpenetrated networks, colored in *green* and *gray*. (b) The same MOF with pendant crown-10 macrocycles included in *red*; only CBPQT<sup>4+</sup> is omitted. (c) Complete view of the MOF structure, in which the CBPQT<sup>4+</sup> cyclophanes are assigned space-filling representations in *blue*. (d) Simplified illustration of the catenated MOF for conceptual purposes

topology; it is hard to imagine a crystal any more jam-packed with mechanical bonds. The cartoon of the MOF in Fig. 15d testifies to the importance of the transition to cartoons.

### 3.4 The Transition to Cartoons

It will be recalled from Sect. 3.1 that first-generation MIMs were primarily represented by primitive line drawings and condensed structural formulas. Although Sauvage took a refreshing step forward into structural diagrams, there was still a need to find a compromise between the simple line drawings that convey only topology and the detailed structural diagrams that detail every atom and bond. Again Sauvage was among the first to pioneer the next evolutionary step: graphical representations, or cartoons. His 1985 report of a [3]catenand [101] included a graphically simplified reaction scheme with attractive shading (Fig. 16a). Few, if

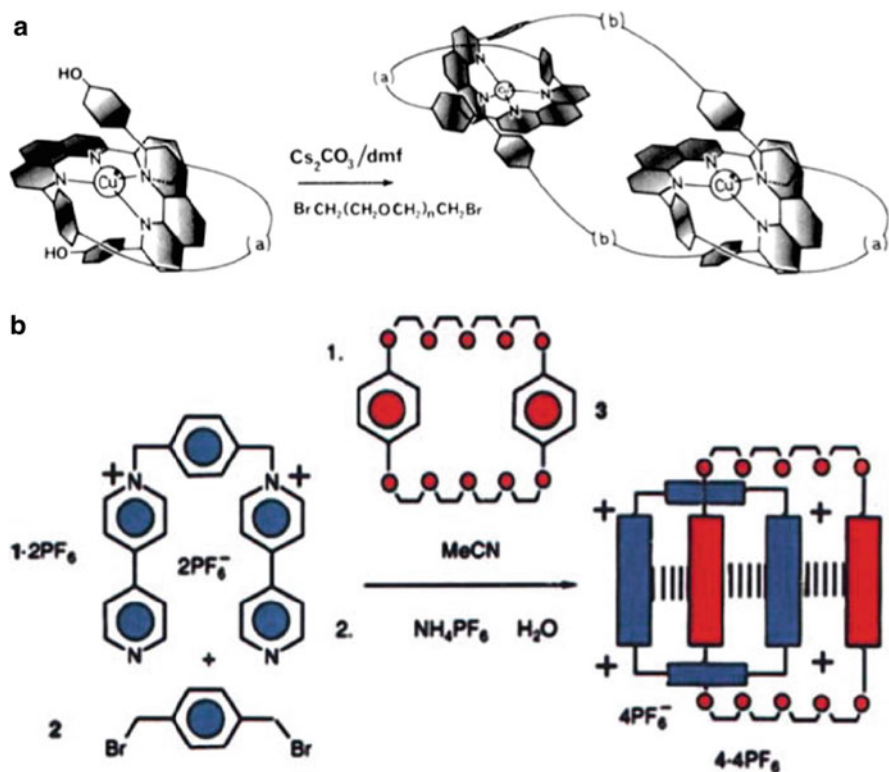


**Fig. 16** Early examples of MIM cartoons. (a) Sauvage's cartoon of a [3]catenand [101]. (b) Synthetic scheme of a donor-acceptor [2]catenane that uses illustration to emphasize topology, noncovalent bonding, and electronic properties [102]. Reproduced with permission from [101] (copyright 1985 American Chemical Society), [102] (copyright 1991 Wiley-VCH)

any, other cartoons existed in the literature until the Stoddart group entered [89] the field of MIMs in 1989 with a donor–acceptor [2]catenane [102]. The importance of our contribution was in the way we communicated information about noncovalent bonding interactions through the use of cartoons. We applied color (vide supra) and rectangles to clarify the topology of the molecule, electronic nature of the components ( $\pi$  donor or acceptor), and to emphasize the noncovalent bonds involved in the formation of the catenane (Fig. 16b).

Though we saw it as an effective means of communication, we received our share of criticism. We nevertheless stuck to our guns with cartoons (Fig. 17), and as

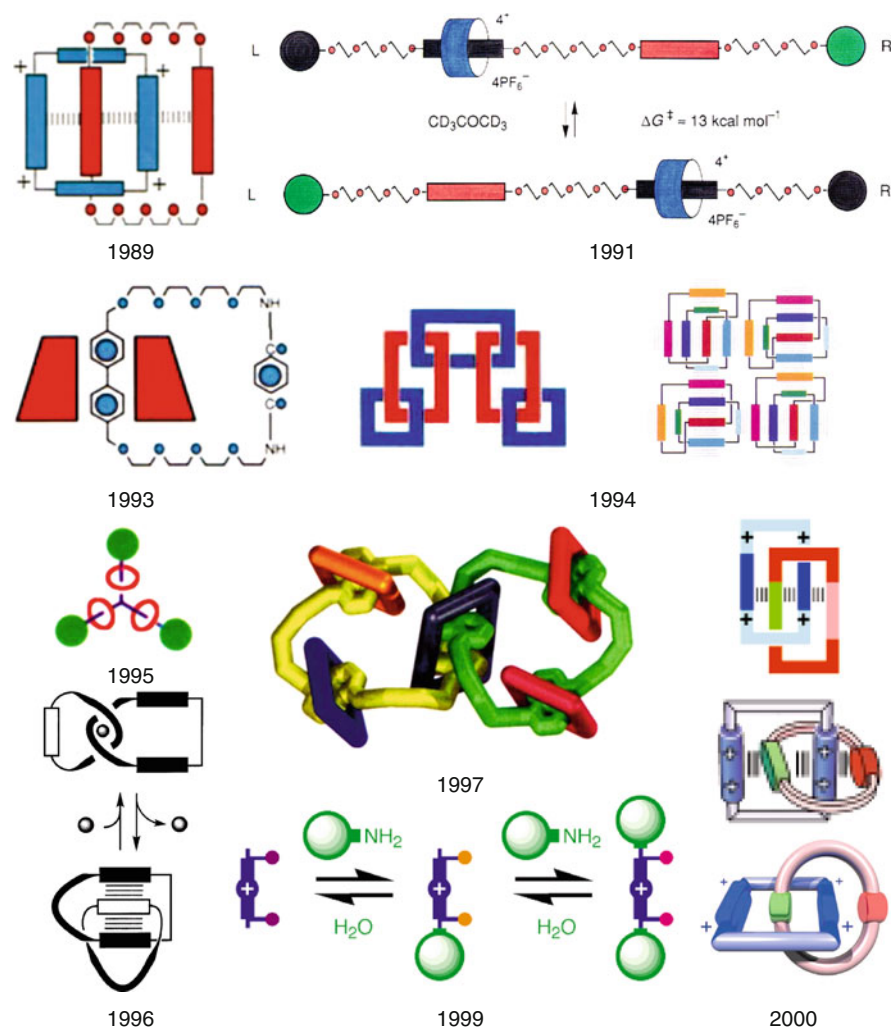
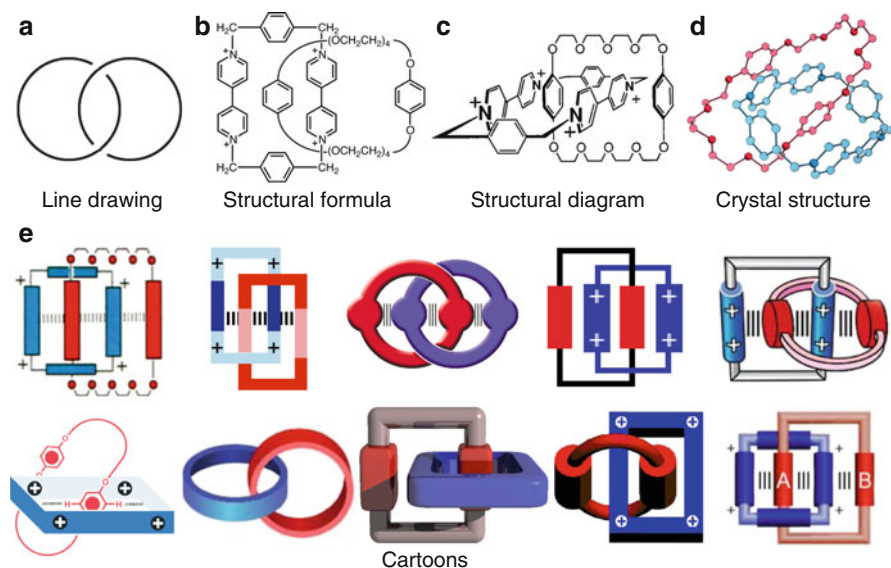


Fig. 17 Chronologically arranged assortment of MIM cartoons from the Stoddart group

the years passed by we began taking the time to make them more aesthetically appealing, paying attention to details like size, shape, shading, and intelligibility above all else. The result is that our cartoons – and graphical representations more generally – have gone through an evolutionary process of their own (represented chronologically in Fig. 17), which was more or less at the point it is today by the year 2000. Two-dimensional cartoons were displaced progressively by three-dimensional ones, which inherently aid in the visualization of molecular stereochemistry by their portrayal of perspective. Our first 3D cartoon was a branched heptacatenane (Fig. 17), which was illustrated directly below the space-filling representation of the solid-state structure (Fig. 14b) in the original paper [84] in 1997. A comparison between the two modes of depiction makes it immediately obvious why there is utility in such cartoons; they do justice to the topology as well as the Euclidean shape of the molecule!

Fig. 18 presents a summary of the different ways to represent the same catenane. It is apparent that venturing into cartoons has opened space for much more freedom and creativity in the representation of molecules (note that every type of cartoon in Fig. 18e has been published in the chemical literature). We conclude that the transition to cartoons has been a boon in the field because cartoons:

1. Highlight topology by de-emphasizing atom and bond details
2. Allow for the denotation of features that structural diagrams and formulas lack (e.g., noncovalent bonding interactions)



**Fig. 18** Different representations of the same donor–acceptor [2]catenane. Line drawings (a) and condensed structural formulas (b) were the order of the day until the modern era of MIMs gave way to structural diagrams (c) and crystal structures (d). Graphical representations, also called cartoons (e), can be a helpful compromise between these representations when attempting to emphasize the topology, noncovalent bonding interactions, shape, beauty, or function of a MIM

3. Provide a representative picture of a molecule's shape in Euclidean space
4. Declutter and beautify figures and schemes
5. Elicit creativity and inspire ideas and future research

The fifth point is related to the subject of Sect. 3.5 on how MIMs have influenced the growth of molecular nanotechnology.

### 3.5 Technomorphism

In some cartoons, a MIM can look less like a molecule and more like an ordinary object, such as a toy or LEGO set. Take the MIMs in Fig. 19 for example; these were drawn intentionally to look as though they were built from pipes, nuts, and bolts. Though they bear the same topology as the molecules they represent, they look more like the handiwork of a plumber than that of a synthetic chemist: chemically meaningless unless placed in the proper context. The objects in the figure hang in tension between the molecular world and the ordinary world, belonging ambiguously to both. The way in which these images refer at once to molecular and ordinary objects has been described by Joachim Schummer as a “gestalt switch in molecular image perception” [103]. Schummer's important thesis about “an aesthetic phenomenon that symbolically linked the world of molecules and the world of ordinary objects, and...prompted the creation of a new sign language” is embodied by images like those in Fig. 19, for which he coined the term “technomorphs.” Note that some cartoons in Fig. 18 are also technomorphs.

The technomorph representations of MIMs and supermolecules are truly valuable from both a practical and an aesthetic standpoint. Practically speaking, they played a role in inspiring chemists to think about molecules as objects and push back the frontiers of molecular nanotechnology. Because of technomorphism, suddenly a molecule that looks like a car should be driven like a car [104], those that look like cages should trap things inside [105], and so on. This mode of thinking applies immensely to MIMs, where a frenzy of creative research

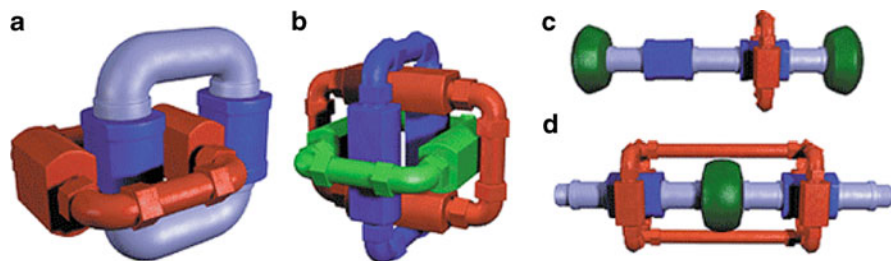


**Fig. 19** Technomorph representations of MIMs: (a) [2]catenane, (b) Borromean Rings, (c) [2]rotaxane, and (d) suit[2]ane



accompanies imaginative project titles. Over the years, we ourselves have fabricated molecular shuttles [106], switches [107], push-buttons [108], trains [109], elevators [110], pistons [111], muscles [112], abacuses [113], motors [114], and valves [115]. Other groups have reported MIMs as molecular necklaces [116–118], locks [119], rotors [120], chameleons [121], charm bracelets [122], and the list goes on and on. It is apparent that the visionary dream of nanotechnology is aided and abetted by the new symbols borne out of supramolecular chemistry [28] and mechanostereochemistry [50].

Though we allow ourselves to talk freely about the beauty of molecular structures, technomorphs are among the few products of chemistry that can currently withstand a formal aesthetic philosophy. Schummer, a philosopher of science, has undertaken a systematic investigation [9] of chemical representations in the context of idealistic aesthetics (Plato, Kant) [123], aesthetics of symbols (Goodman) [124], and Eco's semiotic theory [125], concluding in the negative on all but Eco's theory. In brief, Umberto Eco's modern theory would recognize that technomorph symbols are rich in aesthetic content because they (1) can be interpreted ambiguously, (2) challenge the interpreter to develop new interpretations, and (3) redirect the interpreter's attention to the symbol itself. In other words, an individual's reflection on and interpretation of a technomorph image is a bona fide aesthetic experience.

It is good news that cartoons, particularly the subset referred to as technomorphs, have been accepted by the chemical community as a new symbolic language. The result has been the formation of a symbolic link between molecular and ordinary objects, images that appeal to a broader audience (no background in chemistry necessary!), and a new, powerful driving force for ongoing research.

## 4 The Beauty of MIMs

The various ways to represent MIMs on paper have often been a portrayal of beauty in their own right. In Sect. 3, we tried to engage the beauty of printed molecular representations. There remain many other ways to perceive the beauty of molecular objects, some of them particularly unique to MIMs, but things get messier when we depart from concrete illustrations and images and venture into even more subjective territory. Roald Hoffman, pioneer of molecular aesthetics, has approached beauty in chemistry from the perspective that "beauty is built out of individual pleasure around an object or idea" [126]. The aesthetic experience of molecular structures is therefore inexorably tied together with our subjective biases. Synthetically derived molecules are retroactively beautified out of a psychological need to associate pleasure with hard work. We find reasons to label a molecule beautiful and experiments elegant, because we invested work, time, and failure to achieve them. Nevertheless, these notions of beauty are common to the experiences of

most, if not all, chemists, and are therefore very relevant to a more complete understanding of the discipline of chemistry. The words of Nobel Laureate Charles Pedersen, whose revolutionary discovery of crown ethers eventually opened the field of host–guest chemistry [127], supramolecular chemistry [28], and mechanostereochemistry [50], are a case in point: “One of my first actions was motivated by esthetics more than science. I derived great esthetic pleasure from the three-dimensional structure of [the first crown ether]” [128].

Pedersen’s account demonstrates that molecular beauty is not just an interesting topic for discussion; it can have a profound impact on scientific research. Here we discuss aspects of beauty in MIMs that can be independent of their printed representations. In other words, this section is about where chemists find pleasure in their research into MIMs.

## 4.1 *Topological Beauty*

We must take a moment to clarify the difference between topography and topology. The aspects of a molecule relating to its geometry (tetrahedral, square planar, etc.), symmetry, size, and shape, are characterized by its topography. By contrast, the topology of a molecule (see Sect. 3.1) relates to properties that remain invariant throughout allowed distortions of a molecule’s topographical features (stretching, bending, and compressing bonds without breaking them). It is well accepted that the beauty of a molecular structure is often associated with its shape in Euclidean geometry (topography), but here we recognize that beauty can be associated with topology as well.

David Walba was among the first to discuss topological beauty in the primary literature, noting that “topological stereochemistry is a unique field, esthetically and intellectually pleasing in the extreme” [54]. Two years later, Jean-Pierre Sauvage’s first major review of MIMs paid particular attention to the aesthetic value of catenanes and catenands. He proposed that “the beauty of some molecules might be independent of shape and rest only in [their] topological properties” [129]. A recent review by Amabilino and Pérez-García [130] constitutes a delightful look at topological molecules, very much in the vein of this volume, in the context of how chemists represent them. We humbly refer the reader to these references and to an article by Sauvage [131] for a more complete discussion on topology and beauty.

It is appropriate in this section to recognize contributions from DNA nanotechnology [132–134]. In 1997, Seeman and coworkers ingeniously constructed [135] single-stranded DNA Borromean Rings (Fig. 20a). DNA catenanes (Fig. 20b) and knots have also been prepared [136, 138–140]. Recently, a Möbius strip approach (see Sect. 3.1, Fig. 9) to catenane synthesis was elegantly realized [137] at long last using the rapidly expanding DNA “origami” technique [141] (Fig. 20c–h). DNA is certainly an exciting frontier for those scientists interested in topology.

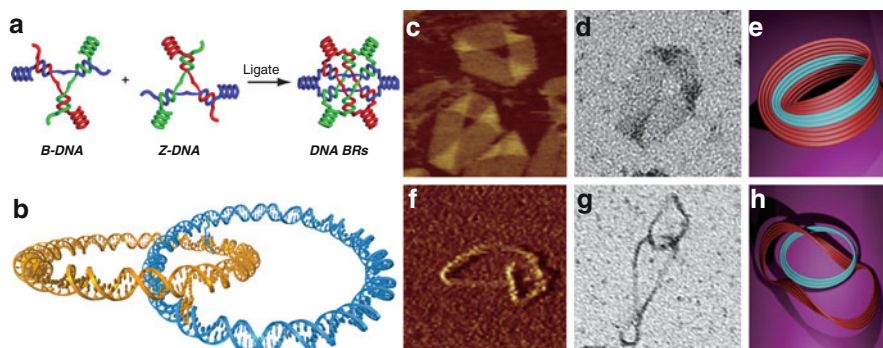


**Fig. 20** DNA nanotechnology ushers in beautiful DNA topologies. (a) Synthesis of DNA Borromean Rings [135] from complimentary three-stranded junctions. (b) Double-helix [2] catenane [136]. (c–h) Images of DNA Möbius strips (c AFM, d TEM, e graphical), and their corresponding [2]catenanes (f AFM, g TEM, h graphical) [137]. Reproduced with permission from [44] (copyright 2005 American Chemical Society), [136] (copyright 2011 American Chemical Society), [137] (copyright 2010 Nature Publishing Group)

In mathematics, links can be characterized by an extension of knot theory using Alexander–Briggs notation, where each link is represented by the number of crossings in its two-dimensional projection, with a superscript denoting the number of interlocked rings and a subscript denoting its (arbitrary) order among links with the same crossing number [142]. Fig. 21 shows the 18 prime links (composite links are a combination of one or more prime links) with less than eight crossings, demonstrating that chemical topology is still a largely unexplored and exciting challenge; only  $2_1^2$ ,  $4_1^2$ , and  $6_3^3$  have been reproduced as synthetic molecules to date. Other novel topologies (effectively composite links) and architectures have also been prepared, and will be addressed in Sect. 4.2.

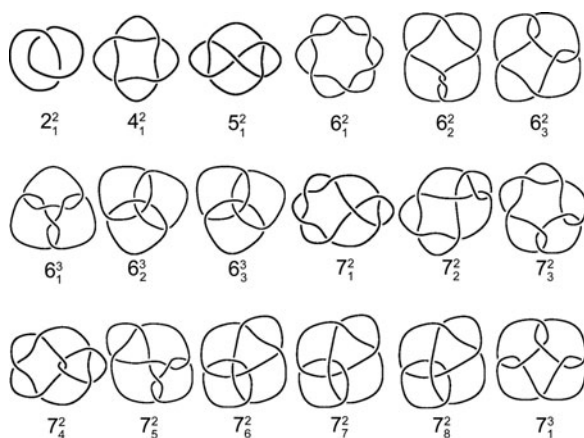


**Fig. 21** Projections of the 18 prime links with less than eight crossings

## 4.2 Architectural Beauty

A synthetic chemist has the opportunity to share the same thrill as architects and artisans, i.e., the pleasure of designing and building something new. We use the term “architecture” to describe mechanically interlocked structures as we widen our scope from mathematical topology to include topologically trivial species such as rotaxanes. The field of MIMs is full of opportunities to create new and exotic architectures like those shown in Figs. 22 & 23. In Fig. 22 we acknowledge a handful of MIMs whose architectures were unprecedented at the time of publication. Fig. 22a is a “pretzelane,” a [2]catenane in which the two macrocycles are covalently connected. The Vögtle group was the first to prepare a pretzelane [143, 149] and has also applied a similar concept to rotaxanes: a [1]rotaxane [150] results when the ring of a [2]rotaxane is connected to its dumbbell; a “molecular 8” [151]

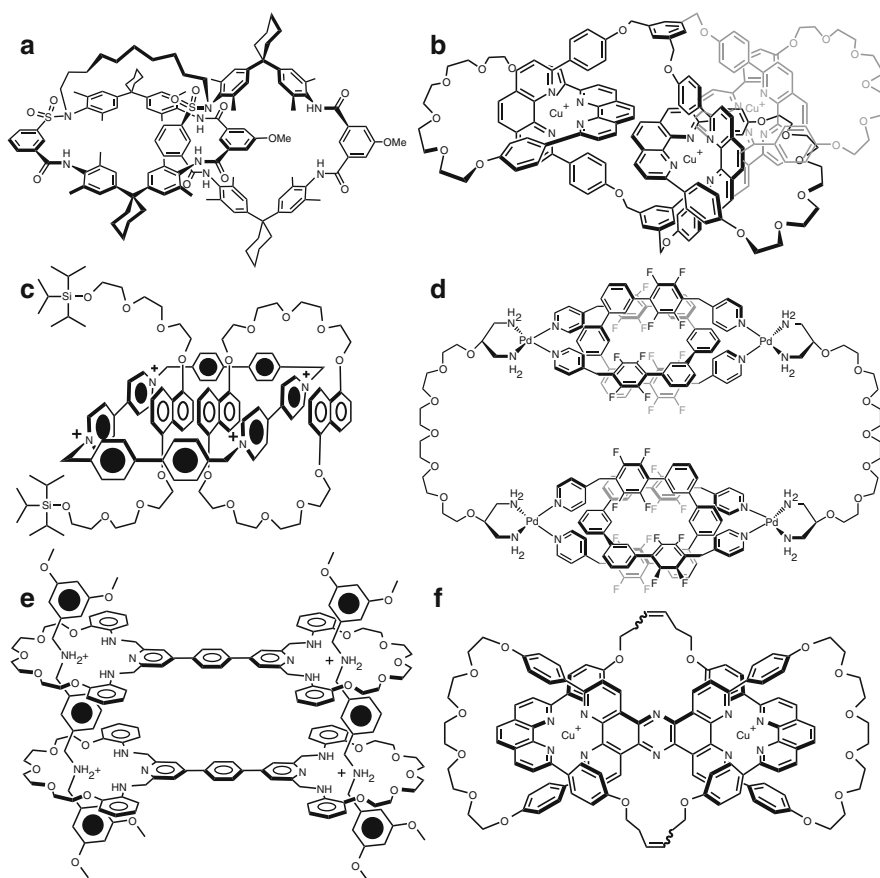


**Fig. 22** Novel MIM architectures: (a) pretzelane [143], (b) macrobicyclic [4]catenane [144], (c) rotacatenane [145], (d) cyclic [2]catenane dimer [146], (e) cyclic [4]rotaxane [147], and (f) doubly threaded [2]catenane [148]

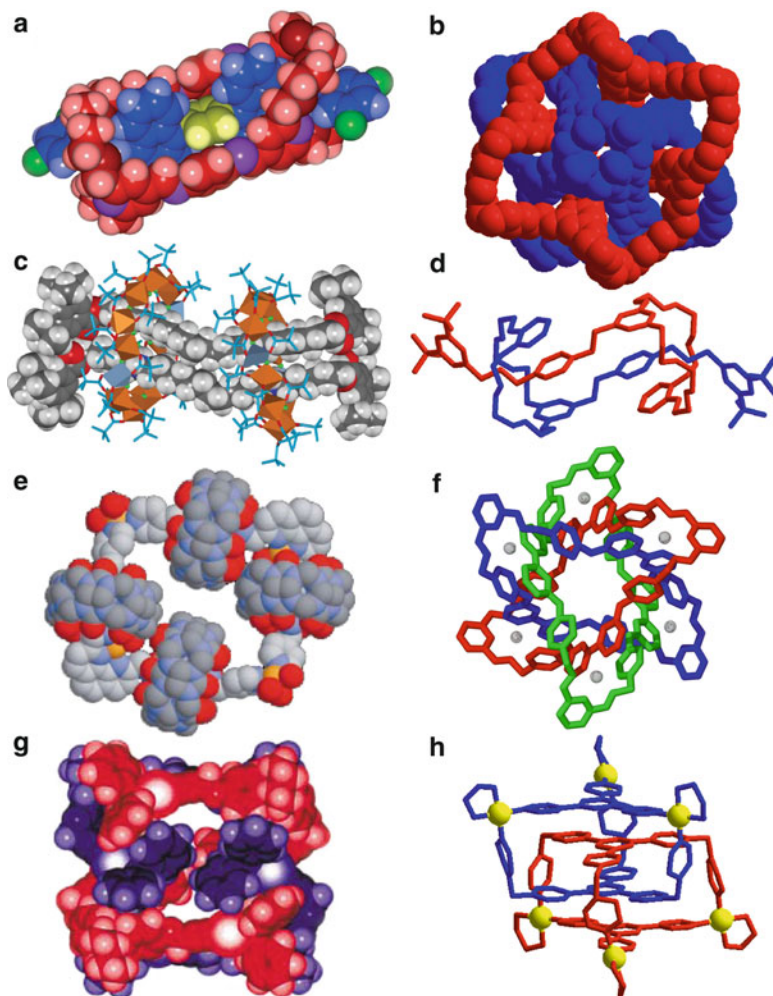


**Fig. 23** Solid-state structures of some beautifully novel MIM architectures: (a) suit[2]ane [33], (b) eightfold interlocked multicatenane [154], (c) hybrid organic–inorganic [4]rotaxane [88], (d) [c2]daisy chain [155], where [c2] denotes that the molecule is cyclic and has two components, (e) [5]catenane “molecular necklace” [116], (f) molecular Borromean Rings [156], (g) molecular Solomon Link [157], and (h) interlocked coordination cages [158]. (a), (c), (e), and (g) reproduced with permission from [33] (copyright 2006 Wiley-VCH), [88] (copyright 2009 Nature Publishing Group), [116] (copyright 1999 Wiley-VCH), [157] (copyright 2000 Wiley-VCH)

arises from doubly connecting the ring on both sides; and a “bonnane” [152] is the product of connecting two or more rotaxane rings together. A joint effort from the Vögtle and Sauvage groups [144] led to the beautifully symmetrical [4]catenane in Fig. 22b with a macrobicyclic core. Fig. 22c is a rotacatenane (rotaxane/catenane combination) [145] from our own group. A cyclic [2]catenane dimer (Fig. 22d) from the Fujita group [146] and a cyclic [4]rotaxane (Fig. 22e) from our group [147]

are macrocycles formed via the mechanical bond. The Sauvage group has recently published a beautiful crystal structure of a cyclic [4]rotaxane [153]. The appealing structure in Fig. 22f by Sauvage is a doubly threaded catenane [148], with one ring passing through two covalently linked “handcuff” macrocycles.

Fig. 23 is a collection of crystal structures of some exceptionally novel architectures, all of them uniquely interlocked. A suitane (Fig. 23a) is so-named because a molecular “suit” mechanically envelops a multilimbed body (a suit[ $n$ ]ane has  $n$  “limbs”) [33, 159]. Böhmer’s multicatene [154] in Fig. 23b consists of interwoven annulated rings with a remarkable eight interlockings among only two components. The Leigh group used novel building materials (inorganic macrocycles) to construct [88] their architecturally new [4]rotaxane in which two rings each encircle two threads (Fig. 23c). The cyclic, double-threaded [2]rotaxane dimer (“daisy chain”) in Fig. 23d is yet another mechanically bonded macrocycle [155, 160, 161]. Bistable daisy chains [162–164] are interesting for their capacity to dramatically change length in response to external stimuli. Trimeric daisy chains have also been reported [165]. Kimoon Kim’s group appropriately calls the large macrocycle with four curcubituril “beads” (a [5]catenane) in Fig. 23e a molecular necklace [116]. The molecular Borromean Rings (Fig. 23f) are a tour de force in self-assembly and chemical topology [156]. Their synthesis is discussed in Sect. 4.3. The Puddephat group obtained a crystal structure [157] for the doubly interlocked [2]catenane known as a Solomon Knot (Fig. 23g), a topology pioneered [166] by Sauvage in 1994. Finally, the multiply interlocked bicyclic coordination cages of Fujita [158] are presented in Fig. 23h.

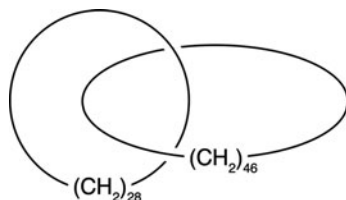
For all of the pleasure, i.e., beauty – derived from creating new interlocked architectures, we have only scratched at the surface of what is possible. Many of the molecules shown in this section were already framed in the context of beauty (Borromean Rings and Solomon Knots), and we expect that aesthetic considerations will continue to motivate new architectural developments.

### 4.3 *Simplicity and Elegance*

Simplicity is probably the least controversial trait that a molecule needs to be beautified in the minds of chemists, who have always been drawn to Platonic notions of beauty. And who could blame chemists for this line of thinking? Simplicity is tied to the pleasing virtues of balance, symmetry, wholeness, and harmony. It is also tied to coherence and comprehension, which is tied to truth, which is tied to beauty. When a chemist examines a simple molecule, a network of these related concepts inevitably leaves him or her with a sense of pleasure and satisfaction.

There is no lack of beautifully simple MIMs. The quintessential example is Schill’s all-hydrocarbon [2]catenane [167], the simplest non-trivial topology composed of the simplest atoms and bonds (Fig. 24). Other MIMs are simplified by highly symmetrical structures that make them “easy on the brain”, such as the

**Fig. 24** Schill's all-hydrocarbon [2]catenane [167]



examples from Sect. 4.2 in Figs. 22b,e-f, 23a,b,e,f, to cite but a few. Though these molecules look relatively simple, it is clear that an IUPAC name – if it could be generated – would be far from simple, a testament to the growing importance of images and their clarity, beauty, and so on.

Though we are, no doubt, aesthetically drawn to simple molecules – recall the Platonic solids from our introduction – experiments are where the beauty of simplicity truly shines. In this context, we often refer to simplicity as elegance. Instead of unraveling a further list of simple MIMs, we wish to highlight elegance in MIM experiments. We will break down elegance in the synthesis of MIMs into four broad categories and provide important references and representative examples in each case. This is our only section on experimental beauty and the list is by no means exhaustive, but we hope it is at least a stimulating exercise for the reader.

### 4.3.1 Template Synthesis

Sauvage revived an all but forsaken discipline by introducing templates for synthesizing MIMs. His solution (Fig. 25) of using transition metals to position organic precursors appropriately to interlock them in subsequent reactions, which

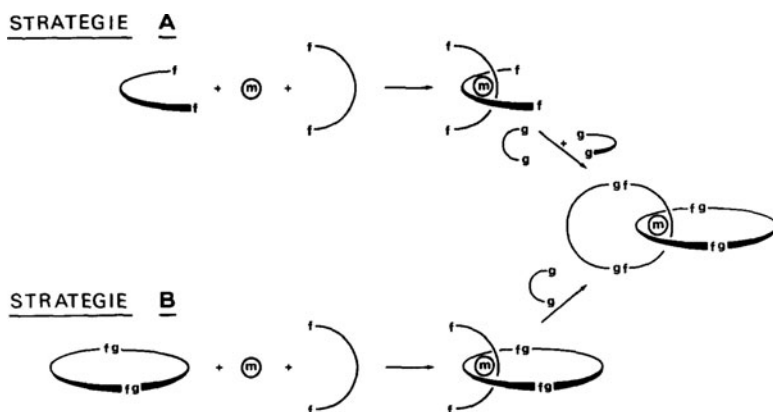


**Fig. 25** Sauvage's conceptual drawing explaining the first template-directed synthetic strategies for synthesizing MIMs. A tetrahedral center orients U-shaped species appropriately for subsequent ring-closure, resulting in a catenane. Reprinted with permission from [72] (copyright 1983 Elsevier)

dramatically reduces the number of steps and increases the yield by orders of magnitude compared with previous MIMs, was supremely elegant. Fig. 25 is his shorthand drawing of the original template strategies for catenane synthesis [72].

Many new elegant templating methods have been invented since Sauvage's revolutionary breakthrough with transition metals. They include donor–acceptor interactions and  $\pi$ – $\pi$  stacking of charged [89, 168] and neutral [169] species, hydrophobic effects [117, 170–172], hydrogen bonding [78, 173–175], salt bridges [176], ion pairing [177, 178], anion binding [179, 180], and radical pairs [181]. There is a 2005 *Topics in Current Chemistry* volume on templates in organic chemistry that includes a review of template-directed protocols in MIM synthesis [182].

### 4.3.2 Active Template Synthesis

A step beyond the template is the “active template,” introduced in 2006 independently by the groups of Saito [183] and Leigh [184]. An active template is a metal center, which acts simultaneously as a template and as a catalyst. It relies on the use of a macrocycle capable of immobilizing a metal ion within its cavity such that it catalyzes a covalent ring-closing reaction (for catenanes) or coupling (for rotaxanes) endotopically, resulting in a mechanical bond. A cartoon depicting the concept of an active metal template is shown in Fig. 26. The elegant dual-role of the template means that the metal can be used in substoichiometric amounts without compromising yield, and permanent coordination sites need not be built into every component of the corresponding MIM. Though they are relatively new to the scene, active templates have already been employed [185] in the synthesis of

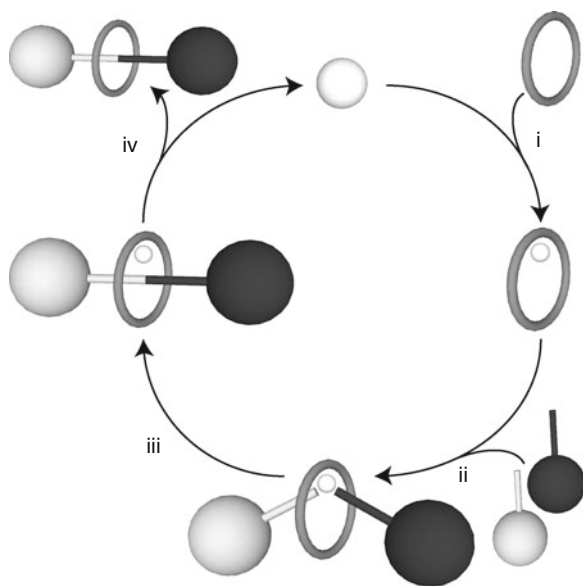


**Fig. 26** Active template synthesis [185]: (i) metal catalyst is bound in the cavity of a macrocycle, (ii) reagents (half-dumbbells in this example) coordinate the metal within the macrocycle, (iii) a covalent bond is catalytically formed, resulting also in a mechanical bond, and (iv) catalyst is regenerated and the MIM is expelled



rotaxanes, catenanes, and shuttles, and have made use of copper-catalyzed Huisgen terminal azide-alkyne 1,3-cyclo additions [184] (“click” chemistry [186]), Glaser terminal alkyne homo-couplings [183, 187], Ullmann-type C–S couplings [183], Cadiot–Chodkiewicz alkyne heterocouplings [188], as well as Pd-mediated alkyne homocouplings [189], oxidative Heck cross-couplings [190], and Michael additions [191], (reaching yields >99% in the final case) marking this method as having versatility in addition to elegance.

### 4.3.3 Thermodynamic Control

By moving from kinetically controlled to thermodynamically controlled reactions (Fig. 27), MIMs can now be synthesized in near-quantitative yields, primarily

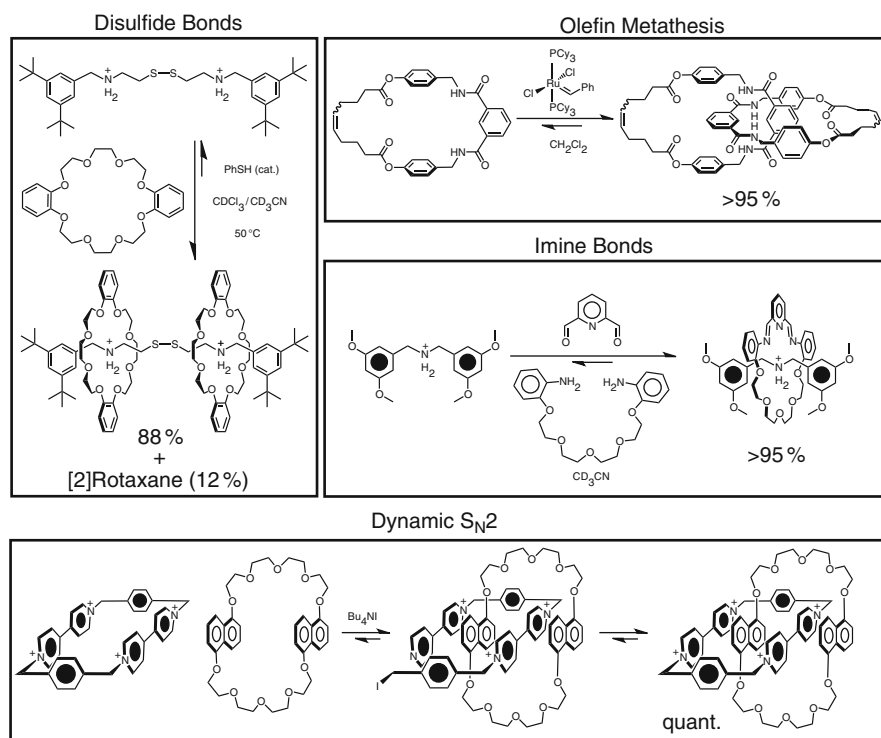
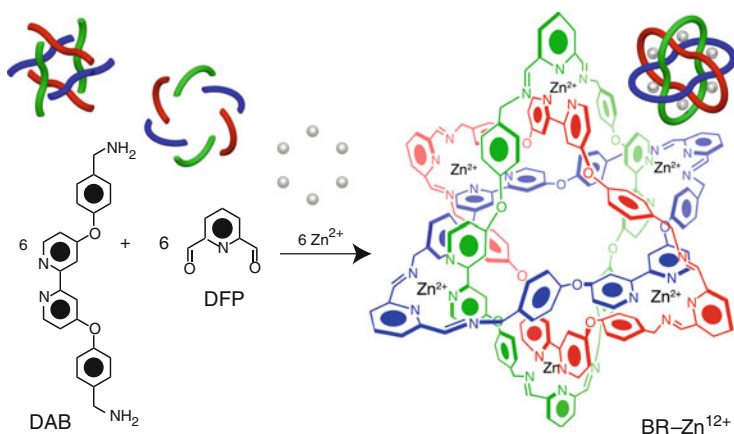


**Fig. 27** Examples of thermodynamically controlled reactions employed in the near-quantitative synthesis of MIMs. (a) Disulfide-exchange reaction permits equilibration between a bis(ammonium) disulfide dumbbell and a crown ether macrocycle to yield a mixture of [2]- and [3]rotaxanes quantitatively [194]. (b) Olefin metathesis at high concentration on a benzylic amide macrocycle greatly favors the catenated species [196]. (c) Self-correcting imine bonds allow for nearly quantitative selection of a [2]rotaxane from an appropriate dynamic combinatorial library [76]. (d) A weak nucleophile ( $I^-$ ) equilibrates the components of a donor–acceptor [2]catenane in a dynamic  $S_N2$  reaction [205]

through the use of dynamic covalent chemistry (DCC) [192]. DCC employs dynamic, reversible (self-correcting) covalent bonds to allow a chemical reaction to reach its energetic minimum. In the synthesis of MIMs, thiol-disulfide exchange [193–195], olefin metathesis [196–200], imine bonds [76, 201–204], and even dynamic  $S_N2$  reactions [205–207] have been used to put template-directed reactions into a thermodynamic regime. Likewise, the Fujita group has pioneered the use of labile coordinative bonds to achieve thermodynamic control in MIM synthesis [208]. Fig. 27 highlights some of these beautiful thermodynamically driven, near-quantitative MIM syntheses. Elegant, one-step quantitative syntheses of simple MIMs are now becoming fairly routine, though we should note that kinetically controlled MIM reactions are also sometimes very high-yielding as well [209].

The Borromean Rings (Fig. 4) are among the most elegant of relevant examples; this previously elusive topology, which had been sought after in a stepwise fashion for over a decade [210], was finally achieved [156] in one step by employing the use of reversible imine bonds among six *exo* bidentate diaminobipyridine (DAB) ligands and six *endo* diformylpyridine (DFP) ligands, in combination with the templating effect of six zinc ions (Scheme 1).



**Scheme 1** The elegant 18-component self-assembly of molecular Borromean rings under thermodynamic control [156], which utilizes reversible imine bonds to incite self-correction of the iconic interlocked structure at equilibrium

#### 4.3.4 Post-Synthesis Modification

An elegant solution to building new mechanically interlocked architectures has been to make them amenable to further modification after their synthesis. This category is particularly broad, as it encompasses all manner of reactions that have been performed on MIMs, including their organization in scaffolds (e.g., MOFs, see Fig. 15, Sect. 3.3) and interfaces, polymerization [211, 212], and other

transformations to connect their components to each other or to other MIMs and molecules, such as Vögtle's pretzelanes, [1]rotaxanes, and bonnananes (see Sect. 3.2), knotaxanes [213], as well as our stepwise route [214] to rotacatenanes (Fig. 22c). Even more than being a road to new architectures, the boon of post-synthetic flexibility has been in the arena of molecular switches and machines, which we discuss in Sect. 4.5. In short, a simple functional group on a MIM can be an elegant way to integrate it.

#### 4.4 *Complexity and Emergence*

In contrast to the pleasure of comprehension, harmony, and tidiness that goes with the connected topics of simplicity and elegance, is the pleasure of surprise and learning that accompanies the related concepts of complexity [215] and emergence [216]. In complexity, those pleasures that ignite at the sight of a simple molecule are silenced and replaced by laborious efforts to grasp and discern, or perhaps plain confusion. Beauty must be sought in tension and challenge rather than in simplicity and harmony. Emergence, however, is immediately pleasing when we recognize it: that "Eureka!" moment, the realization that the whole is greater than the sum of its parts, that the output could not have been predicted by inspection of the input. Emergence arises out of complexity; it is the diamond at the bottom of a dark mine.

We are in danger of conflating "complex" with "complicated". While there is undoubtedly beauty to be found in both, in science they have different meanings. Complexity is related to chaos – dynamic, non-equilibrium, nearly unpredictable phenomena. Chaos theory was borne out of meteorology and mathematics and is conceptually (and hypothetically) demonstrated by the famous "butterfly effect," where the simple flap of a butterfly's wings can be enough to trigger catastrophic weather thousands of miles away. Complexity and chaos is a growing and highly multidisciplinary field of research. By contrast, "complicated" only refers to things that are, well... complicated – having many parts or intricacies, perhaps.

Again we find ourselves in muddy waters, where we must admit that there is a prominent subjective air to this business of complexity and emergence. What is complex to one person might seem only complicated to another, wiser person. What is emergent now will not be emergent in 100 years when it is more deeply understood. Whitesides [215] has noted of complexity that even the simplest organic reactions are complex when considered rigorously; reactants have an enormous variety of conformations and interactions with solvent molecules, ions, other reactants, and so on. Hence, chemistry is an empirical science; we understand these truly complex reactions by correlating structure and reactivity in the light of loads of data. In that sense, emergence might be an area of chemistry where our data is too incomplete to give us a reliable understanding of structure–response relationships. With that disclaimer, we share a few examples that we find of emergence in MIMs.

A promising arena for observing emergent phenomena is dynamic combinatorial chemistry (DCC) [192]. It can take days or weeks for a dynamic combinatorial library (DCL) to reach equilibrium and pass through an array of complex and emergent structures. Even at equilibrium, DCLs can easily be complicated, even complex or emergent when they are highly sensitive to initial conditions. Sanders and coworkers demonstrated this idea beautifully in 2005, when they reported [202] a DCL composed of a peptide (*p*PFm) that equilibrated over 3 days into a variety of cyclic oligomers, but formed a more elaborate [2]catenane composed of two trimeric 42-membered rings as the dominant species upon the presence an acetylcholine additive (Fig. 28). Another emergent interlocked structure obtained by DCC was the Solomon Knot reported by us [217] in 2007. The same DAB and DFP ligands that were used to create Borromean Rings (see Scheme 1, Sect. 4.3) unexpectedly yielded a doubly interlocked [2]catenane (Fig. 29) when a mixture of  $Zn^{2+}$  and  $Cu^{2+}$  ions was added, even though homogenous  $Zn^{2+}$  or  $Cu^{2+}$  templates lead only to Borromean Rings. It is believed that these structures are kinetic products from the DCL, with solvent, counterions, and templates all playing a sensitive role in the (not yet well-understood) kinetically controlled crystallization.

It was discovered recently that a polymer could demonstrate emergent phenomena when catenated under thermodynamic control. The previously developed [205]

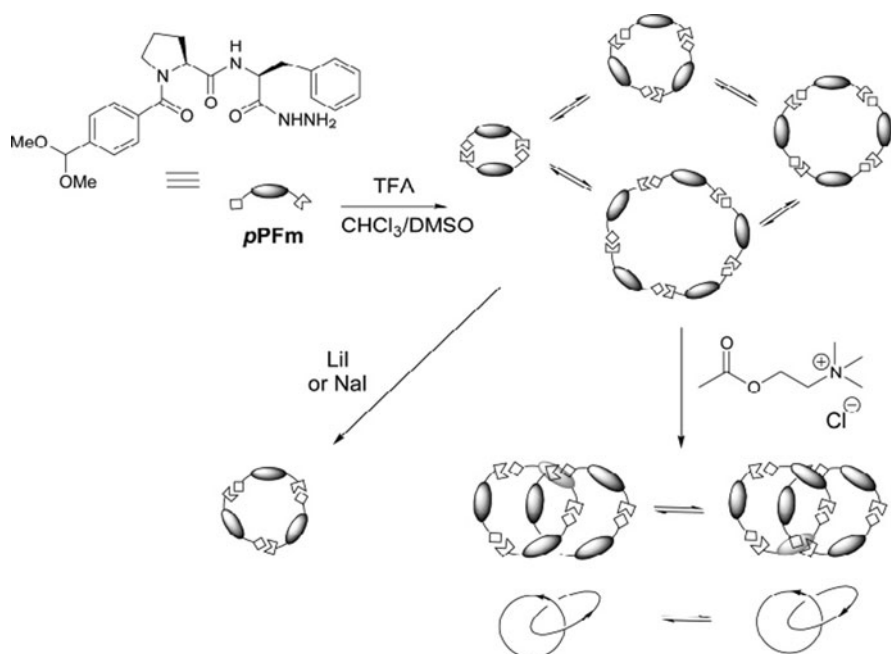
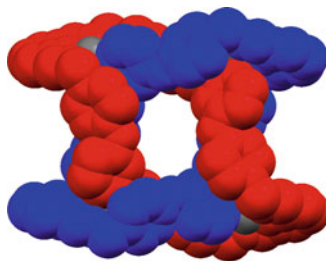


**Fig. 28** Sanders' *p*PFm dynamic combinatorial library, leading to an exquisite [2]catenane in the presence of an acetylcholine template [202]. Reproduced with permission from [192] (copyright 2006 American Chemical Society)

**Fig. 29** Solid-state structure of the doubly interlocked [2] catenane (Solomon Knot) that emerges unexpectedly from a DCL containing DAB, DFP, and a 1:1 mixture of  $Zn^{2+}$  and  $Cu^{2+}$  templates [217]



iodide-catalyzed self-assembly of donor–acceptor [2]catenanes (Fig. 27d) was applied to a polymerizable “blue box” monomer in 84% yield. When dimerized, the catenation proceeded in an unsurprising 49% yield. However, when the catenation was performed on the polymerized species, the reaction unexpectedly went to >99% completion (Fig. 30). This result [207] was subsequently rationalized by postulating a cooperative, synergistic templating effect by nearby cyclophanes on the backbone of the polymer that would not be present in the monomeric and dimeric compounds.

Though there are plenty of gray areas on the subject of complexity and emergence, spectacular examples in the field of MIMs are still rare, but the chemistry of complexity is sure to become a growing, exciting, and pleasing new direction that chemists will inevitably take.

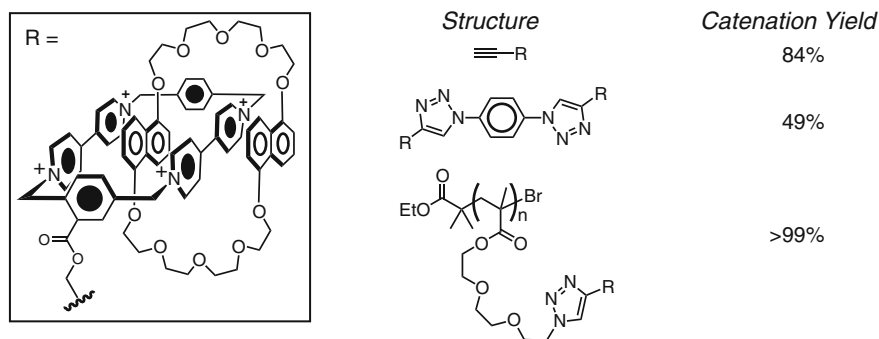


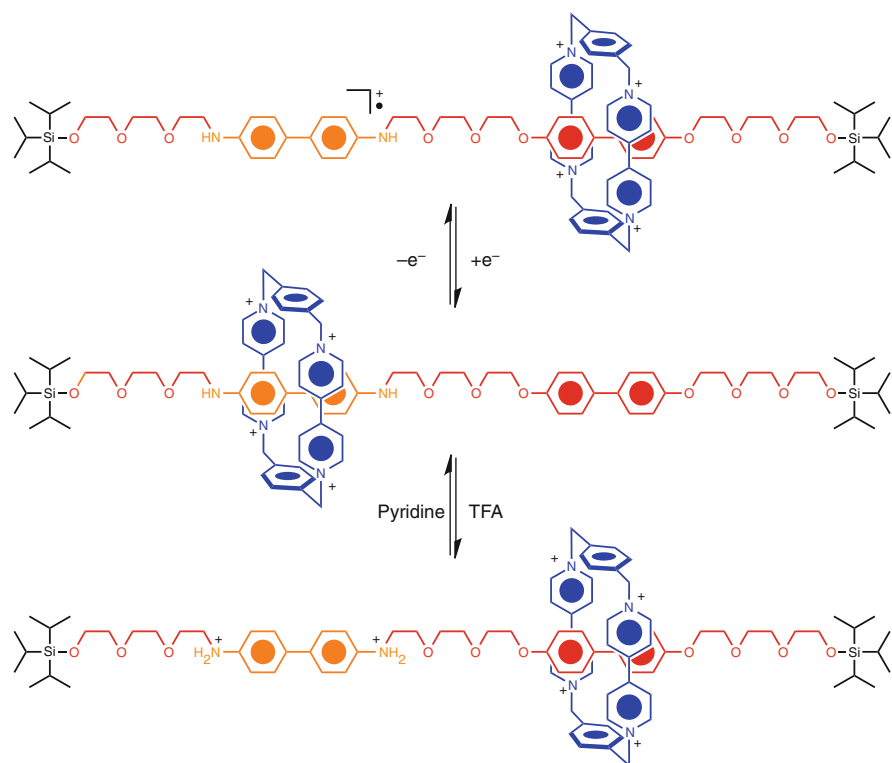
**Fig. 30** Polymeric “blue box” cyclophane displays the emergent property of quantitative thermodynamic catenation by iodide-catalyzed self-assembly with an appropriate crown ether macrocycle. The analogous monomeric and dimeric species do not react quantitatively [207]

#### 4.5 Beautiful Mechanically Interlocked Molecular Machines and Switches

We live in an era that beautifies machines, from automobiles to computers. Arguably the most compelling aspect of MIMs – at least those templated by noncovalent bonding interactions – is their susceptibility to controlled mechanical motion of

their components, manipulated by external stimuli that affect noncovalent bonds. The intramolecular motion of one component in a MIM relative to another gives way to different co-conformational states, which have different stabilities, as well as spectroscopic and physical properties. Controllable bistable (and tristable, etc.) MIMs are often referred to as “motor molecules” or “molecular machines” as a consequence of these unique capabilities, though it would be more accurate to call most of them switches. The macrocycle of a catenane or rotaxane can be moved (“switched”) from one site to another relative to its counterpart under the influence of a wide variety of stimuli, the most common of which are light, chemical or electrochemical redox chemistry, and pH changes (See [218]).

The earliest examples of mechanically bonded molecular switches were two-station rotaxanes and catenanes (a “station” is a recognition site for the macrocyclic component) that could be switched by these common stimuli. Our group reported a bistable rotaxane in 1994 that could be switched chemically and electrochemically, utilizing a  $\pi$ - $\pi$  donor/acceptor recognition motif (see Scheme 2 and explanation in corresponding caption) [107]. Many of the recognition motifs in MIMs that



**Scheme 2** Switchable molecular shuttle. At equilibrium, the cyclophane preferentially encircles the benzidine unit (84%), but can be shuttled to the biphenol unit by oxidation (*top*) or protonation (*bottom*) of benzidine [107]

we have already discussed can also be switched under the appropriate conditions, including Sauvage's transition metal-based MIMs and Leigh's benzylic amide MIMs. Reviews on the subject of mechanically interlocked molecular machines are abundant in the literature [218–222].

We are unlikely to appreciate a car that does not run or a computer that does not compute. Likewise, molecular switches that bump and tumble randomly in solution cannot yield a functional effect; they must be organized in bulk or at interfaces to produce a coherent and cooperative effect of technological relevance [223–225]. Only then might it be possible to dub them machines in the true sense of the word. Thus, the most beautiful molecular machines are those [222] that we put to work for us. Here we provide several examples.

Would not it be amazing if the tiny nanomotions of molecular machines could be cooperatively scaled up to do work on macroscopic objects? Toward that end, it has been demonstrated [226, 227] that a monolayer of “molecular muscles” – palindromic bistable [3]rotaxanes (Fig. 31a) immobilized on the surface of a thin

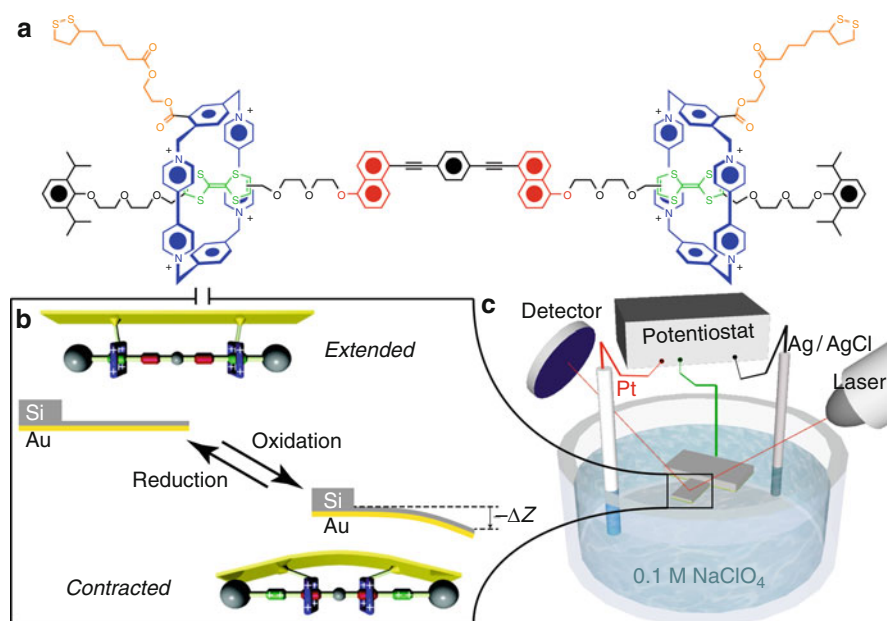


**Fig. 31** Mechanical actuation of a gold-coated microcantilever by “molecular muscles” [227]. (a) Structural formula of a palindromic, bistable [3]rotaxane with gold-binding dithiolane groups attached to the cyclophanes. (b) Reversible bending up and down of a cantilever by actuation of a monolayer (~8 billion molecules) of the rotaxanes on its surface. The gold surface bends when the rotaxanes “contract” under the influence of an electrochemical oxidation that causes the cyclophanes to shuttle inward from the periphery of the molecule. (c) Electrochemical cell (Ag/AgCl, Pt, and the cantilever are the reference, counter, and working electrodes, respectively) and combined AFM device used to measure the bending by detecting a laser beam reflected off of the cantilever’s surface

gold-coated microcantilever – could be actuated in concert to bend the cantilever up and down, which was detected with a laser beam (Fig. 31). Although it was below the macroscopic scale, the experiment was a powerful demonstration that energy can be transduced and work can be done by molecular switches on their immediate environment, converting chemical or electrochemical energy to mechanical energy. Leigh and coworkers [228] devised an ingenious experiment in 2005 that also utilized molecular switches, this time to transport a macroscopic object on a surface. Bistable rotaxanes were physisorbed onto a surface and irradiated with UV light, which photoisomerized an olefin in some rotaxanes and caused the macrocyclic component to shuttle over a fluorinated recognition site, which in turn changed the polarophobicity of the surface. Photoswitching the surface in this manner moved a drop of diiodomethane several millimeters up a 12° incline (Fig. 32). Though the world is still waiting for MIMs to physically do the macroscopic work, these approaches represent noteworthy steps in that direction.

Now for a bit of science fiction: what if single molecules could be utilized to store information like transistors? Joint efforts [229–235] between the Heath and Stoddart groups, which addressed the organization of bistable donor–acceptor MIMs at crossbar interfaces using the Langmuir–Blodgett technique and their actuation in these two-dimensional devices, culminated [236] in 2007 after a decade with a device (Fig. 33) approaching that metric. A monolayer of bistable rotaxanes was incorporated into a crossbar logic architecture in a size regime

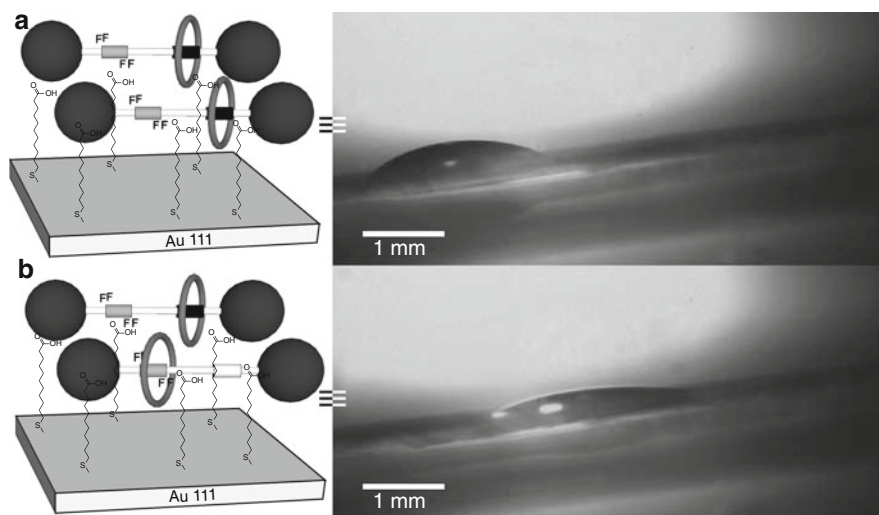


**Fig. 32** Transport of a diiodomethane droplet up a 12° incline on a surface with physisorbed, photoswitchable bistable [2]rotaxanes [228]. (a) Cartoon and photograph of the surface in the ground state. The macrocycle preferentially encircles an unfluorinated recognition site. (b) The same surface in the photostationary state (after UV irradiation). Olefin isomerization in the preferred recognition site causes some macrocycles to shuttle to the fluorinated site, changing the polarophobicity of the surface and moving the droplet several millimeters uphill

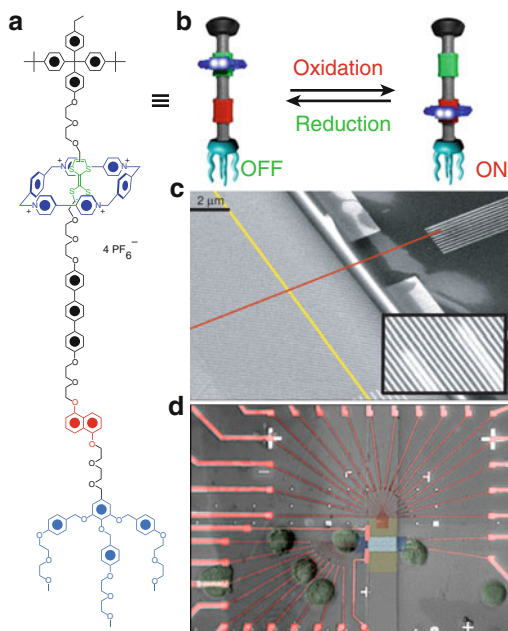


**Fig. 33** A 160-kb molecular electronic memory device [236]. (a) Structural formula of the molecular switches used in the device.

(b) Technomorph representations depicting how the molecular switches can be electrochemically toggled “on” and “off” in the device into co-conformational states with different conductivities.

(c) SEM image of the intersection between top (red) and bottom (yellow) electrodes for the molecular switch tunnel junctions.

(d) Microscopic image of the memory device (blue area) with white blood cells (green circles) and the electrical contacts (red).



corresponding to approximately 250 molecules per junction. Actuation of the bistable switches in these “molecular switch tunnel junctions” validated them as storage elements; about 25% of the bits had sufficient on/off ratios to be configured into a device. The resulting 160-kb memory circuit had a density of  $10^{11}$  bits/cm<sup>2</sup>, for a total memory cell size of 0.0011  $\mu m^2$ , which is approximately the cross-sectional area of a white blood cell (Fig. 33b). A memory circuit of these dimensions is roughly on par with that of a storage density projected [237] to be available in 2020 if Moore’s Law continues to be obeyed.

The question inevitably arises – could we build molecular machines that are “smart” enough to respond to signals within our bodies, releasing therapeutic drugs or diagnostic contrast agents, for example, only at a localized and desired site? Once again, reality is not so far from the dream. A number of research groups are developing a variety of “mechanized nanoparticles” [238] with these applications in mind. Efforts thus far have been associated chiefly with the covalent functionalization of mesoporous silica nanoparticles (MSNPs) [239] that can act as stimulus-responsive gates to the nanopores [240, 241]. Since 2004, bistable rotaxanes and pseudorotaxanes at the surface of these nanoparticles have been demonstrated over and over again to selectively release cargo from MSNPs in response to changes in pH [111, 242–246] light [247–249], redox stimuli [115, 250, 251], and salt concentration [252], as well as oscillating magnetic fields [253] and the application of specific enzymes [254] or small molecules [255]. Fig. 34 provides one example of how they are operated, depicting the release profile of “snap-top” rotaxane-gated

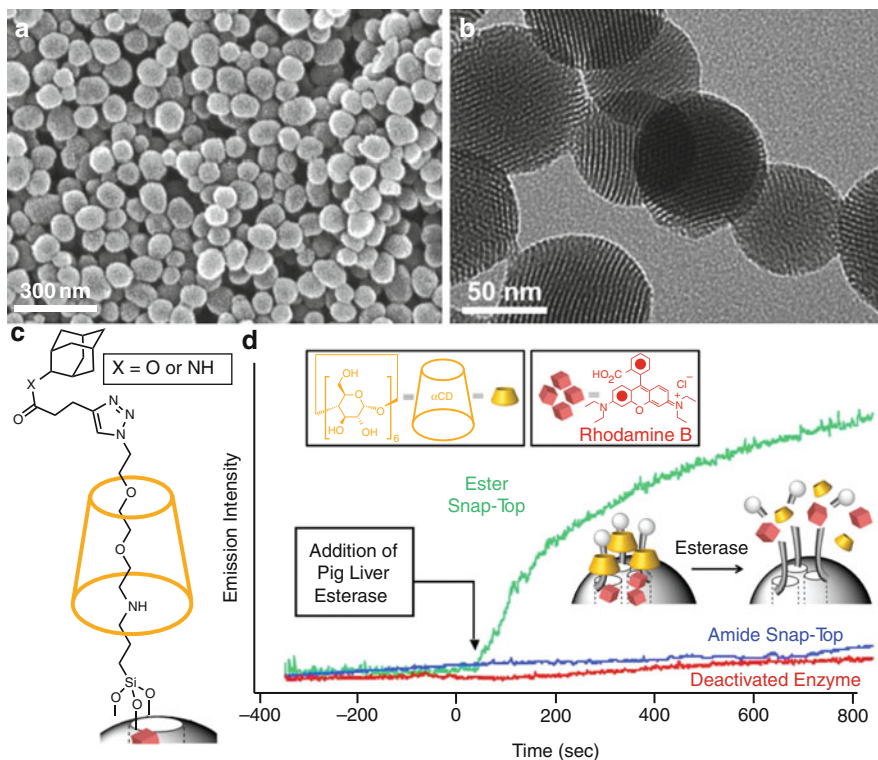


**Fig. 34** Example of mechanized mesoporous silica nanoparticles (MSNPs). SEM (a) and TEM (b) images show the structure and morphology of the MSNP platform [238]. (c) Structural formula of the  $\alpha$ -cyclodextrin-based “snap-top” rotaxane that blocks the pores of an enzyme-cleavable mechanized MSNP. The stopper is connected to the stalk (*dumbbell*) by an ester or an amide bond [254]. (d) Release profile of rhodamine B from the snap-top MSNP. The addition of an esterase enzyme cleaves the ester bond, releasing the stopper,  $\alpha$ -cyclodextrin, and cargo from the nanoparticles, which is monitored by the fluorescence intensity of rhodamine B. Controls employing an amide bond snap-top or deactivated enzyme do not release significant amounts of cargo

nanoparticles that are activated with an enzyme to release cargo. One of the pH-responsive systems has been shown to work autonomously to release cargo in vitro [256], making these materials very promising candidates as drug delivery vehicles. The large number of examples produced in a relatively short time span signifies these nanocarriers as useful, beautiful applications of molecular machinery.

The use of molecular mechanical motions to do work and perform technologically important functions is beautiful in a similar way to technomorphs (Sect. 3.5); it draws a connection to the machines we know and use every day while demanding that we be creative to challenge the limits of what molecular machines can do, coming from a world where Brownian motion rules the roost.

#### 4.6 *The Artwork of MIMs*

Though we consider many of the figures and schemes of MIMs in the primary literature to be artwork in and of themselves, even more deliberate art has been crafted on inspiration from MIMs for journal covers and graphical abstracts for years, along with the occasional work of art for arts' sake. We close Sect. 4 with a collection of commissioned art and cover art inspired by MIMs (Figs. 35–37). We are convinced that MIMs are indeed “a work of art”.



**Fig. 35** MIM-inspired art that decorates the Stoddart Laboratory. The paintings are by artist, Mike Thompson, and the Borromean Ring quilt (*bottom right*) was made by Kirsten E. Griffiths, a former member of the Stoddart Group



**Fig. 36** MIM cover art, reprinted with permission from (in order of appearance): [44] (copyright 2005 American Chemical Society), [257] (copyright 2007 American Chemical Society), [258] (copyright 2007 Royal Society of Chemistry), [89] (copyright 1989 Wiley-VCH), [259] (copyright 2010 Wiley-VCH), [260] (copyright 2000 American Chemical Society), [97] (copyright 2005 Royal Society of Chemistry), [261] (copyright 2008 Royal Society of Chemistry), [262] (copyright 2010 Royal Society of Chemistry)



**Fig. 37** MIM cover art, continued. Reprinted with permission from (in order of appearance): [263] (copyright 2010 Nature Publishing Group), [211] (copyright 2010 Royal Society of Chemistry), [241] (copyright 2009 Royal Society of Chemistry), [264] (copyright 2007 Wiley-VCH), [265] (copyright 2008 Wiley-VCH), [266] (copyright 2005 Wiley-VCH), [267] (copyright 2008 Royal Society of Chemistry), [206] (copyright 2008 Royal Society of Chemistry), [268] (copyright 2006 Royal Society of Chemistry)

## 5 Conclusions and Perspectives

Though it is framed mostly outside the bounds of any formal aesthetic framework, molecular beauty is very much a part of chemists' experience. At the end of the day, MIMs are beautiful because they are researched by hard-working, passionate people who cannot help but to take pleasure in their work. We find beauty in many aspects of the mechanical bond, from its prevalence in society, nature, and art, to the pleasure of building new molecular topologies and architectures, to the appeal of elegant new protocols, the prospect of uncovering emergent phenomena, and the remarkable functionality of molecular switches and machines. At the same time, many chemists are surely artists at heart, sculpting molecules instead of clay, synthesizing masterpieces instead of painting them, even demonstrating a knack for visual presentation as evidenced by the development of new graphical modes of communication, as discussed in Sect. 3, such as the cartoons that simultaneously aid in communication and stimulate innovation. Roald Hoffman has said, "It never ceases to amaze me how a community of people who are not talented at drawing, nor trained to do so, manages to communicate faultlessly so much three-dimensional information" [126]. We add to that our amazement at the beauty such images can bear, and their ability to draw connections between molecules and ordinary objects. Whether we speak of their images, topologies and architectures, experimental elegance, or functional novelty, the research performed on MIMs is indeed a pleasing and beautiful line of work.

## References

1. Wikipedia (2010) Art. <http://en.wikipedia.org/wiki/Art>. Accessed 14 December 2010
2. Chandrasekhar S (1987) Truth and beauty: aesthetics and motivations in science. Chicago University Press, Chicago
3. Pfenninger KH, Shubik VR (2001) The origins of creativity. Oxford University Press, New York
4. Heisenberg W (1974) The meaning of beauty in the exact sciences. In: Anshen RN (ed) Across the frontiers. Harper & Row, New York
5. Spector TI, Schummer J (2003) HYLE 9:3
6. Hoffmann R, Laszlo P (1991) Angew Chem Int Ed Engl 30:1
7. Kretzenbacher HL (2003) HYLE 9:191
8. Laszlo P (2003) HYLE 9:11
9. Schummer J (2003) HYLE 9:73
10. Hoffmann R (1990) J Aesthet Art Critic 48:191
11. Root-Bernstein R (2003) HYLE 9:33
12. Miodownik MA (2007) Pure Appl Chem 79:1635
13. Hoffmann R (1988) Am Sci 76:389
14. Hoffmann R (1988) Am Sci 76:604
15. Hoffmann R (1989) Am Sci 77:177
16. Hoffmann R (1989) Am Sci 77:330
17. Schummer J (1997) Scientometrics 39:125
18. MacGillivray LR, Atwood JL (1999) Angew Chem Int Ed 38:1019

19. Eaton PE, Cole TW (1964) *J Am Chem Soc* 86:3157
20. Paquette LA, Ternansky RJ, Balogh DW, Kentgen G (1983) *J Am Chem Soc* 105:5446
21. Kroto HW, Heath JR, O'Brien SC, Curl RF, Smalley RE (1985) *Nature* 318:162
22. Seidel SR, Stang PJ (2002) *Acc Chem Res* 35:972
23. Tominaga M, Suzuki K, Kawano M, Kusukawa T, Ozeki T, Shakamoto S, Yamaguchi K, Fujita M (2004) *Angew Chem Int Ed* 43:5621
24. Sun Q-F, Iwasa J, Ogawa D, Ishido Y, Sato S, Ozeki T, Sei Y, Yamaguchi K, Fujita M (2010) *Science* 328:1144
25. Nicolaou KC (2009) *J Org Chem* 74:951
26. Ball P (2005) *Elegant solutions: ten beautiful experiments in chemistry*. The Royal Society of Chemistry, Cambridge
27. Hall N (2003) *Chem Commun* 2003:661
28. Lehn J-M (1995) *Supramolecular chemistry: concepts and perspectives*. Wiley-VCH, Weinheim
29. Kreuzer KN, Cozzarelli NR (1980) *Cell* 20:245
30. Subramanian K, Rutvisuttinunt W, Scott W, Myers RS (2003) *Nucleic Acid Res* 31:1585
31. Wikoff WR, Liljas L, Duda RL, Tsuruta H, Hendrix RW, Johnson JE (2000) *Science* 289:2129
32. Mears JA, Lackner LL, Fang S, Ingerman E, Nunnari J, Hinshaw JE (2011) *Nat Struct Mol Biol* 18:20
33. Williams AR, Northrop BH, Chang T, Stoddart JF, White AJP, Williams DJ (2006) *Angew Chem Int Ed* 45:6665
34. Hudson B, Vinograd J (1967) *Nature* 216:647
35. Krasnow MA, Stasiak A, Spengler SJ, Dean F, Koller T, Cozzarelli N (1983) *Nature* 304:559
36. Wasserman SA, Cozzarelli NR (1986) *Science* 232:951
37. Kovall R, Matthews BW (1997) *Science* 277:1824
38. Trakselis MA, Alley SC, Abel-Santos E, Benkovic SJ (2001) *Proc Natl Acad Sci USA* 98:8368
39. Thordarson P, Bijsterveld EJA, Rowan AE, Nolte RJM (2003) *Nature* 424:915
40. Youle RJ, Karbowski M (2005) *Nat Rev Mol Cell Biol* 6:657
41. Cromwell PR (2007) *The Borromean Rings*. <http://www.liv.ac.uk/~spmr02/rings/index.html>. Accessed 20 April 2011
42. Fraser D, Cole HM (eds) (1972) *African art and leadership*. University of Wisconsin Press, Madison
43. Rose LR (2005) *Seeing Solomon's knot*. Lois Rose, Los Angeles
44. Cantrill SJ, Chichak KS, Peters AJ, Stoddart JF (2005) *Acc Chem Res* 38:1
45. Stoddart JF (1992) *Chem Aust* 59:576
46. Cromwell PR, Beltrami E, Rampichini M (1998) *Math Intell* 20:53
47. Greenberg A (2003) *The art of chemistry: myths, medicines, and materials*. Wiley, Hoboken, NJ
48. Obrist B (2003) *HYLE* 9:131
49. Weininger SJ (1998) *HYLE* 4:3
50. Olson MA, Botros YY, Stoddart JF (2010) *Pure Appl Chem* 82:1569
51. Frisch HL, Wasserman E (1961) *J Am Chem Soc* 83:3789
52. Frisch HL, Martin I, Mark H (1953) *Monatsh Chem* 84:250
53. Forgan RS, Sauvage J-P, Stoddart JF (2011) *Chem Rev* 111:5434
54. Walba DM (1985) *Tetrahedron* 41:3161
55. Breault GA, Hunter CA, Mayers PC (1999) *Tetrahedron* 55:5265
56. Dietrich-Buchecker CO, Colasson BX, Sauvage J-P (2005) *Top Curr Chem* 249:261
57. Lüttringhaus A, Cramer F, Prinzbach H, Henglein FM (1958) *Justus Liebigs Ann Chem* 613:185
58. Wasserman E (1960) *J Am Chem Soc* 82:4433
59. Schill G, Lüttringhaus A (1964) *Angew Chem Int Ed Engl* 3:546

60. Wasserman E (1962) *Sci Am* 207:94
61. Harrison IT, Harrison S (1967) *J Am Chem Soc* 89:5723
62. Agam G, Zilka A (1976) *J Am Chem Soc* 98:5212
63. Agam G, Zilka A (1976) *J Am Chem Soc* 98:5214
64. Schill G, Zürcher C (1977) *Chem Ber* 110:2046
65. Schill G, Zürcher C (1977) *Chem Ber* 110:3964
66. Schill G, Rissler K, Fritz H, Vetter W (1983) *Angew Chem Int Ed Engl* 22:889
67. Schill G, Schweickert N, Fritz H, Vetter W (1988) *Chem Ber* 121:961
68. Schill G (1971) *Catenanes, rotaxanes, and knots*. Academic, New York
69. van Gulick N (1993) *New J Chem* 17:619
70. Walba DM, Richards RM, Haltiwanger RC (1982) *J Am Chem Soc* 104:3219
71. Walba DM, Armstrong JDI, Perry AE, Richards RM, Homan TC, Haltiwanger RC (1986) *Tetrahedron* 42:1883
72. Dietrich-Buchecker CO, Sauvage J-P (1983) *Tetrahedron Lett* 24:5095
73. Cesario M, Dietrich CO, Edel A, Guilhem J, Kintzinger J-P, Pascard C, Sauvage J-P (1986) *J Am Chem Soc* 108:6250
74. Dietrich-Buchecker CO, Guilhem J, Khemiss AK, Kintzinger J-P, Pascard C, Sauvage J-P (1987) *Angew Chem Int Ed Engl* 26:661
75. Ashton PR, Brown CL, Chrystal EJT, Goodnow TT, Kaifer AE, Parry KP, Philp D, Slawin AMZ, Spencer N, Stoddart JF, Williams DJ (1991) *J Chem Soc Chem Commun* 1991:634
76. Glink PT, Oliva AI, Stoddart JF, White AJP, Williams DJ (2001) *Angew Chem Int Ed* 40:1870
77. Ibukuro F, Fujita M, Yamaguchi K, Sauvage J-P (1999) *J Am Chem Soc* 121:11014
78. Johnston AG, Leigh DA, Pritchard RJ, Deegan MD (1995) *Angew Chem Int Ed Engl* 34:1209
79. Odell B, Reddington MV, Slawin AMZ, Spencer N, Stoddart JF, Williams DJ (1988) *Angew Chem Int Ed Engl* 27:1547
80. Ashton PR, Odell B, Reddington MV, Slawin AMZ, Stoddart JF, Williams DJ (1988) *Angew Chem Int Ed Engl* 27:1550
81. Gross L, Mohn F, Moll N, Meyer G, Ebel R, Abdel-Mageed WM, Jaspars M (2010) *Nat Chem* 2:821
82. Amabilino DB, Ashton PR, Reder AS, Spencer N, Stoddart JF (1994) *Angew Chem Int Ed Engl* 33:1286
83. Cesario M, Dietrich-Buchecker CO, Guilhem J, Pascard C, Sauvage J-P (1985) *J Chem Soc Chem Commun* 1985:244
84. Amabilino DB, Ashton PR, Boyd SE, Lee JY, Menzer S, Stoddart JF, Williams DJ (1997) *Angew Chem Int Ed Engl* 36:2070
85. Cabezón B, Cao JG, Raymo FM, Stoddart JF, White AJP, Williams DJ (2000) *Angew Chem Int Ed* 39:148
86. Wang C, Olson MA, Fang L, Benítez D, Tkatchouk E, Basu S, Basuray AN, Zhang D, Zhu D, Goddard WA, Stoddart JF (2010) *Proc Natl Acad Sci USA* 107:13991
87. Belowich ME, Valente C, Stoddart JF (2010) *Angew Chem Int Ed* 49:7208
88. Lee C-F, Leigh DA, Pritchard RG, Schultz D, Teat SJ, Timco GA, Winpenny REP (2009) *Nature* 458:314
89. Ashton PR, Goodnow TT, Kaifer AE, Reddington MV, Slawin AMZ, Spencer N, Stoddart JF, Vicent C, Williams DJ (1989) *Angew Chem Int Ed Engl* 101:1396
90. Li H, Eddaoudi M, O'Keeffe M, Yaghi OM (1999) *Nature* 402:276
91. Eddaoudi M, Kim J, Rosi N, Vodak D, Wachter J, O'Keeffe M, Yaghi OM (2002) *Science* 295:469
92. Yaghi OM, O'Keeffe M, Ockwig NW, Chae HK, Eddaoudi M, Kim J (2003) *Nature* 423:705
93. Chae HK, Siberio-Pérez DY, Kim J, Go Y, Eddaoudi M, Matzger AJ, O'Keeffe M, Yaghi OM (2004) *Nature* 427:523
94. Batten SR, Robson R (1998) *Angew Chem Int Ed* 37:1460



95. Reineke TM, Eddaoudi M, Moler D, O'Keeffe M, Yaghi OM (2000) *J Am Chem Soc* 122:4843
96. Chen B, Eddaoudi M, Hyde ST, O'Keeffe M, Yaghi OM (2001) *Science* 291:1021
97. Loeb SJ (2005) *Chem Commun* 2005:1511
98. Vukotic VN, Loeb SJ (2010) *Chem Eur J* 16:13630
99. Li Q, Sue C-H, Basu S, Shveyd AK, Zhang W, Barin G, Fang L, Sarjeant AA, Stoddart JF, Yaghi OM (2010) *Angew Chem Int Ed* 49:6751
100. Li Q, Zhang W, Miljanić OŠ, Knobler CB, Stoddart JF, Yaghi OM (2010) *Chem Commun* 46:380
101. Sauvage J-P, Weiss J (1985) *J Am Chem Soc* 107:6108
102. Ashton PR, Brown CL, Chrystal EJT, Goodnow TT, Kaifer AE, Parry KP, Slawin AMZ, Spencer N, Stoddart JF, Williams DJ (1991) *Angew Chem Int Ed Engl* 30:1039
103. Schummer J (2006) *Found Chem* 8:53
104. Shirai Y, Osgood AJ, Zhao YM, Kelly KF, Tour JM (2005) *Nano Lett* 5:2330
105. Yoshizawa M, Klosterman JK, Fujita M (2009) *Angew Chem Int Ed* 48:3418
106. Anelli PL, Spencer N, Stoddart JF (1991) *J Am Chem Soc* 113:5131
107. Bissell RA, Córdova E, Kaifer AE, Stoddart JF (1994) *Nature* 369:133
108. Spruell JM, Paxton WF, Olsen J-C, Benítez D, Tkatchouk E, Stern CL, Trabolsi A, Friedman DC, Goddard WA, Stoddart JF (2009) *J Am Chem Soc* 131:11571
109. Ashton PR, Brown CL, Chrystal EJT, Parry KP, Pietraszkiewicz M, Spencer N, Stoddart JF (1991) *Angew Chem Int Ed Engl* 103:1042
110. Badjić JD, Balzani V, Credi A, Silvi S, Stoddart JF (2004) *Science* 303:1845
111. Zhao Y-L, Li Z, Kabehie S, Botros YY, Stoddart JF, Zink JI (2010) *J Am Chem Soc* 132:13016
112. Juluri BK, Kumar AS, Liu Y, Ye T, Yang Y-W, Flood AH, Fang L, Stoddart JF, Weiss PS, Huang TJ (2009) *ACS Nano* 3:291
113. Ashton PR, Ballardini R, Balzani V, Credi A, Dress KR, Ishow E, Kleverlaan CJ, Kocian O, Preece JA, Spencer N, Stoddart JF, Venturi M, Wenger S (2000) *Chem Eur J* 6:3558
114. Balzani V, Clemente-Leon M, Credi A, Ferrer B, Venturi M, Flood AH, Stoddart JF (2006) *Proc Natl Acad Sci USA* 103:1178
115. Saha S, Leung KC-F, Nguyen TD, Stoddart JF, Zink JI (2007) *Adv Funct Mater* 17:685
116. Roh S-G, Park K-M, Park G-J, Sakamoto S, Yamaguchi K, Kim K (1999) *Angew Chem Int Ed* 38:638
117. Harada A, Li J, Kamachi M (1992) *Nature* 356:325
118. Whang DM, Park K-M, Heo J, Ashton P, Kim K (1998) *J Am Chem Soc* 120:4899
119. Fujita M, Ibukuro F, Yamaguchi K, Ogura K (1995) *J Am Chem Soc* 117:4175
120. Leigh DA, Wong JKY, Dehez F, Zerbetto F (2003) *Nature* 424:174
121. Leigh DA, Moody K, Smart JP, Watson KJ, Slawin AMZ (1996) *Angew Chem Int Ed Engl* 35:306
122. Clark PG, Guidry EN, Chan WY, Steinmetz WE, Grubbs RH (2010) *J Am Chem Soc* 132:3405
123. Kant I (1892) *Critique of judgement*. Macmillan, London
124. Goodman N (1968) *Languages of art: an approach to a theory of symbols*. Bobbs-Merrill, Indianapolis
125. Eco U (1976) *A theory of semiotics*. Indiana University Press, Bloomington
126. Hoffmann R (2003) *HYLE* 9:7
127. Cram DJ (1988) *Angew Chem Int Ed Engl* 27:1009
128. Pedersen CJ (1988) *Angew Chem Int Ed Engl* 27:1021
129. Dietrich-Buchecker CO, Sauvage J-P (1987) *Chem Rev* 87:795
130. Amabilino DB, Pérez-García L (2009) *Chem Soc Rev* 38:1562
131. Sauvage J-P, Amabilino DB (2011) *Top Curr Chem*. doi: [10.1007/128\\_2011\\_292](https://doi.org/10.1007/128_2011_292)
132. Seeman NC (2007) *Mol Biotechnol* 37:246
133. Aldaye FA, Sleiman HF (2009) *Pure Appl Chem* 81:2157

134. Endo M, Sugiyama H (2009) *Chembiochem* 10:2420
135. Mao CD, Sun WQ, Seeman NC (1997) *Nature* 386:137
136. Schmidt TL, Heckel A (2011) *Nano Lett* 11:1739
137. Han D, Pal S, Liu Y, Yan H (2010) *Nat Nanotech* 5:712
138. Wang H, Du SM, Seeman NC (1993) *J Biomol Struct Dyn* 10:853
139. Seeman NC, Chen J, Du SM, Mueller JE, Zhang Y, Fu TJ, Wang Y, Wang H, Zhang S (1993) *New J Chem* 17:739
140. Weizmann Y, Braunschweig AB, Wilner OI, Cheglakov Z, Willner I (2008) *Proc Natl Acad Sci USA* 105:5289
141. Rothmund PWK (2006) *Nature* 440:297
142. Rolfsen D (1976) *Knots and links. Publish or Perish, Berkeley*
143. Reuter C, Mohry A, Sobanski A, Vögtle F (2000) *Chem Eur J* 6:1674
144. Dietrich-Buchecker CO, Frommberger B, Lüer I, Sauvage J-P, Vögtle F (1993) *Angew Chem Int Ed Engl* 32:1434
145. Amabilino DB, Ashton PR, Bravo JA, Raymo FM, Stoddart JF, White AJP, Williams DJ (1999) *Eur J Org Chem* 1999:1295
146. Hori A, Sawada T, Yamashita K-I, Fujita M (2005) *Angew Chem Int Ed* 44:4896
147. Arico F, Chang T, Cantrill SJ, Khan SI, Stoddart JF (2005) *Chem Eur J* 11:4655
148. Frey J, Kraus T, Heitz V, Sauvage J-P (2005) *Chem Commun* 2005:5310
149. Jäger R, Schmidt T, Karbach D, Vögtle F (1996) *Synlett* 1996:723
150. Jäger R, Händel M, Harren J, Rissanen K, Vögtle F (1996) *Liebigs Ann Chem* 1996:1201
151. Reuter C, Wienand W, Schmuck C, Vögtle F (2001) *Chem Eur J* 7:1728
152. Kishan MR, Parham A, Schelhase F, Yoneva A, Silva G, Chen X, Okamoto Y, Vögtle F (2006) *Angew Chem Int Ed* 45:7296
153. Collin J-P, Durola F, Frey J, Heitz V, Reviriego F, Sauvage J-P, Trolez Y, Rissanen K (2010) *J Am Chem Soc* 132:6840
154. Wang L, Vysotsky MO, Bogdan A, Bolte M, Böhmer V (2004) *Science* 304:1312
155. Chiu S-H, Rowan SJ, Cantrill SJ, Stoddart JF, White AJP, Williams DJ (2002) *Chem Commun* 2002:2948
156. Chichak KS, Cantrill SJ, Pease AR, Chiu S-H, Cave GWV, Atwood JL, Stoddart JF (2004) *Science* 304:1308
157. McArdle CP, Vittal JJ, Puddephatt RJ (2000) *Angew Chem Int Ed* 39:3819
158. Fujita M, Fujita N, Ogura K, Yamaguchi K (1999) *Nature* 400:52
159. Northrop BH, Arico F, Tangchiavang N, Badjić JD, Stoddart JF (2006) *Org Lett* 8:3899
160. Ashton PR, Baxter I, Cantrill SJ, Fyfe MCT, Glink PT, Stoddart JF, White AJP, Williams DJ (1998) *Angew Chem Int Ed* 37:1294
161. Rowan SJ, Cantrill SJ, Stoddart JF, White AJP, Williams DJ (2000) *Org Lett* 2:759
162. Raehm L, Kern J-M, Sauvage J-P (1999) *Chem Eur J* 5:3310
163. Wu J, Leung KC-F, Benítez D, Han J-Y, Cantrill SJ, Fang L, Stoddart JF (2008) *Angew Chem Int Ed* 47:7470
164. Fang L, Hmadeh M, Wu J, Olson MA, Spruell JM, Trabolsi A, Yang Y-W, Elhabiri M, Albrecht-Gary A-M, Stoddart JF (2009) *J Am Chem Soc* 131:7126
165. Hoshino T, Miyauchi M, Kawaguchi Y, Yamaguchi H, Harada A (2000) *J Am Chem Soc* 122:9876
166. Nierengarten J-F, Dietrich-Buchecker CO, Sauvage J-P (1994) *J Am Chem Soc* 116:375
167. Schill G, Schweickert N, Fritz H, Vetter W (1983) *Angew Chem Int Ed Engl* 22:889
168. Coumans RGE, Elemans JAAW, Thordarson P, Nolte RJM, Rowan AE (2003) *Angew Chem Int Ed* 42:650
169. Hamilton DG, Davies JE, Prodi L, Sanders JKM (1998) *Chem Eur J* 4:608
170. Isnin R, Kaifer AE (1991) *J Am Chem Soc* 113:8188
171. Wylie RS, Macartney DH (1992) *J Am Chem Soc* 114:3136
172. Wenz G, Keller B (1992) *Angew Chem Int Ed Engl* 31:197
173. Hunter CA (1992) *J Am Chem Soc* 114:5303

174. Ashton PR, Campbell PJ, Chrystal EJT, Glink PT, Menzer S, Philp D, Spencer N, Stoddart JF, Tasker PA, Williams DJ (1995) *Angew Chem Int Ed Engl* 34:1865
175. Vögtle F, Meier S, Hoss R (1992) *Angew Chem Int Ed Engl* 31:1619
176. Nakatani Y, Furusho Y, Yashima E (2010) *Angew Chem Int Ed* 49:5463
177. Lestini E, Nikitin K, Müller-Bunz H, Fitzmaurice D (2008) *Chem Eur J* 14:1095
178. Barrell MJ, Leigh DA, Lusby PJ, Slawin AMZ (2008) *Angew Chem Int Ed* 47:8036
179. Hübner GM, Gläser J, Seel C, Vögtle F (1999) *Angew Chem Int Ed* 38:383
180. Wisner JA, Beer PD, Drew MGB, Sambrook MR (2002) *J Am Chem Soc* 124:12469
181. Li H, Fahrenbach AC, Dey SK, Basu S, Trabolsi A, Zhu Z, Botros YY, Stoddart JF (2010) *Angew Chem Int Ed* 49:8260
182. Arico F, Badjić JD, Cantrill SJ, Flood AH, Leung KC-F, Liu Y, Stoddart JF (2005) *Top Curr Chem* 249:203
183. Saito S, Takahashi E, Nakazono K (2006) *Org Lett* 8:5133
184. Aucagne V, Hänni KD, Leigh DA, Lusby PJ, Walker DB (2006) *J Am Chem Soc* 128:2186
185. Crowley JD, Goldup SM, Lee A-L, Leigh DA, Mcburney RT (2009) *Chem Soc Rev* 38:1530
186. Rostovtsev VV, Green LG, Fokin VV, Sharpless KB (2002) *Angew Chem Int Ed* 41:2596
187. Sato Y, Yamasaki R, Saito S (2009) *Angew Chem Int Ed* 48:504
188. Berná J, Goldup SM, Lee A-L, Leigh DA, Symes MD, Teobaldi G, Zerbetto F (2008) *Angew Chem Int Ed* 47:4392
189. Berná J, Crowley JD, Goldup SM, Hänni KD, Lee A-L, Leigh DA (2007) *Angew Chem Int Ed* 46:5709
190. Crowley JD, Hänni KD, Lee A-L, Leigh DA (2007) *J Am Chem Soc* 129:12092
191. Goldup SM, Leigh DA, Lusby PJ, McBurney RT, Slawin AMZ (2008) *Angew Chem Int Ed* 47:3381
192. Corbett PT, Leclaire J, Vial L, West KR, Wietor J-L, Sanders JKM, Otto S (2006) *Chem Rev* 106:3652
193. Furusho Y, Hasegawa T, Tsuboi A, Kihara N, Takata T (2000) *Chem Lett* 2000:18
194. Furusho Y, Oku T, Hasegawa T, Tsuboi A, Kihara N, Takata T (2003) *Chem Eur J* 9:2895
195. Wang W, Wang LQ, Palmer BJ, Exarhos GJ, Li ADQ (2006) *J Am Chem Soc* 128:11150
196. Kidd TJ, Leigh DA, Wilson AJ (1999) *J Am Chem Soc* 121:1599
197. Hannam JS, Kidd TJ, Leigh DA, Wilson AJ (2003) *Org Lett* 5:1907
198. Kilbinger AFM, Cantrill SJ, Waltman AW, Day MW, Grubbs RH (2003) *Angew Chem Int Ed* 42:3281
199. Guidry EN, Cantrill SJ, Stoddart JF, Grubbs RH (2005) *Org Lett* 7:2129
200. Badjić JD, Cantrill SJ, Grubbs RH, Guidry EN, Orenes R, Stoddart JF (2004) *Angew Chem Int Ed* 43:3273
201. Rowan SJ, Stoddart JF (1999) *Org Lett* 1:1913
202. Lam RTS, Belenguer A, Roberts SL, Naumann C, Jarrosson T, Otto S, Sanders JKM (2005) *Science* 308:667
203. Hutin M, Schalley CA, Bernardinelli G, Nitschke JR (2006) *Chem Eur J* 12:4069
204. Kawai H, Umehara T, Fujiwara K, Tsuji T, Suzuki T (2006) *Angew Chem Int Ed* 45:4281
205. Miljanić OŠ, Stoddart JF (2007) *Proc Natl Acad Sci USA* 104:12966
206. Patel K, Miljanić OŠ, Stoddart JF (2008) *Chem Commun* 2008:1853
207. Olson MA, Coskun A, Fang L, Basuray AN, Stoddart JF (2010) *Angew Chem Int Ed* 49:3151
208. Fujita M, Ibukuro F, Hagihara H, Ogura K (1994) *Nature* 367:720
209. Dichtel WR, Miljanić OŠ, Zhang W, Spruell JM, Patel K, Aprahamian I, Heath JR, Stoddart JF (2008) *Acc Chem Res* 41:1750
210. Huang TJ, Kolchinski AG, Vance AL, Busch DH (1999) *Adv Supramol Chem* 5:237
211. Fang L, Olson MA, Benítez D, Tkatchouk E, Goddard WA, Stoddart JF (2010) *Chem Soc Rev* 39:17
212. Harada A, Hashidzume A, Yamaguchi H, Takashima Y (2009) *Chem Rev* 109:5974
213. Lukin O, Kubota T, Okamoto Y, Schelhase F, Yoneva A, Müller WM, Müller U, Vögtle F (2003) *Angew Chem Int Ed* 42:4542

214. Barin G, Coskun A, Friedman DC, Olson MA, Colvin MT, Carmielli R, Dey SK, Bozdemir OA, Wasielewski MR, Stoddart JF (2011) *Chem Eur J* 17:213
215. Whitesides GM, Ismagilov RF (1999) *Science* 284:89
216. Gibb BC (2011) *Nat Chem* 3:3
217. Pentecost CD, Chichak KS, Peters AJ, Cave GWV, Cantrill SJ, Stoddart JF (2007) *Angew Chem Int Ed* 46:218
218. Kay ER, Leigh DA, Zerbetto F (2007) *Angew Chem Int Ed* 46:72
219. Balzani V, Gómez-López M, Stoddart JF (1998) *Acc Chem Res* 31:405
220. Balzani V, Credi A, Raymo FM, Stoddart JF (2000) *Angew Chem Int Ed* 39:3348
221. Balzani V, Credi A, Venturi M (2008) *Molecular devices and machines: concepts and perspectives for the nanoworld*. Wiley-VCH, Weinheim
222. Browne WR, Feringa BL (2006) Making molecular machines work. *Nat Nanotechnol* 1:25
223. Stoddart JF (2009) *Nat Chem* 1:14
224. Deng H, Olson MA, Stoddart JF, Yaghi OM (2010) *Nat Chem* 2:439
225. Boyle MM, Smaldone RA, Whalley AC, Ambrogio MW, Botros YY, Stoddart JF (2011) *Chem Sci* 2:204
226. Liu Y, Flood AH, Bonvallet PA, Vignon SA, Northrop BH, Tseng H-R, Jeppesen JO, Huang TJ, Brough B, Baller M, Magonov S, Solares SD, Goddard WA, Ho C-M, Stoddart JF (2005) *J Am Chem Soc* 127:9745
227. Juluri BK, Kumar AS, Liu Y, Ye T, Yang Y-W, Flood AH, Fang L, Stoddart JF, Weiss PS, Huang TJ (2009) *ACS Nano* 3:291
228. Berná J, Leigh DA, Lubomska M, Mendoza SM, Pérez EM, Rudolf P, Teobaldi G, Zerbetto F (2005) *Nat Mater* 4:704
229. Collier CP, Wong EW, Bělohorský M, Raymo FM, Stoddart JF, Kuekes PJ, Williams RS, Heath JR (1999) *Science* 285:391
230. Wong EW, Collier CP, Bělohorský M, Raymo FM, Stoddart JF, Heath JR (2000) *J Am Chem Soc* 122:5831
231. Collier CP, Mattersteig G, Wong EW, Luo Y, Beverly K, Sampaio J, Raymo FM, Stoddart JF, Heath JR (2000) *Science* 289:1172
232. Collier CP, Jeppesen JO, Luo Y, Perkins J, Wong EW, Heath JR, Stoddart JF (2001) *J Am Chem Soc* 123:12632
233. Luo Y, Collier CP, Jeppesen JO, Nielsen KA, DeIonno E, Ho G, Perkins J, Tseng H-R, Yamamoto T, Stoddart JF, Heath JR (2002) *ChemPhysChem* 3:519
234. DeIonno E, Tseng H-R, Harvey DD, Stoddart JF, Heath JR (2006) *J Phys Chem B* 110:7609
235. Choi JW, Flood AH, Steuerman DW, Nygaard S, Braunschweig AB, Moonen NNP, Laursen BW, Luo Y, DeIonno E, Peters AJ, Jeppesen JO, Xu K, Stoddart JF, Heath JR (2006) *Chem Eur J* 12:261
236. Green JE, Choi JW, Boukai A, Bunimovich Y, Johnston-Halperin E, DeIonno E, Luo Y, Sheriff BA, Xu K, Shin YS, Tseng H-R, Stoddart JF, Heath JR (2007) *Nature* 445:414
237. Semiconductor Industry Association (2005) *The International Technology Roadmap for Semiconductors: Process Integration, Devices, and Structures*. SIA, Washington D.C. <http://www.itrs.net/reports.html>. Accessed 19 April 2011
238. Cotí KK, Belowich ME, Liong M, Ambrogio MW, Lau YA, Khatib HA, Zink JI, Khashab NM, Stoddart JF (2009) *Nanoscale* 1:16
239. Klichko Y, Liong M, Choi E, Angelos S, Nel AE, Stoddart JF, Tamanoi F, Zink JI (2009) *J Am Ceram Soc* 92:S2
240. Angelos S, Johansson E, Stoddart JF, Zink JI (2007) *Adv Funct Mater* 17:2261
241. Liong M, Angelos S, Choi E, Patel K, Stoddart JF, Zink JI (2009) *J Mater Chem* 19:6251
242. Angelos S, Yang Y-W, Patel K, Stoddart JF, Zink JI (2008) *Angew Chem Int Ed* 47:2222
243. Angelos S, Khashab NM, Yang Y-W, Trabolsi A, Khatib HA, Stoddart JF, Zink JI (2009) *J Am Chem Soc* 131:12912
244. Du L, Liao S, Khatib HA, Stoddart JF, Zink JI (2009) *J Am Chem Soc* 131:15136

245. Khashab NM, Belowich ME, Trabolsi A, Friedman DC, Valente C, Lau Y, Khatib HA, Zink JI, Stoddart JF (2009) *Chem Commun* 2009:5371
246. Park C, Oh K, Lee SC, Kim C (2007) *Angew Chem Int Ed* 46:1455
247. Hernandez R, Tseng H-R, Wong JW, Stoddart JF, Zink JI (2004) *J Am Chem Soc* 126:3370
248. Ferris DP, Zhao Y-L, Khashab NM, Khatib H, Stoddart JF, Zink JI (2009) *J Am Chem Soc* 131:1686
249. Park C, Lee K, Kim C (2009) *Angew Chem Int Ed* 48:1275
250. Nguyen TD, Tseng H-R, Celestre P, Flood AH, Liu Y, Stoddart JF, Zink JI (2005) *Proc Natl Acad Sci USA* 102:10029
251. Khashab NM, Trabolsi A, Lau YA, Ambrogio MW, Friedman DC, Khatib HA, Zink JI, Stoddart JF (2009) *Eur J Org Chem* 2009:1669
252. Nguyen TD, Leung KC-F, Liong M, Pentecost CD, Stoddart JF, Zink JI (2006) *Org Lett* 8:3363
253. Thomas CR, Ferris DP, Lee J-H, Choi E, Cho MH, Kim ES, Stoddart JF, Shin J-S, Cheon J, Zink JI (2010) *J Am Chem Soc* 132:10623
254. Patel K, Angelos S, Dichtel WR, Coskun A, Yang Y-W, Zink JI, Stoddart JF (2008) *J Am Chem Soc* 130:2382
255. Ambrogio MW, Pecorelli TA, Patel K, Khashab NM, Trabolsi A, Khatib HA, Botros YY, Zink JI, Stoddart JF (2010) *Org Lett* 12:3304
256. Meng H, Xue M, Xia T, Zhao Y-L, Tamanoi F, Stoddart JF, Zink JI, Nel AE (2010) *J Am Chem Soc* 132:12690
257. Pentecost CD, Tangchaivang N, Cantrill SJ, Chichak KS, Peters AJ, Stoddart JF (2007) *J Chem Ed* 84:855
258. Meyer CD, Joiner CS, Stoddart JF (2007) *Chem Soc Rev* 36:1705
259. Zalewski L, Wykes M, Brovelli S, Bonini M, Breiner T, Kastler M, Dötz F, Beljonne D, Anderson HL, Cacialli F, Samorì P (2010) *Chem Eur J* 16:3933
260. Balzani V, Credi A, Matternsteig G, Matthews OA, Raymo FM, Stoddart JF, Venturi M, White AJP, Williams DJ (2000) *J Org Chem* 65:1924
261. Suzaki Y, Taira T, Osakada K, Horie M (2008) *Dalton Trans* 2008:4823
262. Collin J-P, Durola F, Lux J, Sauvage J-P (2010) *New J Chem* 34:34
263. Baumes JM, Gassensmith JJ, Giblin J, Lee J-J, White AG, Culligan WJ, Leevy WM, Kuno M, Smith BD (2010) *Nat Chem* 2:1025
264. Bäuerle P, Ammann M, Wilde M, Götz G, Mena-Osteritz E, Rang A, Schalley CA (2007) *Angew Chem Int Ed* 46:363
265. Goldup SM, Leigh DA, Lusby PJ, McBurney RT, Slawin AMZ (2008) *Angew Chem Int Ed* 47:6999
266. Lukin O, Vögtle F (2005) *Angew Chem Int Ed* 44:1456
267. Dawson RE, Lincoln SF, Easton CJ (2008) *Chem Commun* 2008:3980
268. Ng K-Y, Cowley AR, Beer PD (2006) *Chem Commun* 2006:3676

# The Beauty of Chemistry in the Words of Writers and in the Hands of Scientists

Margherita Venturi, Enrico Marchi, and Vincenzo Balzani

**Abstract** Chemistry is a central science because all the processes that sustain life are based on chemical reactions, and all things that we use in everyday life are natural or artificial chemical compounds. Chemistry is also a fantastic world populated by an unbelievable number of nanometric objects called molecules, the smallest entities that have distinct shapes, sizes, and properties. Molecules are the words of matter. Indeed, most of the other sciences have been permeated by the concepts of chemistry and the language of molecules. Like words, molecules contain specific pieces of information that are revealed when they interact with one another or when they are stimulated by photons or electrons. In the hands of chemists, molecules, particularly when they are suitably combined or assembled to create supramolecular systems, can play a variety of functions, even more complex and more clever than those invented by nature. The wonderful world of chemistry has inspired scientists not only to prepare new molecules or investigate new chemical processes, but also to create masterpieces. Some nice stories based on chemical concepts (1) show that there cannot be borders on the Earth, (2) underline that there is a tight connection among all forms of matter, and (3) emphasize the irreplaceable role of sunlight.

**Keywords** Catenanes · Dendrimers · Molecular logic · Molecules as words · Rotaxanes · Supramolecular chemistry · Writers and chemistry

---

M. Venturi (✉) and V. Balzani  
Dipartimento di Chimica “G. Ciamician”, Alma Mater Studiorum, Università di Bologna,  
via Selmi 2, 40126 Bologna, Italy  
e-mail: [margherita.venturi@unibo.it](mailto:margherita.venturi@unibo.it); [vincenzo.balzani@unibo.it](mailto:vincenzo.balzani@unibo.it)

E. Marchi  
Centro di Ricerca Interuniversitario per la Conversione Chimica dell’Energia Solare, Università di  
Bologna, via Selmi 2, 40126 Bologna, Italy  
e-mail: [enrico.marchi@unibo.it](mailto:enrico.marchi@unibo.it)

## Contents

1	Chemistry: A Central Science .....	74
2	Language and Chemistry .....	74
3	Beautiful Molecules .....	75
4	Chemistry in the Words of Scientists and Writers .....	78
5	Clever Molecules .....	79
6	From Molecules to Molecular Devices and Machines .....	82
7	Molecular Devices .....	83
	7.1 Molecular Plug/Socket System .....	83
	7.2 Electrical Extension Cable at the Molecular Level .....	85
	7.3 Dendrimers: Appealing Structures and Useful Compounds .....	87
8	Molecular Machines .....	91
	8.1 Linear Movements in Rotaxanes .....	92
	8.2 Ring Movements in Catenanes .....	96
9	Conclusions .....	102
	References .....	102

## 1 Chemistry: A Central Science

Chemistry is a central science. Its language, the language of molecules, permeates several other fields of science. Today the most important part of biology is molecular biology, and in the near future the chemical concepts that underlie our mental activity (learning, thought, memory, and even conscience) will be recognized. Chemistry is the necessary link between physics and biology, and it is also the basis of emerging fields like ecology and material science. Without chemistry there would be no hope of finding solutions to the four most important problems of our society: food, health, energy, and environment.

Everybody knows that chemistry is useful and important: it allows us to treat diseases, to live a more pleasant life, to understand the laws of Nature, and to change the world around us. Many people wrongly believe that chemistry is only a dirty industrial activity. Only a few know that Chemistry is a beautiful science strictly connected with arts [1].

## 2 Language and Chemistry

There is a close parallelism between language and chemistry. Atoms are the letters of chemistry, and the periodic table is the chemistry alphabet. A combination of letters according to the rules of language forms a word, a combination of atoms according to Nature's laws forms a molecule. A combination of words forms a sentence, a combination of molecules forms a supramolecular system. Going on towards increasing complexity, language takes the forms of paragraphs, articles, books, and libraries, while chemistry merges into biology and ends with its highest expression: man. But chemistry is much more complex than language. The books of

a very large library, such as the Bibliothèque Nationale de France, contain all together about  $10^{13}$  letters, whereas in the body of a man there are about  $10^{28}$  atoms: one million billion times more!

Atoms, like letters, are indispensable, but they do not have much meaning by themselves. As in a language, words are the smallest units with a meaning; in chemistry, molecules are the smallest entities that can play a function: they are indeed the smallest entities of matter that have distinct shapes, sizes and properties. Therefore, like words, molecules contain specific pieces of information that can be seen as “the meaning” of a molecule.

Both words and molecules can have a strong impact on our life. Both the word “rose” and the molecule responsible for the perfume of a rose give us a pleasant sensation. Words and molecules can be sweet, bitter, light, heavy, sour, cutting. There are words and molecules that can save or kill a life.

There is another important analogy between language and chemistry. The meaning of a word depends not only on the number and types of letters by which it is formed, but also on the order of the letters. For example, in Italian by using 2a, 1g, 1i, 1l, 1o, 1r, 1t, 1v we can write two words with very different meanings, *giravolta* (complete turn) and *travaglio* (torment). Analogously, the same atoms, namely 2C, 6H, 1O, constitute the molecules of methyl alcohol and dimethyl ether that have the same formula,  $C_2H_6O$ , but very different properties because of the different order in which the atoms are linked together. Both words and molecules can be disassembled and then reassembled to give rise to other words or molecules. The Latin poet Lucretius was a master in doing that with words [2]. But Nature is much better. Our body is a book in which some molecules are continuously erased and others written: our skin is fully replaced in a month, our liver is renewed every 6 weeks.

The field of chemistry is much broader than the field of any language. In Italian we have about 160,000 words, whereas at least 5 million types of molecules can be found in Nature and about 15 million types of artificial molecules have been synthesized by chemists. Leonardo da Vinci did not know chemistry; nevertheless, his sentence “Where nature finishes producing its species, there man begins with natural things to make with the aid of this nature an infinite number of species” [3] is quite appropriate to comment the outstanding development of chemistry. Chemists, indeed, started as explorers of Nature, but very soon they also became inventors and today they continue to play such dual role. As a consequence, chemistry is at the same time a book that we can read and a collection of white sheets that we can write on. A large part of the book has not yet been read (undiscovered natural molecules and processes) and the number of white sheets to be written on (artificial molecules and processes) is endless.

### 3 Beautiful Molecules

Molecules of nearly any shape have been synthesized in recent years. Instead of using conventional chemical names, chemists often call these molecules by names derived from the similarity of the molecular shapes to those of objects



encountered in everyday life: barrels, baskets, belts, bowls, boxes, bridges, butterflies, cages, catenanes, crowns, cryptands, cylinders, dendrimers, fences, footballene, gates, gondola, grids, helicates, helicenes, hinges, knots, ladders, lantern, lepidopterene, octopus, ovalene, pagodanes, podands, propellanes, racks, rotaxanes, scorpiands, sepulchrand, speleands, spherands, staffanes, stellanes, torand, trinacene, tweezers, vessels, wires [4].

If we could see molecules, we would realize that in several cases they have high symmetries and fascinating shapes [5, 6]. We have a clue of that from CPK molecular models (Corey–Pauling–Koltun space-filling models), which are one hundred million time larger. Some examples of esthetically appealing molecules are shown in Figs. 1 [7, 8] and 2 [9]. As Primo Levi noticed [10]: “In fact it happens also in chemistry as in architecture that ‘beautiful’ edifices, that is, symmetrical and simple, are also the most sturdy: in short, the same thing happens with molecules as with the cupolas of cathedrals or the arches of bridges.”

Molecules have indeed been taken as models for creating beautiful sculptures (Fig. 3) [11].

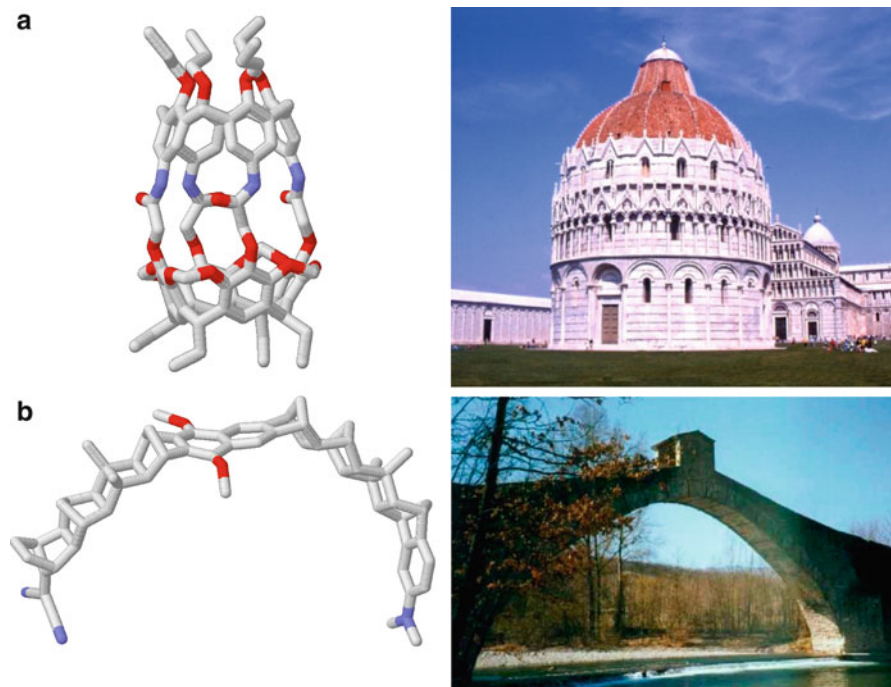


**Fig. 1** Molecular architecture: two fascinating nanometer-scale supramolecular species and the corresponding macroscopic counterparts. (a) Resorcarene-calixarene carcerand [7] and the Battistero of Pisa (Italy). (b) Norbornylogous-type compound [8] and the Olina medieval bridge, Modena (Italy). The geometries of the molecules are constructed by molecular mechanics calculations

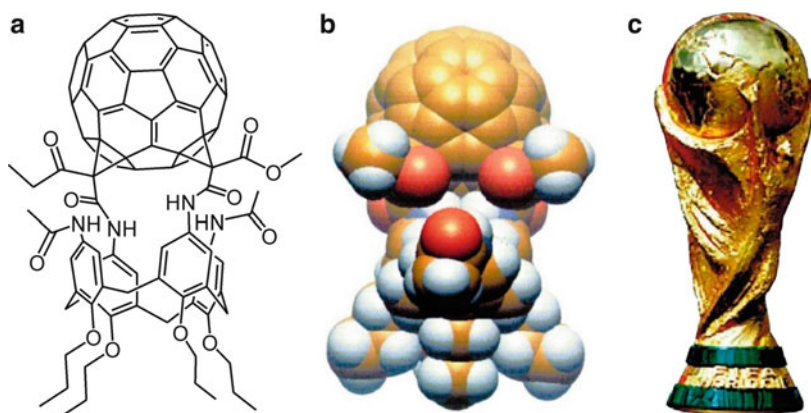


**Fig. 2** Supramolecular system consisting of a fullerene covalently linked to a calixarene [9]; the authors say that the synthesis of the nanocup was a tribute to the French football team of 1998: (a) classical chemical representation; (b) computer-generated space-filling model, showing the shape relationship of this supramolecular structure; and (c) the football World Cup. Reproduced by permission of The Royal Society of Chemistry (RSC) and the Centre National de la Recherche Scientifique (CNRS)



**Fig. 3** Sculptures by Vizi Béla representing four classical supramolecular systems [11]

## 4 Chemistry in the Words of Scientists and Writers

Language and chemistry have been beautifully combined by scientists and writers. An outstanding example is the definition of a tree given by Richard Feynman [12]: “A tree is essentially made of air and sun. When it is burned, it goes back to air, and in the flaming heat is released the flaming heat of the sun which was bound in to convert the air into tree, and in the ash is the small remnant of the part which did not come from air that came from the solid earth, instead.”

It is difficult to explain by words the beauty and complexity of chemistry. Primo Levi, a great writer and chemist, in his book *The Monkey's Wrench* [13], in talking with a construction worker named Faussone succeeded in giving a poetical description of the profession of a chemist: “My profession, my real one, the profession I studied in school and that has kept me alive so far is the profession of chemist. I don't know if you have a clear idea of it, but it is a bit like yours; only we rig and dismantle very tiny constructions. We are divided into two main branches, those who rig and those who dismantle or break down, and both kinds are like blind people with sensitive fingers. I say blind because, actually, the things we handle are too small to be seen, even with the most powerful microscopes: so we have invented various intelligent gadgets to recognize them without seeing them. . . . Those who dismantle, the analytical chemists, in other words, have to be able to take a structure apart piece by piece without damaging it, or at least without damaging it too much; then they have to line up the pieces on the desk, naturally without ever seeing them, but recognizing them one by one. Then, they say in what order the pieces were attached.”

In another book entitled *The Periodic Table* [14], Primo Levi describes, in a poetical and fascinating way, the endless travel of a carbon atom: “. . . firmly clinging to two oxygen companions, it issued from the chimney and took the path of the air. . . . It was caught by the wind, flung down on the earth, lifted ten kilometers high. It was breathed in by a falcon, descending into its precipitous lungs, but did not penetrate its rich blood and was expelled. It dissolved three times in the water of the sea, one in the water of a cascading torrent, and again was expelled. It traveled with the wind for eight years: now high, now low, on the sea and among clouds, over forests, deserts, and limitless expanses of ice; then it stumbled into capture and the organic adventure. . . . Our atom of carbon enters the leaf, colliding with other innumerable molecules of nitrogen and oxygen. It adheres to a large and complicated molecule that activates it, and simultaneously receives the decisive message from the sky, in the flashing form of a packed of solar light: in an instant, like an insect caught by a spider, it is separated from its oxygen, combined with hydrogen and finally inserted in a chain, whether long or short does not matter, but is the chain of life.” This nice story shows that there cannot be borders for chemistry and, most important, it underlines the tight connections among all forms of matter present on Earth.

Chemistry, words, and life are amazingly blended in the recent poem *Sustainable Development* [15] by Roald Hoffmann, a chemist, poet and philosopher, who

shared the 1981 Nobel Prize in Chemistry. Such a poem, which describes the “divine” growing of a vine around a tall tree, begins with the following lines: “Alive? The /vines just push/the question/aside, a/green muff for/these trees, coat-/ing them real/tight like a crosslinked po-/lymer gone/mad. The prob-/lem in spring/ is the trees’-/are they? And /will they be?” This poem is another marvelous description of the power of photosynthesis.

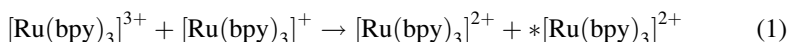
## 5 Clever Molecules

Although the most creative act in chemistry is frequently considered to be “the design and creation of new molecules” [16], creativity in chemistry in the last few years has more often arisen from novel conceptual interpretations of well-known chemical reactions of established molecules [17–21]. In many fields of art and science, creativity results indeed from reconsidering old materials with a new design in mind. A typical example of exploiting well-known properties of old molecules for new achievements concerns the field of information processing.

In 1993 the analogy between molecular switches and logic gates was experimentally demonstrated [22]. Since then, processing photonic, electronic, and chemionic signals by molecules in solution has been proposed [17–20, 23–28] as an alternative route to solid-state molecular electronics towards the design and construction of the much-sought chemical computer [29, 30]. The field has recently developed from simple switches to produce more complex molecular systems that are capable of performing a variety of classical logic functions [23–28].

A particularly interested case of “clever” molecule is the very simple and well-known metal complex,  $[\text{Ru}(\text{bpy})_3]^{2+}$  ( $\text{bpy} = 2,2'$ -bipyridine), which was found to perform as both an encoder and a decoder of a combination of electronic and photonic inputs and outputs [31].

The chemical, photochemical, and electrochemical behavior of  $[\text{Ru}(\text{bpy})_3]^{2+}$  and of hundreds of its derivatives has been extensively investigated in the past 30 years [32, 33]. The ground state complex (Fig. 4) can be excited by visible light with formation of a spin-allowed excited state,  $^*[\text{Ru}(\text{bpy})_3]^{2+}$ , which undergoes fast and efficient radiationless deactivation to form the spin-forbidden, long-lived, and luminescent  $^*[\text{Ru}(\text{bpy})_3]^{2+}$  excited state.  $[\text{Ru}(\text{bpy})_3]^{2+}$  can also undergo reversible one-electron oxidation and reduction processes (e.g., in acetonitrile solution), which become energetically much more favorable starting from  $^*[\text{Ru}(\text{bpy})_3]^{2+}$  because of the extra energy available to the excited state (photoinduced electron transfer, Fig. 4). It is also well known that the comproportionation reaction between the oxidized  $[\text{Ru}(\text{bpy})_3]^{3+}$  and the reduced  $[\text{Ru}(\text{bpy})_3]^+$  species (1) is strongly exergonic and can in fact generate a ground  $[\text{Ru}(\text{bpy})_3]^{2+}$  and an excited  $^*[\text{Ru}(\text{bpy})_3]^{2+}$  species, followed by radiative deactivation of the latter (luminescence induced by electron transfer):



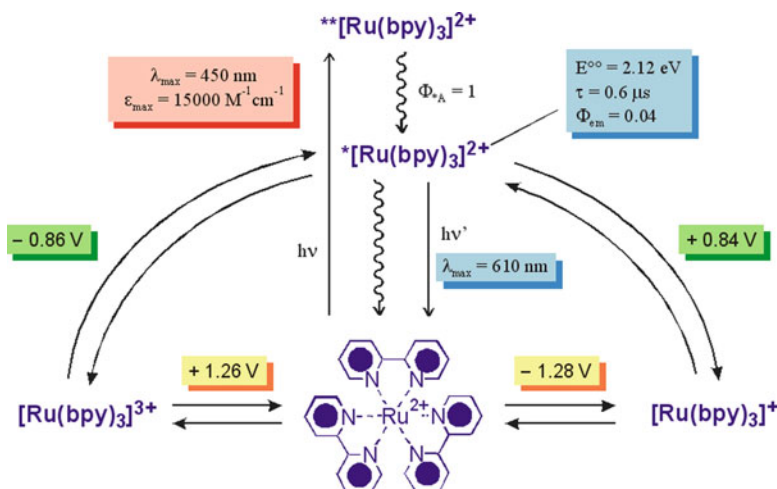


**Fig. 4** [Ru(bpy)<sub>3</sub>]<sup>2+</sup> and its photoexcited and redox forms that can be obtained by light and electrochemical inputs [32, 33]

These results show that [Ru(bpy)<sub>3</sub>]<sup>2+</sup> is able to process, and even interchange, photonic and electronic inputs (Fig. 4). The absorption spectra of the [Ru(bpy)<sub>3</sub>]<sup>3+</sup>, [Ru(bpy)<sub>3</sub>]<sup>2+</sup> and [Ru(bpy)<sub>3</sub>]<sup>+</sup> species are substantially different and it is not difficult to choose appropriate absorbance thresholds related to the three interconverting species at three different wavelengths (310, 450, and 530 nm). Furthermore, [Ru(bpy)<sub>3</sub>]<sup>2+</sup> exhibits a luminescence band (λ<sub>max</sub> 620 nm), whereas [Ru(bpy)<sub>3</sub>]<sup>3+</sup> and [Ru(bpy)<sub>3</sub>]<sup>+</sup> are not luminescent. By elaborating these spectroscopic properties and the photochemical and electrochemical processes, it has been found that [Ru(bpy)<sub>3</sub>]<sup>2+</sup> can indeed perform as both an encoder and a decoder (Fig. 5) [31].

The example described above is only one of the many systems developed with the aim of mimicking Boolean logic function at the molecular level [28]. Leaving aside futuristic applications related to the construction of a chemical computer, recent work shows that molecular logic devices could lead to practical applications in a not-too-distant future. An example is the use of molecular logic gates for tagging and identification of small objects in a large population [34], a method termed molecular computational identification (MCID) [35]. Populations of microscopic objects that need encoding are, e.g., cells in diagnostics or polymer beads in combinatorial chemistry. In this approach, a tag is represented by the unique signature from a set of logic gates that is obtained in response to a defined set of inputs under given experimental conditions.

To test the MCID method, single-input molecular logic gates 1–3 (Fig. 6) were linked to Tentagel-S-NH<sub>2</sub> polymer beads (100 μm) by peptide coupling [35]. Compounds 1, 2, and 3 give a fluorescent output with PASS 1, YES, and NOT logic, respectively, under the action of a proton input in solution, whereas underivatized beads implement PASS 0 logic. Figure 6b shows that beads tagged

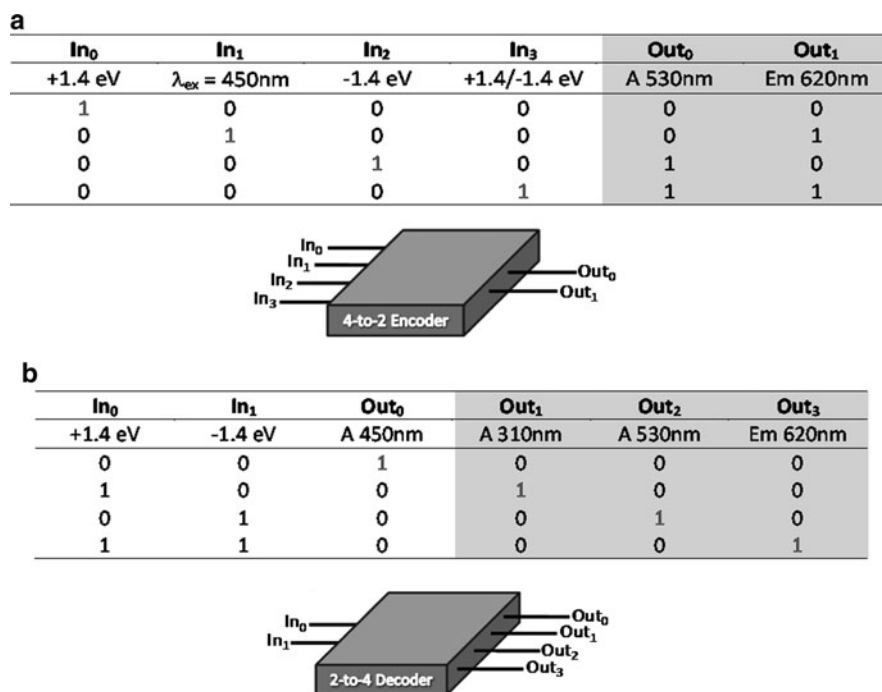


**Fig. 5** Representation and truth tables of (a) 4-to-2 encoder, and (b) 2-to-4 decoder based on  $[\text{Ru}(\text{bpy})_3]^{2+}$  [31]

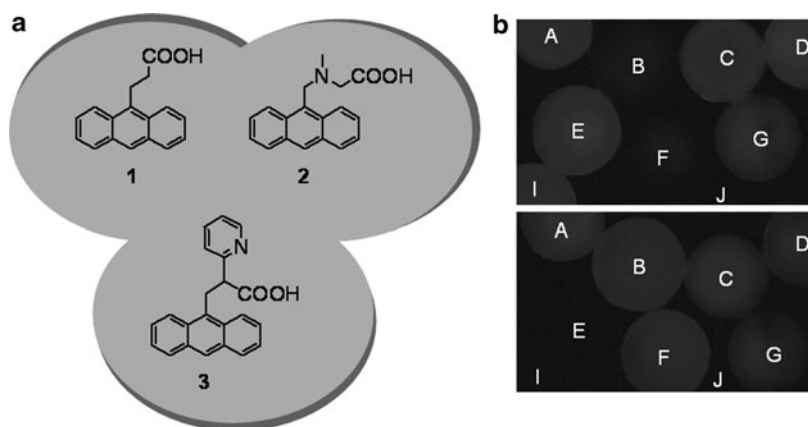


**Fig. 6** (a) Structural formulas of PASS 1 gate **1**, YES gate **2**, and NOT gate **3** that were linked to polymer beads for tagging and identification. (b) Fluorescence microscopic image ( $\lambda_{exc} = 366\text{ nm}$ ) of mixed beads with different logic tags in  $\text{CH}_3\text{OH}/\text{H}_2\text{O}$  1:1v/v in the presence of  $\text{HCl}$  (top) and  $\text{NaOH}$  (bottom). Each bead in the picture can be clearly identified from its logic response to the chemical inputs employed. A, C, G PASS 1; B, F NOT; D PASS 1 + YES (1:1); E, I YES; F NOT; and J PASS 0. Adapted from [31]

with different molecular logic elements can be easily distinguished in an ensemble on the basis of the logic response of their fluorescence upon addition of acid and alkali solutions. The number of distinct chemically switched tags available can be scaled up by increasing the number of logic types and including those that respond to more than one input (AND, OR, XOR, INH, etc.). Luminophores other than the anthracene signaling unit used in compounds **1–3** could be employed, each having characteristic excitation/emission spectral features and luminescence lifetime.

This study shows that a large number of molecular logic gates can be designed such that each displays a unique signature (luminescence output) in response to chemical (inputs of ions or molecules) or physical (light or heat) stimulation under determined experimental conditions (excitation/emission wavelengths, input threshold values, temperature, etc.). This starting set of tags can be increased further if the targeted objects are marked with mixtures of logic gates in a chosen molar ratio, and more than two output levels are considered. The final MCID tag address of a given object can be represented by a sequence of terms, like a car license plate or an Internet Protocol address, for instance,  $(\lambda_{\max,exc}).(\lambda_{\max,em}).(\text{logic types and combinations}).(\text{input types}).(\text{input thresholds})$ . To give an example, the tag of bead D in Fig. 6b can be represented as (368).(422).(PASS 1 + YES, 1:1).( $H^+$ ,  $H^+$ ).(none, pH = 4.9) [35].

Molecular logic can also be useful for the development of nanosystems for therapeutic applications. Molecular devices able to generate a chemical output by processing chemical inputs according to programmed logic functions can be viewed as “secured” or “smart” delivery systems. Such systems could release a drug molecule only in response to a predetermined set of external inputs, or when the concentrations of a given number of chemical inputs signaling a specific condition (e.g., a disease) rise above (or fall below) appropriate threshold values.

An interesting example is a semibiological molecular device capable of controlling the folding of a protein with AND logic in response to ATP (adenosine triphosphate) and light stimulations [36]. Noticeably, a molecular automaton based on DNA (deoxyribonucleic acid) and DNA-manipulating enzymes [37, 38] has been utilized to achieve logical analysis of gene expression and consequent controlled administration of a biologically active molecule. The automaton was programmed to identify and analyze *in vitro* messenger RNAs (ribonucleic acid) of disease-related genes associated with some forms of cancer, and generate a single-stranded DNA molecule modeled after an anticancer drug [38]. This work is an important step towards the construction of molecular computers operating *in vivo* and capable of autonomously diagnosing a disease and effecting a therapy.

## 6 From Molecules to Molecular Devices and Machines

In the last 30 years, chemists have learnt to assemble molecules [18] and now, by exploiting the molecule-by-molecule “bottom-up” approach [39, 40], they have virtually unlimited possibilities to design and construct supramolecular species and enter the field of nanotechnology.

Roald Hoffmann has defined nanotechnology as the “The marriage of the synthetic talent of Chemists with a ‘device driven’ ingenuity” [41]. Roald Hoffmann reacted in this way when asked about the goal of nanotechnology: “I’m glad you guys (that includes women, of course) found a new name for chemistry. Now you have the incentive to learn what you didn’t want to learn in college. Chemists have been practicing nanotechnology, structure and reactivity and properties, for two centuries, and for 50 years by design. What is exciting about modern nanotechnology is (a) the marriage of chemical synthetic talent with a direction provided by “device-driven” ingenuity coming from engineering, and (b) a certain kind of courage provided by those incentives, to make arrays of atoms and molecules that ordinary, no, extraordinary chemists just wouldn’t have thought of trying. Now they’re pushed to do so. And of course they will. They can do anything. Nanotechnology is the way of ingeniously controlling the building of small and large structures, with intricate properties; it is the way of the future, a way of precise, controlled building, with, incidentally, environmental benignness built in by design.” Indeed, the macroscopic concepts of a device and a machine have been extended by chemists to the molecular level [39, 40, 42–54]. A *molecular-level device* can be defined as an assembly of a discrete number of molecular components (that is, a supramolecular structure) designed to achieve a specific function. Each molecular component performs a single act, while the entire supramolecular assembly performs a more complex function, which results from the cooperation of the various components. A *molecular-level machine* is a particular type of molecular-level device in which the component parts can display changes in their relative positions as a result of some external stimulus. Like macroscopic devices and machines, molecular-level devices and machines need energy to operate and signals to communicate with the operator.

Interestingly, the bottom-up approach to the construction of molecular level devices and machines was poetically anticipated by Primo Levi in his already-cited book *The Monkey’s Wrench* [55]:

It is reasonable to proceed a bit at a time, first attaching two pieces, then adding a third, and so on. . . . we don’t have those tweezers we often dream of at night . . . If we had those tweezers (and it’s possible that, one day, we will), we would have managed to create some lovely things that so far only the Almighty has made, for example, to assemble – perhaps not a frog or a dragonfly - but at least a microbe or the spore of a mold.

Up until now, nobody has succeeded in constructing a chemical system as complex as a microbe or the spore of a mold; in recent years, however, a number of very simple molecular-level devices and machines have been built.

## 7 Molecular Devices

### 7.1 *Molecular Plug/Socket System*

Supramolecular species, whose components are connected by means of non-covalent forces, can be disassembled and re-assembled [56] by modulating the interactions



that keep the components together, thereby allowing switching of energy- or electron-transfer processes. Two-component systems of this type are reminiscent of plug/socket electrical devices and, like their macroscopic counterparts, must be characterized by: (1) the possibility of connecting/disconnecting the two components in a reversible way, and (2) the occurrence of an electron or electronic energy flow from the socket to the plug when the two components are connected. Hydrogen-bonding interactions between ammonium ions and crown ethers are particularly convenient for constructing molecular-level plug/socket devices, since they can be switched on and off quickly and reversibly by means of acid–base inputs.

A plug/socket system that deals with the transfer of electronic energy is illustrated in Fig. 7 [57]. The absorption and fluorescence spectra of a  $\text{CH}_2\text{Cl}_2$  solution containing equal amounts of binaphthocrown ether **4** and amine **5** indicate

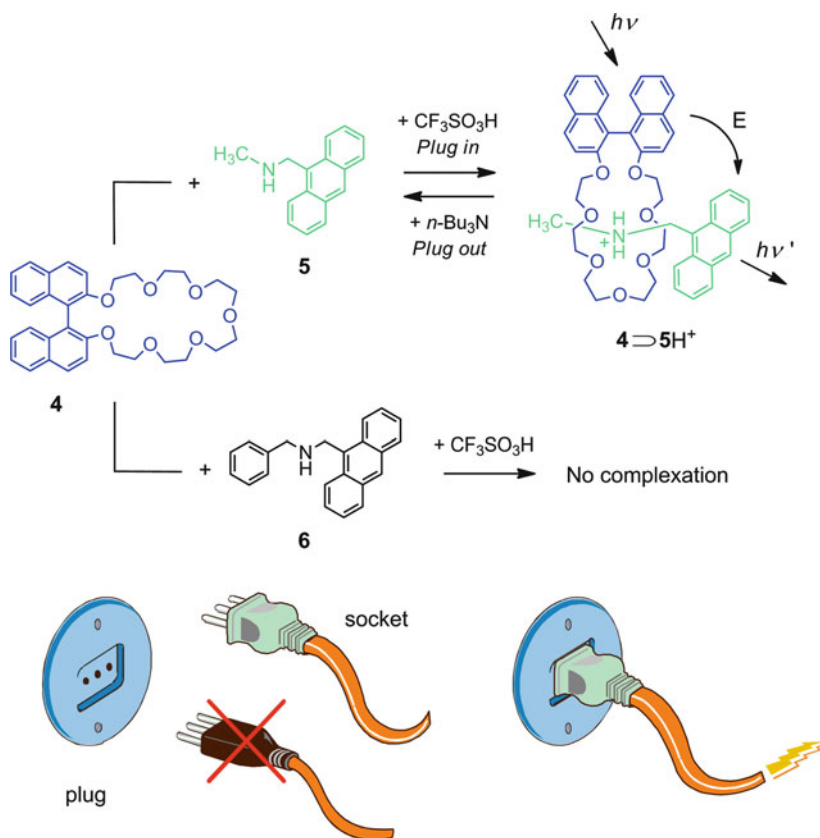


**Fig. 7** Molecular-level plug/socket system for energy transfer based on the reversible acid–base driven threading–dethreading motions in the hydrogen bonded pseudorotaxane  $4 \supset 5\text{H}^+$  ( $\text{CH}_2\text{Cl}_2$ ; room temperature). The acid-driven threading of compound **6**, incorporating a bulky benzyl group, through the macrocyclic cavity of **4** does not occur [57]

the absence of any interaction between the two compounds. Addition of a stoichiometric amount of acid causes profound changes in the fluorescence behavior of the solution, namely (1) the fluorescence of **4** is quenched, and (2) the fluorescence of **5-H<sup>+</sup>** is sensitized upon excitation with light absorbed exclusively by the crown ether. These observations show that a pseudorotaxane adduct, **4**⊃**5H<sup>+</sup>**, is formed wherein very efficient energy transfer takes place from the binaphthyl unit of the crown ether to the anthracenyl group incorporated in the component containing the dialkylammonium ion. Such a pseudorotaxane can be disassembled by the subsequent addition of a stoichiometric amount of base, thereby interrupting the photoinduced energy flow, as indicated by the fact that the initial absorption and fluorescence spectra are restored. Interestingly, the plug-in process does not take place when a plug component incompatible with the size of the socket, such as the benzyl-substituted amine **6**, is employed (Fig. 7).

## 7.2 Electrical Extension Cable at the Molecular Level

The plug-socket concept described above can be used to design molecular systems that mimic the function played by a macroscopic electrical extension cable. The operation of an extension cable is more complex than that of a plug/socket system, since it involves three components that must be held together by two connections that have to be controllable reversibly and independently; in the fully connected system, an electron (or electronic energy) flow must take place between the remote donor and acceptor units (Fig. 8).

A system of this type is made of the three components **7<sup>2+</sup>**, **8H<sup>+</sup>**, and **9<sup>2+</sup>** shown in Fig. 9a [58]. Component **7<sup>2+</sup>** consists of two moieties [59]: a [Ru(bpy)<sub>3</sub>]<sup>2+</sup> unit, which behaves as an electron donor under light excitation, and a dibenzo[24]crown-8 macrocycle, capable of playing the role of a hydrogen-bonding first socket. The second component **8H<sup>+</sup>** is made up [60] of a dialkylammonium ion, that can insert itself as a plug into a dibenzo[24]crown-8 socket by virtue of hydrogen-bonding

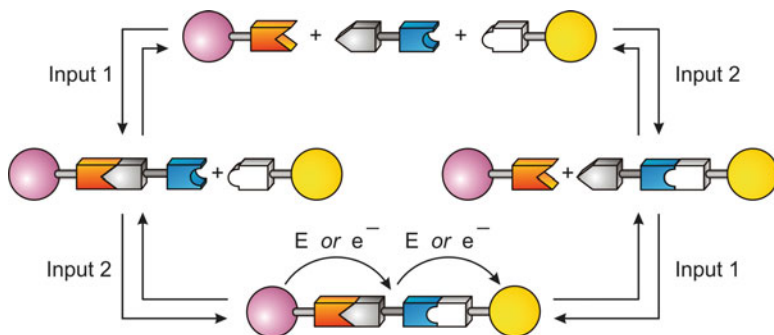


**Fig. 8** Working mechanism of an electrical extension cable

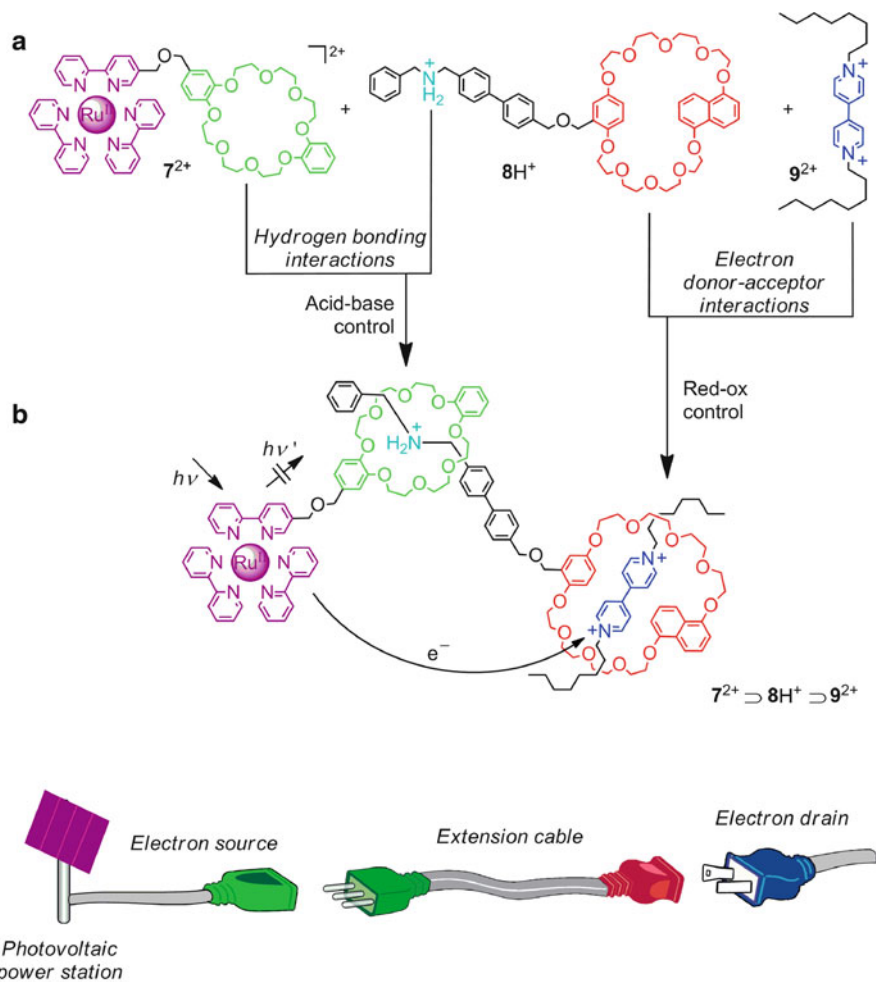


**Fig. 9** Chemical system for mimicking an electrical extension cable. Structural formulas of the three molecular components  $7^{2+}$ ,  $8H^+$  and  $9^{2+}$  (a), which self-assemble in solution ( $CH_2Cl_2$ ; room temperature) to give the  $7^{2+} \supset 8H^+ \supset 9^{2+}$  triad (b). In the fully connected system, excitation with visible light of the Ru-based unit of  $7^{2+}$  is followed by electron transfer to  $9^{2+}$ , with  $8H^+$  playing the role of an extension cable [58]

interactions, a biphenyl spacer, and a benzonaphtho[36]crown-10 unit, which fulfils the role of a  $\pi$ -electron-rich socket. Finally, the 1,1'-dioctyl-4,4'-bipyridinium dication  $9^{2+}$  can play the role of an electron drain plug. In  $CH_2Cl_2$  solution, reversible connection–disconnection of the two plug–socket junctions can be controlled independently by acid–base and redox stimulation, respectively, and monitored by changes in the absorption and emission spectra, owing to the different nature of the interactions (hydrogen bonding and  $\pi$ -electron donor–acceptor) that connect the components. In the fully assembled triad,  $7^{2+} \supset 8H^+ \supset 9^{2+}$ , light

excitation of the Ru-based unit of  $7^{2+}$  is followed by electron transfer to  $9^{2+}$ , with  $8H^+$  playing the role of an extension cable (Fig. 9b). The occurrence of this process is confirmed by nanosecond-laser flash-photolysis experiments, showing a transient absorption signal assigned to the 4,4'-bipyridinium radical cation formed by photoinduced electron transfer within the self-assembled triad. Interestingly, the extension cable component  $8H^+$  exists in a self-threaded conformation [60], that cannot host the electron drain until it is opened up by complexation with the socket unit of the source component. This feature, which can be viewed as a limitation because it reduces the efficiency, in fact plays the function of a safety-catch device. Moreover, the photoinduced electron-transfer process can be powered by sunlight because the  $7^{2+}$   $[Ru(bpy)_3]^{2+}$ -type component shows a broad and intense absorption band in the visible spectral region.

### 7.3 Dendrimers: Appealing Structures and Useful Compounds

Highly branched molecules having tree-like structures are called dendrimers from the Greek word *dendron* (Fig. 10). Like trees, dendrimers usually exhibit esthetically pleasant structures, but they are more interesting if they are able to produce “fruit,” i.e., to perform useful functions.

#### 7.3.1 Light-Harvesting Antennas

In the last 10 years, much attention has been devoted to the design and synthesis of dendrimers [61, 62] capable of playing the role of antennas (Fig. 11) in artificial

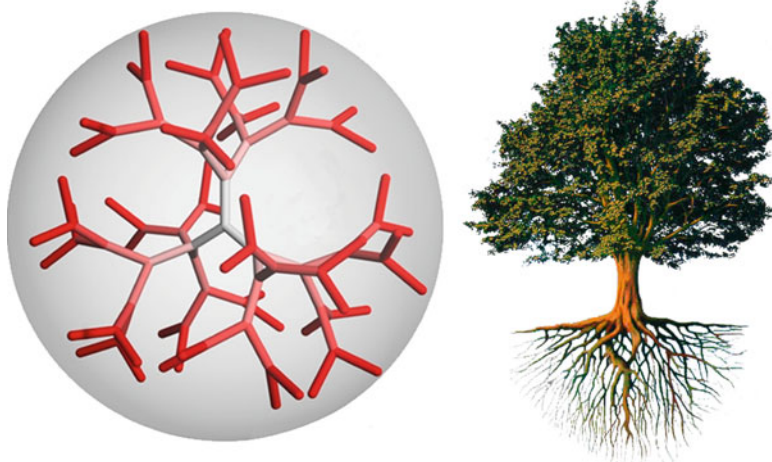


**Fig. 10** Dendrimers are highly branched molecules with a tree-like structure

**Fig. 11** Light-harvesting antenna

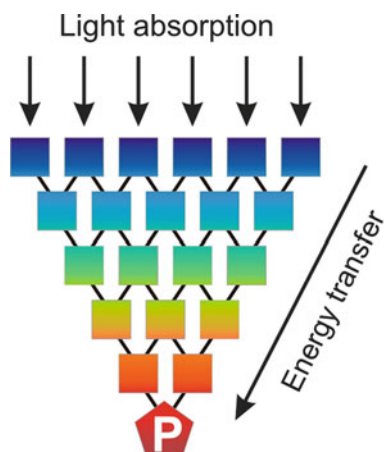
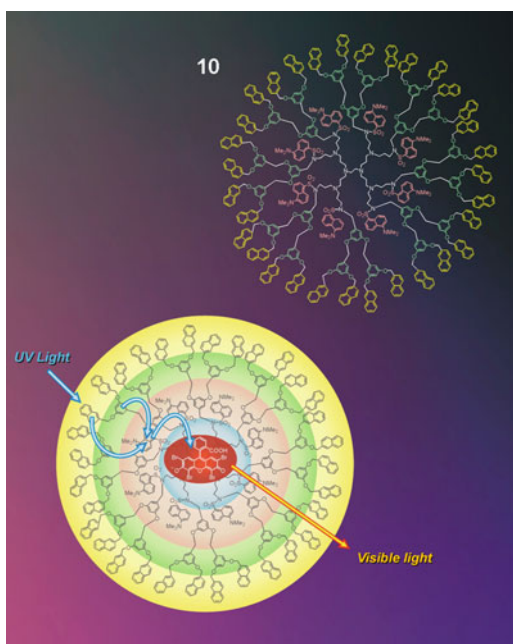


**Fig. 12** Structural formula of dendrimer **10** (*top*) and energy transfer occurring from the peripheral dimethoxybenzene and naphthalene units to the light-emitting dansyl unit (*bottom*) [63]



systems for the photochemical conversion of solar energy, like solar cells, and in the future for the development of an artificial photosynthesis.

Taking advantage of the dynamic cavities present in dendrimers, energy transfer from the numerous chromophoric units of a suitable dendrimer to a luminescent guest may be exploited to construct systems for light harvesting and for changing the light frequency. An advantage shown by such host–guest systems compared with dendrimers with a luminescent core is that the wavelength of the sensitized

emission can be tuned by changing the luminescent guest hosted in the same dendrimer.

An example of this behavior is exhibited by dendrimer **10** (Fig. 12, top). It consists of a hexamine core with appended four branches, which carry a great number of units capable of absorbing and emitting light. More specifically, this dendrimer contains eight dansyl-, 24 dimethoxybenzene-, and 32 naphthalene-type units [63]. Upon light absorption, energy transfer from the peripheral dimethoxybenzene and naphthalene units to the light-emitting dansyl unit occurs with high efficiency (>90%). When the dendrimer hosts a molecule of the eosin dye (Fig. 12, bottom), the dansyl light-emission is no longer observed and the characteristic emission of the eosin guest takes place instead. The encapsulated eosin molecule collects electronic energy from all the 64 light-absorbing units of the dendrimer (antenna effect), so that UV input signals are converted into visible output signals. By using different dyes, a fine tuning of the visible output signal can be achieved.

### 7.3.2 Molecular Batteries

A dendrimer consisting of multiple identical and non-interacting redox units, able to reversibly exchange electrons with another molecular substrate or an electrode, can perform as a molecular battery [64, 65]. The redox-active units should exhibit chemically reversible and fast electron transfer processes at easily accessible potential difference and chemical robustness under the working conditions.

Because of their reversible electrochemical properties, ferrocene and its methyl derivatives are the most common electroactive units used to functionalize dendrimers. A recently reported example of this class of dendrimers is constituted by giant redox dendrimers (see e.g., the 81-Fc second generation compound **11** shown in Fig. 13) with ferrocene and pentamethylferrocene termini up to a theoretical number of  $3^9$  tethers (seventh generation), evidencing that lengthening of the tethers is a reliable strategy to overcome the bulk constraint at the dendrimer periphery [66].

These redox metallodendrimers were investigated with a variety of techniques: (1) Cyclic voltammetry has revealed a full chemical and electrochemical reversibility up to the seventh generation with a single redox wave corresponding to the oxidation of all the ferrocene units at the same potential. (2) Coulometry has evidenced that the number of exchanged electrons is equal to the number of peripheral ferrocene units (the difference of 17% between the theoretical and experimental numbers found for the largest dendrimer was attributed to structural defects). (3) Chemical oxidation was used to isolate and characterize the blue 17-electron ferrocenium and deep-green mixed-valence Fe(III)/Fe(II) dendritic complexes. (4) Atomic force microscopy, employed to study the behavior of the dendrimers on a mica surface, enabled a comparison of the size of the oxidized cationic form of the dendrimers with that of their neutral form. For the fifth generation dendrimer it was found that the average height of the oxidized species ( $6.5 \pm 0.6$  nm) is much larger than that of its neutral form ( $4.5 \pm 0.4$  nm).

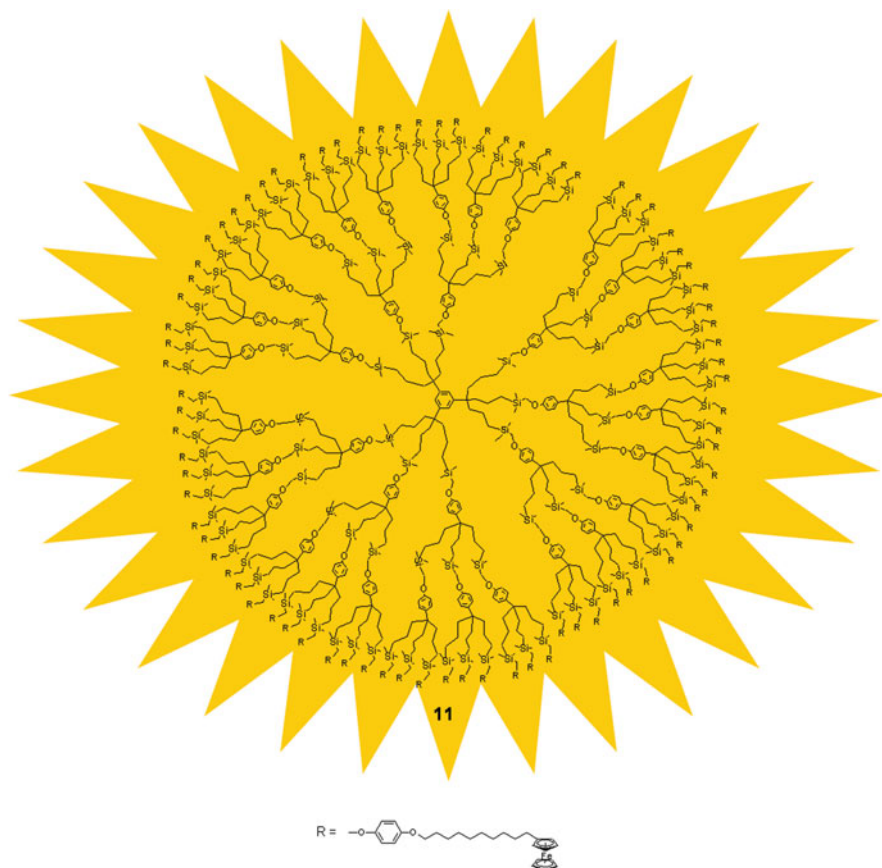


**Fig. 13** Structural formula of the second generation metallodendrimer **11** containing 81 ferrocene units at its periphery [66]

Thus, these giant redox metallodendrimers exhibit a “breathing mechanism” controlled by the redox potential.

A molecular battery behavior is also exhibited by polyviologen (viologen is commonly used to indicate 4,4'-bipyridinium-type units) dendrimers because of their capability of storing, at easy accessible potentials, a number of electrons twice that of the viologen units incorporated in the structure, as shown by the first investigations on this kind of compound [67, 68]. A different behavior, however, has been observed for two families of dendrimers that only differ in the peripheral groups (Fig. 14) [69–71]. Electrochemical experiments have indeed revealed that in all cases only a fraction of the viologen units can be reduced, and that this fraction corresponds (within experimental error) to the number of the viologen units present in the outer shell (six for **A9**<sup>18+</sup> and **B9**<sup>18+</sup>, and 12 for **A21**<sup>42+</sup> and **B21**<sup>42+</sup>). The electrochemical reduction experiments have also shown that in each dendrimer, the first reduction process of all its reducible viologen units occurs at the same potential

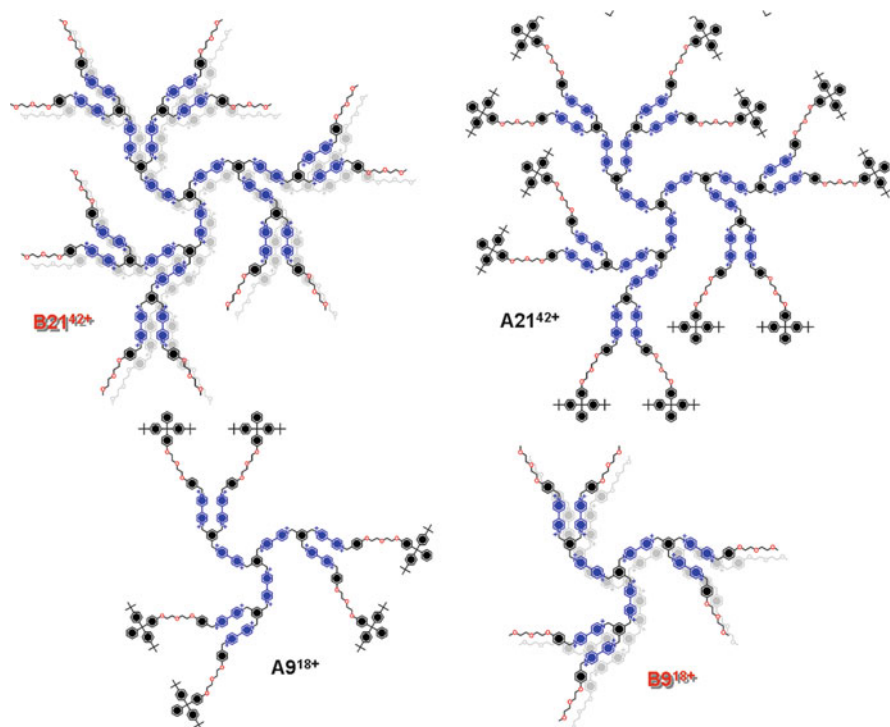


**Fig. 14** Structural formulas of two families of dendrimers containing a 1,3,5-trisubstituted benzenoid core and 9 ( $A9^{18+}$  and  $B9^{18+}$ ) and 21 ( $A21^{42+}$  and  $B21^{42+}$ ) viologen units in their branches [69–71]

and that the first reduction process of all the reducible viologen units in all the dendrimers occurs at the same potential. An interesting result is that the reduction potential of a reducible unit is not affected by the state of the other reducible units, which is an ideal property for a charge pooling system. Photosensitized reduction experiments have shown that the numbers of viologen units photochemically reducible are in reasonable agreement with those obtained by electrochemical experiments, confirming that only the viologens in the external shells can be reduced. Photosensitized reduction experiments have also revealed that formation of the one-electron reduced viologen units is accompanied by their dimerization, a well-known process called pimerization [72] and already observed in viologen-based dendrimers [67, 68, 73].

## 8 Molecular Machines

The development of civilization has always been strictly related to the design and construction of devices, from wheel to jet engine, capable of facilitating man's movement and travelling. Nowadays the miniaturization race leads scientists to



investigate the possibility of designing and constructing machines at the nanometer scale, i.e., at the molecular level. Molecular machines are already present in Nature (e.g., ATP synthase) [74], but they are extremely complex systems; any attempt to construct systems of such a complexity by using the bottom-up molecular approach would be hopeless. At present what can be done in the field of artificial molecular-level machines is to construct simple prototypes consisting of a few molecular components, capable of moving in a controllable way.

### 8.1 Linear Movements in Rotaxanes

A rotaxane is a supramolecular system composed of a macrocyclic and a dumbbell-shaped component. The macrocycle encircles the linear rod-like portion of the dumbbell-shaped component and is trapped mechanically around it by two bulky stoppers. Thus, the two components cannot dissociate, but the ring component can shuttle along the axis component (Fig. 15).

When the dumbbell component contains two different recognition sites (stations) for the macrocycle, a shuttling process between the two states 0 and 1 can be induced by external energy stimulation [39, 40]. Rotaxanes are, therefore, appealing systems for the construction of linear molecular machines that, depending on the nature of the energy inputs, can be photochemically, chemically, or electrochemically driven. It is important to add that the controlled shuttling movement in a rotaxane is interesting not only from a mechanical viewpoint, but also for information processing at the molecular level.

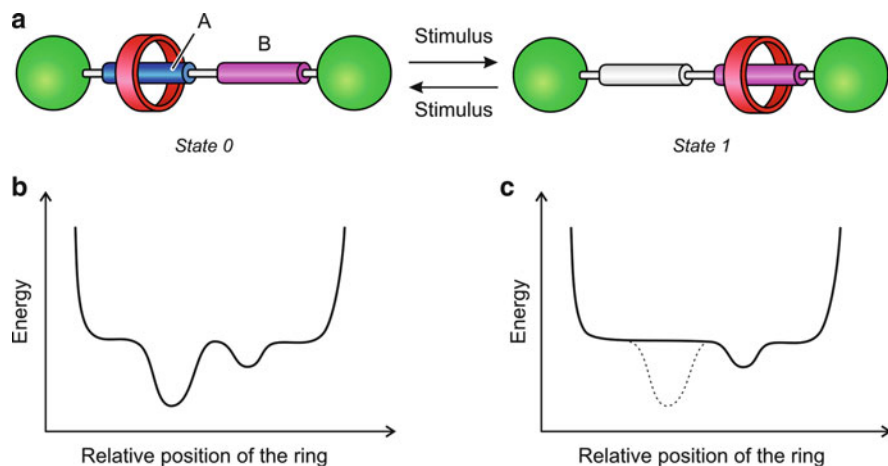


**Fig. 15** (a) Two-station rotaxane and its operation as a controllable molecular shuttle. *A* and *B* are the two different recognition sites. (b, c) Idealized representations of the potential energy of the system as a function of the position of the ring relative to the axle before (b) and after (c) switching off station *A*

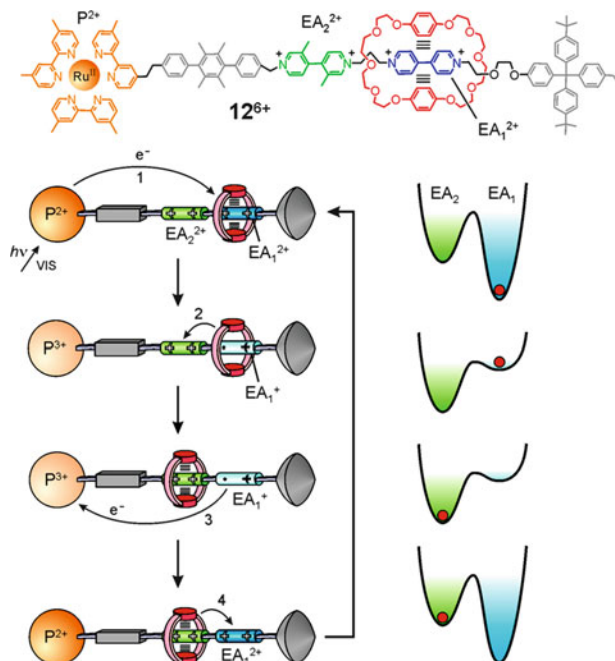


**Fig. 16** Structural formula of rotaxane  $12^{6+}$  (top) and intramolecular working mechanism for the photochemically induced ring shuttling (bottom). Right: Potential energy profile for each molecular structure illustrated on the left [75, 76]. Steps 1–4 are described in the text

As an example of rotaxanes in which the ring shuttling is photochemically driven, rotaxane  $12^{6+}$  [75, 76] (Fig. 16) is briefly discussed. It is a carefully designed multicomponent system that upon light stimulation behaves as a four-stroke linear motor. It is made of the electron-donor macrocycle, and a dumbbell-shaped component that contains  $[\text{Ru}(\text{bpy})_3]^{2+}$  ( $\text{P}^{2+}$ ) as one of its stoppers, a *p*-terphenyl-type ring system as a rigid spacer, a 4,4'-bipyridinium unit ( $\text{EA}_1^{2+}$ ) and a 3,3'-dimethyl-4,4'-bipyridinium unit ( $\text{EA}_2^{2+}$ ) as electron-accepting stations, and a tetraarylmethane group as the second stopper.

The stable translational isomer is the one in which the ring component encircles the  $\text{EA}_1^{2+}$  unit, as expected because this station is a better electron acceptor than the other. The photoinduced ring shuttling between the two station occurs with an intramolecular working mechanism (Fig. 16) based on the following four operations [76]:

1. *Destabilization of the stable translational isomer.* Light excitation of the photoactive unit  $\text{P}^{2+}$  is followed by transfer of an electron from the excited state to the  $\text{EA}_1^{2+}$  station, which is encircled by the ring (step 1), with the consequent deactivation of this station; such a photoinduced electron-transfer process must compete with the intrinsic decay of the excited state of  $\text{P}^{2+}$ .

2. *Ring displacement.* The ring moves from the reduced station  $EA_1^+$  to  $EA_2^{2+}$  (step 2), a step that must compete with the back-electron-transfer process from  $EA_1^+$  (still encircled by ring) to the oxidized photoactive unit  $P^{3+}$ . This is the most difficult requirement to meet in the intramolecular mechanism.
3. *Electronic reset.* A back electron-transfer process from the free reduced station  $EA_1^+$  to  $P^{3+}$  (step 3) restores the electron-acceptor power to the  $EA_1^{2+}$  station.
4. *Nuclear reset.* As a consequence of the electronic reset, back movement of the ring from  $EA_2^{2+}$  to  $EA_1^{2+}$  occurs (step 4).

Each absorbed photon could, in principle, cause the occurrence of a forward and back ring movement (i.e., a full cycle) without generation of any waste product. In practice, the efficiency is very low, because 84% of the excited  $*P^{2+}$  species undergoes deactivation in competition with electron transfer (step 1), and 88% of the reduced  $EA_1^+$  species undergoes back electron transfer before ring displacement (step 2) can occur [77]. The somewhat disappointing quantum efficiency for ring shuttling (2%) is compensated by the fact that the investigated system is a unique example of an artificial linear nanomachine, because it gathers together the following features: (1) it is powered by visible light (in other words, sunlight); (2) it exhibits autonomous behavior, like motor proteins; (3) it does not generate waste products; (4) its operation can rely only on intramolecular processes, allowing in principle operation at the single-molecule level; (5) it can be driven at a frequency

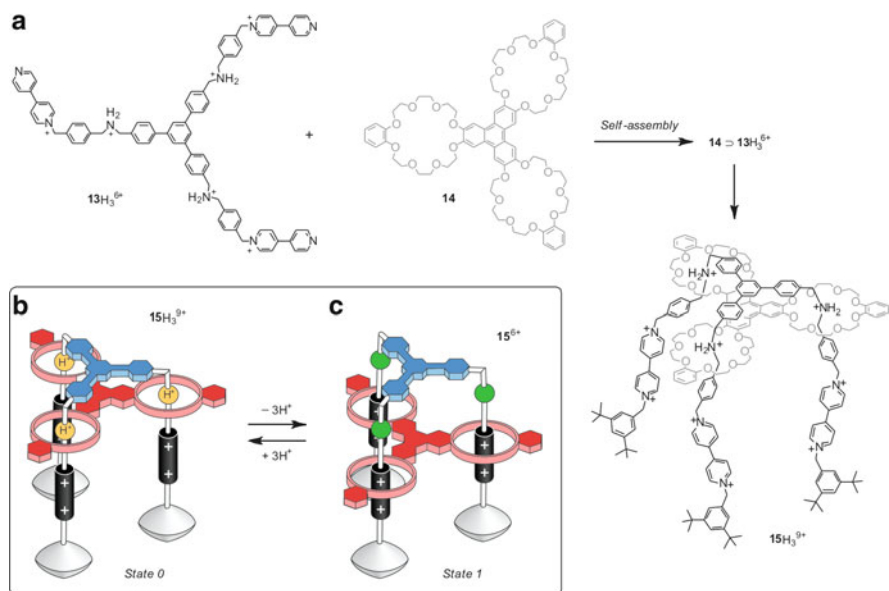


**Fig. 17** (a) Self-assembly of the triply threaded supramolecular system  $14 \supset 13H_3^{6+}$  and the subsequent synthesis of the triply interlocked species  $15H_3^{9+}$ . (b, c) Operation of  $15H_3^{9+}$  as an acid-base controlled molecular elevator [78–80]

of  $\sim 1$  kHz; (6) it works in mild environmental conditions (i.e., fluid solution at ambient temperature); and (7) it is stable for at least  $10^3$  cycles.

A chemically driven rotaxane-based molecular machine, fascinating from the structural viewpoint, has been obtained by extending the idea of a one-dimensional two-station dumbbell to a three-dimensional system [78]. It is made of the trifurcated compound  $13\text{H}_3^{6+}$ , which contains two stations in each of its three arms (Fig. 17a) threaded into the tritopic receptor **14**, in which three benzo[24] crown-8 macrorings are fused on to a triphenylene core. The assembled system  $14 \supset 13\text{H}_3^{6+}$  was then converted into the rotaxane species  $15\text{H}_3^{9+}$  by functionalization with bulky groups [79, 80]. This compound, which behaves like a nanometer-scale elevator, is  $\sim 2.5$  nm in height and has a diameter of  $\sim 3.5$  nm. It consists of a tripod component containing two different notches – one ammonium center and one 4,4'-bipyridinium unit – at different levels in each of its three legs. Such legs are interlocked by the tritopic host, which plays the role of a platform that can be made to stop at the two different levels. Initially, the platform resides exclusively on the “upper level,” i.e., with the three rings surrounding the ammonium centers (Fig. 17b, state 0). Because the molecular elevator operates in solution, i.e., with no control of the orientation of the molecules relative to a fixed reference system, the words “upper” and “lower” are used only for descriptive purposes. On addition of a strong, non-nucleophilic phosphazene base to an acetonitrile solution of  $15\text{H}_3^{9+}$ , deprotonation of the ammonium center occurs and, as a result, the platform moves to the lower level, i.e., with the three crown ether rings surrounding the bipyridinium units (Fig. 17c, state 1). The distance travelled by the platform is  $\sim 0.7$  nm and the potential force that can be generated is 200 pN, which is more than one order of magnitude larger than that generated by natural linear motors like kinesin. This structure is stabilized mainly by charge-transfer interactions between the electron-rich aromatic units of the platform and the electron-deficient bipyridinium units of the tripod component. Subsequent addition of acid to  $15^{6+}$  restores the ammonium centers, and the platform moves back to the upper level. The “up and down” elevator-like motion can be repeated many times, can be monitored by  $^1\text{H}$  NMR spectroscopy, electrochemistry, and absorption and fluorescence spectroscopy [79, 80]. Detailed spectroscopic investigations have shown that the platform operates by taking three distinct steps associated with each of the three deprotonation processes. In this regard, the molecular elevator is more reminiscent of a legged animal than it is of a passenger or freight elevator.

The base–acid controlled mechanical motion in  $15\text{H}_3^{9+}$  is associated with interesting structural modifications, such as the opening and closing of a large cavity (1.5 nm by 0.8 nm) and the control of the positions and properties of the bipyridinium legs. This behavior can in principle be used to control the uptake and release of a guest molecule, a function of interest for the development of drug delivery systems.

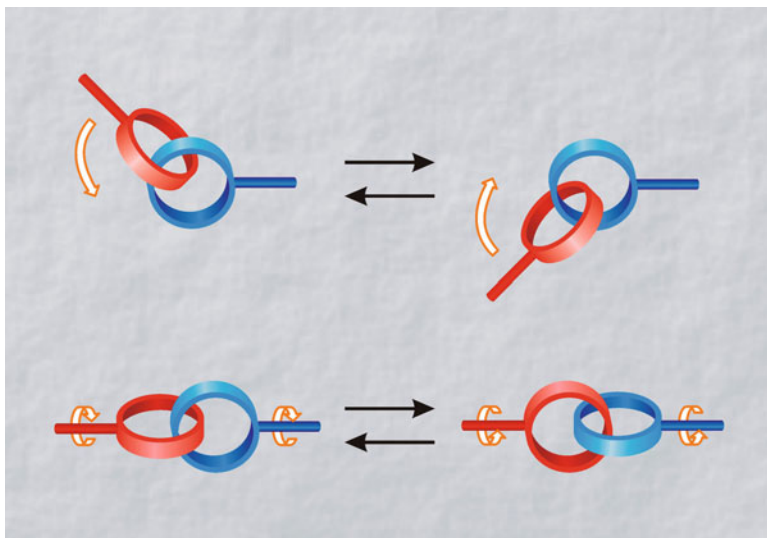


**Fig. 18** Mechanical movements of one ring relative to the other in a catenane, which from a macroscopic viewpoint are reminiscent of movements of a “ball and socket joint” (*top*) and of a “universal joint” (*bottom*)

## 8.2 Ring Movements in Catenanes

A catenane is a molecule composed of two or more interlocked macrocyclic components. From a macroscopic mechanical viewpoint the movement of one ring relative to the other in a catenane is reminiscent of a “ball and socket joint” (Fig. 18, top) [81]. Similarly, twisting of one ring around the main axis of the catenane forces the other ring to rotate in the same direction in a manner reminiscent of an “universal joint” (Fig. 18, bottom) [81].

As already pointed out in the case of rotaxanes, mechanical movements can also be induced in catenanes by chemical, electrochemical, and photochemical stimulation. Catenanes  $16^{4+}$  and  $17^{4+}$  (Fig. 19) are examples of systems in which the conformational motion can be controlled electrochemically [82, 83]. They are made of a symmetric electron acceptor, tetracationic cyclophane, and a desymmetrized ring comprising two different electron donor units, namely a tetrathiafulvalene (TTF) and a dimethoxybenzene (DOB) ( $16^{4+}$ ) or a dimethoxynaphthalene (DON) ( $17^{4+}$ ) unit. Because the TTF moiety is a better electron donor than the dioxyarene units, as witnessed by the potentials values for their oxidation, the thermodynamically stable conformation of these catenanes is that in which the symmetric cyclophane encircles the TTF unit of the desymmetrized macrocycle (Fig. 19a, state 0).

Monoelectronic oxidation of the TTF unit is accompanied by the circumrotation of the desymmetrized ring through the cavity of the tetracationic cyclophane. Indeed, after oxidation, the newly formed monocationic tetrathiafulvalene unit

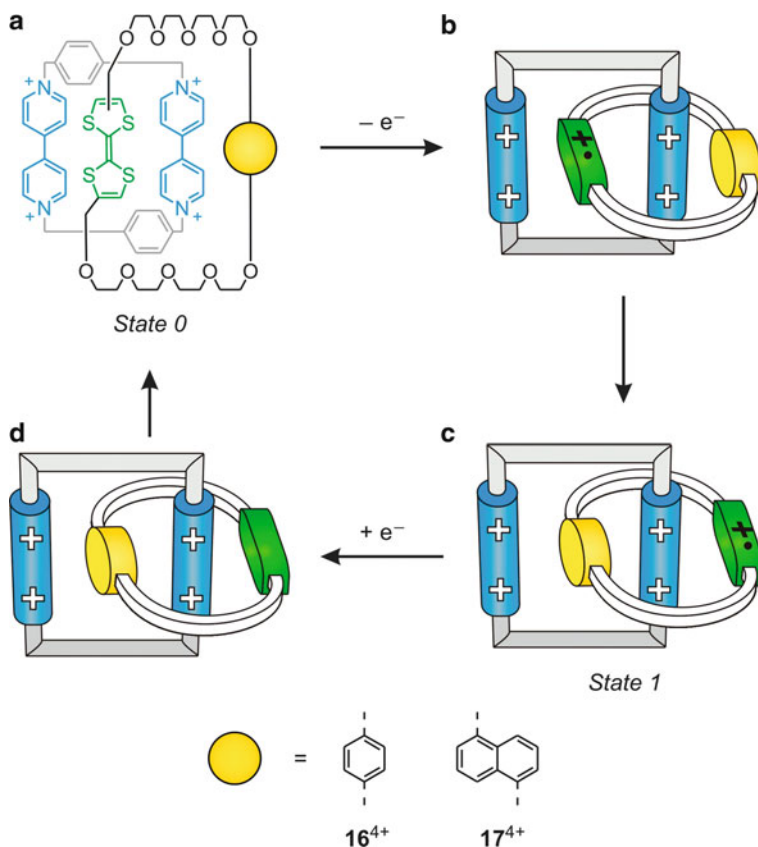


**Fig. 19** Redox controlled ring rotation in catenanes  $16^{4+}$  and  $17^{4+}$ , which contain a symmetric electron-acceptor cyclophane and a desymmetrized electron-donor ring [82, 83]. Steps *a–d* are explained in the text

(Fig. 19b) loses its electron-donor power; as a consequence it is expelled from the cavity of the tetracationic cyclophane and is replaced by the neutral dioxyarene unit (Fig. 19c, state 1). Back-reduction of the TTF unit restores the original conformation (Fig. 19d) as the neutral TTF unit replaces the dioxyarene unit inside the cavity of the tetracationic cyclophane. Ring rotation in these catenanes can also be obtained chemically. The tendency of *o*-chloranil to stack against TTF has been indeed exploited [82, 83] to lock this unit alongside the cavity of the tetracationic cyclophane. On addition of a mixture of  $\text{Na}_2\text{S}_2\text{O}_5$  and  $\text{NH}_4\text{PF}_6$  in  $\text{H}_2\text{O}$ , the adduct formed between the TTF unit and *o*-chloranil is destroyed, and the original conformation with tetrathiafulvalene inside the cavity of the tetracationic cyclophane is then restored.

Catenane  $17^{4+}$  was also incorporated in a solid state device that could be used for random access memory (RAM) storage [84, 85]. Additionally, this compound

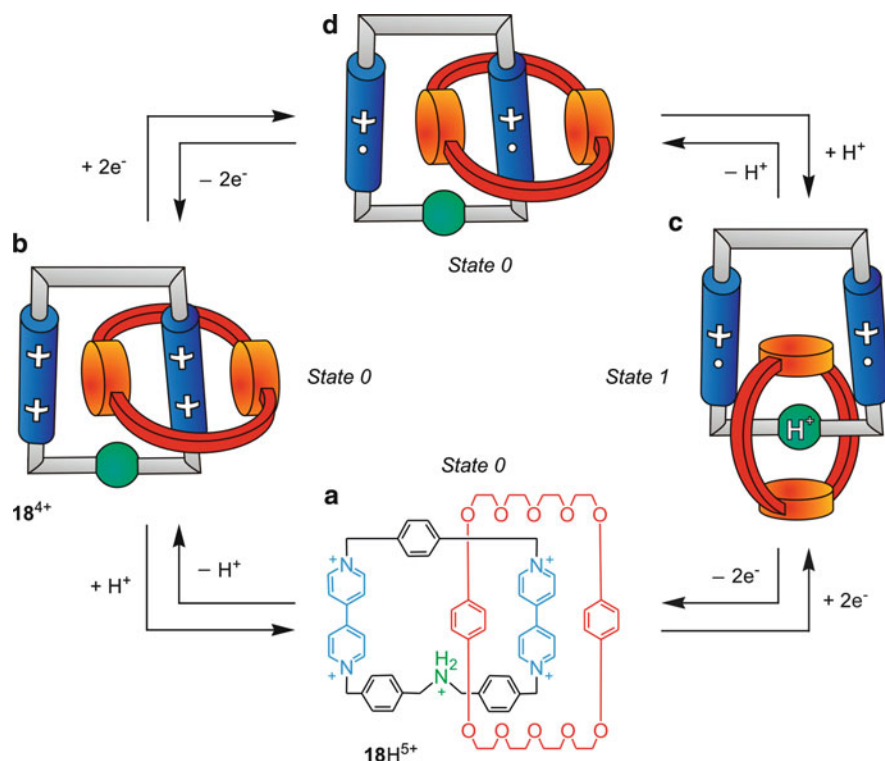


**Fig. 20** Switching processes of catenane  $18H^{5+}$ . In the deprotonated catenane  $18^{4+}$ , the position of the ring switches are under acid–base and redox inputs according to AND logic [87]. Steps *a–d* are explained in the text

could be employed for the construction of electrochromic systems, because its various redox states are characterized by different colors [82, 83, 86].

By an appropriate choice of the functional units that are incorporated in the catenane components, more complex functions can be obtained. An example is represented by catenane  $18H^{5+}$  (Fig. 20), composed of a symmetric crown ether and a cyclophane ring containing two bipyridinium and one ammonium recognition sites [87]. The electrochemical properties, as well as the absorption spectra, show that the crown ether surrounds a bipyridinium unit of the other ring both in  $18H^{5+}$  (Fig. 20a) and in its deprotonated form  $18^{4+}$  (Fig. 20b), indicating that deprotonation–protonation of the ammonium unit does not cause any displacement of the ring (state 0). Electrochemical measurements also show that, after one-electron reduction of both the bipyridinium units of  $18H^{5+}$ , the ring is displaced on the ammonium function (Fig. 20c, state 1), which means that an electrochemically induced conformational switching does occur. Furthermore, upon deprotonation of the two-electron reduced form of the catenane (Fig. 20d), the crown ether moves to one of the monoreduced bipyridinium units (state 0). Therefore, in order to achieve the motion

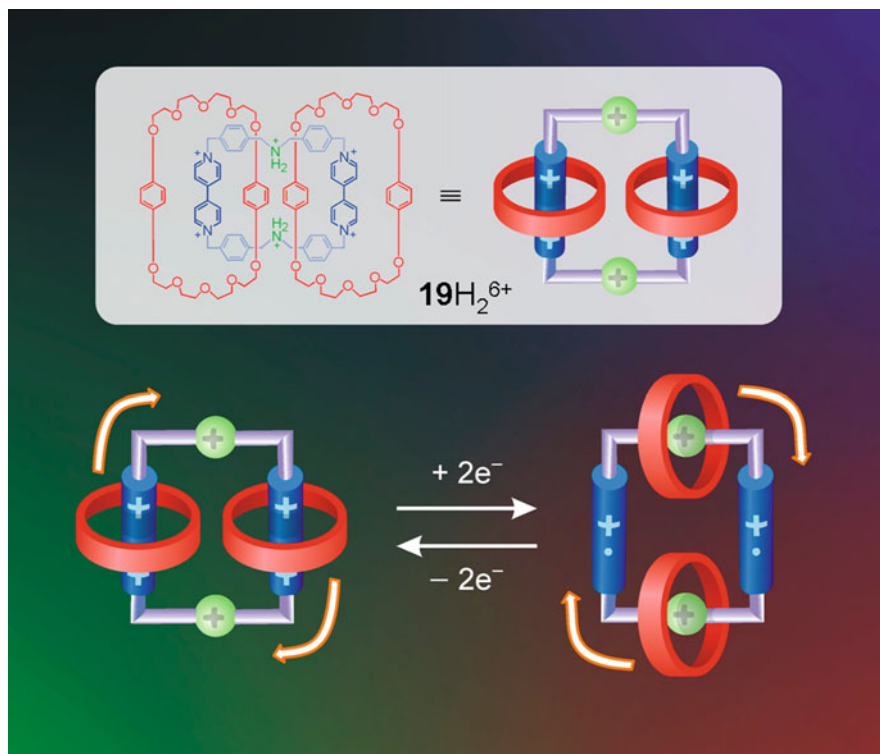


**Fig. 21** Redox controlled movements of the ring components in catenane  $19H_2^{6+}$ , composed of three interlocked macrocycles. These motions are obtained upon reduction–oxidation of the bipyridinium units of the cyclophane [87]

of the ring in the deprotonated catenane  $18^{4+}$ , it is necessary *both* to reduce (switch off) the bipyridinium units *and* protonate (switch on) the amine function. The mechanical motion in such a catenane occurs according to an AND logic [88], a function associated with two energy inputs of different nature.

Controlled rotation of the molecular rings has also been achieved in catenanes composed of three interlocked macrocycles. For example, catenane  $19H_2^{6+}$  (Fig. 21) is made up of two identical dioxybenzene-based macrocycles interlocked with a cyclophane containing two bipyridinium and two ammonium units [87].

Because of the type of the macrocycles used, the stable conformation of  $19H_2^{6+}$  is that in which the two rings surround the bipyridinium units. Upon addition of one electron in each of the bipyridinium units, the two macrocycles move on the ammonium stations, and move back to the original position when the bipyridinium units are reoxidized.

It should be remarked that for the described catenanes, but also for most of the catenane-based machines developed so far, the repeated switching between the two translational states does not need to occur through a full rotation. In fact, because of



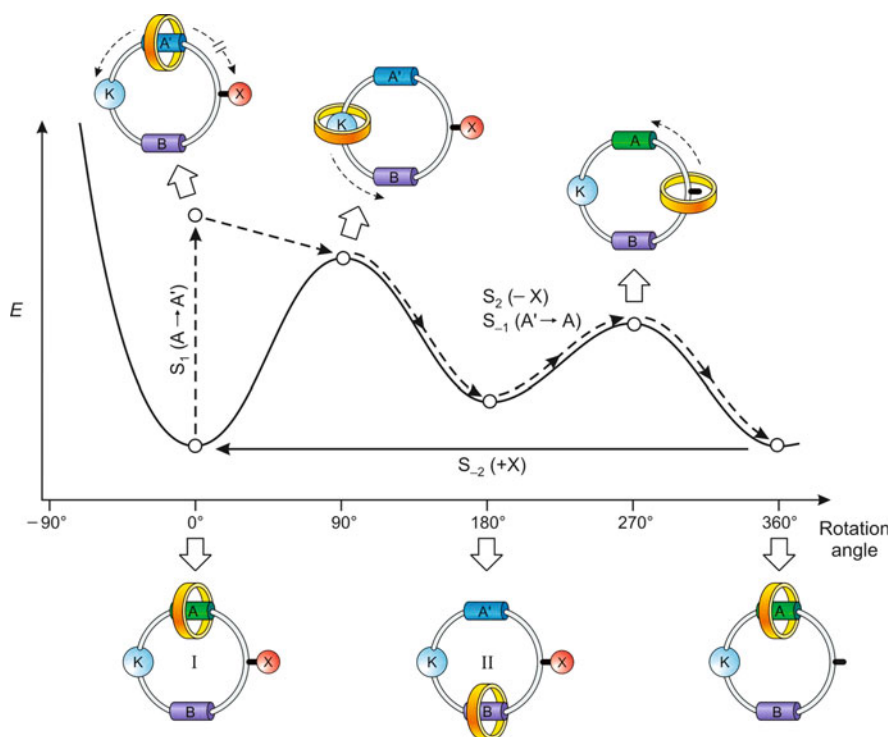


**Fig. 22** Design of a bistable catenane that performs as a molecular rotary motor controlled by two pairs of independent stimuli ( $S_1$  and  $S_2$ ). The working scheme is based on the potential energy changes expected for the chemical reactions and co-conformational rearrangements brought about by stimulation with independent inputs. A, B recognition sites; A' site A is switched on, K hindering group, X blocking group

the intrinsic symmetry of the system, both movement from the initial state to the final state and that from the final state to the initial state can occur with equal probabilities along a clockwise or anticlockwise direction. A unidirectional full ( $360^\circ$ ) rotation movement can be obtained only in ratchet-type systems (i.e., in the presence of dissymmetry elements, which can be structural or functional in nature) and requires a careful design of the system [52, 89, 90]. A bistable catenane can be a starting point to make a rotary motor, but an additional control element has to be added, as illustrated in Fig. 22 [49]. The track ring of the catenane should contain, besides two different recognition sites A and B, a hindering group K, and a blocking group X. In the starting co-conformation (I), the “moving” ring surrounds the most efficient site (A) on the track ring. On application of the stimulus  $S_1$ , site A is switched off ( $A'$ ) and the ring moves from it. The system has to reach the new stable co-conformation II wherein the ring surrounds site B. The presence of a blocking group X makes anticlockwise rotation faster than clockwise rotation. At this stage, application of stimulus  $S_2$  causes the cleavage of the blocking group, and a reset

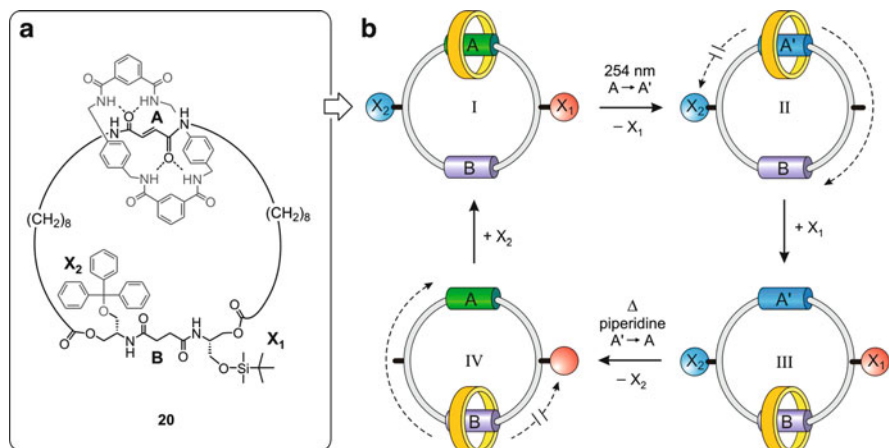


**Fig. 23** (a) Structural formula of catenane **20**. (b) Processes that enable unidirectional ring rotation [92]. A, B recognition sites;  $X_1$ ,  $X_2$  blocking groups

stimulus  $S_{-1}$  restores the recognition ability of site A. The system has now to reach the starting co-conformation wherein the moving ring surrounds site A. The presence of the hindering group K again makes anticlockwise rotation faster than clockwise rotation. The original catenane structure is then obtained with a reset stimulus  $S_{-2}$ , by which the blocking group X is put back in place. Unidirectional rotation in such a catenane occurs by a “flashing ratchet” mechanism [90, 91], which is based on a periodic change of the potential energy surface viewed by the moving part (Fig. 22) by orthogonal (i.e., independent) reactions. It is worth noting that the direction of rotation can be inverted by reversing the order of the two input stimuli.

This concept was cleverly realized using light as a stimulus with catenane **20** shown in Fig. 23a [92]. Its larger ring contains two recognition sites for the smaller ring – namely, a photoisomerizable fumaramide unit (A) and a succinamide unit (B) – and two bulky substituents that can be selectively detached and reattached – namely, a silyl ( $X_1$ ) and a triphenylmethyl ( $X_2$ ) group. In the starting isomer (I in Fig. 23b), the smaller ring surrounds the fumaramide site. On  $E \rightarrow Z$  photoisomerization of such a unit with 254 nm light and subsequent desilylation (II in Fig. 23b), the smaller ring moves in the clockwise direction to surround the succinamide site. At this point, a silyl group is reattached at the original position (III in Fig. 23b). Piperidine-assisted back-isomerization of the maleamide unit to the fumaramide unit, followed by removal of the triphenylmethyl group (IV in Fig. 23b), causes another half-turn of the smaller ring in the clockwise direction to surround the fumaramide unit. Reattachment of a triphenylmethyl substituent regenerates the starting isomer (I in Fig. 23b). The overall result is a net clockwise rotation of the smaller ring about the larger one. Exchanging the order in which the two blocking groups are manipulated produces an equivalent anticlockwise rotation of the smaller ring. The structures of the compounds obtained after each of the above reaction steps, and particularly the position of the smaller ring, were determined by  $^1\text{H}$  NMR

spectroscopy [92]. This system is more complex than that described in Fig. 22 because it contains two independently addressable blocking groups. Hence, unidirectional rotation is achieved with three pairs of different stimuli (one for driving the co-conformational rearrangement, and two for the ratcheting of the energy barriers).

The time scales and number of reactions involved for unidirectional ring rotation in catenane **20** and in other similar catenanes [93] make their operation as rotary motors somewhat unpractical. Nevertheless, analysis of the thermodynamic and kinetic aspects of the operation mechanisms provides a fundamental insight on how energy inputs can be used to harness thermal fluctuations and drive unidirectional motion.

## 9 Conclusions

Chemistry is inside and around us: all the processes that sustain life are based on chemical reactions, and most things we use in everyday life are natural (e.g., water, wheat, oil, wood) or artificial (plastics, glass, medicines, pesticides) molecules. For these reasons Chemistry is a central science. Its importance and extension can be better perceived by a comparison with language. Molecules, the words of matter, are the smallest entities that have distinct shapes, sizes and properties. Like words, molecules contain specific pieces of information that are revealed when they interact with one another.

Much more complex functions can be achieved by assembling molecules into supramolecular systems. Upon excitation with chemical species, electrons, and photons, suitably designed supramolecular systems can indeed perform a variety of useful functions related to energy- and electron-transfer processes and to mechanical movements.

Besides being important and useful, Chemistry has also a beautiful side that has inspired writers, poets, and sculptors. Chemistry is a wonderful book that continues to expand every day: new ideas and new concepts are developed, previously unknown natural molecules are discovered, novel artificial molecules are synthesized, more complex supramolecular species are assembled, and more and more interesting molecular devices and machines are created.

**Acknowledgments** Authors acknowledge Alberto Credi for fruitful discussion and artistic suggestions. Support by Alma Mater Studiorum – Università di Bologna, Ministero dell'Università e della Ricerca (PRIN 2008HZJW2L), and Fondazione CARISBO is gratefully acknowledged.

## References

1. Greenberg A (2003) *The art of chemistry – Myths, medicine, and materials*. Wiley, Hoboken
2. Smith MF (2001) *Lucretius: on the nature of things*. Hackett, Indianapolis/Cambridge
3. *The literary works of Leonardo da Vinci*, compiled and edited from the original manuscripts by Richter J-P, commentary by Pedretti C (1977) Phaidon, Oxford, p 102

4. Balzani V, Scandola F (1991) *Supramolecular photochemistry*. Horwood, Chichester
5. Vögtle F (1992) *Fascinating molecules in organic chemistry*. Wiley, Chichester
6. Hopf H (2000) *Classics in hydrocarbon chemistry. Syntheses, concepts, perspectives*. Wiley-VCH, Weinheim
7. Timmerman P, Verboom W, Van Veggel FCJM, Vanhoorn WP, Reinhoudt DN (1994) *Angew Chem Int Ed Engl* 33:1292–1295
8. Lawson JM, Paddon-Row MN (1993) *J Chem Soc Chem Commun* 1641–1643
9. Soi A, Hirsch A (1998) *New J Chem* 22:1337–1339
10. Levi P (2000) *The periodic table*. Penguin, London, p 149
11. Béla V (1990) *Chemistry in sculptures*. <http://www.vizibela.hu/>. Last accessed 8 Sept 2011
12. Feynman RP (1969) *Phys Teach* 7:313–320
13. Levi P (1995) *The monkey's wrench*. Penguin, New York, pp 142–143
14. Levi P (2000) *The periodic table*. Penguin, London, pp 189–191
15. Hoffmann R (2011) *Clin Chem* 57:144
16. Breslow R (1997) *Chemistry today and tomorrow – The central, useful, and creative science*. American Chemical Society and Jones and Bartlett Publishers, Washington DC
17. Balzani V, Credi A, Venturi M (2008) *Chem Eur J* 14:26–39
18. Lehn J-M (1995) *Supramolecular chemistry: concepts and perspectives*. VCH, Weinheim
19. Lehn J-M (2007) *Chem Soc Rev* 36:151–160
20. de Silva AP, Uchiyama S (2007) *Nat Nanotechnol* 2:399–410
21. Chichak KS, Cantrill SJ, Pease AR, Chiu S-H, Cave GWV, Atwood JL, Stoddart JF (2004) *Science* 304:1308–1312
22. de Silva AP, Gunaratne HQN, McCoy CP (1993) *Nature* 364:42–44
23. de Silva AP, Gunaratne HQN, Gunnlauugsson T, Huxley AJM, McCoy CP, Rademacher JT, Rice TE (1997) *Chem Rev* 97:1515–1566
24. Tian H, Wang QC (2006) *Chem Soc Rev* 35:361–374
25. Raymo FM, Tomasulo M (2006) *Chem Eur J* 12:3186–3193
26. Pischel U (2007) *Angew Chem Int Ed Engl* 46:4026–4040
27. Szacilowski K (2008) *Chem Rev* 108:3481–3548
28. Balzani V, Credi A, Venturi M (2008) *Molecular devices and machines – Concepts and perspectives for the nanoworld*, 2nd edn. Wiley-VCH, Weinheim, pp 259–311
29. Pimentel GC, Coonrod AJ (1985) *Opportunities in chemistry*. National Academy of Sciences, National Academy Press, Washington
30. Credi A (2007) *Angew Chem Int Ed Engl* 46:5472–5475
31. Ceroni P, Bergamini G, Balzani V (2009) *Angew Chem Int Ed Engl* 48:8516–8518
32. Juris A, Balzani V, Barigelletti F, Campagna S, Belser P, von Zelewsky A (1988) *Coord Chem Rev* 84:85–277
33. Campagna S, Puntoriero F, Nastasi F, Bergamini G, Balzani V (2007) *Top Curr Chem* 280:117–214
34. Webb R (2006) *Nature* 443:39
35. de Silva AP, James MR, McKinney BOF, Pears DA, Weir SM (2006) *Nat Mater* 5:787–789
36. Muramatsu S, Kinbara K, Taguchi H, Ishii N, Aida T (2006) *J Am Chem Soc* 128:3764–3769
37. Benenson Y, Paz-Elizur T, Adar R, Keinan E, Livneh Z, Shapiro E (2001) *Nature* 414:430–434
38. Benenson Y, Gil B, Ben-Dor U, Adar R, Shapiro E (2004) *Nature* 429:423–429
39. Balzani V, Venturi M, Credi A (2003) *Molecular devices and machines: a journey into the nanoworld*, 1st edn. Wiley-VCH, Weinheim
40. Balzani V, Credi A, Venturi M (2008) *Molecular devices and machines: concepts and perspectives for the nanoworld*, 2nd edn. Wiley-VCH, Weinheim
41. Hoffmann R (1995) Nobel chemist on nanotechnology. *Foresight Update* 20 <http://www.foresight.org/Updates/Update20/Update20.1.html#anchor176004>. Accessed 23 June 2011
42. Stoddart JF (ed) (2001) *Special issue on molecular machines*. *Acc Chem Res* 34(6):409–522
43. Sauvage J-P (ed) (2001) *Molecular machines and motors. Structure and bonding*, vol 99. Springer, Berlin

44. Flood AH, Ramirez RJA, Deng WQ, Muller RP, Goddard WA III, Stoddart JF (2004) *Aust J Chem* 57:301–322
45. Kelly TR, Sestelo JP (2005) Rotary motion in single-molecule machines. In: Sauvage J-P (ed) *Molecular machines and motors. Structure and bonding*, vol 99. Springer, Berlin
46. Sauvage J-P (2005) *Chem Commun*:1507–1510
47. Kinbara K, Aida T (2005) *Chem Rev* 105:1377–1400
48. Kottas GS, Clarke LI, Horinek D, Michl J (2005) *Chem Rev* 105:1281–1376
49. Balzani V, Credi A, Silvi S, Venturi M (2006) *Chem Soc Rev* 35:1135–1149
50. Browne WR, Feringa BL (2006) *Nat Nanotech* 1:25–35
51. Balzani V, Credi A, Venturi M (2007) *Nano Today* 2:18–25
52. Kay ER, Leigh DA, Zerbetto F (2007) *Angew Chem Int Ed Engl* 46:72–191
53. Credi A, Tian H (eds) (2007) Special issue: molecular machines and switches. *Adv Funct Mater* 17(5):671–840
54. Mateo-Alonso A, Guldi DM, Paolucci F, Prato M (2007) *Angew Chem Int Ed Engl* 46:8120–8126
55. Levi P (1995) *The monkey's wrench*. Penguin Books, New York, p 144
56. Balzani V, Credi A, Venturi M (2002) *Proc Natl Acad Sci USA* 99:4814–4817
57. Ishow E, Credi A, Balzani V, Spadola F, Mandolini L (1999) *Chem Eur J* 5:984–989
58. Ferrer B, Rogez G, Credi A, Ballardini R, Gandolfi MT, Balzani V, Liu Y, Tseng H-R, Stoddart JF (2006) *Proc Natl Acad Sci USA* 103:18411–18416
59. Ballardini R, Balzani V, Clemente-Leon M, Credi A, Gandolfi MT, Ishow E, Perkins J, Stoddart JF, Tseng H-R, Wenger S (2002) *J Am Chem Soc* 124:12786–12795
60. Rogez G, Ferrer Ribera B, Credi A, Ballardini R, Gandolfi MT, Balzani V, Liu Y, Northrop BH, Stoddart JF (2007) *J Am Chem Soc* 129:4633–4642
61. Balzani V, Ceroni P, Maestri M, Vicinelli V (2003) *Curr Opin Chem Biol* 7:657–665
62. Puntoriero F, Nastasi F, Cavazzini M, Quici S, Campagna S (2007) *Coord Chem Rev* 251:536–545
63. Hahn U, Gorka M, Vögtle F, Vicinelli V, Ceroni P, Maestri M, Balzani V (2002) *Angew Chem Int Ed* 41:3595–3598
64. Ceroni P, Venturi M (2010) In: Ceroni P, Credi A, Venturi M (eds) *Electrochemistry of functional supramolecular systems*. Wiley, Hoboken, pp 145–184
65. Astruc D, Ornelas C, Ruiz J (2009) *Chem Eur J* 15:8936–8944
66. Ornelas C, Ruiz J, Belin C, Astruc D (2009) *J Am Chem Soc* 131:590–601
67. Heinen S, Walder L (2000) *Angew Chem Int Ed* 39:806–809
68. Heinen S, Meyer W, Walder L (2001) *J Electroanal Chem* 498:34–43
69. Marchioni F, Venturi M, Credi A, Balzani V, Belohradsky M, Elizarov AM, Tseng H-R, Stoddart JF (2004) *J Am Chem Soc* 126:568–573
70. Marchioni F, Venturi M, Ceroni P, Balzani V, Belohradsky M, Elizarov AM, Tseng H-R, Stoddart JF (2004) *Chem Eur J* 10:6361–6368
71. Ronconi CM, Stoddart JF, Balzani V, Baroncini M, Ceroni P, Giansante C, Venturi M (2008) *Chem Eur J* 14:8365–8373
72. Monk PMS (1998) *The Viologens – Physicochemical properties, synthesis and applications of the salts of 4,4'-bipyridine*. Wiley, Chichester
73. Baker WS, Lemon BI III, Crooks RM (2001) *J Phys Chem B* 105:8885–8894
74. Elston T, Wang H, Oster G (1998) *Nature* 391:510–513
75. Ashton PR, Ballardini R, Balzani V, Credi A, Dress R, Ishow E, Kleverlaan CJ, Kocian O, Preece JA, Spencer N, Stoddart JF, Venturi M, Wenger S (2000) *Chem Eur J* 6:3558–3574
76. Balzani V, Clemente-León M, Credi A, Ferrer B, Venturi M, Flood AH, Stoddart JF (2006) *Proc Natl Acad Sci USA* 103:1178–1183
77. Inverting the positions of  $\text{EA1}^{2+}$  and  $\text{EA2}^{2+}$  increases the quantum yield of photoinduced electron transfer ( $F_2 = 0.50$ ) but prevents ring displacement because the back-electron-transfer reaction becomes exceedingly fast: Balzani V, Clemente-León M, Credi A, Semeraro M, Venturi M, Tseng H-R, Wegner S, Saha S, Stoddart JF (2006) *Aust J Chem* 59:193–206

78. Balzani V, Clemente-León M, Credi A, Lowe JN, Badjic JD, Stoddart JF, Williams DJ (2003) *Chem Eur J* 9:5348–5360
79. Badjic JD, Balzani V, Credi A, Silvi S, Stoddart JF (2004) *Science* 303:1845–1849
80. Badjic JD, Ronconi CM, Stoddart JF, Balzani V, Silvi S, Credi A (2006) *J Am Chem Soc* 128:1489–1499
81. Sauvage J-P (1998) *Acc Chem Res* 31:611–619
82. Asakawa M, Ashton PR, Balzani V, Credi A, Hamers C, Matternsteig G, Montalti M, Shipway AN, Spencer N, Stoddart JF, Tolley MS, Venturi M, White AJP, Williams DJ (1998) *Angew Chem Int Ed* 37:333–337
83. Balzani V, Credi A, Matternsteig G, Matthews OA, Raymo FM, Stoddart JF, Venturi M, White AJP, Williams DJ (2000) *J Org Chem* 65:1924–1936
84. Collier CP, Matternsteig G, Wong EW, Luo Y, Beverly K, Sampaio J, Raymo FM, Stoddart JF, Heath JR (2000) *Science* 289:1172–1175
85. Luo Y, Collier CP, Jeppesen JO, Nielsen KA, Delonno E, Ho G, Perkins J, Tseng H-R, Yamamoto T, Stoddart JF, Heath JR (2002) *Chemphyschem* 3:519–525
86. Steuerman DW, Tseng H-R, Peters AJ, Flood AH, Jeppesen JO, Nielsen KA, Stoddart JF, Heath JR (2004) *Angew Chem Int Ed* 43:6486–6491
87. Ashton PR, Baldoni V, Balzani V, Credi A, Hoffmann HDA, Martinez-Diaz MV, Raymo FM, Stoddart JF, Venturi M (2001) *Chem Eur J* 7:3482–3493
88. Balzani V, Credi A, Venturi M (2003) *ChemPhysChem* 4:49–59
89. Ballardini R, Balzani V, Credi A, Gandolfi MT, Venturi M (2001) *Acc Chem Res* 34:445–455
90. Astumian RD (2005) *Proc Natl Acad Sci USA* 102:1843–1847
91. Astumian RD (2005) *J Phys Condens Matter* 17:S3753–S3766
92. Hernandez JV, Kay ER, Leigh DA (2004) *Science* 306:1532–1547
93. Leigh DA, Wong JKY, Dehez F, Zerbetto F (2003) *Nature* 424:174–179

# The Beauty of Knots at the Molecular Level

Jean-Pierre Sauvage and David B. Amabilino

**Abstract** What makes a given object look beautiful to the observer, be it in the macroscopic world or at the molecular level? This very general question will be briefly addressed at the beginning of this essay, in relation to contemporary molecular chemistry and biology, leading to the general statement that, most of the time, beauty is tightly connected to function as well as to the cultural background of the observer. The main topic of the present article will be that of topologically non-trivial molecules or molecular ensembles and the fascination that such species have exerted on molecular or solid state chemists. Molecules with a graph identical to Kuratowski's  $K_5$  or  $K_{3,3}$  graphs are indeed highly attractive from an aesthetical viewpoint, but perhaps even more fascinating and beautiful are molecular knots. A general discussion will be devoted to these compounds, which are still considered as exotic species because of the very limited number of efficient synthetic strategies leading to their preparation. Particularly efficient are templated approaches based either on transition metals such as copper(I) or on organic groups able to form hydrogen bonds or acceptor–donor stacks. A particularly noteworthy property of knots, and in particular of the trefoil knot, is their topological chirality. The isolation of both enantiomers of the trefoil knot ( $3_1$ ) could be achieved and showed that such species have fascinating chiroptical properties. Finally, various routes to more complex and beautiful knots than the trefoil knot, which is the simplest non-trivial knot, will be discussed in line with the remarkable ability of transition metals to gather and orient in a very precise fashion several organic

---

J.-P. Sauvage (✉)

Institut de Science et d'Ingénierie Supramoléculaires, Université de Strasbourg, 8 Allée Gaspard Monge, 67000 Strasbourg, France  
e-mail: [jpsauvage@unistra.fr](mailto:jpsauvage@unistra.fr)

D.B. Amabilino (✉)

Institut de Ciència de Materials de Barcelona (ICMAB-CSIC), Campus Universitari de Bellaterra, 08193 Cerdanyola del Vallès, Barcelona, Spain  
e-mail: [amabilino@icmab.es](mailto:amabilino@icmab.es)

components in their coordination spheres, thus leading to synthetic precursors displaying geometries which are perfectly well adapted to the preparation of the desired knots or links.

**Keywords** Catenanes · Copper complexes · Interlaced design · Knots · Kuratowski's graphs · Möbius strip · Topological chirality · Topology

## Contents

1	Introduction: Beauty and Molecules .....	108
2	The Beauty of Knots .....	111
3	Chemical Approaches to Knots .....	114
4	Molecular Knot Characteristics and Beauty .....	119
5	Conclusion and Outlook .....	123
	References .....	123

## 1 Introduction: Beauty and Molecules

Beauty in general refers to the perception of the observer. For an object, a person, a concept or a place to appear as beautiful implies that the observer perceives it as such. As far as the entity itself is concerned, it is obvious that there are no absolute criteria able to define its beauty. For objects or their two- or three-dimensional representations, several factors can be put forward as contributing to give the observer the feeling that he or she is contemplating something beautiful. Symmetry is certainly one of them. Similarly, the relation between the object that is observed and entities found in Nature or in our urban environment is also important, as well as the possible function of the object or of what it may evoke. In any case, the most important criterion is without doubt on the observer's side: his or her cultural background determines whether the observer perceives the object as beautiful or not.

Such considerations can be extended to molecules or, rather, their representations [1]. All we chemists are more or less attracted by certain molecules or sets of molecules that we would regard as beautiful species or not. Infinite networks [2], whose structures as obtained by X-ray crystallography, can sometimes be considered as wonderful architectures, making them particularly attractive because of the geometrical arrangement of the various components in the three-dimensional lattice. In this review article, we will deliberately exclude such networks, although they constitute a huge class of beautiful systems. We will focus on molecules or finite molecular sets.

As for other objects, a given molecule can appear beautiful for several distinct reasons. Here again, symmetry is often an important factor. Platonic solids and other high-symmetry geometrical objects have often been a source of inspiration for molecular chemists [3, 4], as testified by the attraction exerted on chemists by dodecahedrane, cubane or the various fullerenes, C<sub>60</sub> fullerene being the archetype [5]. The success of calixarenes [6, 7], to take a particularly representative example,



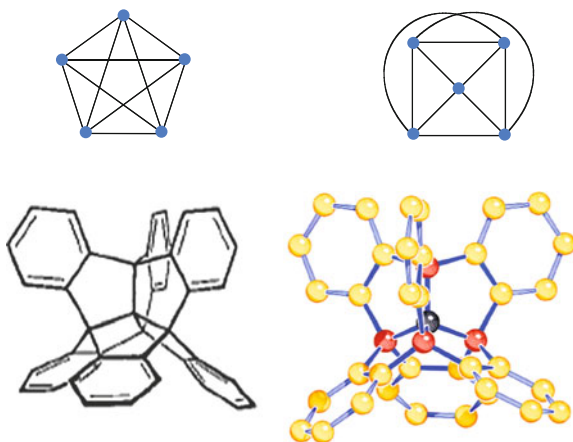
or cucurbituril [8] is certainly also related to their symmetry and the aesthetic appeal they exert on chemists, although their host–guest properties certainly play a major role on the interest they have triggered among the supramolecular chemists. The same can be put forward for the ancestors of molecular containers such as crown-ethers or cryptands, with their nice-looking representations and structures [9].

The function of a molecule or an ensemble of molecules can also contribute substantially to the perception of the observer when looking at them. Complex natural products are beautiful, although some of them have strictly no element of symmetry. Brevetoxin A or Maitotoxin appear as aesthetically very attractive compounds mostly because of their complexity and of the challenge that their total synthesis represented (for Brevetoxin A) or still represents (for Maitotoxin). In biology, beauty can be found in many molecular systems. Particularly noteworthy are some elements of natural photosynthetic systems. A spectacular example is that of the light-harvesting antenna complex (LH<sub>2</sub>) from *Rhodospseudomonas acidophila* (a purple photosynthetic bacterium), with its two rings of 18 and 9 bacteriochlorophyll molecules [10]. In this example, the disc-shaped ensemble, with its ninefold symmetry, was certainly not expected but it demonstrated that Nature also loves beautiful arrangements. Another example is that of the photosynthetic reaction centre from the purple bacterium *Rhodospseudomonas viridis*. Not only is the structure of the reaction centre very complex, with a pseudo-symmetry axis (C<sub>2</sub>), but its function makes the structure fascinating. For the first time, one can “see” the very centre of photosynthesis in an incredibly old organism, which brings us close to the origin of life and to the most primitive organisms that appeared on Earth more than 3 billion years ago [11].

The main topic of this chapter will be to discuss the beauty of compounds in relation to their topology [12]. Topologically trivial molecules will not be considered. In other words, if one can draw the molecule on a sheet of paper (i.e. embed it in a two-dimensional space) without intersections between bonds by distorting the bonds and angles by our mind, the molecule will be considered as trivial and thus of no topological interest. Topologically, beautiful molecules have to display a non-trivial molecular graph (the graph of a molecule is the figure built on the two sets of bonds and atoms, or to use topological vocabulary, edges and vertices). A non-trivial graph cannot be represented in a plane without edge crossings, regardless of the distortions one may impose on the system. A particularly beautiful class of topologically non-trivial compounds is that of molecules having the topology of Kuratowski’s K<sub>5</sub> graph. K<sub>5</sub> is the complete graph on five vertices: It consists of five vertices and, connecting these vertices, it contains ten edges. This graph is the example par excellence of a simple object having a non-trivial topology: It is impossible to draw the corresponding figure in a plane without at least one crossing point. A few molecules with the same topological properties exist but one of them is particularly attractive since it contains a K<sub>5</sub> core and six phenyl rings disposed in a symmetrical fashion [13]. K<sub>5</sub> and Kuck’s compound are depicted in Fig. 1.

The other elemental non-trivial graph is Kuratowski’s graph K<sub>3,3</sub>. K<sub>3,3</sub> is the complete bipartite graph on six vertices, three of which connect to each of the other three. In any object, if one can identify a subgraph K<sub>5</sub> or K<sub>3,3</sub>, then the object is

**Fig. 1**  $K_5$ . *Top*: The complete graph on five vertices (*left*) and one-crossing presentation (*right*). *Bottom*: Classical representations of  $K_5$  and the molecule made by Kuck and Schuster in 1988 [13], which has the same topology as  $K_5$



topologically non-trivial. Almost 30 years ago, in a seminal piece of work, Walba and co-workers prepared a compound with the topology of  $K_{3,3}$  [14]. The molecule is also a Möbius strip, identical to a three-rung ladder that has been twisted before connecting the two upper ends to the lower ones.  $K_{3,3}$  and Walba's compounds are represented in Fig. 2. To those interested in molecules and topology, Kuck's compound and Walba's Möbius strip are very attractive and can definitively be regarded as beautiful molecules.

The second class of topologically non-trivial compounds that we will consider consists of knots and links. Links are sets of two or more interlocking rings. In chemistry, the word "link" was replaced by the word "catenanes" many years ago and it is now of standard usage. Single component knots are simply rings that have been disposed in a three-dimensional space in such a way that any projection on a plane will have to contain intersections. In other words, embedding of a knot in a two-dimensional space cannot be realised without crossings, and is thus impossible. The simplest link, consisting of two interlocking rings, is also called a "Hopf link" by topologists. Chemists would call it a [2]catenane since it consists of a "chain" (*catena* in Latin) of two cyclic components. The simplest non-trivial knot is very different because it is a single closed curve that requires three crossings to be drawn in a plane. A "normal" ring such as a circle is obviously topologically trivial. It is often called an "unknot". The three-crossing knot is symbolised by  $3_1$ . A Hopf link and  $3_1$  are represented in Fig. 3.

Many catenanes have been reported since the origin of the field in the 1960s [15], but mostly since the introduction of efficient synthesis strategies based on template effects at the beginning of the 1980s. Dramatically different is the situation as far as molecular knots are concerned. Very few syntheses of knots have been described in the literature and even less X-ray structures have been reported. Today, the only knots that can be prepared by molecular chemists are the trefoil knot and a composite knot based on the trefoil knot. Considering the number of single-component knots that have been identified by topologists, the achievements of synthetic chemists in the field of knots at the molecular level is still extremely modest [16]!

**Fig. 2**  $K_{3,3}$ . *Top:* The complete bipartite graph on five vertices (*left*) and one-crossing presentation (*right*). *Center:* Structure of Walba's compound. *Bottom:* Kuratowski's graph  $K_{3,3}$  and Walba's compound, with the same topology as  $K_{3,3}$  (*left*) or with a trivial geometry (*right*)

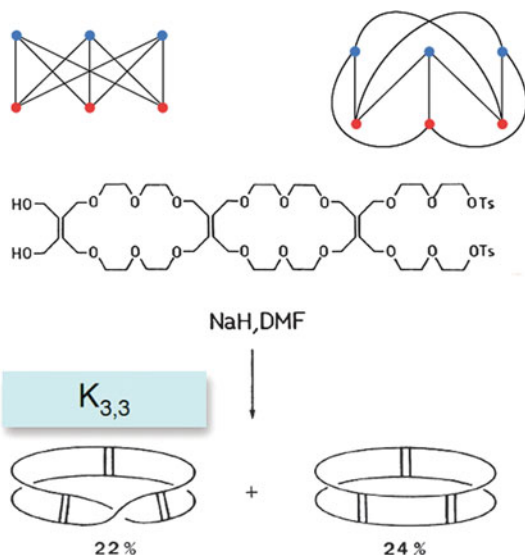
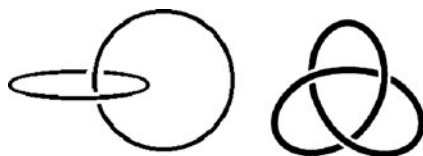


**Fig. 3** The simplest link and the simplest non-trivial knot,  $3_1$



## 2 The Beauty of Knots

Ancient Asiatic and eastern Mediterranean art are replete with representations of interlaced and knotted designs and objects, symbols of continuity and eternity. The Endless Knot (Fig. 4) is a Buddhist symbol believed to represent the cycle of life and rebirth, although there are other interpretations. The symbol itself is a very angular design in which the knot traces linear sections that form right angles, which is a representation that might help a chemist design a pathway to this beautiful object. The central section is a grid in which each line has three crossing points, a very suggestive drawing for a coordination chemist! It is the start of a plaiting, weaving or basketry-type crossing, which was to find imitation to an extreme level of beauty in the Book of Kells, an eighth century work created by Celtic monks. In the cloisters of certain abbeys from the twelfth century, one can even find signs of humankind's desire to thread and weave immortalised in stone (Fig. 4).

The fascination with interweaved structures shown by the Celts was undoubtedly related with beauty and perfection, which has lasted to the present day, spreading and changing. The remarkable sixteenth century designs created by Albrecht Durer and Leonardo da Vinci (Fig. 5) were engraved and printed for subsequent use by painters, goldsmiths, weavers, damaskeeners and needle workers [17].



**Fig. 4** *Top:* The Endless Knot, a symbol from Buddhist belief (*left*), and an ornated capital letter from the Book of Kells (*right*). *Bottom:* A figure in the cloister of the Monastery of Sant Cugat del Vallès, Catalonia, Spain, showing a man weaving a chord

The examples of interwoven and knotted structures have prevailed in all walks of architecture, symbolism and art, and it is not our aim here to give an exhaustive list of where one may encounter different representations of knots. Be that as it may, this short journey through the history of knot representation would not be complete without mentioning the great Dutch graphical artist M.C. Escher, whose beautiful representations of the Möbius strip and the trefoil knot are renowned. They prove a great inspiration for chemists wishing to adorn the covers of chemistry journals.

The beauty of a molecular knot is naturally related to its representation and to the shape of the molecule itself [18] and, in all walks of chemistry, there are more and less beautiful representations of knotted structures. Few people envisage these beautiful molecules as the clouds of electron density and atomic nuclei that they are, but with computer-aided design it is likely that these attractive molecules will find renewed interest from those eager to attempt totally synthetic challenges in synthesis through template methods. One has simply to behold the remarkable and

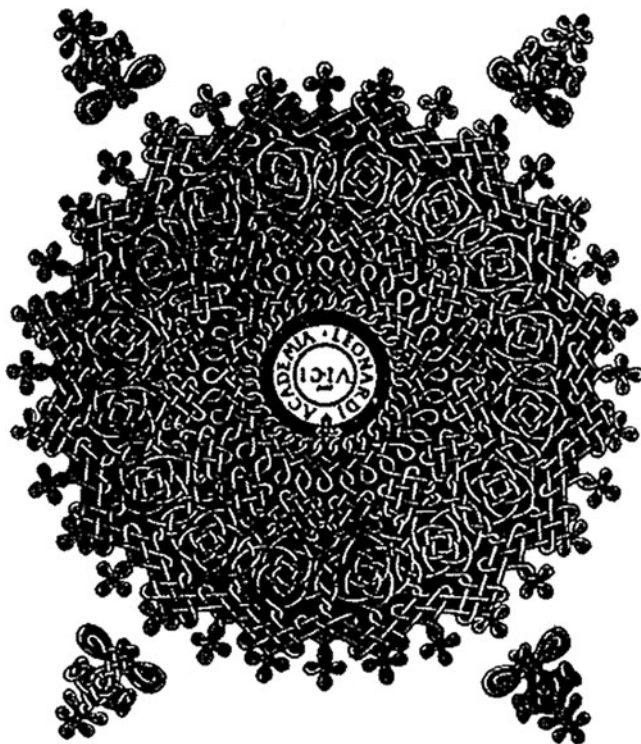


Fig. 5 “Concatenation” by Leonardo da Vinci

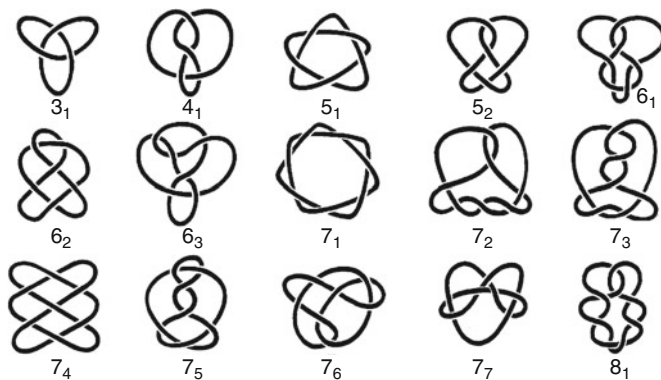


Fig. 6 Representations of the first 15 prime knots

beautiful prime knots (Fig. 6) to begin to chart routes through treacherous waters to rewarding synthetic challenges. Especially appealing to the writers is the  $7_4$  knot, which has exactly the same topology as the endless knot drawn centuries ago – and there are beautiful chemical grids that might lead to this kind of structure. The  $5_1$

and  $7_1$  knots also stand out for their beautiful symmetry. In Sect. 3 we will outline some of the “linking synthons” that might be useful to approach these objects.

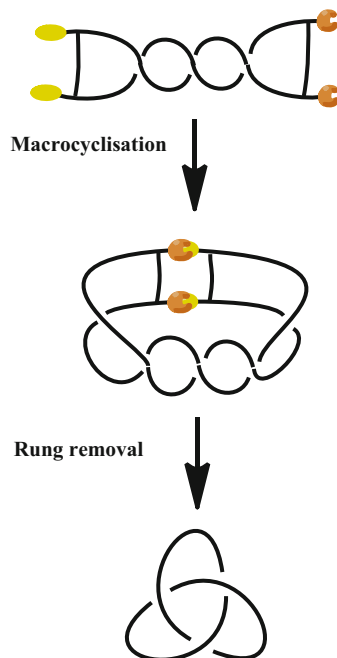
### 3 Chemical Approaches to Knots

The synthetic chemist can see beauty in an approach to a chemical object, be it in the form of the perceived elegance, efficiency, directness, or combination of approaches. Covalent bond forming, coordination chemistry and purely non-covalent possibilities are all important of course, but each one on its own is weak. Take the statistical approach to link formation: A flexible linear molecule in random motion is not likely to form a knot, and it is even less likely that we could separate and characterise it even if it did. There is no direction in the reactivity. Covalent bonds can be used to hold fragments together, and then those bonds used to orient the fragments are removed to leave the linked molecule. With today’s control over molecular conformation and covalent bond making and breaking, this has to be considered a viable approach. But, those approaches based on coordination chemistry and non-covalent bonds are more direct and efficient for the moment.

What a beautiful object the “Möbius strip” is! The one-sided strip with two edges, even today a formidable synthetic challenge, is perhaps destined not to be attempted in these days of use-oriented research. Yet what might the electronic properties of a Möbius strip be? The Möbius strip is in fact a plausible precursor to a trefoil knot (Fig. 7), a feature first suggested by Frisch and Wasserman in 1961 [19]. Of course, this task is nigh on impossible to perform by covalent bond-forming chemistry alone. The brave and ingenious synthetic approach by Schill and colleagues to reach a knot through a Möbius strip-like molecule was perhaps plausible [20], but the number of steps and unwanted topologies formed in some of the reactions left the end unreached. A non-covalent strategy has not been reported to date, but awaits a valiant champion! It is interesting, in the context of molecules capable of charge transport, to wonder how charge conjugation would flow around a Möbius strip.

It is clear that, in general, the formation of knots requires the controlled formation of crossing points. Also, the molecular fragments must be mutually orthogonal or at least form an appreciable angle, preferably a controlled one. The molecule should be stable under the conditions required to prepare the knot. Therefore, simple square planar complexes, for example, are intuitively of little use for templating interlocked systems because, although they are stable, the four divergent ligands do not have an easy way to cross each other. Notwithstanding, square planar complexes or the hydrogen-bonded side-on equivalents of them could aid in the orientation of fragments for covalent linkage, an interesting possibility in the Möbius strip approach to knots. Several examples of orthogonality in chemical structures exist: perhaps the tetrahedral copper(I) complexes developed in Strasbourg [21], or maybe the threaded systems based on donor–acceptor systems and combining hydrogen bonding [22], and why not the hydrogen-bonding

**Fig. 7** Depiction of the Möbius strip approach to a trefoil knot



system that leads to two strands whose planes are held at a large angle to one another [23–25].

A very suggestive route to knots is through multiply ravelled species in the form of helices, the double helix for example. The double helix itself attracts great interest in itself as a beautiful object. In the age of genetics, we are almost constantly bombarded with images of the DNA double helix. Indeed, many authors refer to this intertwined structure when describing their work on helices, simply because it is a beautiful object that demonstrates intricate function with relative simplicity of structure.

Hypothetical joining of the termini of helices with covalent bonds [26] (Fig. 8) – joined in the right way of course thanks to the correct positioning of reactive ends – gives a route to a series of knots and multiply interlocked catenanes. The double helical coordination complexes, which are relatively frequent [27], are ideal precursors for this purpose, where transition metal ions are surrounded by winding coordinating strands to give the double helix. Connecting the termini of the strands in the correct way gives knots and multiply ravelled [2]catenanes.

The preparation of double helices from different bis-chelate ligands and transition metals in all likelihood occurred long ago, yet it is only relatively recently that the first such system was recognised and characterised. Apart from their beauty, their scientific relevance was not at all apparent. One of the earliest dinuclear helical complexes was discovered by Fuhrhop and co-workers in 1976 [28]. Since then, several double helical complexes have been created and characterised, and

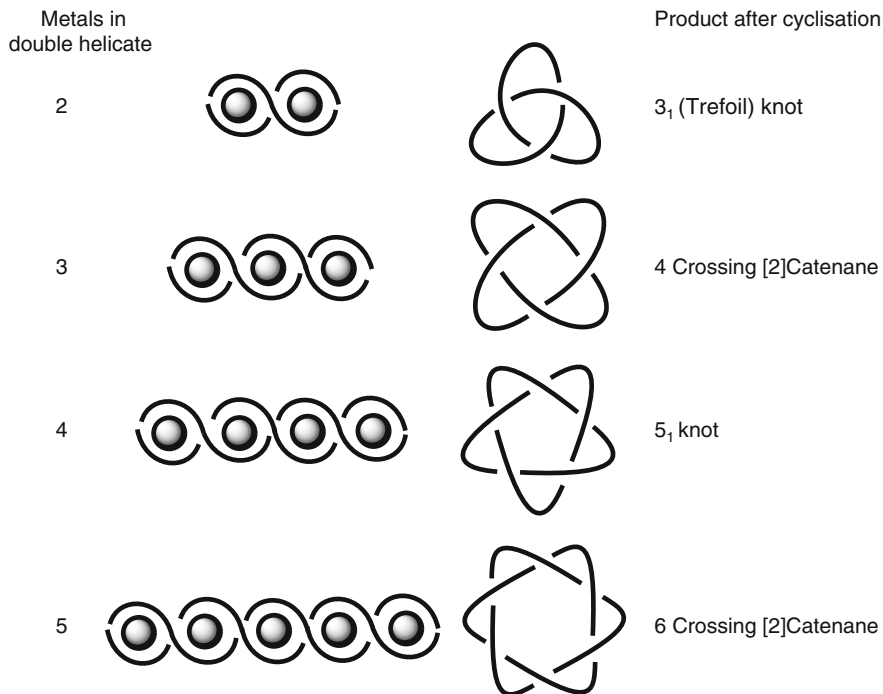


**Fig. 8** Double-stranded helicates (with metal ion centres depicted by *filled circles*) and the molecular knots and catenanes derived from them by appropriate joining of the ends in the helical strands. Half turns give multiply crossed [2]catenanes whereas an integral number of turns leads to knots

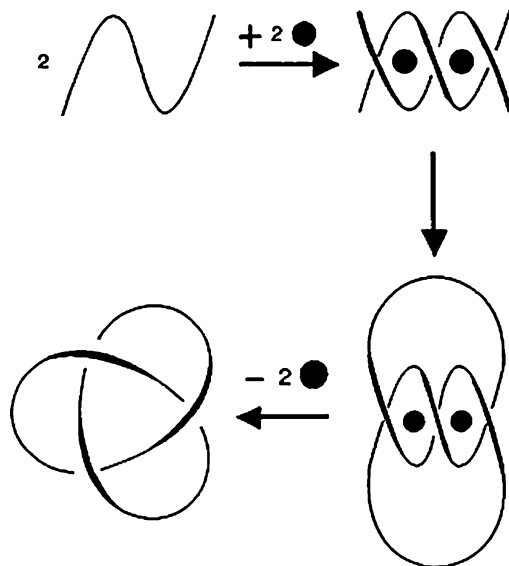
their interest in the context of interlocking molecular structures has been discussed [29]. In particular, if synthesis is to be done, the helices must be formed efficiently and must be stable to the conditions of the covalent bond-forming reactions. As we shall see, the advances in softer reactions for covalent bond forming are proving extremely useful for the preparation of complex molecular forms.

The synthesis of trefoil knots based on copper(I) coordination by phenanthroline ligands as the template is a reliable and flexible route to knots in which the metal ion can be removed to liberate the free “knotand” (a knot that behaves as a ligand). The route is conceptually simple: Linking the termini of strands in a double helical strand gives the knot as its copper complex, which upon removal of the templating metal ion leaves the knotand. The route shown in Fig. 9 illustrates the approach elegantly. It relies on linking the strand termini on the same side of the double helix, rather than at the ends, which leads to the macrocycle.

Many attempts with various linkers were carried out before it was found that 1,10-phenanthroline moieties, connected via their 2-positions by a butyl chain, form a double helix when complexed with two copper(I) ions. In addition, by introducing appropriate functions at the 9-positions, the strategy of Fig. 9 could be followed to achieve the synthesis of a molecular knot. The route to the knot, showing the



**Fig. 9** Double helicate approach to a trefoil knot



chemical transformations and structures at each step is shown in Fig. 10. Purification of the complexed knot after the cyclisation procedure was a long and difficult process, but the bis-copper(I) complex was isolated in 3% yield [30].

The low yield achieved for the first dicopper knotted 86-membered macrocycle was improved significantly by changing the length of the linker connecting the two chelates and the long functionalised linker used in the cyclisation step [31–33]. The best yields for the cyclisation reaction were around 8%. The use of a 1,3-phenylene spacer between the coordinating units caused a great improvement [34].

The double-stranded helical precursor with copper (I) using the 1,3-phenylene linker was formed quantitatively from its components, and reaction of this tetraphenolic double helix with two equivalents of the di-iodo derivative of hexaethyleneglycol, in the presence of caesium carbonate, gave a single isolable copper (I) complex: The isolated yield of the dicopper(I) knot was 29%. The compact helical core was fully confirmed by its subsequent X-ray structure determination [35]. The spectacularly improved yield can be increased even further by optimising the covalent bond-forming reactions, whose conditions can harm the helical precursors, using the ring-closing metathesis (RCM) reactions [36, 37]. These beautiful molecules are therefore now available to the skilled chemist in gram quantities!

In the field of molecular knots templated by transition metal ions, another remarkable achievement deserves to be mentioned. Hunter and co-workers recently prepared a trefoil knot in a very satisfactory fashion by first wrapping a string-like molecule around a single transition metal ion with an octahedral coordination sphere ( $\text{Zn}^{2+}$ ) so as to obtain an open knotted structure and, subsequently, they could link the two ends of the string to form a real trefoil knot [38]. This nice piece of work again confirms the power of transition metals when it comes to preparing topologically novel species.

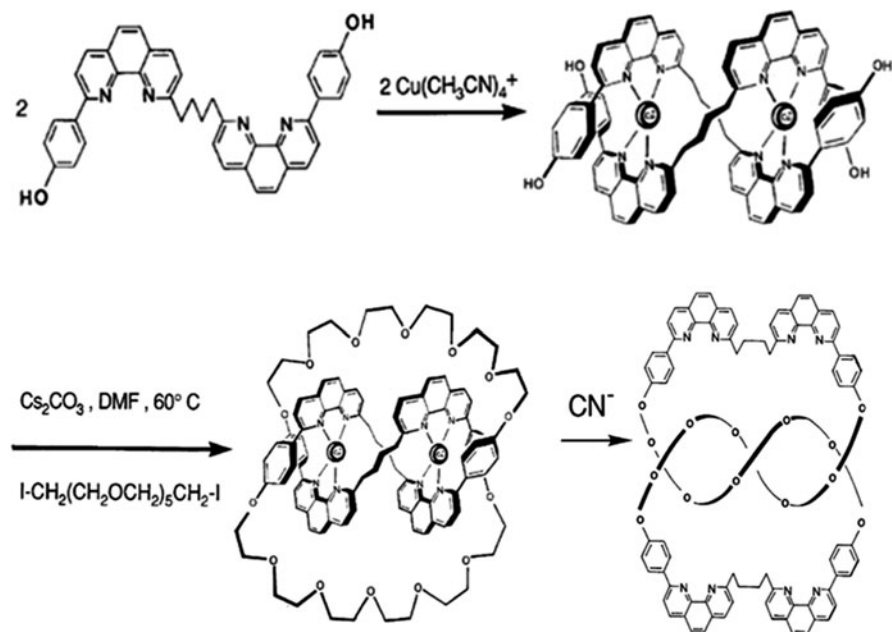


**Fig. 10** Synthesis of the first trefoil knot

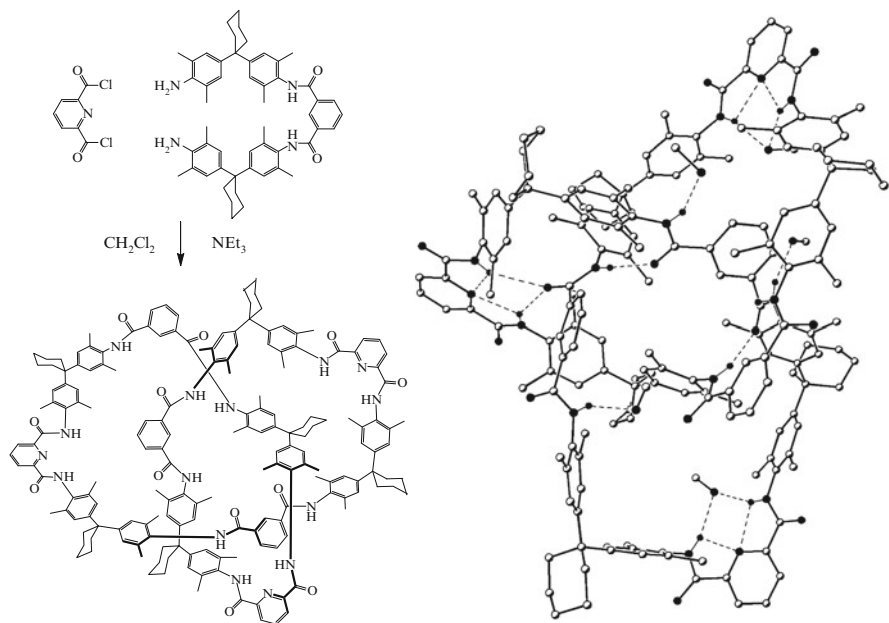


**Fig. 11** *Left*: Synthesis of a trefoil knot thanks to hydrogen bonding. *Right*: Crystal structure of the compound, with the non-covalent interactions indicated by dashed lines

We have seen how elegantly transition metals can template the formation of knots, but what about Nature's favourite templating interaction, the hydrogen bond? A remarkably efficient molecular trefoil knot synthesis based on this interaction was reported by Vögtle and co-workers, who made a knotane in 20% yield [39]. This amazing route (Fig. 11) was uncovered serendipitously during the synthesis of catenanes. The crystal structure of the compound was the definitive proof for the structure, because neither NMR nor mass spectrometry could tell it apart conclusively from the macrocycles that are also formed.

The hydrogen bonded knot can also be synthesised by a step-wise route, which helps determine the way in which it is formed in the one-step reaction [40]. A string-like molecule was prepared in order to ascertain if indeed it is an intermediate on the pathway to the knot (Fig. 12). The reaction of this "pre-knot" with a di-acid chloride generated the knot in 11% yield. The creative chemist will immediately have realised that using the knot precursor as a reagent with different di-acid chlorides is possible, and indeed this path leads to a variety of substituted knot molecules and analogues, especially in combination with different [41, 42] and quite exotic and beautiful knotty structures [43]. The formation of compounds that contain various knots was achieved by the functionalisation of the 5-position of the pyridine rings with different functional groups, which makes possible selective reaction at each external loop, which can be appreciated in the X-ray structure of the native compound. To give just one case, the functionalisation of the knots with allyloxy units facilitates the preparation of linear and branched oligomers of knots [44].

This section would not be complete without mention of the beautiful objects prepared using DNA. Single-stranded DNA is a practical building block for the preparation of topologically complex unnatural interlocked structures in awe-inspiring manner [45]. Mutually compatible sequences of DNA (designed so as to form interlocked structures) pair through the Watson–Crick code and allow precise control of the ravelling necessary to form knots. A  $4_1$  knot has been made by precise double helix formation and control of the directionality of the strands [46]. This figure-eight knot has two positive and two negative nodes, defined as such by the direction the strands cross each another. Defining the DNA direction as the 5' to 3' vector, the right-handed B-DNA double helix has only negative nodes, and the left-handed Z-DNA double helix contains exclusively positive nodes. The type of DNA encoded at each crossing results in the stereoselective formation of the knots, an approach that is inspirational for the purely synthetic approach to knots. Indeed, three knotted topologies can be achieved with a synthetic DNA molecule [47].

## 4 Molecular Knot Characteristics and Beauty

When a chemist working with molecules incorporating organic fragments makes an object as beautiful as a knot, one might expect that the symmetry of this object be reflected in some of its characteristic spectroscopic signatures, such as its nuclear magnetic resonance spectrum. NMR spectra of apparently large and complex

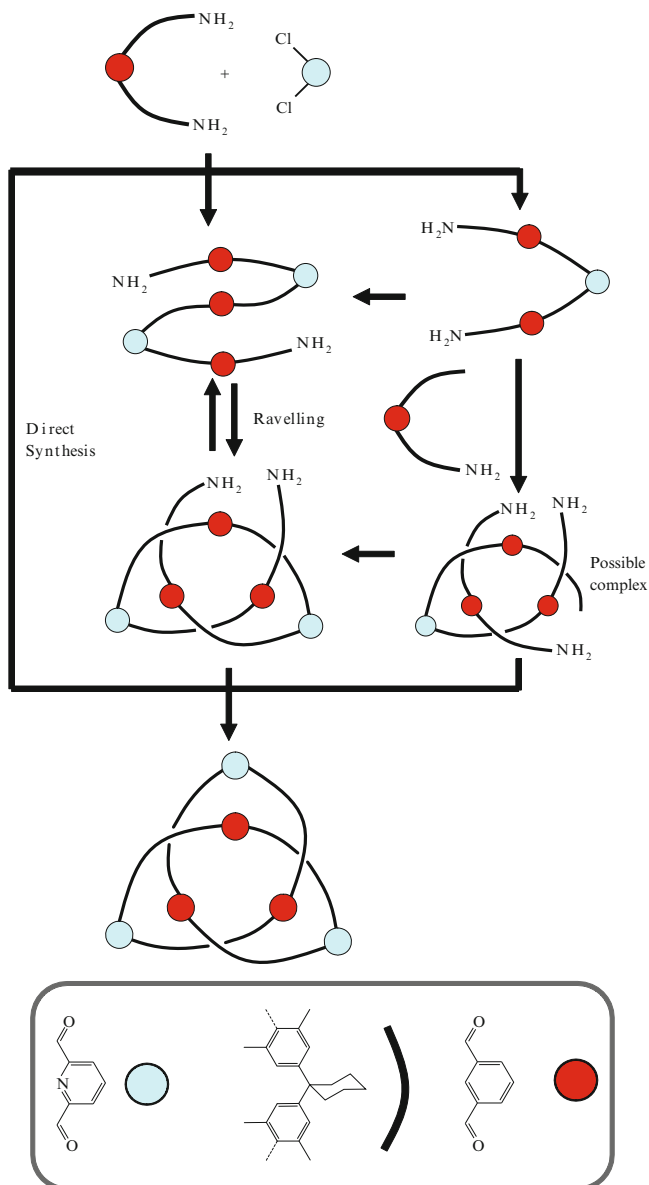


**Fig. 12** Representation of the synthetic pathway to a trefoil knot by hydrogen bond-mediated weaving

molecules can be beautifully simple. Hope for this kind of situation might be founded when one thinks of the NMR spectra of folded peptide structures in natural systems, which are often very well defined because of the strongly held secondary and tertiary structures. Certainly, the knots based on copper template chemistry

have very well-defined form when the metal ions are present, holding the phenanthroline groups tightly in their tetrahedral clutches! No motion in the backbone is permitted, and the self-wrapped ring might as well be a piece of static jewellery. The coordination forces that templated the formation of the knot “live on” (to quote Fraser Stoddart) in the knot after it is formed.

The knotted topology of the first synthetic trefoil was first demonstrated by mass and NMR spectroscopy, but was later fully confirmed by an X-ray structure determination showing this situation [48] (Fig. 13).

Of course, static things can be beautiful, but movement can be far more seductive! Removal of the metal ion from the double helical core of the knots leads to molecules with no strong non-covalent interactions between the moieties in the ring. The NMR of this molecule is now far from pretty, though. The slow motions that result from the tight intertwining on the one hand and the lack of specific interaction on the other mean that the ring slides through itself at a rate that is slow on the NMR timescale, with multiple conformations that are poorly defined. For now, seeing how the knot glides through itself will tease us.

The pattern of crossings in knots means that they can be chiral objects. This is particularly the case for the three-crossing knot  $3_1$  (trefoil knot). However,  $4_1$ , the four-crossing knot already discussed above, is not chiral, which could be very

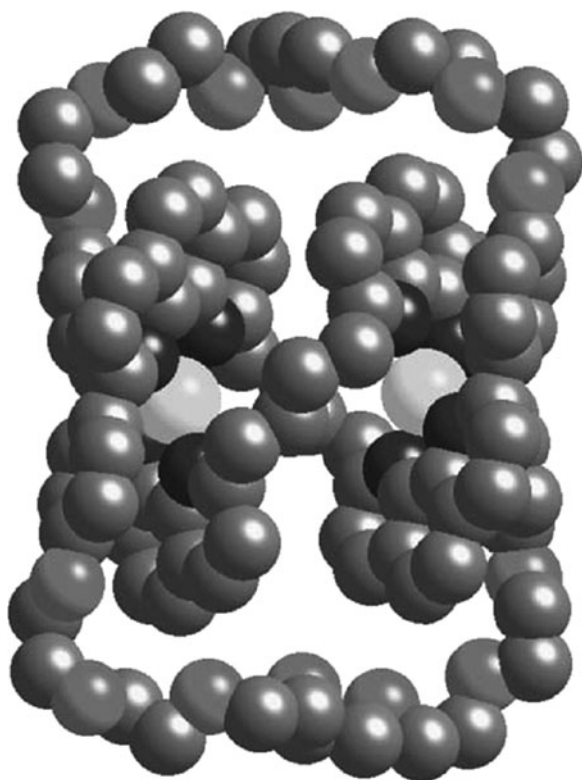


**Fig. 13** Structure of the first trefoil knot as it exists in its crystals, with the copper(I) ions shown as *clear spheres* in the tetrahedral coordination sphere of two phenanthroline ligands

surprising to the observer! Topological chirality lies beyond Euclidean geometry, where the relative disposition of groups in a chemical object (in the case of stereochemistry) defines its chirality, because it involves objects with non-planar graphs. This means that they cannot be drawn on a plane of paper without crossing points and that they cannot be converted into their enantiomers even upon total distortion (not the case for Euclidean geometry). Therefore, molecules with a trefoil knot backbone are topologically chiral, and when an excess of one enantiomer is present they should be optically active. Indeed, the homochirality in knots leads to beautiful circular dichroism (CD) spectra (Fig. 14). The enantiomers show opposite CD bands arising from the metal-to-ligand charge transfer band at approximately 500 nm and from the ligand itself at around 300 nm.

The copper(I)-templated strategy for knot synthesis leads to the target molecules as di-cationic dicopper(I) complexes, with a one-handed helix running through an axis of the molecule. Thus, diastereomeric salts can be formed by combining them with optically active anions, although a careful strategy is required to achieve interchange of the counterions. Binaphthyl phosphate (BNP) exists as enantiomorphous atropoisomers on account of the twisted disposition of the naphthyl rings and the high barrier to interconversion of the enantiomers. The chiral anion is labile, unlike the usual  $\text{BF}_4^-$  or  $\text{PF}_6^-$  anions, which are hard to exchange. Triflate can be introduced in the formation step of the double helix of the bischelating diphenolic strand with the 1,3-phenylene spacer. One equivalent of copper(I) triflate was added to the strand in a reductive medium. The dinuclear copper(I) double helix was

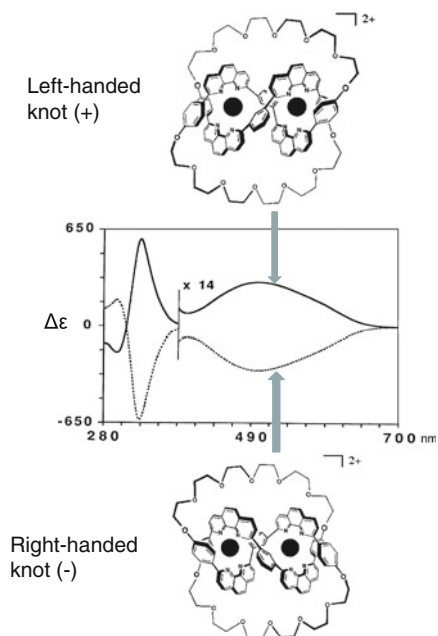


**Fig. 14** Circular dichroic spectra of knot enantiomers

formed quantitatively, with  $\text{CF}_3\text{SO}_3^-$  as the counteranion. The bicyclisation reaction afforded the racemic copper(I) knot triflate in 23% yield.

Liquid extraction was used to make diastereomers, exploiting the high solubility of potassium triflate in water compared with the binaphthylphosphate salts. The two diastereomers have different solubilities and the (+) isomers of knot and anion crystallise together [49, 50], while the laevorotatory knot remains soluble. Counterion exchange with hexafluorophosphate gave the pure topological enantiomers. The optical rotatory power of the copper(I) knots is very high: At the sodium D-line (589 nm), the optical rotatory power was  $\pm 7,000^\circ \text{mol}^{-1} \text{L dm}^{-1}$ . They are beautiful molecules with a remarkable property!

## 5 Conclusion and Outlook

Knots are all around us, and even within us in our DNA, and their beauty is undeniable. The elegance of knot synthesis has yielded synthetic nanometre scale knots that look beautiful when represented simply, yet whose complexity and mystery make them even more appealing. Modern society is plagued with huge scientific challenges, and that of making topologically complex and attractive molecules is not obviously relevant. Funding bodies requiring impact on innovation and generation of wealth will never prioritise this recreational approach to science. Yet so much has been learned on the journey to these molecules that society is richer. Those practising the arts are funded, and their work can be appreciated by the general public, whereas the chemist generally struggles to convince the man in the street of the value of this kind of molecular artistry. Yet the beauty of these molecules is a seductive way of gaining societal interest, and it should be our duty to use the tools now available to us [51] to help capture the imagination and spirit of adventure in the pursuit of new science. The making of such species can also be regarded as a search for new synthetic methodologies, analogous to the research done by natural substance chemists who contribute to the development of new synthetic approaches while being very conscious that the compounds that they are making in tens of individual chemical steps will probably never be prepared using their approach by pharmaceutical companies.

**Acknowledgements** We warmly thank all the researchers that have contributed to the research in this area, and we especially wish to remember the late Christiane Dietrich-Buchecker from whose hands and mind so many molecular knots were made.

## References

1. Hoffmann R, Laszlo P (1991) *Angew Chem Int Ed Engl* 30:1
2. Batten SR, Robson R (1998) *Angew Chem Int Ed Engl* 37:1460
3. Seidel SR, Stang PJ (2002) *Acc Chem Res* 35:972
4. Hu GA, Qiu WY, Cheng XS, Liu SY (2010) *J Math Chem* 48:401

5. Kroto HW, Allaf AW, Balm SP (1991) *Chem Rev* 91:1213
6. Gutsche CD (1998) *Calixarenes revisited*. RSC, Cambridge
7. Mandolini L, Ungaro R (2000) *Calixarenes in action*. Imperial College Press, London
8. Lagona J, Mukhopadhyay P, Chakrabarti S, Isaacs L (2005) *Angew Chem Int Ed Engl* 44:4844
9. Seel C, Vögtle F (1992) *Angew Chem Int Ed Engl* 31:528
10. McDermott G, Prince SM, Freer AA, Hawthornthwaite-Lawless AM, Papiz MZ, Gogdell RJ, Isaacs NW (1995) *Nature* 374:517
11. Deisenhoffer J, Epp O, Miki K, Huber R, Michel H (1985) *Nature* 318:518
12. Sauvage J-P, Dietrich-Buchecker C (eds) (1999) *Molecular catenanes, rotaxanes and knots: a journey through the world of molecular topology*. Wiley-VCH, Weinheim
13. Kuck D, Schuster A (1988) *Angew Chem Int Ed Engl* 27:1192
14. Walba D, Richards RM, Haltiwanger RC (1982) *J Am Chem Soc* 104:3219
15. Schill G, Lüttrinhof A (1964) *Angew Chem Int Ed Engl* 3:546
16. Forgan RS, Sauvage J-P, Stoddart JF (2011) *Chem Rev* 111: 5434–5464
17. Coomaraswamy AK (2009) The iconography of Dürer's "Knots" and Leonardo's "concatenations". In: *Eye of the heart*, vol 4. La Trobe University, Bendigo, 11–40
18. Dietrich-Buchecker Ch, Sauvage J-P (1992) *New J Chem* 16:277
19. Frisch HL, Wasserman E (1961) *J Am Chem Soc* 83:3789
20. Schill G, Doerjter G, Logemann E, Fritz H (1979) *Chem Ber* 112:3603
21. Dietrich-Buchecker CO, Sauvage J-P Kern JM (1984) *J Am Chem Soc* 106:3043
22. Philp D, Stoddart JF (1991) *Synlett* 1991:445
23. Hunter CA (1992) *J Am Chem Soc* 114:5303
24. Vogtle F, Meier S, Hoss R (1992) *Angew Chem Int Ed Engl* 31:1619
25. Johnston AG, Leigh DA, Pritchard RJ, Deegan MD (1995) *Angew Chem Int Ed Engl* 34:1209
26. Sauvage J-P (1990) *Acc Chem Res* 23:319
27. Furusho Y, Yashima E (2007) *J Synth Org Chem* 65:1121
28. Fuhrhop JH, Struckmeier G, Thewalt U (1976) *J Am Chem Soc* 98:278
29. Amabilino DB, Stoddart JF (1995) *Chem Rev* 95:2725
30. Dietrich-Buchecker CO, Sauvage JP (1989) *Angew Chem Int Ed Engl* 28:189
31. Dietrich-Buchecker CO, Nierengarten JF, Sauvage JP (1992) *Tetrahedron Lett* 33:3625
32. Dietrich-Buchecker CO, Nierengarten JF, Sauvage JP, Armaroli N, Balzani V, De Cola L (1993) *J Am Chem Soc* 115:11237
33. Albrecht-Gary AM, Dietrich-Buchecker CO, Guilhem J, Meyer M, Pascard C, Sauvage JP (1993) *Recl Trav Chim Pays-Bas* 112:427
34. Dietrich-Buchecker CO, Sauvage JP, De Cian A, Fischer J (1994) *J Chem Soc Chem Commun* 1994:2231
35. Dietrich-Buchecker CO, Rapenne G, Sauvage JP (1999) *Coord Chem Rev* 185–186:167
36. Dietrich-Buchecker CO, Rapenne G, Sauvage JP (1997) *Chem Commun* 1997:2053
37. Rapenne G, Dietrich-Buchecker CO, Sauvage JP (1999) *J Am Chem Soc* 121:994
38. Guo J, Mayers PC, Breault GA, Hunter CA (2010) *Nat Chem* 2:218
39. Safarowsky O, Nieger M, Fröhlich R, Vögtle F (2000) *Angew Chem Int Ed Engl* 39:1616
40. Brüggemann J, Bitter S, Müller S, Müller WM, Müller U, Maier NM, Lindner W, Vögtle F (2007) *Angew Chem Int Ed Engl* 46:254
41. Vögtle F, Hüntgen A, Vogel E, Buschbeck S, Safarowsky O, Recker J, Parham AH, Knott M, Müller WM, Müller U, Okamoto Y, Kubota T, Lindner W, Francotte E, Grimme S (2001) *Angew Chem Int Ed Engl* 40:2468
42. Lukin O, Müller WM, Müller U, Kaufmann A, Schmidt C, Leszczynski J, Vögtle F (2003) *Chem Eur J* 9:3507
43. Lukin O, Kubota T, Okamoto Y, Schelhase F, Yoneva A, Müller WM, Müller U, Vögtle F (2003) *Angew Chem Int Ed Engl* 42:4542
44. Lukin O, Kubota T, Okamoto Y, Kaufmann A, Vögtle F (2004) *Chem Eur J* 10:2804
45. Seeman NC (1998) *Angew Chem Int Ed Engl* 37:3220
46. Du SM, Seeman NC (1992) *J Am Chem Soc* 114:9652



47. Du SM, Stollar BD, Seeman NC (1995) *J Am Chem Soc* 117:1194
48. Dietrich-Buchecker CO, Guilhem J, Pascard C, Sauvage JP (1990) *Angew Chem Int Ed Engl* 29:1154
49. Dietrich-Buchecker CO, Rapenne G, Sauvage JP, De Cian A, Fischer J (1999) *Chem Eur J* 5: 1432
50. Chambron JC, Dietrich-Buchecker CO, Rapenne G, Sauvage JP (1998) *Chirality* 10:125
51. Amabilino DB, Perez-Garcia L (2009) *Chem Soc Rev* 38:1562

# Living in a Cage Is a Restricted Privilege

Luigi Fabbrizzi

**Abstract** There exist molecules, whose shape is reminiscent of a cage, that are able to include either metal ions or anions or both. In contrast to what happens in the macroscopic world, where a kinetic barrier prevents the escaping of the guest from the cage, the inclusion–extrusion of an ion from a molecular cage is in most cases thermodynamically controlled and the ion can get in or out of the cage at will. This gives the basis for highly selective ion recognition processes by cage-shaped ligands or receptors for metal ions and anions. Nobody in everyday life would say that a cage (for birds or wild animals), even if nicely designed and splendidly decorated, was beautiful and appealing, due to the consciousness of its reprehensible function. This does not happen in chemistry and we admire the ingenuity and skilfulness of synthetic chemists for the design of cage-shaped polycyclic hosts, made for the inclusion of a variety of guests, but also capable of generating in the viewer emotion and gratification of aesthetical origin. We have tried to outline, in this chapter, the development of cages in metal coordination chemistry and in anion coordination chemistry, over the last 50 years.

**Keywords** Anion coordination chemistry • Cryptands • Ligands • Metal coordination chemistry • Molecular recognition • Receptors • Sarcophagines

## Contents

1	Cages in Life and in Art .....	128
2	From Ammonia to Sarcophagine: Cages for Metals Made by Metals .....	129
3	Cryptands and Cryptates: Cages Made to Measure for s-Block Metals .....	139
4	Cages for Anions .....	145
5	Bis-Tren Cages: Comfortable Shelters for Metal Ions, Anions and Both Metal Ions and Anions Together .....	150

---

L. Fabbrizzi (✉)

Dipartimento di Chimica, via Taramelli 12, 50136 Pavia, Italy

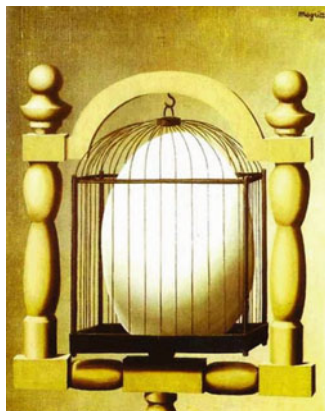
e-mail: [luigi.fabbrizzi@unipv.it](mailto:luigi.fabbrizzi@unipv.it)

6 Small Cages for the Smallest Anion .....	158
7 Is it the Shape or the Function that Defines a Cage? .....	163
References .....	163

## 1 Cages in Life and in Art

Cages are not artistic items. At least in the sense that they are not loved by artists. In fact, they do not appear in famous paintings and sculptures of any age and culture. The only relevant painting featuring a cage is quite recent, on the time scale of art history, being due to René Magritte (1898–1967) during his first surrealist period – *Elective Affinities*, 1933 (see Fig. 1). The painting shows a caged egg and it probably intends to provoke a shock in the viewer through the delayed affinity of two objects to each other, the cage and the egg, from which the typical guest of the cage, a bird, originates. The rare appearance of cages in art is not due to the intrinsically poor relevance of the object itself. Benvenuto Cellini (1500–1571) completed in 1543 for King Francis I of France an object for everyday life, a salt cellar, as a splendid ivory, gold and vitreous enamel table sculpture, but neither a Pope nor an Emperor nor a rich merchant commissioned a golden cage from him. The poor attention of artists and gifted craftsmen to cages is probably to be ascribed to the blameworthy concept of a cage, which is related to deprivation of freedom, constriction in a reduced space, and forced exhibition of one's private life. In addition, the most frequent and usual guest of a cage is one of the most undefended and tender of living beings: a small bird (a canary, a parrot). Thus, humans use cages mostly for leisure, but are not proud of this practise and do not want to emphasise it.

Chemistry is different: synthesising a molecular cage and putting into it a chemical entity (metal ion, anion or molecule) is considered a deserving and admirable action. The design and synthesis of cages at a molecular level has become so common and distinguished an activity to be mentioned in the

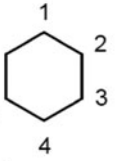
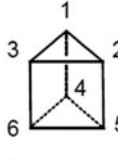
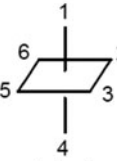


**Fig. 1** René Magritte,  
*Elective Affinities* (1933) – oil  
on canvas. Private collection

Merriam-Webster dictionary online as “an arrangement of atoms or molecules so bonded as to enclose a space in which another atom or ion (as of a metal) can reside” [1]. We can add that a caged chemical can profit from some special properties that are not granted to non-caged counterparts, which makes living in a molecular cage a notable privilege, as we will try to demonstrate.

## 2 From Ammonia to Sarcophagine: Cages for Metals Made by Metals

Transition metal ions are among the most demanding guests of a cage. They engage in bonding  $d$  orbitals, which possess well-defined directional properties and, depending upon their electronic configuration, they discriminate between different coordination geometries in order to profit to the largest extent from ligand field stabilisation effects. The most common coordination geometry is the octahedral one and the electronic configuration that profits most from octahedral geometry (24 Dq, in the language of Crystal Field Theory) is  $d^6$  low-spin. It is not accidental that coordination chemistry began with the synthesis and characterisation of octahedral complexes of  $\text{Co}^{\text{III}}$  ( $d^6$  low-spin) with the most common and cheapest ligand: ammonia. The founder of coordination chemistry, Alfred Werner (1866–1919), thanks to the substitutional inertness of the  $\text{Co}^{\text{III}}$  centre, a property related to the stable electronic configuration, isolated a variety of cobalt ammonia complexes, which could be characterised by elemental analysis and simple reactivity tests. Even in the absence any direct physico-chemical technique (e.g. single crystal X-ray diffraction), Werner was able to induce not only stoichiometry, but also the geometrical structure of the investigated complexes [2]. The most famous example refers to the complex of formula  $\text{Co}(\text{NH}_3)_4\text{Cl}_3$ , which was isolated in two isomeric forms of distinct colour: green and violet. Addition of  $\text{AgNO}_3$  to the solutions of the two complexes, at room temperature, caused in both cases the precipitation of 1 equiv. of  $\text{AgCl}$ , which indicated that only two  $\text{Cl}^-$  ions were directly bound to the metal, to which the following formula corresponded:  $[\text{Co}^{\text{III}}(\text{NH}_3)_4\text{Cl}_2]^+$ . Then, Werner considered that, for coordination number 6, three coordination geometries were possible: hexagonal, trigonal prismatic and octahedral. Of the three geometrical arrangements, the hexagon and the trigonal prism would give rise to three isomers, as shown in Fig. 2. Thus, the correct geometry had to be the octahedral one, whose expected isomers are just two. Professor Werner was pretty sure of his ability at the bench for not missing a “third” isomer (but he had investigated 20 series of compounds showing this type of isomerism). Also the “configuration allocation”, i.e. the discrimination of *cis* and *trans* isomers was carried out on a chemical basis: Werner noted that on substitution by two  $\text{Cl}^-$  ions of the bound bidentate carbonate ion in the complex  $[\text{Co}^{\text{III}}(\text{NH}_3)_4\text{CO}_3]^+$ , which had to necessarily exhibit a *cis* configuration, the violet form was obtained, to which the *cis* configuration could be unequivocally assigned. The advantage of the octahedron

number of found isomers			
	hexagon	trigonal prism	octahedron
2	possible isomers 3 (1,2;1,3;1,4)	possible isomers 3 (1,2; 1,4; 1,5)	possible isomers 2 (1,2; 1,4)

**Fig. 2** How Alfred Werner assigned an octahedral structure to the two isomeric complexes of formula  $[\text{Co}^{\text{III}}(\text{NH}_3)_4\text{Cl}_2]\text{Cl}$ . Only the octahedral geometry is consistent with the formation of two isomers: the green (1,4) *trans* isomer and the violet (1,2) *cis* isomer

with respect to the other six-coordinating arrangements was later supported by valence shell electron pair repulsion (VSEPR) theory and also by crystal field stabilisation energy (CFSE) arguments. Indeed, Werner introduced in chemistry, from the inorganic side, a second Platonic solid (the octahedron), which followed the most famous and well-established polyhedron, coming from the organic counterpart (the tetrahedron). Since then, chemists became used to “seeing” six-coordinated metal complexes, including aquaions, arranged in the highly symmetric octahedral structure, explaining on this geometrical basis their physical properties and reactivity.

Over the last century, ligands containing more amine groups and displaying an increasing degree of sophistication were synthesised and were found to impart novel and interesting properties to the bound metal ions. Only a few chosen transition metal ions exhibit substitutional inertness, which is related to their stable electronic configuration, e.g.  $\text{Co}^{\text{III}}$  and  $\text{Rh}^{\text{III}}$ ,  $d^6$  low-spin octahedral;  $\text{Cr}^{\text{III}}$ ,  $d^3$  octahedral;  $\text{Pt}^{\text{II}}$ ,  $d^8$  planar, just to mention those investigated by Werner. On the other hand, divalent 3d metal ions are labile, undergoing fast substitution processes. Thus, their ammonia complexes cannot be isolated in different isomeric forms, as can those of  $\text{Co}^{\text{III}}$ . Nevertheless, they presented interesting properties, which allowed the introduction of new concepts in chemistry. In particular, the coordination chemistry of multidentate ligands developed, i.e. molecules containing more amine groups (Fig. 3), also defined as chelating agents. It was observed that a given metal complex of an  $n$ -dentate ligand was thermodynamically more stable than the corresponding complex with  $n$  molecules of  $\text{NH}_3$  (the chelate effect) and that such an extra stability increased with the ligand’s denticity [3]. Later, comparison of the solution behaviour of the divalent 3d metal complexes of aliphatic tetra-amines, whether open-chain or cyclic, disclosed further interesting properties. In particular, the cyclic tetramine ligand (the macrocycle) forms a more stable complex (by three orders of magnitude or more) with a given metal than its non-cyclic counterpart (the so called thermodynamic macrocyclic effect) [4].

As an example, Fig. 4 illustrates the  $\text{Ni}^{\text{II}}$  complexation equilibria in water involving 2.3.2-tet (1), champion of non-cyclic tetra-amines, and cyclam (2),

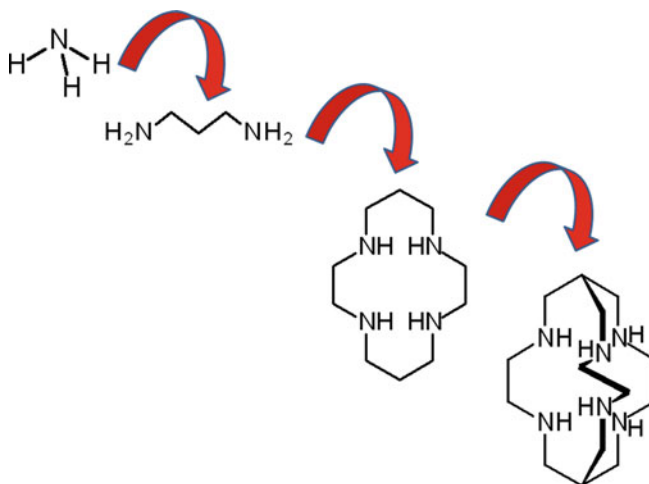


**Fig. 3** Evolution of ligands containing  $sp^3$  nitrogen donor atoms: from ammonia, to ethylenediamine, to cyclam, to sarcophagine

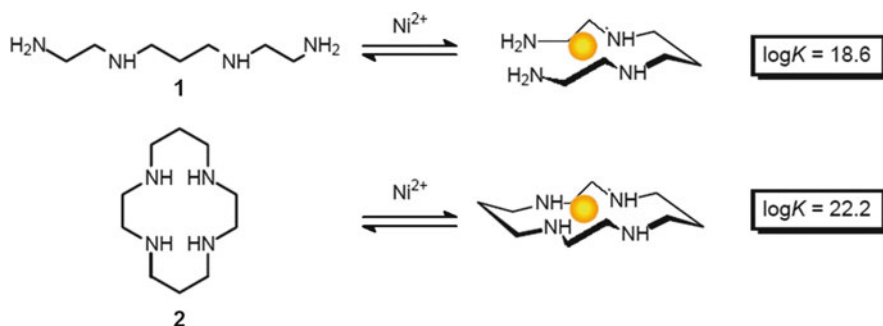
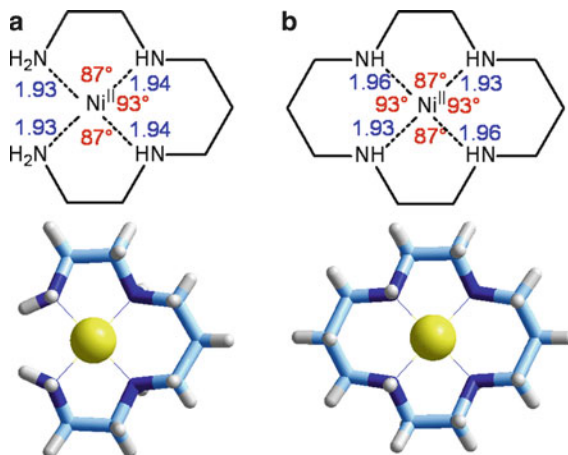


**Fig. 4** Thermodynamic macrocyclic effect: complexation equilibria involving the  $Ni^{II}$  aqua.ion and the champions of non-cyclic tetra-amines **1** (2.3.2-tet) and of the tetra-amine macrocycles **2** (cyclam)

champion of tetramine macrocycles. The macrocyclic complex is ca. 4,000-fold more stable than that of the open-chain ligand. Figure 5 shows some structural details of the low-spin  $Ni^{II}$  complexes of 2.3.2-tet [5], and cyclam [6], as obtained from X-ray diffraction studies on crystalline salts. Both complexes exhibit a square planar coordination geometry.  $Ni^{II}$ -N distances and N- $Ni^{II}$ -N angles are nearly the same for both complexes, which indicates the establishing of metal-ligand interactions of comparable intensity. Thus, the thermodynamic macrocyclic effect does not depend upon a different strength of coordinative bond, and, in particular, it has to be ascribed to the fact that cyclam is perfectly preorganised for metal coordination, whereas the open-chain ligand must spend energy (both enthalpic and entropic in nature) in folding itself in order to fulfil the geometrical requirements of

**Fig. 5** Molecular structures of low-spin nickel(II) tetramine complexes: (a)  $[\text{Ni}^{\text{II}}(2.3.2\text{-tet})]^{2+}$  [5] and (b)  $[\text{Ni}^{\text{II}}(\text{cyclam})]^{2+}$  [6]. Counterions have been omitted for clarity: tetraethynylborate and chloride for (a) and triflate for (b). Bond distances are given in Å



the metal ion. Moreover, there exists also a kinetic macrocyclic effect [7]. In fact, the  $[\text{Ni}^{\text{II}}(\text{cyclam})]^{2+}$  complex does not demetallate on addition of strong acid. In particular,  $[\text{Ni}^{\text{II}}(\text{cyclam})]^{2+}$  persists in a 1 M  $\text{HClO}_4$  solution with a lifetime,  $\tau$ , of 30 years [8]. On the other hand,  $[\text{Ni}^{\text{II}}(2.3.2\text{-tet})]^{2+}$  decomposes instantaneously in acidic solution. In fact,  $\text{Ni}^{\text{II}}$  is a labile metal and allows terminal ethylamine arms to quickly detach/attach from/attach to coordination sites. In the presence of  $\text{H}^+$  ions, detached primary amine groups are protonated and cannot bind the metal again, thus starting the demetallation process. On the other hand, the four amine groups of the  $[\text{Ni}^{\text{II}}(\text{cyclam})]^{2+}$  complex are mechanically blocked in the corners of the coordination square, do not undergo any flip–flop motion and cannot be protonated.

Sequestering in a cyclic environment imparts to the metal novel properties and favours redox activity. For instance,  $[\text{Ni}^{\text{II}}(\text{cyclam})]^{2+}$  in 1 M  $\text{HCl}$  is oxidised to the indefinitely stable  $[\text{Ni}^{\text{III}}(\text{cyclam})]^{3+}$  complex, at a moderately positive potential (0.72 V vs. NHE) [9]. The acidic medium is required to prevent intramolecular electron transfer processes, leading to decomposition [10]. Moreover,  $[\text{Ni}^{\text{II}}(\text{cyclam})]^{2+}$  can be electrochemically reduced to  $[\text{Ni}^{\text{I}}(\text{cyclam})]^+$  at a mercury electrode, where it catalyses the reduction of  $\text{CO}_2$  to  $\text{CO}$  and  $\text{HCOO}^-$  (in an aqueous solution buffered to pH 5) [11]. This is nothing especially new: encircling by tetra-aza macrocycles (e.g. porphyrins) is a trick known to Nature for billions of years to favour and control the redox activity of metal ions.

Multidentate ligands (e.g. polyamines) of desired structural features can be designed and synthesised, sometimes through multistep and tedious procedures, then made to react with a chosen metal ion to give a complex of predetermined geometry, hopefully displaying wanted properties and reactivity. However, the synthesis of cyclam can be carried out in one pot, with the help of the  $\text{Ni}^{\text{II}}$  ion, which controls and addresses the course of the reaction, acting as a template.

The reaction, illustrated in Fig. 6, takes place in water, open air, at room temperature. The  $\text{Ni}^{2+}$  ion, on coordination of the linear tetramine 3.2.3-tet (3), places the two primary amine groups in the positions (the adjacent corners of a square)

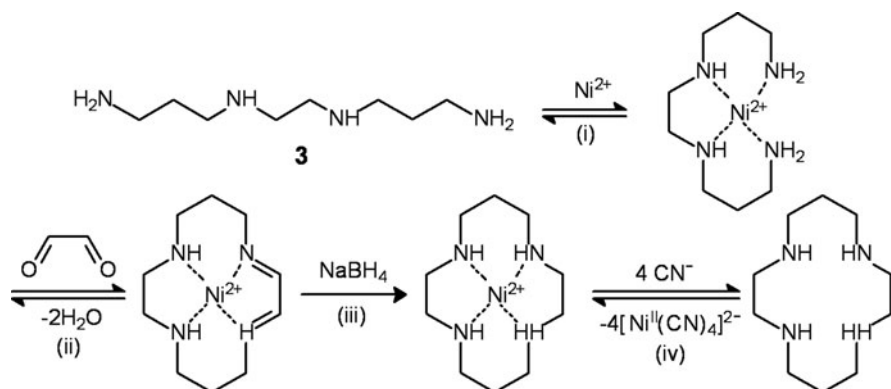


**Fig. 6** Template synthesis of  $[\text{Ni}^{\text{II}}(\text{cyclam})]^{2+}$  from linear 3,2,3-tet **3** and its demetallation to give the uncomplexed cyclam ligand. Steps *i–iv* are described in the text

suitable for Schiff base condensation with one molecule of glyoxal, to form the diene macrocycle. The reversibility of the formation of the  $\text{C}=\text{N}$  double bond favours the attainment of the thermodynamically most stable species (the macrocyclic complex) with respect to non-cyclic oligomers. Then,  $\text{NaBH}_4$  is added in the same vessel in order to hydrogenate the two  $\text{C}=\text{N}$  bonds, thus giving weaker, but kinetically stable  $\text{C}-\text{N}$  single bonds. The  $[\text{Ni}^{\text{II}}(\text{cyclam})]^{2+}$  complex can be precipitated as a yellow–orange perchlorate salt by addition of concentrated perchloric acid. If wished, boiling an aqueous solution of  $[\text{Ni}^{\text{II}}(\text{cyclam})](\text{ClO}_4)_2$ , in the presence of excess  $\text{CN}^-$  (and  $\text{OH}^-$ ), demetallates the complex and the cyclam ligand can be isolated as a white solid. The  $\text{Ni}^{\text{II}}$  template synthesis of cyclam was reported in 1972 by Barefield [12, 13]. This was the natural evolution of the pioneering work on the template synthesis of tetra-aza macrocycles carried out by Busch and Curtiss during the preceding decade [14, 15].

“Template” is a widely used term in chemistry and in biology. Looking at its etymology, “template” is the phonetic English version of the French word *templet*, diminutive of temple, which hints at the pediment of a Greek–Latin temple (see Fig. 7): in fact, the shape of the pediment provides the most simple pattern to be used as a guide to the form of a piece being made: the triangle. Triangular shapes are not common in coordination chemistry, where the most simple template remains the square, which can be conveniently provided by 3d metals,  $\text{Ni}^{\text{II}}$  and  $\text{Cu}^{\text{II}}$  *in primis*.

However, transition metals can also act as templates to make shapes in three dimensions. In 1977, Alan Sargeson reported the astonishing one-pot synthesis of a cage-shaped polyamine, templated by  $\text{Co}^{\text{III}}$ , which offered an octahedral pattern [16]. Mechanistic details of the synthesis, taking place in water, in open air, at room temperature, are illustrated in Fig. 8.

The labile  $\text{Co}^{2+}$  ion was made to react with three molecules of ethylenediamine (en), to give the octahedral  $[\text{Co}^{\text{II}}(\text{en})_3]^{2+}$  complex, which was then oxidised by air to the inert  $[\text{Co}^{\text{III}}(\text{en})_3]^{3+}$  (Fig. 8, step i). Then, Schiff base condensation with six





**Fig. 7** The Temple of Concordia at Agrigentum. The shape of the pediment provides the simplest template: the triangle

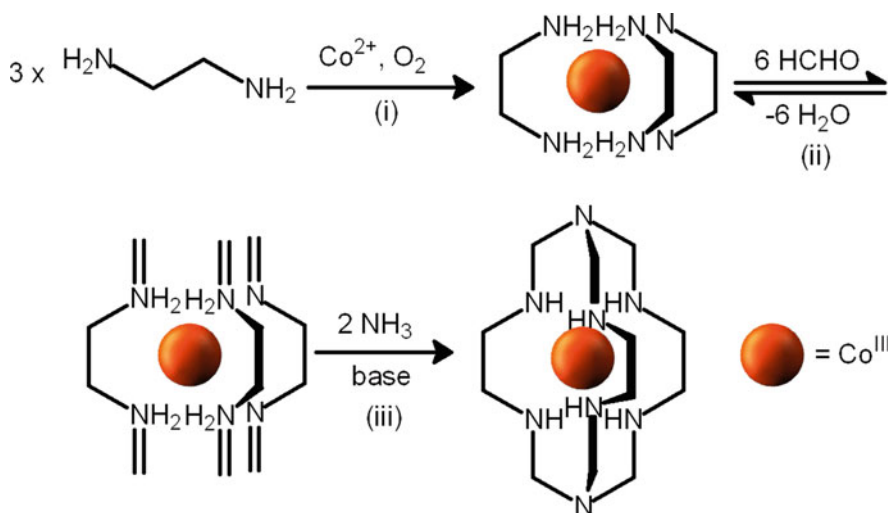


**Fig. 8** Template synthesis of the cobalt(III) sepulchrate complex,  $[\text{Co}^{\text{III}}(\text{sep})]^{3+}$ . *Step i* complex formation and oxidation by air; *step ii* Schiff base condensation; *step iii* nucleophilic attack to the C=N double bond by the deprotonated forms of ammonia

molecules of formaldehyde takes place at the six  $-\text{NH}_2$  groups (Fig. 8, step ii). Finally, in the presence of base, nucleophilic attacks to the C=N double bonds by the varying deprotonated forms of the triprotic acid  $\text{NH}_3$  occur, which eventually lead to the formation of the cage (Fig. 8, step iii). The reaction is unique in that 12 distinct particles (the metal ion, three en, six HCHO, and two  $\text{NH}_3$ ) give a well-concerted sequence of reactions, addressed by the  $\text{Co}^{\text{III}}$  template, leading to the formation of an intrinsically complicated and highly symmetrical molecular system. Inspired by the solemn, funereal fashion of naming ligands introduced by Lehn (with cryptands and cryptates), Sargeson christened the octamine cage “sepulchrand” (sep) and its

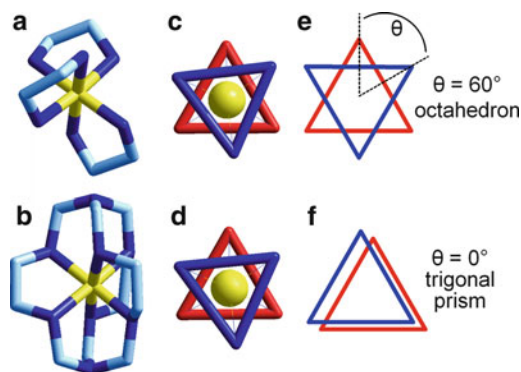
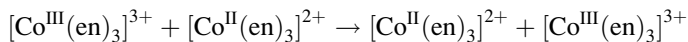


**Fig. 9** (a) Structure of the  $[\text{Co}^{\text{III}}(\text{en})_3]^{3+}$  complex [16] and (b) structure of the  $[\text{Co}^{\text{III}}(\text{sep})]^{3+}$  complex [17]; for both complex salts, chloride counterions and hydrogen atoms have been omitted for clarity. (c) Top view of the triangles obtained by joining the nitrogen atoms of the primary amine groups of each coordinated en molecule. (d) Top view of the triangles obtained by joining the nitrogen atoms of the secondary amine groups linked to each one of the two caps of sepulchrand. (e, f) Top view of two opposite triangular faces of an octahedron and of a trigonal prism; the two different geometrical arrangements are defined by the torsion angle  $\theta$ . Values of  $\theta$  are:  $53.58^\circ$  for  $[\text{Co}^{\text{III}}(\text{en})_3]^{3+}$  (c), and  $54.5 \pm 0.3^\circ$  for  $[\text{Co}^{\text{III}}(\text{sep})]^{3+}$  (d)

complexes “sepulchrates”. The term is nevertheless appropriate considering that the metal centre in the  $[\text{Co}^{\text{III}}(\text{sep})]^{3+}$  complex is insensitive to any exotic ligand and inert to the demetallation, as if it were dead and buried in the octamine framework.

In Fig. 8, for convenience, the structural formulae of  $[\text{Co}^{\text{III}}(\text{en})_3]^{3+}$  and  $[\text{Co}^{\text{III}}(\text{sep})]^{3+}$  complexes have been represented according to a trigonal prismatic coordination geometry. However, structural studies on crystalline trichloride salts have shown that both complexes exhibit a slightly distorted octahedral geometry, as illustrated in Fig. 9a, b [16, 17]. Notice that in a perfectly regular octahedron, two opposite triangular faces should be staggered with a torsion angle  $\theta = 60^\circ$ , as illustrated in Fig. 9e. Conversely, a value of  $\theta = 0^\circ$  (eclipsed triangles, Fig. 9f) defines the other possible six-coordinating geometrical arrangement: the trigonal prism. The observed torsion angles are very similar for the two complexes,  $[\text{Co}^{\text{III}}(\text{en})_3]^{3+}$   $\theta = 53.58$  [16] and  $[\text{Co}^{\text{III}}(\text{sep})]^{3+}$   $\theta = 54.5 \pm 0.3$ , and are very close to the value for a regular octahedron [17].  $\text{Co}^{\text{III}}\text{-N}$  bond distances are those expected for  $\text{Co}^{\text{III}}$  low-spin amine complexes ( $[\text{Co}^{\text{III}}(\text{en})_3]^{3+}$   $1.96 \pm 0.01 \text{ \AA}$ ;  $[\text{Co}^{\text{III}}(\text{sep})]^{3+}$   $1.99 \pm 0.01 \text{ \AA}$ ) and  $\text{N-Co}^{\text{III}}\text{-N}$  bond angles are very similar for both complexes. Thus, being coordinated by three distinct en molecules or by three ethylenediamine fragments incorporated in a cage framework does not seem to change very much the binding tendencies of the  $\text{Co}^{\text{III}}$  centre, which in any case imposes its bonding and geometrical preferences. However, deep differences are observed in the reactivity of the  $[\text{Co}^{\text{III}}(\text{en})_3]^{3+}$  and of the  $[\text{Co}^{\text{III}}(\text{sep})]^{3+}$  complex, in particular as far as the redox behaviour is concerned. Cobalt(III) hexamine complexes undergo a one-electron reduction process to the corresponding  $\text{Co}^{\text{II}}$  species at a moderately negative potential: for instance, for the

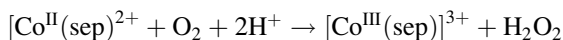
$[\text{Co}^{\text{III}}(\text{en})_3]^{3+}/[\text{Co}^{\text{II}}(\text{en})_3]^{2+}$  couple,  $E^\circ = -0.02$  V versus the normal hydrogen electrode (NHE) [18]. Such an electron transfer is especially slow. In particular, for the self-exchange process:



the rate constant  $k_{11}$  is  $2.9 \times 10^{-5} \text{ M}^{-1} \text{ s}^{-1}$  [18]. As a consequence, all reductions processes involving  $[\text{Co}^{\text{III}}(\text{en})_3]^{3+}$ , as well as oxidation processes involving  $[\text{Co}^{\text{II}}(\text{en})_3]^{2+}$ , are slow. Sluggishness of the  $\text{Co}^{\text{III}}/\text{Co}^{\text{II}}$  electron transfer process is well interpreted in terms of the Marcus theory: on moving from the  $[\text{Co}^{\text{III}}(\text{en})_3]^{3+}$  complex ( $d^6$ , low-spin) to the  $[\text{Co}^{\text{II}}(\text{en})_3]^{2+}$  ( $d^7$ , high-spin), a substantial increase in the Co–N bond distance from 1.96 to 2.16 Å is observed. This makes the reorganisation energy and the free energy of activation  $\Delta G^\ddagger$  especially high and the electron transfer slow.

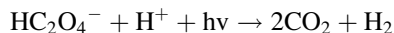
On the other hand, while the  $E^\circ$  value for the  $[\text{Co}^{\text{III}}(\text{sep})]^{3+}/[\text{Co}^{\text{II}}(\text{sep})]^{2+}$  ( $-0.30$  V vs. NHE) is close to that observed for the en analogue, the rate constant of the self-exchange process is more than five orders of magnitude higher ( $k_{11} = 5.1 \text{ M}^{-1} \text{ s}^{-1}$ ) [18]. Such a behaviour is surprising in that the  $[\text{Co}^{\text{III}}(\text{sep})]^{3+}/[\text{Co}^{\text{II}}(\text{sep})]^{2+}$  reduction process also involves a low-spin to high-spin conversion and a drastic increase of the bond distances (from 1.99 to 2.16 Å), to which a similarly high value of reorganisation energy and of  $\Delta G^\ddagger$  should correspond. However, attention should be addressed not only to the metal–ligand interaction, but also to the overall energy of the complex, including the strain energy of the ligating framework [19]. The strain energy, which is intuitively larger in the cage system than in a bidentate ligand, brings the  $\text{Co}^{\text{III}}$  and  $\text{Co}^{\text{II}}$  complexes closer to the transition state, making  $\Delta G^\ddagger$  much lower and the electron transfer much faster.

As a further advantage, the  $[\text{Co}^{\text{II}}(\text{sep})]^{2+}$  complex can be generated in aqueous solution by reducing the  $\text{Co}^{\text{III}}$  complex with zinc dust or zinc amalgam in the 5–7 pH range and investigated for its redox properties. For instance,  $[\text{Co}^{\text{II}}(\text{sep})]^{2+}$  reacts with dioxygen to give hydrogen peroxide [20], according to the a fast process:



Non-caged  $\text{Co}^{\text{II}}$  polyamine complexes, e.g.  $[\text{Co}^{\text{II}}(\text{NH}_3)_6]^{2+}$ , do not give such a reaction, but form stable  $\text{Co}^{\text{III}}$  peroxy dimers,  $[(\text{NH}_3)_5\text{Co}^{\text{III}}\text{O}-\text{O}-\text{Co}^{\text{III}}(\text{NH}_3)_5]^{4+}$ . Moreover, encapsulation provides a redox couple whose oxidised and reduced form are protected from undesired side reactions. This makes the  $[\text{Co}^{\text{III}}(\text{sep})]^{3+}/[\text{Co}^{\text{II}}(\text{sep})]^{2+}$  a convenient and robust electron relay in many processes. For instance, it can successfully replace methylviologen ( $\text{MV}^{2+}$ ) as an efficient electron transfer agent from photoexcited  $[\text{Ru}^{\text{II}}(\text{bpy})_3]^{2+}$  to  $\text{H}^+$  in the photoreduction of water (in the presence of colloidal platinum, and excess EDTA as a sacrificial electron donor) [21]. In particular, it works for more than 5,000 turnovers, as compared with the 55 turnovers of the more fragile  $\text{MV}^{2+}$ .  $[\text{Co}^{\text{III}}(\text{sep})]^{3+}$  can act as a photosensitiser itself and, when irradiated at 331 nm in a solution adjusted to

pH = 3, in the presence of oxalate, it promotes the formation of H<sub>2</sub> and CO<sub>2</sub>, according to the reaction:



with a turnover number >700 [22]. This unique reactivity results from the combination of two properties: (1) the relatively high-rate of the electron transfer, derived from the strained arrangement of the cage framework; and (2) the stability of the Co<sup>II</sup> complex in a moderately acidic solution (whereas non-caged Co<sup>II</sup> complexes decompose). At this stage, it could seem convenient to verify whether other metals, encapsulated by the sepulchrand, display unusual and unprecedented properties. However, any attempt to demetallate the complex, in order to obtain the free sepulchrand, failed. In particular, in the absence of an encapsulated metal, the sepulchrand decomposes, due to intrinsic instability of methylenediamine groups. For instance, reduction of [Co<sup>III</sup>(sep)]<sup>3+</sup> with Zn in 1 M HCl induces decomposition to Co<sup>2+</sup>(aq), <sup>+</sup>H<sub>3</sub>NCH<sub>2</sub>CH<sub>2</sub>NH<sub>3</sub><sup>+</sup> and NH<sub>4</sub><sup>+</sup>, practically reversing the process illustrated in Fig. 8.

In conclusion, a metal centre has built up around itself a superb container, of which it remains prisoner. The only, but unhappy, way to escape is to crash the beautiful vase. This tale is reminiscent of a short story by Luigi Pirandello (1867–1936) entitled *The jar* [23]. A Sicilian landowner bought an enormous earthenware jar, large enough to contain the great amount of olive oil he expects to produce. To his disappointment, he realises that the jar is broken in two distinct pieces. Therefore he calls a renowned craftsman to repair the huge amphora. The repairman decides to fix the jar with glue and iron wire and asks that the two pieces of the jar are closed around him, because he wants to make the repair from inside. At the end, the jar is perfectly fixed, but the craftsman remains prisoner. Then, a long contest begins involving the repairman, who wants to break the jar, and the landowner, who insists that the jar must not be broken, in the presence of many partaking wits. Finally, the frustrated landowner kicks the jar, which rolls down a bank to crash into a tree, freeing the craftsman.

Fortunately, things at the molecular level can go better than in the real (or literary) world. In fact, a very stable and indestructible version of polyamine cages of the sepulchrand type was obtained by Sargeson by simply replacing NH<sub>3</sub>, in the template reaction illustrated in Fig. 8, with the stronger triprotic acid CH<sub>3</sub>NO<sub>2</sub>, to give the [Co<sup>III</sup>(NO<sub>2</sub>)<sub>2</sub>sar]<sup>3+</sup> complex [24]. Notice first that the substituents on the caps can be modified and finally eliminated according to the sequence of reactions illustrated in Fig. 10. To these hexamines, the general trivial name of “sarcophagines” (abbreviated to sar) was given, in keeping with the current necrophilic nomenclature. The sar framework is robust and resistant to the most drastic conditions, which allows demetallation and isolation of the metal-free hexamine, whether (NH<sub>2</sub>)<sub>2</sub>sar or sar, in good yield [25]. Demetallation was carried out on the Co<sup>II</sup> cage complex, to avoid the intrinsic inertness of the Co<sup>III</sup> centre, according to two main procedures. In one process, a suspension of the [Co<sup>II</sup>(NH<sub>3</sub>)<sub>2</sub>sar]Cl<sub>4</sub> complex salt in a deoxygenated 48% HBr solution was heated at reflux for 3 h under dinitrogen, to give a clear solution of the blue [Co<sup>II</sup>Br<sub>4</sub>]<sup>2-</sup>

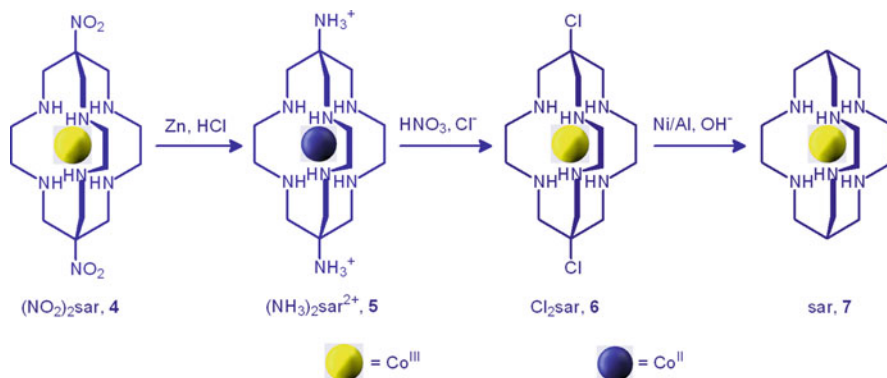


**Fig. 10** Different cobalt sarcophagine complexes **5–7** derived from the  $[\text{Co}^{\text{III}}(\text{NO}_2)_2\text{sar}]^{3+}$  precursor **4**, obtained from a template reaction

complex and of the protonated sarcophagine. Then, the solution was exposed to air and eluted with HCl on a Dowex column, to give the  $[(\text{NH}_3)_2\text{sar}]\text{Cl}_2$  hydrochloride. According to a milder procedure, a deoxygenated yellow–orange solution, containing equimolar amounts of  $[\text{Co}^{\text{III}}(\text{NH}_3)_2\text{sar}]\text{Cl}_3$  and  $\text{CoCl}_2 \cdot 6\text{H}_2\text{O}$  plus excess of  $\text{CN}^-$ , was heated at  $70^\circ\text{C}$  for 6 h. The resulting colourless solution was taken to dryness, to give a white precipitate of  $(\text{NH}_3)_2\text{sar}$ . In the latter process,  $[\text{Co}^{\text{III}}(\text{NH}_3)_2\text{sar}]^{3+}$  is first reduced by  $[\text{Co}^{\text{II}}(\text{CN})_6]^{4-}$  to  $[\text{Co}^{\text{II}}(\text{NH}_3)_2\text{sar}]^{2+}$ , which is then demetallated by  $\text{CN}^-$ , with formation of  $[\text{Co}^{\text{II}}(\text{CN})_6]^{4-}$ .

Availability of the free sarcophagines allowed the synthesis of a variety of metal complexes, showing distinct structural differences. Some selected examples are shown in Fig. 11. In particular, the complexes showed coordination geometries varying from the trigonal prism to the octahedron, while the degree of distortion changed with the electronic configuration of the metal ion. In the  $[\text{Mg}^{\text{II}}(\text{NH}_3)_2\text{sar}]^{4+}$  complex [25], the torsion angle  $\theta$  ( $27.6 \pm 0.1^\circ$ ) is midway between that of the trigonal prism ( $\theta = 0^\circ$ ) and that of octahedron ( $\theta = 60^\circ$ ).  $\text{Mg}^{\text{II}}$  is a spherical ion that does not present any geometrical preference. This suggests that the coordinated sarcophagine framework, in the  $[\text{Mg}^{\text{II}}(\text{NH}_3)_2\text{sar}]^{4+}$  complex, is in its most stable conformation from a purely steric point of view. Things change with the  $[\text{Cr}^{\text{III}}(\text{NH}_3)_2\text{sar}]^{3+}$  complex, whose torsion angle ( $\theta = 48.9 \pm 0.2^\circ$ ) has moved to a value much closer to that of the octahedron [26]. This may reflect the fact that a transition metal profits more from the octahedral than from the trigonal prismatic coordination geometry, in terms of crystal field stabilisation energy (CFSE) [29]. In particular, for a  $d^3$  cation like  $\text{Cr}^{\text{III}}$ , the CFSE is  $-10.72$  Dq for the trigonal prism and  $-12$  Dq for the octahedron. However, the greatest advantage of the octahedron is expected for a low-spin  $d^6$  electronic configuration, that of  $\text{Co}^{\text{III}}$  with CFSE =  $-24$  Dq, versus  $-21.44$  Dq for the trigonal prism. Indeed, in the  $[\text{Co}^{\text{III}}(\text{NH}_3)_2\text{sar}]^{5+}$  complex, the closest value to  $60^\circ$  is observed ( $\theta = 55.4 \pm 0.3^\circ$ ), which makes the coordination geometry almost octahedral [27]. On the other hand, the  $\text{Mn}^{\text{II}}$  metal centre, of high-spin  $d^5$ , has a CFSE =  $0$  Dq in any coordination

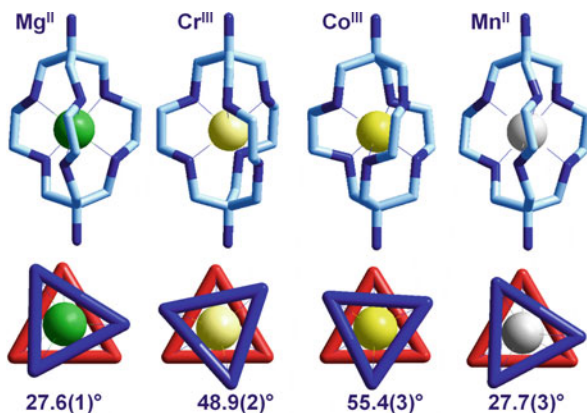


**Fig. 11** *Top*: Structures of metal complexes of sarcophagines, as obtained from X-ray diffraction studies [25–28]; Cr<sup>III</sup> is complexed by (NH<sub>3</sub>)<sub>2</sub>sar; all other metals are complexed by (NH<sub>3</sub>)<sub>2</sub>sar<sup>2+</sup>. *Bottom*: Top view of the triangles obtained by joining the nitrogen atoms of the secondary amine groups linked to each one of the two caps of sarcophagine ligands, with the values of torsion angles  $\theta$

geometry and its [Mn<sup>II</sup>(NH<sub>3</sub>)<sub>2</sub>sar]<sup>4+</sup> complex shows a torsion value  $\theta = 27.7 \pm 0.3^\circ$  [28]. This is the same value observed for the Mg<sup>II</sup> complex, which corresponds to the less-strained conformational arrangement of the coordinated sarcophagine, in the absence of any crystal field effect.

### 3 Cryptands and Cryptates: Cages Made to Measure for s-Block Metals

Coordination chemistry was born with transition metals, a circumstance that reflects the relatively high energy of the metal–ligand interaction. The  $sp^3$  amine nitrogen atom is the deputed donor for establishing strong  $\sigma$  coordinative interactions and ammonia is the prototype ligand for transition metal ions. On the other hand, for s-block metal ions, it is the  $sp^3$  oxygen that is the donor atom displaying the highest affinity and water is expected to be the prototype ligand. Indeed, alkali and alkaline earth metal salts dissolve in water, where the metal is surrounded by a shell of coordinating solvent molecules. However, such aqua-complexes are not stable enough to be isolated and, on crystallisation, salts are formed in which the metal ion directly interacts (electrostatically) with the anion.

Transition metal coordination chemistry has taught some tricks for enhancing the stability of complexes, for instance making use of multidentate ligands. However, the intrinsic stability of the complexes of s-block metal ions with ligands containing  $sp^3$  oxygen donor atoms is so low that the simple chelate effect fails: in fact, poorly stable complexes are formed with glycols, the analogues of polyamines. But, if the chelate effect does not work, the macrocyclic effect does. This was

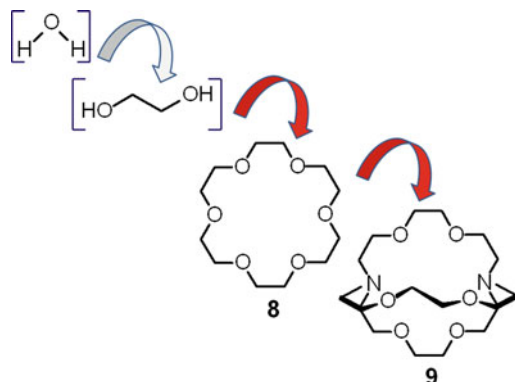


**Fig. 12** Evolution of ligands containing  $sp^3$  oxygen donor atoms. Only crown-ethers (e.g. **8**, 18-crown-6) and cryptands (e.g. **9**, 2.2.2-crypt) form stable complexes with s-block metal ions

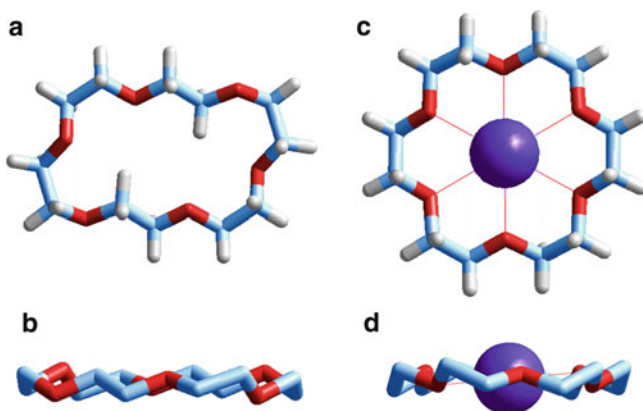


**Fig. 13** Structures of the free cyclic polyether 18-crown-6, **8** (a, b) and of its  $K^+$  complex (c, d) [31]. The puckered arrangement of the  $sp^3$  hybridised carbon and oxygen atoms of the polyether accounts for the trivial name of “crown”

demonstrated in 1967 by Charles Pedersen through the synthesis of a spectacular collection of cyclic polyethers [30]. The ideal evolution of ligands for an s-block cation, containing  $sp^3$  oxygen donor atoms is illustrated in Fig. 12. Figure 13 shows the structure of the cyclic polyether **7** constituted of 18 atoms and containing six oxygen atoms [31], which was given the trivial name of 18-crown-6. The term “crown” was suggested by the puckered arrangement of the  $sp^3$  carbon and  $sp^3$  oxygen atoms, which is shown, for instance, in Fig. 13c, d. The  $K^+$  ion on complexation makes the ligand reorganise to a more symmetric arrangement, which allows it to receive six equivalent bonds from the ethereal oxygen atoms. Indeed, the crown seems made to measure for  $K^+$ , which is perfectly inserted into the crown.

The study of the interaction in solution of a variety of cyclic polyethers of different cavity size with a homogeneous class of spherical cations of differing

**Fig. 14** Log  $K$  values for the equilibrium:  $M^+ + L \rightleftharpoons [ML]^+$  in MeOH, at 25 °C ( $M$  = alkali metal;  $L$  = 18-crown-6, **8**) [32]

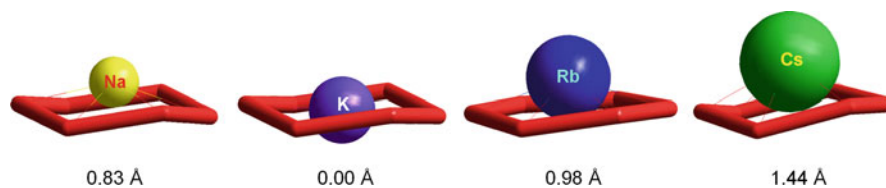
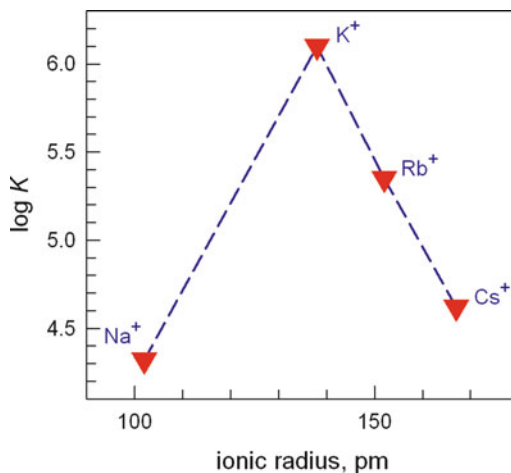


**Fig. 15** Position of alkali metal ions with respect to the six oxygen atoms of 18-crown-6, **8**, which are linked by segments, in the corresponding complexes. Values in Å give the distance between the metal and the mean least-squares plane of the six oxygen atoms of the ligand. These values are related to the stability of the complexes in solution: the lower the distance, the higher the complexation constant [31, 33, 34]

radius, e.g. alkali metals, offered the opportunity to evaluate geometrical effects on the thermodynamic stability of the complexes and to introduce the concept of size selectivity. This is illustrated, for instance, by the diagram in Fig. 14, in which log  $K$  values of the complexation equilibria of 18-crown-6 in MeOH, at 25 °C, have been plotted against the ionic radius of the alkali metal [32]. A sharp peak selectivity in favour of  $K^+$  is observed, which apparently has the right radius to fit the cavity of the crown ether relaxed to its more stable conformation. Figure 15 shows the position of each alkali metal ion with respect to the six oxygen atoms of 18-crown-6, which have been linked together by segments, as observed from X-ray diffraction studies on crystalline complexes. The distance of the ion from the least-squares mean plane of the six oxygen atoms is also reported in the figure.  $K^+$  is perfectly coplanar with the  $O_6$  mean plane (distance 0.00 Å) [31].  $Rb^+$  (Jaenschke, Wilde and Olbrich, private communication; CCDC refcode: XESWIB) and  $Cs^+$  [33] are too big and must stay above the plane, at 0.98 and 1.44 Å, respectively, thus profiting from less intense metal–ligand interactions. On the other hand, the small  $Na^+$  ion [34] would be lost if fully inserted in the cavity and prefers to interact from



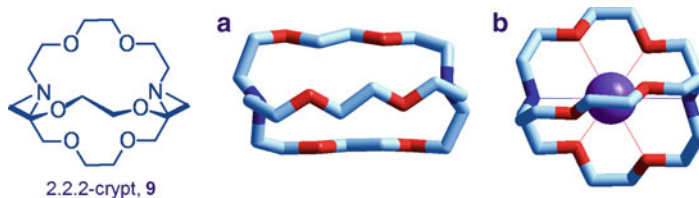


**Fig. 16** Structures of 2.2.2-crypt, **9**, (a) [36] and of its potassium complex (b) [37], as obtained from X-ray diffraction studies on the crystalline compounds. Hydrogen atoms have been omitted for clarity

outside with properly oriented oxygen atoms (to the detriment of the complex stability).

In metal polyamine chemistry, the evolution from macrocycles to cages took decades. In polyether coordination chemistry, such progress took only 2 years. In 1969, Jean-Marie Lehn, a young professor at the Université Louis Pasteur, Strasbourg, with students Bernard Dietrich and Jean-Pierre Sauvage, reported the synthesis of a family of tridimensional analogues of crown ethers, which were given the trivial name of “cryptands” (making reference to the secret Chapel of a Cathedral, where the most precious objects of the worship are kept, hopefully including the remains of the patron saint) [35].

Structural features of a classical cryptand are shown in Fig. 16. The cryptand contains six ethereal oxygen atoms, plus two tertiary amine nitrogen atoms that act as pivots. Indeed, the two nitrogen atoms do not play a mere structural role, but are usually involved in the coordination of the included metal. The name of the cryptand in Fig. 16 has been abbreviated to 2.2.2-crypt, where the numbers indicate the number of ethereal oxygen atoms contained in each one of the three polyoxoethylene chains. Figure 16 shows the structure of 2.2.2-crypt, as it is in the crystalline state, showing an ellipsoidal cavity [36]. On inclusion of the  $K^+$  ion (Fig. 16b), the cryptand rearranges to provide the spherical metal with a spheroidal cavity [37]. In the cryptate complex, the metal establishes coordinative interactions with the six oxygen atoms *and* with the two nitrogen atoms.

Cryptands display enhanced size selectivity with respect to alkali metal ions. Figure 17 refers to 2.2.2-crypt, which shows peak selectivity for  $K^+$ , in a 95/5 MeOH/water mixture (circles in Fig. 17) [38]. This effect is much more pronounced than that exerted by 18-crown-6 in pure MeOH (triangles in Fig. 17), a behaviour which may reflect the higher degree of steric restraint granted by a cage compared to a ring.

Knowledge of structural details may help the interpretation of the peak selectivity exerted by 2.2.2-crypt. Figure 18 shows the structures of the alkali metal complexes of 2.2.2-crypt, obtained from X-ray diffraction studies on crystalline salts [39–42]. First, it is clear that the low stability of the  $Li^+$  complex depends upon the circumstance that the smallest alkali metal ion is lost in the cavity and misses the interaction with an oxygen atom and with one tertiary amine group. The other

**Fig. 17** Size selectivity in the complexation of alkali metal ions by 2.2.2-crypt. Circles  $\log K$  values for the equilibrium  $M^+ + L \rightleftharpoons [ML]^+$  in MeOH/water 95/5, at 25 °C (M = alkali metal; L = cryptand, **9**) [38]; triangles  $\log K$  values for analogous equilibria with L = 18-crown-6 (**8**) in 100% MeOH [32]

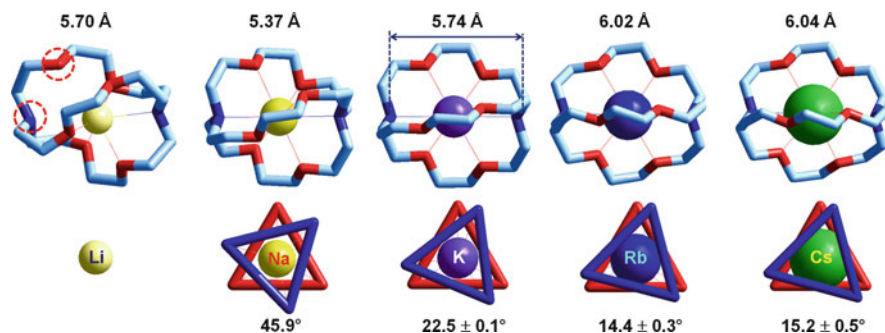
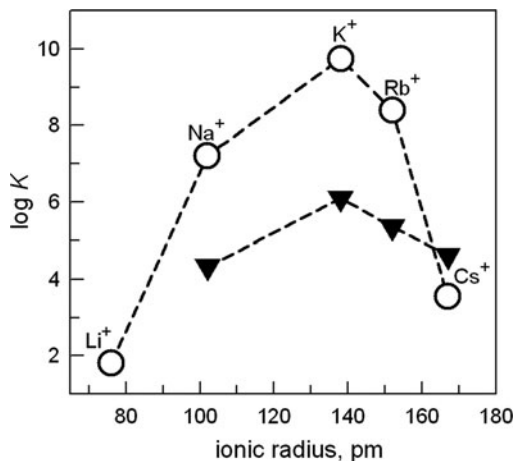


**Fig. 18** Top: Structures of alkali metal complexes of 2.2.2-crypt, **9** (hydrogen atoms omitted for clarity) [39–42]. Bottom: Torsion angles defined by the two triangles obtained by linking the two sets of three oxygen atoms. The smaller the torsion angle, the higher the distance between the two pivot nitrogen atoms (and the larger the cavity size of the cryptand)

metals are bound to all donor atoms of the cryptand, which, as the metal ion radius increases, expands its cavity. The magnitude of the enlargement can be monitored by the distance between the two bridgehead nitrogen atoms, which increases along the series  $Na^+ < K^+ < Rb^+ \approx Cs^+$ . The  $N \cdots N$  axis behaves as a spring and its length can be adjusted by rotating one set of three coordinated oxygen atoms with respect to the opposite set, according to a screw mode: the smaller the torsion angle between the two  $O_3$  triangles, the higher the distance between the two nitrogen atoms (and the larger the size of the cavity provided by the cryptand). Apparently, 2.2.2-crypt, relaxed to its most stable conformation, provides a tailor-made cavity for  $K^+$ . Very interestingly, and this is the most significant contribution of these studies by Lehn and coworkers, the cryptand's cavity size and complexation selectivity can be finely adjusted by design. Thus, 2.1.1-crypt displays sharp peak

selectivity for  $\text{Li}^+$  and 2.2.1-crypt for  $\text{Na}^+$  [38]. The structures of the two cryptate complexes are shown in Fig. 19 [43, 44]. Metal ions fit the cavity well and receive coordinative bonds from all the available donor atoms in the framework (both oxygen and nitrogen).

Preorganisation and complementarity stay at the basis of host–guest chemistry [45], a vast discipline that includes, among other sub-disciplines, metal coordination chemistry. In the case of the alkali metal cryptates, size complementarity (i.e. matching of the radii of the spherical cation and of the spheroidal cavity of the cryptand in its relaxed conformation) defines selectivity. On the other hand, the ligand's preorganisation imparts the required thermodynamic stability. For just this reason, coordination chemistry of alkali metals did not exist before the introduction of crown ethers and cryptands. Even the universal chelating agent EDTA (**12**), six-coordinating and detaining a quadruple negative charge, forms poorly stable complexes in water with  $\text{Na}^+$  and  $\text{K}^+$  ( $\log K = 1.79$  and  $0.96$ , respectively [46]), to be compared with  $[\text{Na}(2.2.1\text{-crypt})]^+$  ( $\log K = 5.40$ ) and  $[\text{K}(2.2.2\text{-crypt})]^+$  ( $\log K = 5.4$ ) [38]. The cryptate advantage results from the fact that the ligand is (almost) perfectly conformationally prepared to coordinate the metal and does not lose energy on complexation. The situation is different for EDTA, as we have tried to illustrate in Fig. 20. On placing its six donor atoms in the coordination sites

**Fig. 19** Structures of  $[\text{Li}(2.1.1\text{-crypt})]^+$  **10** [43], and of  $[\text{Na}(2.2.1\text{-crypt})]^+$  **11** [44], as obtained from X-ray diffraction studies. Hydrogen atoms have been omitted for clarity

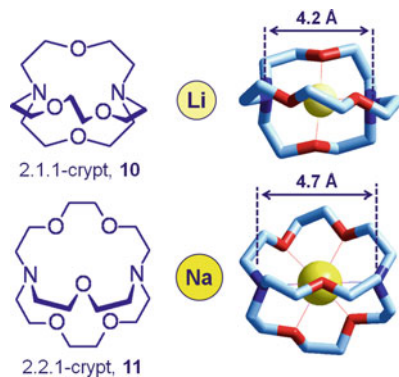
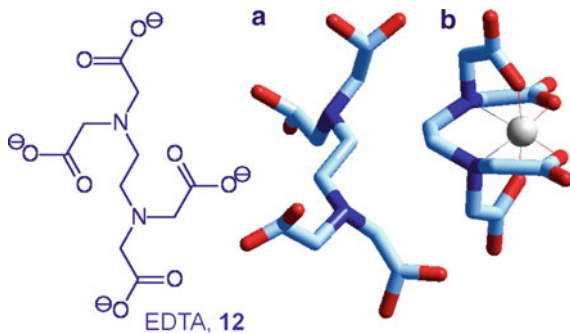


**Fig. 20** The universal chelating agent EDTA ( $\text{Y}^{4-}$ , **12**): (a) structure of the uncomplexed ligand, calculated through a semiempirical method (PM3); and (b) crystal structure of the  $[\text{Al}^{\text{III}}\text{Y}]^-$  complex [47]. Hydrogen atoms have been omitted for clarity



preferred by the metal ion ( $Al^{III}$ , in the crystal structure in Fig. 20b [47]), the sexidentate ligand suffers an extensive energy loss, of both enthalpic and entropic nature, which substantially reduces the free energy change associated with complexation. Such a detrimental contribution is, however, less important in complexation of alkaline earth dications, for which the electrostatic effects are significant, and more than compensate conformational disadvantages:  $\log K$  for  $[CaY]^{2-}$  and for  $[SrY]^{2-}$  are 11.0 and 8.8, respectively [46], distinctly higher than values observed for  $[Ca(2.2.1-crypt)]^{2+}$  ( $\log K = 6.9$ ) and  $[Sr(2.2.2-crypt)]^{2+}$  ( $\log K = 7.3$ ) [38].

In any case, we perceive the metal cryptates shown in Figs. 18 and 19 as much more aesthetically agreeable than EDTA complexes such as that shown in Fig. 20. Surely, we admire the ingenuity of the synthetic chemist who was able to guess the bonding expectations of the envisaged metal ion, which were fulfilled by design. But, we are also fascinated by the geometrical properties of the chemical object itself, the cryptate: symmetry, harmony and, ultimately, beauty.

## 4 Cages for Anions

Metal coordination chemistry was able to produce cages after nearly one century of intense synthetic exercise. Its younger sister, anion coordination chemistry, was born with cages. Such a circumstance is not accidental and derives from the intrinsically low energy of the interaction an anion can establish with its ligand (usually called a “receptor”), whether electrostatic or hydrogen bonding. In particular, anion complex formation is strongly favoured by the receptor’s preorganisation and rigidity. In this vein, the first example of anion complexation is due to Park and Simmons [48], who in 1968 reported on the inclusion of chloride in doubly protonated triple-stranded diammonium alkanes of the type shown in Fig. 21, as investigated through  $^1H$  NMR studies. The numbers in square brackets in the abbreviated name of the cage, e.g. [10.10.10], indicate the number of carbon atoms present in each of the three aliphatic strands linking the two bridgehead nitrogen atoms. The diammonium ion shown in Fig. 21, in a 50/50 solution of

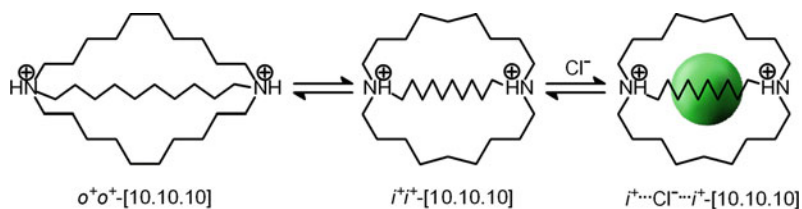


**Fig. 21** Katapinand: a triple-stranded diammonium alkane, which, in a 50% trifluoroacetic acid aqueous solution, “swallows” a chloride ion. Anion inclusion is preceded by a structural reorganisation of the diammonium receptor from the *out,out* isomer ( $o^+o^+$ , the two N–H fragments pointing outside of the cavity) to the *in,in* isomer ( $i^+i^+$ , N–H fragments pointing inside)

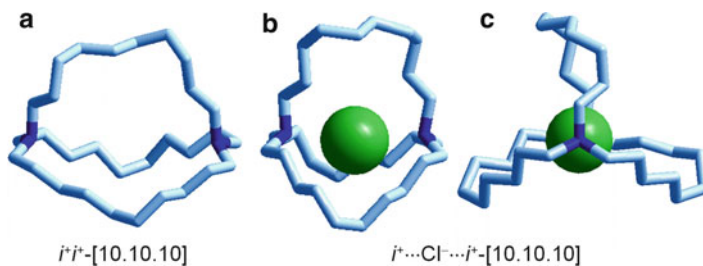


**Fig. 22** Calculated structures (PM3) of the  $i^+i^+-[10.10.10]$  diammonium cage (**a**) and of its inclusion complex with chloride; (**b**) lateral, and (**c**) longitudinal view

deuterated trifluoroacetic acid and  $\text{D}_2\text{O}$ , exists as an equilibrium mixture of the *out*, *out* ( $o^+o^+$ ) isomer, in which the ammonium N–H fragments point outside the cavity (23%) and of the *in*, *in* ( $i^+i^+$ ) isomer, with N–H fragments pointing inside the cavity (77%). The interconversion equilibrium is fast. Quite interestingly, addition of NaCl makes the resonance of  $\alpha\text{-CH}_2$  protons shift upfield, which indicates the occurrence of a fast and reversible anion encapsulation process. The equilibrium constant  $K$  for the inclusion equilibrium was estimated to be  $>10$ . Similar behaviour was observed on addition of  $\text{Br}^-$  and  $\text{I}^-$ , which accounts for the flexible nature and consequent poor selectivity of the  $i^+i^+-[10.10.10]$  diammonium cage. No crystal structures have been reported for salts of the  $i^+i^+-[10.10.10]$  diammonium cage nor of its chloride inclusion complex. The structures in Fig. 22 have been calculated by a semiempirical method (PM3) and may give an idea of the encapsulation process. Structures suggest that the  $i^+i^+-[10.10.10]$  isomer contracts its cavity in order to accommodate the anion and to establish collinear hydrogen bonding interactions  $\text{N-H}\cdots\text{Cl}\cdots\text{H-N}$ .

Park and Simmons gave triple-stranded diammonium derivatives of the type described above the trivial name of “katapinands”, from the ancient Greek *καταπίνειν*, to swallow, thus imagining them like big fishes quietly swimming in solution and looking for smaller fishes (anions) to ingest. It is worth noting that the trivial name katapinand (reserved for anion inclusion [48]) precedes by 1 year that of cryptand (metal ion inclusion [35]), which is much more widely used.

Anion coordination chemistry then grew sleepily for 7 years, until Lehn reported the macrotricyclic **13** [49], whose formula and calculated structure are shown in Fig. 23. According to the orientation of the four  $sp^3$  nitrogen atoms, whether *in* or *out*, the molecule may give rise to five topological forms. The structure in Fig. 23b refers to the all-*in* form, in which the four amine nitrogens are located at the corners of a tetrahedron and the six ethereal oxygens are at the corners of an octahedron. The tetrahedron is inserted into the octahedron and the centres of the two polyhedra coincide (Fig. 23c). In the pertinent article [49], Lehn noted: “In addition to its chemical interest, such a ligand is not without aesthetic appeal!” Oxygen and nitrogen atoms lie on the same sphere, which account for the trivial name of “spherical cryptand”.

**13** provides a spheroidal cavity made by six oxygen atoms (like, for instance 2.2.2-crypt) and includes alkali metal ions in pure water. In particular, **13** forms with  $\text{K}^+$  a complex less stable than that of 2.2.2-crypt ( $\log K = 3.4$  and  $5.4$ , respectively), a  $\text{Rb}^+$  complex of comparable stability ( $\log K = 4.2$  and  $4.3$ ), and a more stable  $\text{Cs}^+$  complex ( $\log K = 3.4$  and  $<2$ ).

On the other hand, the spherical cryptand can be turned in a powerful anion receptor by acidifying the solution. In particular, in an aqueous solution adjusted to  $\text{pH} = 1.5$  with  $\text{HNO}_3$ , the macrotricyclic exists in its tetraprotonated form  $\text{LH}_4^{4+}$ , which, as an  $i^+i^+i^+i^+$  isomer, offers four highly polarised N–H fragments placed at the corners of a tetrahedron and pointing inside the cavity, thus favouring the encapsulation of spherical anions [50]. Indeed, in an acidic aqueous solution **13**  $\text{H}_4^{4+}$  forms an inclusion complex with  $\text{Cl}^-$ , with an association constant  $\log K > 4$ , at least three orders of magnitude higher than that estimated for [10.10.10] katapinand under the same conditions. The cascade process from the spherical cryptand **13** to the chloride complex  $[\mathbf{13H}_4 \cdots \text{Cl}]^{3+}$  is illustrated in Fig. 24.

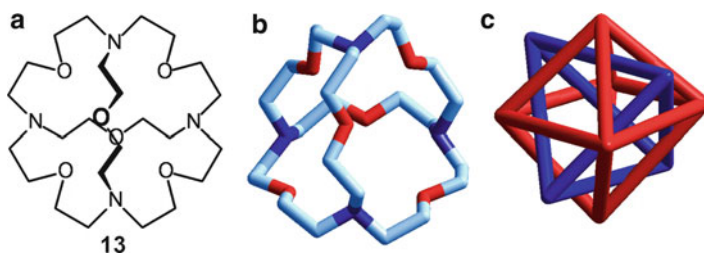


**Fig. 23** (a) Lehn's spherical cryptand, **13**, and (b) calculated structure (MM+) of **13**, in which each  $sp^3$  nitrogen atom points its lone pair inside the cavity. (c) The six oxygen atoms are placed at the corners of an octahedron, and the four nitrogen atoms at the corners of a tetrahedron. The tetrahedron is inserted into the octahedron. Hydrogen atoms have been omitted for clarity

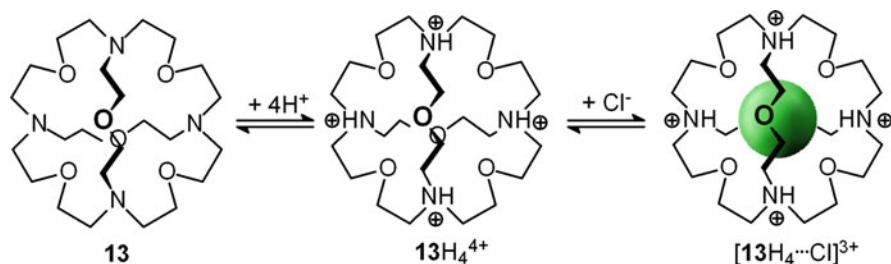
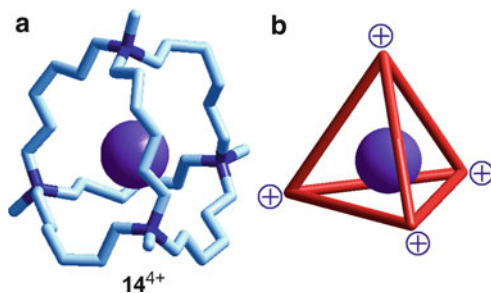


**Fig. 24** Consecutive equilibria for protonation of the spherical cryptand **13** and inclusion of  $\text{Cl}^-$  in the tetraprotonated receptor  $\mathbf{13H}_4^{4+}$ . In the  $[\mathbf{13H}_4 \cdots \text{Cl}]^{3+}$  complex, the anion is tetrahedrally coordinated by four highly polarised N–H fragments, as shown in the crystal structure. Unavailability of coordinates at the Cambridge Crystallographic Database prevented any redrawing of such a structure

**Fig. 25** Iodide inclusion in a macrotricyclic quaternary ammonium receptor.

(a) Crystal structure of the  $[14\cdots I]^{3+}$  complex [52].

(b)  $I^-$  is placed in the centre of the nearly regular tetrahedron described by the four nitrogen atoms;  $N\cdots I$  distance  $4.54 \pm 0.04 \text{ \AA}$ , tetrahedron side  $7.4 \pm 0.3 \text{ \AA}$



Diprotonated katapinands and the tetraprotonated spherical cryptand  $13H_4^{4+}$  are comfortable cages for anions, but, in order to maintain a positive charge, they must operate under strongly acidic conditions. On the other hand, a permanent positive charge can be imparted to the receptor by alkylating, rather than protonating, tertiary amine groups. Such a progress in anion receptor design was achieved by Schmidthen, who, in 1977, reported receptor  $14^{4+}$ , containing four quaternary nitrogen atoms linked by  $-(CH_2)_6-$  aliphatic chains [51]. In particular, each nitrogen is linked to the other three nitrogen atoms, according to a connectivity that is expected to generate a tetrahedral arrangement of the four quaternary ammonium groups. The crystal and molecular structure of the iodide inclusion complex is shown in Fig. 25a [52].  $I^-$  is placed in the middle of a regular tetrahedron whose vertices are the four nitrogen atoms (Fig. 25b). In the present case, the complex is held together only by ionic attractive interactions. In this context, a tetrahedral arrangement of the quaternary ammonium groups maximises attractive electrostatic attraction and minimises electrostatic repulsion between positive charges.  $14^{4+}$  forms stable complexes in water with  $Br^-$  and  $I^-$  ( $\log K = 3.0$  and  $2.7$ , respectively). Increasing the length of the linking aliphatic chains from  $-(CH_2)_6-$  to  $-(CH_2)_8-$  inverts selectivity in favour of  $I^-$  ( $\log K = 2.0$  for  $Br^-$  and  $2.5$  for  $I^-$ ).

Papers by Lehn and Schmidthen were well received by the chemical community and stimulated the development of the novel discipline of anion coordination chemistry. The numerous anion receptors synthesised over the last three decades are not necessarily cage shaped. However, a polycyclic arrangement of the receptor was and is still highly required because it favours the formation of stable complexes in solution and may allow stringent recognition selectivity based on size/shape complementarity. Further examples of positively charged cage shaped receptors will be presented in Sects. 5 and 6.

In the evolution of anion coordination chemistry, it was discovered that neutral molecules can also operate as effective receptors for anions provided that they contain polarised N–H fragments (e.g. of amides [53], ureas [54], thioureas [55] or pyrroles [56]), which act as H-bond donors for anions. These receptors cannot compete for hydrogen bonding with water and alcohols and must be studied in aprotic solvents of varying polarity, e.g.  $CHCl_3$ , MeCN, DMSO. In this vein,

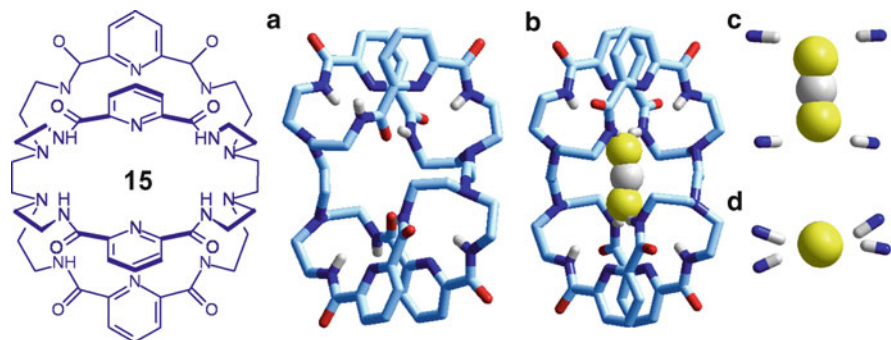


**Fig. 26** Neutral anion receptor consisting of two tetraamide macrocycles linked by two ethylenediamine spacers (**15**) [58]: (a) crystal structure of uncomplexed **15**; (b) crystal structure of the hydrogendifluoride complex [**15**...FHF]<sup>−</sup>, in which each fluorine atom is bound to only two N–H fragments of the proximate tetraamide macrocycle; (c) lateral and (d) top views, highlighting the interaction of HF<sub>2</sub><sup>−</sup> with N–H fragments

a variety of neutral cage-shaped receptors for anions have been synthesised [57]. A nice example is given by the tricyclic receptor **15**, reported by Kristin Bowman-James, whose formula is shown in Fig. 26 [58]. The receptor consists of two tetraamide macrocycles linked together by two ethylenediamine spacers. Figure 26a shows the crystal structure of the receptor alone, which is not perfectly preorganised for anion inclusion. In fact, not all amide N–H fragments point inside the cavity. In any case, the receptor provides an ellipsoidal opening, which could favour the encapsulation of linear polyatomic anions. Indeed, receptor **15** is able to include the elusive hydrogen difluoride anion HF<sub>2</sub><sup>−</sup>. The isolation of the [**15**...FHF]<sup>−</sup> complex was serendipitous. The authors tried to grow crystals of the fluoride complex by evaporation of a solution of **15** in MeCN/CHCl<sub>3</sub> containing an excess of [Bu<sub>4</sub>N]F and, to their surprise, obtained crystals of [Bu<sub>4</sub>N] [**15**...FHF]·3H<sub>2</sub>O. Tetrabutylammonium fluoride is commercially available as a trihydrate salt and is hygroscopic. It is possible that the hydrogen difluoride anion was generated by the following reaction: 2F<sup>−</sup> + H<sub>2</sub>O → HF<sub>2</sub><sup>−</sup> + OH<sup>−</sup>. The crystal structure of the [**15**...FHF]<sup>−</sup> complex is shown in Fig. 26b. Each fluorine atom of HF<sub>2</sub><sup>−</sup> receives two hydrogen bonds from two N–H fragments of a macrocyclic subunit (H...F distances: 1.84 and 2.03 Å). The other two N–H hydrogens are far away and are not H-bonded (H...F distances: 3.22 and 3.31 Å). It is worth noting that the F...F distance in the encapsulated anion (2.74 Å) is distinctly longer than observed in the isolated ion HF<sub>2</sub><sup>−</sup> in crystalline alkali metal salts (2.26 Å), which indicates a rather strong hydrogen bonding interaction of the terminal fluorine atoms. The association constant for [**15**...FHF]<sup>−</sup> (log *K* = 3.74 in DMSO) is higher than for any other anion, including the linear triatomic N<sub>3</sub><sup>−</sup> (log *K* = 2.53), which forms an essentially isomorphous complex [58] with **15**.



## 5 Bis-Tren Cages: Comfortable Shelters for Metal Ions, Anions and Both Metal Ions and Anions Together

Tren, the trivial name for tris(2-aminoethyl)amine **16**, is a classical tetradentate ligand of metal coordination chemistry [59]. Due to its tripodal structure, tren favours the formation of five-coordinate complexes of trigonal bipyramidal geometry, in which the four amine nitrogen atoms occupy four sites of the coordination polyhedron, the fifth one being left available to a solvent molecule or to an anion. Figure 27a shows the crystal structure of the  $[\text{Cu}^{\text{II}}(\text{tren})(\text{H}_2\text{O})]^{2+}$  complex [60]. The complex exhibits a compressed trigonal bipyramidal geometry, which means that axial bonds (e.g.  $\text{Cu}^{\text{II}}$ –tertiary amine nitrogen) are shorter than equatorial bonds ( $\text{Cu}^{\text{II}}$ –secondary amine nitrogen). This implies that the fifth ligand, whether a solvent molecule or an anion, being axial, profits from especially strong coordinative interactions. The situation is opposite to that observed with the twin tetramine ligand trien (trivial name for triethylenetetramine **17**), which gives five-coordinate complexes of square pyramidal geometry with copper(II). In view of its linear connectivity, trien spans the corners of the square with its donor atoms, establishing rather strong coordinative interactions. On the other hand, the distance between  $\text{Cu}^{\text{II}}$  and the apical ligand (a solvent molecule or an anion) is usually large, which gives evidence for a relative weak bonding interaction. The crystal structure of the  $[\text{Cu}^{\text{II}}(\text{trien})(\text{H}_2\text{O})]^{2+}$  complex is shown in Fig. 27b, for comparative purposes [61].

Thus, the flexible ligand tren, in the presence of a metal, gives rise to a nice cavity. Quite interestingly, such a cavity can be made permanent through the reactions illustrated in Fig. 28. In particular, two molecules of tren undergo Schiff base condensation with three molecules of a chosen dialdehyde, to give a cage-shaped Schiff base derivative [62]. Precipitation of the base favours the displacement to the right of the equilibrium. The “reversibility” of the  $\text{C}=\text{N}$  bond (i.e. its

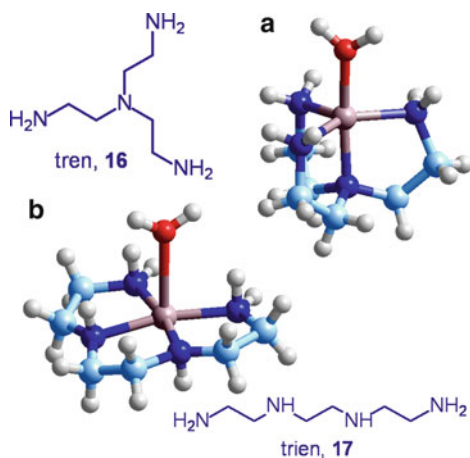


**Fig. 27** Crystal and molecular structures of (a)  $[\text{Cu}^{\text{II}}(\text{tren})(\text{H}_2\text{O})]^{2+}$ , displaying a compressed trigonal bipyramidal coordination geometry [60]; and (b)  $[\text{Cu}^{\text{II}}(\text{trien})(\text{H}_2\text{O})]^{2+}$ , which shows a square pyramidal geometry [61]. The  $\text{Cu}^{\text{II}}$ – $\text{OH}_2$  distance is distinctly smaller in the tren complex than in the trien complex

tendency to undergo a fast hydrolysis) is essential because it allows the achievement of a complex structure, which cannot be obtained without a “trial and error” mechanism. Then, “reversible” C=N bonds are hydrogenated with NaBH<sub>4</sub> to give the weaker, but “irreversible” C–N bonds and a stable cage is ready for further use.

Bistren derivatives of the type illustrated in Fig. 28 are probably the most investigated cages. Their success certainly depends on the convenient synthetic procedure, but also on the versatility of the design. In fact, the distance between the two tren subunits (and the size of the cavity) can be modulated at will through thoughtful choice of the dialdehyde, which acts as a spacer. They have been given the trivial name “bistren cryptands”, firstly because the first members of the series was reported and christened by Lehn, and secondly because they have the same framework as classical cryptands, provided that ethereal oxygen atoms are replaced by secondary amine groups.

The smallest bistren derivative contains –CH<sub>2</sub>CH<sub>2</sub>– spacers (**18**, see Fig. 29) and is reminiscent of Sargeson’s polyamine cages sepulchrand and sarcophagine, in that

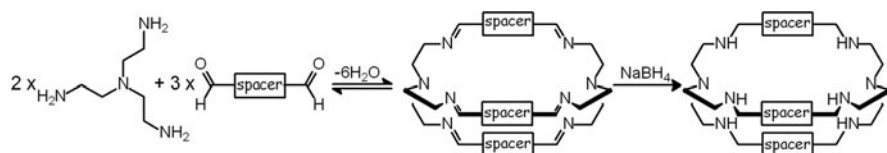


**Fig. 28** Facile synthesis of bistren cages. Tren (2 mol) undergoes a Schiff base condensation with a selected dialdehyde (3 mol), to give an unsaturated cage, whose six C=N double bonds can be hydrogenated with NaBH<sub>4</sub>, to give a stable fully saturated cage

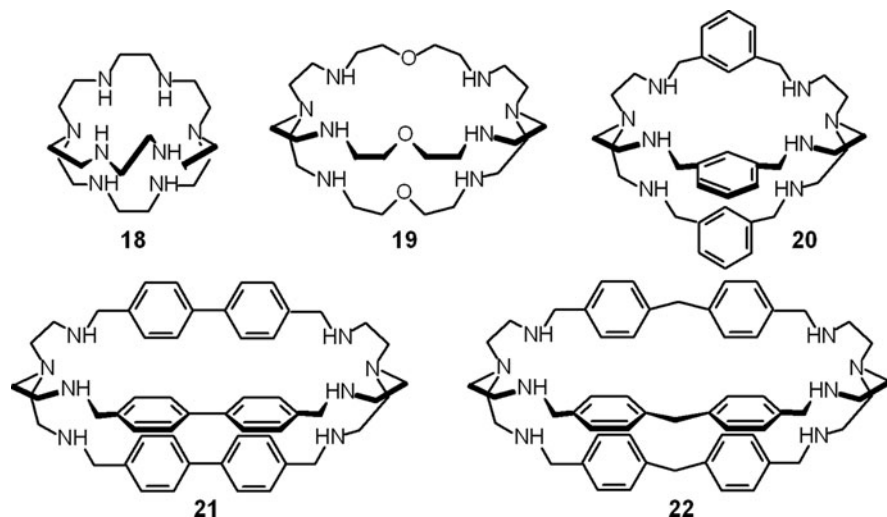


**Fig. 29** Some bistren cages (**18–22**). Shape and size of the cavity are defined by the spacers linking the two tren subunits

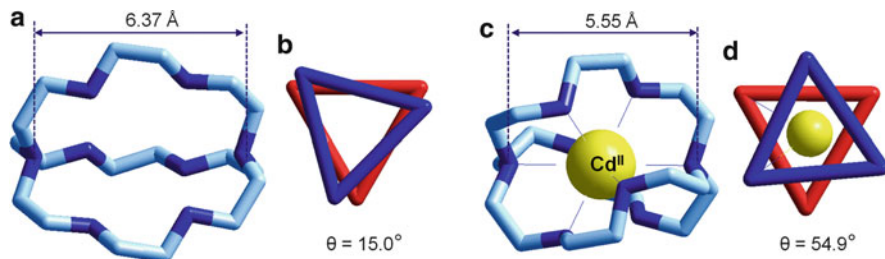


**Fig. 30** (a) Crystal structure of the bistren cryptand **18** [63]. (b) Triangles obtained by linking the secondary amine nitrogen atoms of each tren subunit of the uncomplexed ligand **18**. (c) Crystal structure of the  $[\text{Cd}^{\text{II}}(\mathbf{18})]^{2+}$  complex [64]. (d) Triangles obtained by linking the secondary amine nitrogen atoms of each tren subunit in the  $[\text{Cd}^{\text{II}}(\mathbf{18})]^{2+}$  complex; the *sphere* represents the  $\text{Cd}^{\text{II}}$  ion

it possesses a set of three ethylenediamine fragments, suitable for metal coordination. However, the similarity is only formal and metal complexes of **18** display totally different properties and reactivity with respect to the corresponding sep and sar complexes. The differences derive from the fact that the two tertiary nitrogen atoms of tren (exhibiting an *in, in* configuration) play an active role in the coordination of the included metal(s). Moreover, the two tren caps impart to the cage a flexibility absent in sep and sar derivatives.

Figure 30 compares the crystal structures of the uncomplexed ligand **18** (Fig. 30a) [63], and of its complex with  $\text{Cd}^{\text{II}}$  (Fig. 30c) [64]. The cryptand presents an ellipsoidal cavity (the distance between the apical tertiary nitrogen atoms is 6.37 Å). The spherical  $\text{Cd}^{\text{II}}$  ion ( $4d^{10}$  electronic configuration) is bound to all the eight amine groups (distance  $\text{Cd}^{\text{II}}\text{-NH}(\text{secondary})$  2.52 Å;  $\text{Cd}^{\text{II}}\text{-N}(\text{tertiary})$  2.72 Å). In order to guarantee full amine coordination, the ligand contracts its cavity, bringing the distance between tertiary nitrogen atoms to 5.55 Å. To do that, it profits from the well-established mechanism that involves the rotation by  $40^\circ$  of the triangle defined by the secondary amine nitrogen atoms of a tren subunit, with respect to triangle of the other tren subunit.

In contrast to what is observed with sarcophagines, labile transition metal ions (e.g. the divalent ones of the 3d series) get in/get out of the cavity of **18** according to a fast and reversible mechanism. This opens the way to the evaluation of the stability in solution of metal complexes through classical potentiometric titration experiments. For instance, when titrating with standard NaOH, an acidic solution containing equimolar amounts of **18** and of  $\text{Ni}(\text{ClO}_4)_2$ , a species of formula  $[\text{Ni}^{\text{II}}(\mathbf{18H})]^{3+}$  began to form at pH = 5.5 and reached its maximum concentration (70%) at pH = 7 [65]. On evaporation of a solution adjusted to neutral pH, crystals of a salt of formula  $[\text{Ni}^{\text{II}}(\mathbf{18H})(\text{ClO}_4)_3]$  were obtained. Figure 31a shows the crystal structure of the complex cation  $[\text{Ni}^{\text{II}}(\mathbf{18H})]^{3+}$  [65]. It is observed that the  $\text{Ni}^{\text{II}}$  ion is six-coordinate, according to a rather distorted octahedral geometry. In particular, the metal is bound to four nitrogen atoms of a tren subunit and to two secondary amine nitrogen atoms of the other tren subunit. The remaining secondary amine group is protonated. On further base addition, during the titration experiment, the

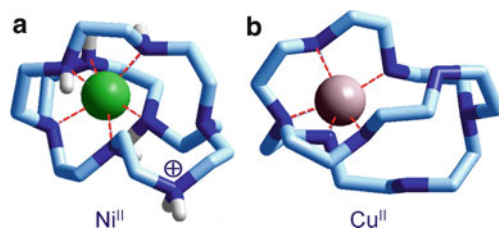


**Fig. 31** Crystal structures of (a) the nickel(II) complex of the monoprotonated form of **18**:  $[\text{Ni}^{\text{II}}(\mathbf{18H})]^{3+}$  [65]; C–H hydrogen atoms omitted for clarity; and (b) the  $[\text{Cu}^{\text{II}}(\mathbf{18})]^{2+}$  complex [66]; all hydrogen atoms omitted for clarity

ammonium group deprotonates and the  $[\text{Ni}^{\text{II}}(\mathbf{18})]^{2+}$  complex forms, which reaches 100% concentration at  $\text{pH} = 10$ .  $[\text{Ni}^{\text{II}}(\mathbf{18})]^{2+}$  undergoes demetallation in acidic solution, a process that has to be monitored using a stopped-flow spectrophotometric technique: in particular, the lifetime of the  $[\text{Ni}^{\text{II}}(\text{L})]^{2+}$  complex in 0.5 M  $\text{HClO}_4$  is 3 s. In the case of  $\text{Cu}^{\text{II}}$ , three main complex species are present at equilibrium, along the investigated pH range:  $[\text{Cu}^{\text{II}}(\mathbf{18H}_2)]^{4+}$ , which forms at  $\text{pH} = 3$ ;  $[\text{Cu}^{\text{II}}(\mathbf{18H})]^{3+}$ , present at 100% over the 4–8 pH interval;  $[\text{Cu}^{\text{II}}(\mathbf{18})]^{2+}$ , the dominating species at  $\text{pH} \geq 10$  [65]. The crystal structure of the latter complex has been determined and is shown in Fig. 31b [66]. The  $\text{Cu}^{\text{II}}$  centre is five-coordinate, profiting from the coordination of a full tren subunit and from that of a secondary nitrogen atom of the other tren subunit. Three nitrogen atoms remain available for metal–ligand interaction, but  $\text{Cu}^{\text{II}}$  maintains its well-defined preference for five-coordination.

At this stage, one could wonder whether the flexible bistren derivative **18** could accommodate two metal ions in its cavity. Indeed, on reaction of **18** with two equivalents of  $\text{Cu}^{\text{II}}(\text{NO}_3)_2$ , a salt of formula  $[\text{Cu}_2(\mathbf{18})](\text{NO}_3)_3$  was obtained, which should formally contain a  $\text{Cu}^{\text{II}}$  and a  $\text{Cu}^{\text{I}}$  cation [67]. One electron reduction is operated by the solvent (MeOH or EtOH). The crystal structure, shown in Fig. 32a, indicates that the two copper centres are equivalent. Electron spin resonance (ESR) studies revealed that the unpaired electron is delocalised over the short Cu–Cu bond (2.36 Å), disclosing the occurrence of a  $\sigma$  bonding interaction between the metal centres. Thus, each copper centre exhibits the average valence of 1.5. Each  $\text{Cu}^{1.5}$  centre experiences a trigonal bipyramidal five-coordination and protrudes from the equatorial triangle towards the other  $\text{Cu}^{1.5}$  metal centre, in order to establish metal–metal covalent interaction (Fig. 32b). It is probably this interaction that stabilises the dimetallic cryptate. On the other hand, stronger electrostatic repulsions should destabilise the  $\text{Cu}^{\text{II}}\text{--Cu}^{\text{II}}$  system with respect to the average valence dimetallic complex.

Bistren cryptands have been deservedly more successful in anion coordination chemistry than in traditional coordination chemistry. In particular, the bistren framework has provided the basis for the design of a variety of receptors that are suitable for the inclusion of polyatomic anions of varying size and shape. A number

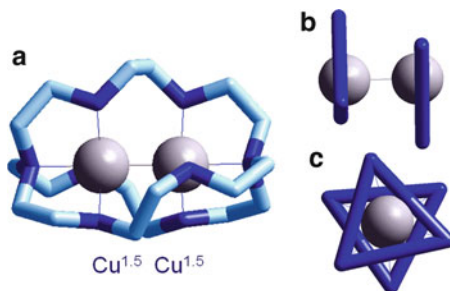


**Fig. 32** (a) Crystal structure of the  $[\text{Cu}^{1.5}\text{-Cu}^{1.5}(\mathbf{18})]^{3+}$  complex (hydrogen atoms omitted for clarity) [67]. (b, c) Triangles obtained by linking the nitrogen atoms of the secondary amine groups of each tren subunit: (b) lateral view: notice how the two  $\text{Cu}^{1.5}$  ions protrude from the triangles in order to establish an intermetallic  $\sigma$  bonding interaction; (c) view along the longitudinal axis

of bistren cages have been synthesised over the last three decades, showing a versatile aptitude for anion encapsulation. The formulae of some bistren derivatives are illustrated in Fig. 29. They can be easily converted to anion receptors by protonating amine groups. In particular, in a slightly acidic solution ( $\text{pH} = 3\text{--}5$ ), these cages exist as a hexa-ammonium cation, with the six secondary amine groups protonated. Due to the strong electrostatic repulsions, protonation of the two tertiary amine groups takes place in much stronger acidic conditions ( $\text{pH} < 2$ ).

The bistren derivative **19** was the first derivative of the family to be synthesised, and, curiously, was not obtained by the Schiff base condensation illustrated in Fig. 28, but through a multistep synthesis involving protection and deprotection of amine groups [68]. The hexaprotonated receptor,  $\mathbf{19H}_6^{6+}$ , present at 100% at  $\text{pH} \leq 4$ , includes a variety of anions, either mono- or polyatomic [69]. Figure 33 shows the crystal structure of the inclusion complexes of  $\text{Br}^-$  and  $\text{N}_3^-$  [70].  $\mathbf{19H}_6^{6+}$  establishes with both anions six hydrogen bonds, each one involving an H atom of the secondary ammonium groups. In view of the flexibility of the  $\text{-(CH}_2\text{)}_2\text{O(CH}_2\text{)}_2\text{-}$  spacers, the cage offers both a spheroidal and an ellipsoidal cavity, depending upon the geometrical requirements of the anion. In particular the “length” of the cage, expressed by the distance between the two tertiary nitrogen atoms, can be modulated through a typical spring and screw mechanism, which involves the rotation of one of the two triangles described by the ammonium nitrogen atoms of each tren subunit, with respect to the other. Thus, generation of the ellipsoidal cavity for  $\text{N}_3^-$  requires a torsion of  $27^\circ$ , whereas for the formation of the spheroidal cavity for  $\text{Br}^-$ , the two triangles must be rotated by  $58^\circ$ .

Moreover, and very interestingly from the point of view of anion recognition, bistren cryptands can interact in sequence with metals and anions, according to the cascade process illustrated in Fig. 34. In particular, a bistren ligand (e.g. **20**) includes two transition metal ions, e.g. two  $\text{Cu}^{\text{II}}$  (step i in Fig. 34). Each metal is coordinated by a tren subunit, which imposes the typical trigonal bipyramidal geometry. In an aqueous solution, an  $\text{H}_2\text{O}$  molecule (or an  $\text{OH}^-$  ion, depending

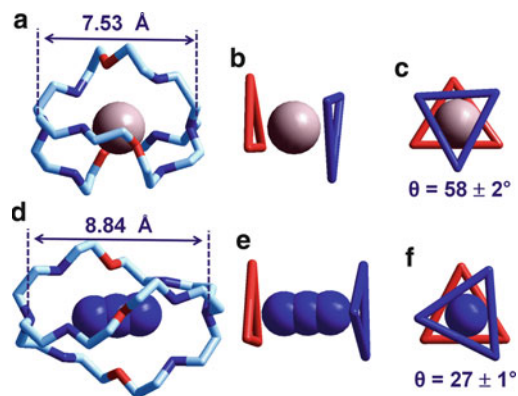


**Fig. 33** Crystal structures of the inclusion complexes involving the hexaprotonated form of the bistren derivative **19** and bromide (**a**), and azide ions (**d**) [70]. The six secondary amine groups are protonated. All hydrogen atoms have been omitted for clarity. (**b**, **c**, **e**, **f**) Triangles have been obtained by linking the nitrogen atoms of the ammonium groups of each tren subunit. (**c**, **f**)  $\theta$  is the torsion angle for each pair of triangles

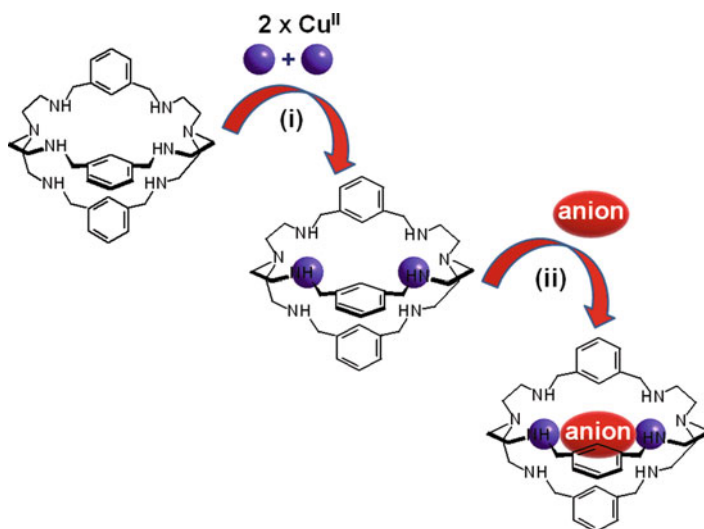
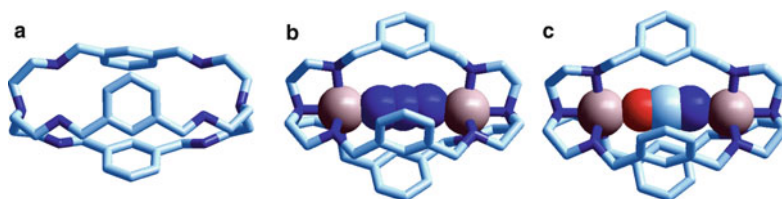


**Fig. 34** Cascade process for the formation of a ternary dicopper(II) bistren cryptate, including an ambidentate anion. The bistren cryptand **20** has been chosen as an example

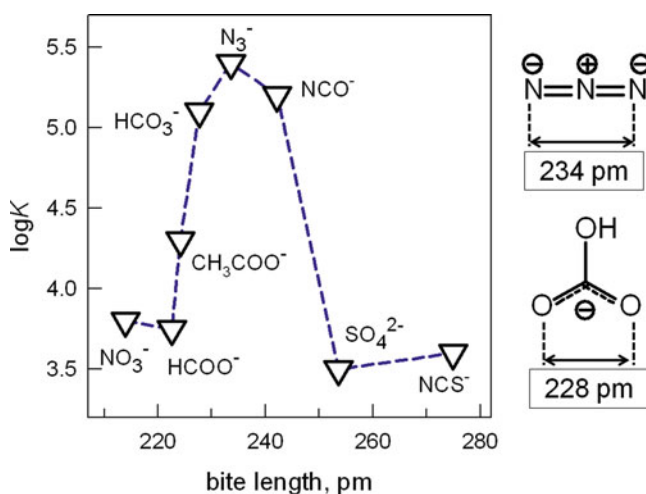
upon pH) occupies the apical position left available in each  $[\text{Cu}^{\text{II}}\text{tren}]^{2+}$  moiety. Then, an ambidentate anion can displace the two labile solvent molecules, to bridge the two metal centres, giving rise to a ternary complex (step ii in Fig. 34), completing the cascade process.

Figure 35a shows the crystal structure of the bistren derivative **20** alone, which discloses an elongated ellipsoidal cavity [71]. It appears, at the first sight, that the

corresponding dicopper(II) complex could include the rod-like pseudohalide anions. Indeed, ternary complexes of  $\text{N}_3^-$  and  $\text{NCO}^-$  have been isolated in their crystalline form [72]. Corresponding structures are shown in Fig. 35b, c. In particular, the two linear anions are well accommodated in the cavity of the dimetallic cryptate. However, although the crystal structures demonstrate that  $[\text{Cu}_2^{\text{II}}(\mathbf{20})]^{4+}$  is a good receptor for rod-like anions, they cannot provide any quantitative information on inclusion selectivity. Such information came from equilibrium studies carried out in a neutral aqueous solution at 25 °C, which disclosed the existence of a stringent geometrical selectivity of the anion inclusion in this cryptate. Such a selective behaviour, however, is not related to the shape of the anion, but to its “bite length” [73, 74]. The bite length, as illustrated in Fig. 36, is the distance between two



**Fig. 35** Crystal structures of the bistren cryptand **20** alone [71] (a) and its ternary dicopper(II) complexes encapsulating  $\text{N}_3^-$  (b) and  $\text{NCO}^-$  (c) [72]. The distances between tertiary nitrogen atoms in the three bistren derivatives are 10.9 Å, 10.1 Å and 10.3 Å, respectively



**Fig. 36** Anion inclusion in the  $[\text{Cu}_2^{\text{II}}(\mathbf{20})]^{2+}$  cryptate in aqueous solution. The stability of the ternary inclusion complex, expressed by  $\log K$  for the equilibrium:  $[\text{Cu}_2^{\text{II}}(\mathbf{20})]^{4+} + \text{X}^- \rightleftharpoons [\text{Cu}_2^{\text{II}}(\mathbf{20})(\text{X})]^{3+}$ , at pH = 7 and 25 °C, is related to the bite length of the anion  $\text{X}^-$ , with a sharp peak selectivity. The  $\text{N}_3^-$  ion has the right bite length to encompass the dimetallic cryptate, without inducing any serious conformational rearrangement of the dimetallic cryptate [73, 74]

consecutive donor atoms of the ambidentate anion. In a linear anion like  $\text{N}_3^-$ , it coincides with anion length.

The plot of  $\log K$  versus bite length, shown in Fig. 36, indicates the existence of a sharp selectivity in favour of  $\text{N}_3^-$ . The azide ion has the right bite length to place its donor atoms in the available apical positions of the two  $\text{Cu}^{\text{II}}$  centres, without inducing any serious endergonic conformational rearrangement of the dimetallic cryptate.  $\text{HCO}_3^-$  and  $\text{NCO}^-$  ions form slightly less (but still detectable) stable inclusion complexes than  $\text{N}_3^-$ , because they have a somewhat smaller and larger bite length, respectively. Anion shape does not play any major role: linear  $\text{NCS}^-$  forms a poorly stable complex because it is too long to encompass the  $\text{Cu}^{\text{II}}\text{-Cu}^{\text{II}}$  distance in the relaxed receptor and its inclusion may involve a severe endothermic conformational rearrangement of the bistren framework.

Anion inclusion selectivity can be modulated by varying the nature of the spacers of the dimetallic cryptate used as a receptor. An example is provided by the dicopper(II) complex of the bistren derivative **21**, whose crystal structure is shown in Fig. 37 [75]. The tetranitrate complex salt was crystallised from water and contained two water molecules apically coordinated to the two metal centres. The complex displays selectivity for the inclusion of linear aliphatic dicarboxylates, as shown in Fig. 38. In particular it is observed that the most stable inclusion

**Fig. 37** Crystal structure of the  $[\text{Cu}_2^{\text{II}}(\mathbf{21})(\text{H}_2\text{O})_2]^{4+}$  complex [75]. Hydrogen atoms of the cryptand and the four  $\text{NO}_3^-$  counterions have been omitted for clarity

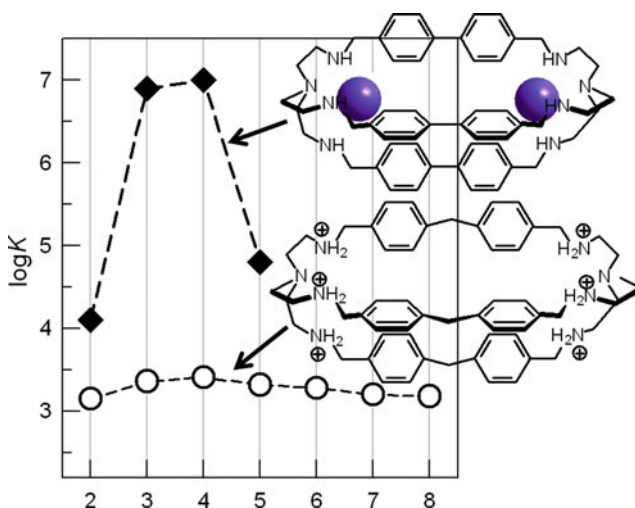
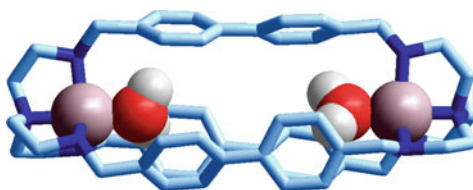


**Fig. 38** Equilibrium constants for the inclusion of linear aliphatic dicarboxylates by  $[\text{Cu}_2^{\text{II}}(\mathbf{21})]^{4+}$  (diamonds, pH = 7) [75], and by the hexaprotonated bistren receptor  $\mathbf{22H}_6^{6+}$  (circles, pH = 6) [76]



complexes (aqueous solution, buffered at  $\text{pH} = 7$ ,  $25\text{ }^\circ\text{C}$ ) are formed with dicarboxylates with spacers consisting of  $n = 3$  (glutarate) and  $n = 4$   $-\text{CH}_2-$  groups (adipate), whose length seem to encompass quite well the  $\text{Cu}^{\text{II}}-\text{Cu}^{\text{II}}$  distance in the relaxed dimetallic receptor. Encapsulation of dicarboxylates with a shorter ( $n = 2$ , succinate) and longer ( $n = 5$ , pimelate) spacer probably induces drastic conformational rearrangements, which are reflected in a substantial decrease of the thermodynamic stability of the corresponding complexes. For comparative purposes, Fig. 38 reports the  $\log K$  values for the inclusion equilibria of linear aliphatic dicarboxylates by the hexaprotonated form of the bistren derivative **22** [76]. No selectivity is observed on varying the number of  $-\text{CH}_2-$  groups present in the dianion from two to eight. This may be due to the higher flexibility of the diphenylmethane spacer, but should also reflect the poor directional nature of hydrogen bonding and electrostatic interactions. On the other hand, intense and directional metal–ligand interactions impose stringent geometrical restrictions, which generate a valuable selective behaviour in anion recognition.

## 6 Small Cages for the Smallest Anion

Probably the most precious occurrence of anion recognition is that related to size exclusion selectivity. This takes place when the receptor, providing for instance a spheroidal cavity, includes only spherical anions of radius less than or equal to a definite value. In this context, the smallest anion, fluoride, has offered vast opportunities.

One of the first investigated receptors for selective fluoride encapsulation was the bistren derivative **18**, in its hexaprotonated form  $\mathbf{18H}_6^{6+}$ . Equilibrium studies in aqueous acidic solution revealed the formation of a very stable inclusion complex, with an extremely high constant of the inclusion equilibrium,  $\log K = 10.7$  [77]. The complex was isolated as a crystalline salt and its structure is shown in Fig. 39 [78]. The fluoride ion receives six hydrogen bonds from the six secondary ammonium groups of the cage. In particular, only one N–H fragment of each secondary ammonium group is close enough to the  $\text{F}^-$  ion to establish an H-bond interaction

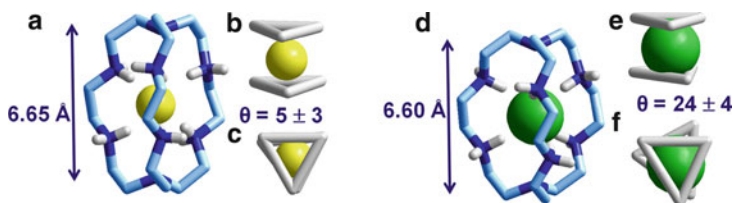


**Fig. 39** Crystal structures of the inclusion complexes of  $\mathbf{18H}_6^{6+}$  with fluoride (a) [78], and chloride (d) [79]; carbon bound hydrogen atoms have been omitted for clarity. (b, c, e, f) Triangles have been obtained by linking the hydrogen atoms of the secondary ammonium groups of each tren subunit, involved in hydrogen bonding

(average distance  $2.0 \pm 0.2 \text{ \AA}$ ), whereas the other N–H fragment points outside of the cavity (average distance  $3.0 \pm 0.5 \text{ \AA}$ ). Looking at the triangles obtained by linking the anion-bound hydrogen atoms of each tren subunit, it appears that the fluoride ion profits from an almost regular trigonal prismatic coordination.  $\mathbf{18H}_6^{6+}$  emerges as an excellent receptor for fluoride recognition in water. However, it is selective, but not specific. In fact,  $\mathbf{18H}_6^{6+}$  also forms a 1:1 complex with chloride under the same conditions, with an association constant that is seven orders of magnitude lower than fluoride [77]. The crystal structure (Fig. 39d) shows that  $\text{Cl}^-$  receives six H-bonds from the six secondary ammonium groups, like  $\text{F}^-$  [79]. However, the coordination geometry is not exactly the same, but it is midway between the trigonal prism and the octahedron (Fig. 39f). Thus, the cage framework, due to the presence of the  $-\text{CH}_2\text{CH}_2-$  spacers, is flexible enough to accommodate two anions of distinctly different size ( $r_{\text{F}^-} = 1.33 \text{ \AA}$ ,  $r_{\text{Cl}^-} = 1.81 \text{ \AA}$ ) and does not exert size exclusion selectivity in favour of  $\text{F}^-$ . The much higher stability of the fluoride complex may result from the higher basicity of  $\text{F}^-$  and from its tendency to establish stronger H-bond interactions than  $\text{Cl}^-$ . Bromide ( $r_{\text{Br}^-} = 1.96 \text{ \AA}$ ) is too large for encapsulation by  $\mathbf{18H}_6^{6+}$ . In the isolated crystalline complex salt  $[\mathbf{18H}_6]\text{Br}_6 \cdot \text{H}_2\text{O}$ , the cavity is empty and all the six bromide ions lie outside [78].

On reaction of **18** with triethylorthoformate at  $120^\circ\text{C}$  in dry xylene, a white solid can be obtained, which corresponds to the tris-imidazolidinium cage  $\mathbf{23}^{3+}$ , shown in Fig. 40 [80]. The trication  $\mathbf{23}^{3+}$  contains three imidazolidinium subunits. The C–H fragment of imidazolidinium is highly polarised and can behave as an effective H-bond donor for anions. However, the crystal structure of the  $[\mathbf{23}](\text{ClO}_4)_3 \cdot \text{H}_2\text{O}$  salt (shown in Fig. 40) indicated that the three C–H fragments do not point towards the cavity, but outside, a circumstance unfavourable to anion encapsulation. The interaction of  $\mathbf{23}^{3+}$  with fluoride was investigated through  $^1\text{H}$  NMR titration of a  $\text{D}_2\text{O}$  solution of the tris-imidazolidinium cage, adjusted to  $\text{pD} = 1$ , with  $\text{NaF}$ . The formation of a 1:1 complex was ascertained, and an extremely high association constant of  $\log K = 12.5$  was measured (such a high  $K$  value could be determined

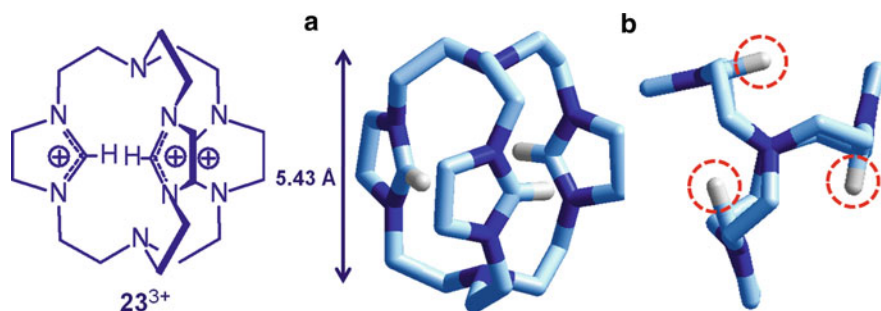


**Fig. 40** (a) Crystal structure of the tris-imidazolidinium cage  $\mathbf{23}^{3+}$  [80]. Only C–H fragments of the imidazolidinium subunits are shown. (b) Top view of the trication indicates that such C–H fragments do not point towards the cavity

by competition with the  $Zr^{IV}$  cation present in excess, forming  $Zr^{IV}F^{3+}$ , which suggested anion encapsulation. X-ray diffraction studies on the salt isolated under the same conditions,  $[23H_2 \cdots F](ClO_4)_2(BF_4)_3 \cdot H_2O$ , disclosed the formation of a fluoride inclusion complex, whose structure is shown in Fig. 41 [80]. The fluoride ion does not interact with the imidazolidinium N–H fragments, which still point outside of the cavity, but it receives two H-bonds from the protonated tertiary amine nitrogen atoms, exhibiting a *in* configuration ( $F \cdots H$  distances: 1.68 and 1.74 Å). Fluoride binding does not seem to induce any serious rearrangement of the receptor, as judged from the distance between the two pivot nitrogen atoms, 5.23 Å, only slightly smaller than that observed in the uncomplexed unprotonated system  $23^{3+}$  (5.43 Å). Very interestingly, titration with  $Cl^-$  under the same conditions (pD = 1) did not induce any modification in the  $^1H$  NMR spectrum of the receptor. Thus,  $23H_2^{5+}$  exerts specific recognition of  $F^-$ . Notice also that  $23H_2^{5+}$  rightfully belongs to the ancient class of katapinands. The short and rigid spacers linking the tertiary ammonium groups (in their  $i^+i^+$  configuration) afford size exclusion selectivity in favour of the smallest anion.

However, there exists another class of even smaller cages that can afford exclusive fluoride encapsulation, whose formulae are shown in Fig. 42. These

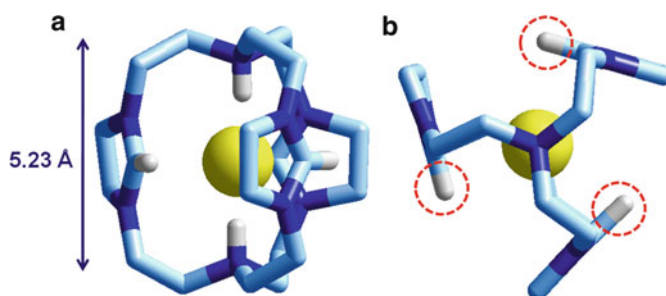


**Fig. 41** (a) Crystal structure of the fluoride inclusion complex of the diprotonated tris-imidazolidinium cage,  $23H_2^{5+}$  [80]. Only C–H fragments of the imidazolidinium subunits and N–H fragments of the tertiary ammonium groups are shown.  $F^-$  receives two H-bonds from the two tertiary ammonium nitrogen atoms. (b) Top view of the pentacation indicates that imidazolidinium C–H fragments do not point towards the cavity and are not involved in anion coordination

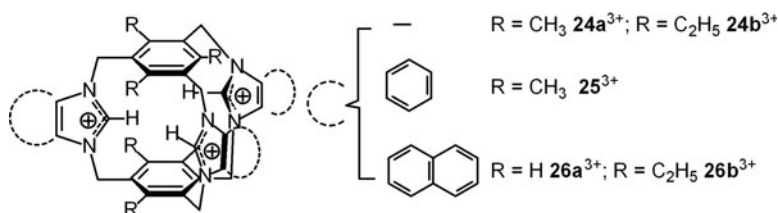


**Fig. 42** Family of tris-imidazolium receptors suitable for exclusive encapsulation of  $F^-$

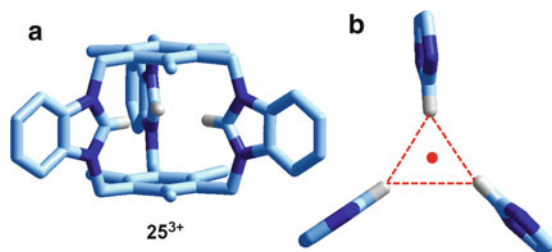


**Fig. 43** (a) Crystal structure the tris-benzimidazolium cage  $25^{3+}$  [84]; only hydrogen atoms belonging to C–H fragments of the imidazolium subunits are shown. (b) Top view showing only the three imidazolium subunits; the *circle* is the centroid of the nearly regular equilateral triangle obtained by linking the hydrogen atoms of the imidazolium C–H fragments

trications possess three imidazolium subunits that are potentially suitable for tight binding of an encapsulated fluoride anion. Indeed, crystal structures of derivatives  $24^{3+}$ – $26^{3+}$  revealed that in all cases the three imidazolium fragments point towards the cavity [81–84]. As an example, the structure of derivative  $25^{3+}$  is shown in Fig. 43 [84]. The cage is highly symmetric and, most interestingly, the three imidazolium C–H fragments point inside the cavity, ready to interact with an included anion, if any. In particular, C–H hydrogen atoms lie at the corners of a nearly regular equilateral triangle and the distances between these hydrogen atoms and the centroid of the triangle are: 1.64, 1.77 and 1.84 Å. These values fall in the range observed for strong  $F\cdots H$  hydrogen bonds in receptor–anion complexes and allow one to predict effective fluoride inclusion in cage  $25^{3+}$ . Indeed, titration experiments in  $CH_3CN$  ( $CD_3CN$ ) solution, using UV–vis (and  $^1H$  NMR) techniques, indicated the formation of a stable complex of 1:1 stoichiometry ( $\log K \geq 7$ ) [84]. Addition of  $Cl^-$  and of any other mono- or polyatomic anion did not cause any modification of the spectral pattern of the receptor, which suggests exclusive fluoride inclusion. Formation of a 1:1  $F^-$  complex in solution was also observed with receptor  $26b^{3+}$ , an event also corroborated by calorimetric titration experiments and by ab initio calculations [85]. However, crystalline salts containing the fluoride inclusion complex have not been obtained (yet) for any of the  $24^{3+}$ – $26^{3+}$  tris-imidazolium receptors, a disappointing circumstance that may not diminish the importance of the investigation, but leaves the readership (viewership) unsatisfied.

This raises a point of some relevance to the story developed in this chapter and, in general, to the subject of this volume. The beauty of any object, including a molecule, is related to its shape, to the harmony of its design or to the combination of novel and unexpected visual features. In the macroscopic world, there exists a single and neutral instrument, the eye, which provides objective perception and information that is subsequently elaborated to generate pleasure, surprise, fun, desire or, in the opposite direction, disgust or revulsion. On the other hand, the shape of a molecule is perceived as a structural formula, which may be a simple drawing made with a pencil by the chemist, deduced on the basis of several physical

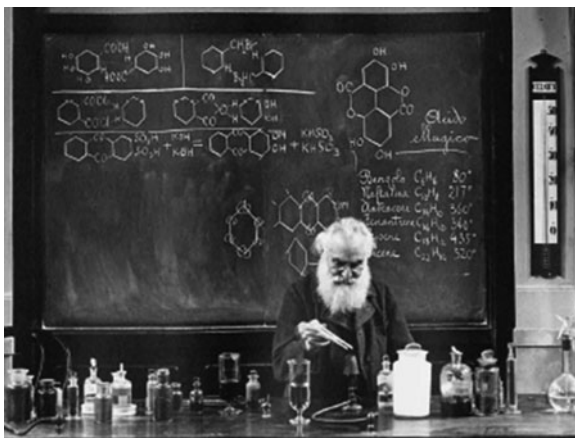


**Fig. 44** Professor Hugo Schiff (1834–1915) giving one of his last lectures in the Amphitheatre of Chemistry of the Institute of Advanced Studies in Florence, Italy, on 26 April 1915

responses, or an image on the screen, drawn by the computer, which has been elaborated on the basis of complex physical responses, following instructions provided by the chemist. Undoubtedly, the image obtained through the elaboration of X-ray diffraction data on a crystalline compound provides the most complete information on the molecular structure, thanks to the effectiveness of the methodology and the power and versatility of computing technology. Moreover, the use of diverse and appealing graphical applications and the utilisation of colour has made the drawing of molecules into a form of art, so that the covers of current issues of journals of chemistry often show graphics featuring appealing molecular structures obtained from X-ray diffraction studies (or by theory), which could rightfully be exhibited in galleries of modern art. However, the feeling that molecular aesthetics is limited to crystal structures is incorrect and misleading. This implies, for instance, that before the availability of diffractometric techniques, chemists could not appreciate and take enthusiasm from beautiful and intriguing molecular shapes. In this context, the photograph in Fig. 44 shows Hugo Schiff giving one of his last lectures on 26 April 1915, at the Institute of Advanced Studies in Florence, Italy. He died, aged 81, a few months later on 8 September 8 1915. The structural formulae on the blackboard, which had been deduced from the rather scarce pieces of physico-chemical information available at that time (mainly thanks to a well-developed chemical intuition) raised admiration and pleasure in the students attending the lecture. The writer of these notes had, about 50 years later, the pleasant opportunity to attend classes of chemistry in the same amphitheatre and to verify that a young assistant, before class, came and drew on the blackboard complicated molecular structures to save the time of the incoming professor, keeping a tradition that may have been introduced by Professor Schiff himself.

To conclude, using a historical approach, one could state that beauty is an intrinsic and immutable property of molecules and molecular assemblies, whose

perception can be modified by progresses in technology and in graphical representation. In this chapter, most of the reported molecular structures have a crystallographic origin and have been taken from the Cambridge Crystallographic Data Centre (CCDC). However, they may have generated a deeper emotion and aesthetical pleasure in the viewer (a student, a coworker or a visiting scientist) when roughly drawn by the inventor with a pencil on a piece of paper or on a tile of a bench in the laboratory.

## 7 Is it the Shape or the Function that Defines a Cage?

Everyday words are currently being used in chemistry for a direct illustration of molecular shapes and/or functions and, in some cases, for keeping a complex official nomenclature. “Cage” is one of these words, whose chemical connotation reached a honourable mention in Merriam-Webster Dictionary. However, looking at a cage, the correspondence between the macroscopic and the molecular world may not be fully justified. In fact, an individual in a cage (for either an animal or a human) remains under an unpleasant kinetic control: it may have (and in general it has) the greatest tendency to get out from the cage, but this event is prevented by an insurmountable activation barrier (a firmly locked gate). On the molecular side, such a kinetically controlled situation has been observed, for instance, in transition metal complexes of sarcophagines. On the other hand, no or a very moderate kinetic barrier between the inner and the outer state exists for s-block metal ions (with cryptands) and for anions (with any kind of polycyclic receptors): the ion can get in or out at will and its permanence in the cage is thermodynamically controlled. Thus, the term “cage” may be appropriate from the point of view of the shape, but not if one considers the function.

Systems providing a cavity suitable for the accommodation of molecules or ions can be designated with a more benign nomenclature than “cage”. For instance, when an anion interacts with the N–H fragments along a protein backbone, the ensemble of binding sites is termed a “nest” [86, 87]. The nest is a place where the “egg” (the anion) can be comfortably accommodated, waiting for opening [88, 89]. Curiously, this gentle metaphor offers a more subtle chemical interpretation of Magritte’s disquieting painting in Fig. 1, with which this chapter began.

## References

1. See <http://www.merriam-webster.com/dictionary/cage>. Accessed 20 July 2011
2. Werner A (1913) On the constitution and configuration of higher-order compounds (Nobel Lecture, 11 Dec 1913) [http://nobelprize.org/nobel\\_prizes/chemistry/laureates/1913/werner-lecture.pdf](http://nobelprize.org/nobel_prizes/chemistry/laureates/1913/werner-lecture.pdf). Accessed 20 July 2011
3. Schwarzenbach G (1952) *Helv Chim Acta* 35:2344–2359
4. Cabbiness DK, Margerum DW (1970) *J Am Chem Soc* 92:2151–2152

5. Kukina GA, Porai-Koshits MA, Shevchenko YN (1995) *Koord Khim* (Russ) 21:318, CCDC: ZASROA
6. Boiocchi M, Fabbrizzi L, Foti F, Vazquez M (2004) *Dalton Trans* 2004:2616–2620
7. Cabbiness DK, Margerum DW (1969) *J Am Chem Soc* 91:6540–6541
8. Billo EJ (1984) *Inorg Chem* 23:236–238
9. Fabbrizzi L, Foti F, Licchelli M, Poggi A, Taglietti A, Vázquez M (2007) *Adv Inorg Chem* 59:81–108
10. De Santis G, Fabbrizzi L, Poggi A, Taglietti A (1994) *Inorg Chem* 33:134–139
11. Beley M, Collin J-P, Ruppert R, Sauvage J-P (1984) *J Chem Soc Chem Commun* 1984:1315–1316
12. Barefield EK (1972) *Inorg Chem* 11:2273–2274
13. Barefield EK, Wagner F, Herlinger AW, Dahl AR (1976) *Inorg Synth* 16:220–225
14. Busch DH (1967) *Helv Chim Acta* (Fasciculus Extraordinarius Alfred Werner) pp 174–206
15. Curtis NF (1968) *Coord Chem Rev* 3:3–47
16. Takamizawa S, Akatsuka T, Ueda T (2008) *Angew Chem Int Ed* 47:1689–1692
17. Creaser II, MacB Harrowfield J, Herlt AJ, Sargeson AM, Springborg J, Geue RJ, Snow MR (1977) *J Am Chem Soc* 99:3181–3182
18. Hendry P, Ludi A (1990) *Adv Inorg Chem* 35:117–198
19. Comba P, Sickmüller AF (1997) *Inorg Chem* 36:4500–4507
20. Sargeson AM (1979) *Chem Br* 15:23–31
21. Lay PA, Mau AWH, Sasse WHF, Creaser II, Gahan LR, Sargeson AM (1983) *Inorg Chem* 22:2347–2349
22. Pina F, Mulazzani QG, Venturi M, Ciano M, Balzani V (1985) *Inorg Chem* 24:848–851
23. Pirandello L (1995) *The oil jar and other stories*. Dover Thrift, Mineola, NY
24. Geue RJ, Hambley TW, Harrowfield JM, Sargeson AM, Snow MR (1984) *J Am Chem Soc* 106:5478–5488
25. Bottomley GA, Clark IJ, Creaser II, Engelhardt LM, Geue RJ, Hagen KS, Harrowfield JM, Lawrance GA, Lay PA, Sargeson AM, See AJ, Skelton BW, White AH, Wilner FR (1994) *Aust J Chem* 47:143–179
26. Comba P, Creaser II, Gahan LR, Harrowfield JM, Lawrance GA, Martin LL, Mau AWH, Sargeson AM, Sasse WHF, Snow MR (1986) *Inorg Chem* 25:384–389
27. Clark IJ, Crispini A, Donnelly PS, Engelhardt LM, Harrowfield JM, Jeong S-H, Kim Y, Koutsantonis GA, Lee YH, Lengkeek NA, Mocerino M, Nealon GL, Ogden MI, Park YC, Pettinari C, Polanzan L, Rukmini E, Sargeson AM, Skelton BW, Sobolev AN, Thuery P, White AH (2009) *Aust J Chem* 62:1246–1260
28. Creaser II, Engelhardt LM, Harrowfield JM, Sargeson AM, Skelton BW, White AH (1993) *Aust J Chem* 46:465–476
29. Comba P, Sargeson AM, Engelhardt LM, Harrowfield JM, White AH, Horn E, Snow MR (1985) *Inorg Chem* 24:2327–2333
30. Pedersen CJ (1967) *J Am Chem Soc* 89:7017–7036
31. Seiler P, Dobler M, Dunitz JD (1974) *Acta Crystallogr B* 30:2744–2745
32. Frensdorff HK (1971) *J Am Chem Soc* 93:600–606
33. Dobler M, Phizackerley RP (1974) *Acta Crystallogr B* 30:2748–2750
34. Petrosyants SP, Ilyukhin AB (2007) *Koord Khim* (Russ) 33:747, CCDC: EFOROH
35. Dietrich B, Lehn J-M, Sauvage J-P (1969) *Tetrahedron Lett* 10:2889–2892
36. Metz B, Moras D, Weiss R (1976) *J Chem Soc Perkin Trans* 2:423–429
37. Metz B, Moras D, Weiss R (1973) *Acta Crystallogr B* 29:383–388
38. Lehn J-M, Sauvage J-P (1975) *J Am Chem Soc* 97:6700–6707
39. Guzei IA, Spencer LC, Su JW, Burnette RR (2007) *Acta Crystallogr B* 63:93–100
40. Guzei IA, Su JW, Spencer LC, Burnette RR (2009) *Acta Crystallogr E* 65:m1381–m1382
41. Moras D, Metz B, Weiss R (1973) *Acta Crystallogr B* 29:388–395
42. Metz B, Weiss R (1973) *Acta Crystallogr B* 29:388–395
43. Moras D, Weiss R (1973) *Acta Crystallogr B* 29:400–403

44. Mathieu F, Metz B, Moras D, Weiss R (1978) *J Am Chem Soc* 100:4412–4416
45. Cram DJ (1988) *Science* 240:760–767
46. Sillen LG, Martell AE (1971) Stability constants of metal-ion complexes, supplement no. 1, Chemical Society Special Publication No. 25. The Chemical Society, London
47. Ilyukhin AB, Petrosyants SP (2001) *Kristallografiya* (Russ) 46:845, CCDC: FADJUQ
48. Park CH, Simmons HE (1968) *J Am Chem Soc* 90:2431–2432
49. Graf E, Lehn J-M (1975) *J Am Chem Soc* 97:5022–5024
50. Graf E, Lehn J-M (1976) *J Am Chem Soc* 98:6403–6405
51. Schmidtchen FP (1977) *Angew Chem Int Ed Engl* 16:720–721
52. Schmidtchen FP, Muller G (1984) *Chem Commun* 1984:1115–1116
53. Bondy CR, Loeb SJ (2003) *Coord Chem Rev* 240:77–99
54. Amendola V, Fabbri L, Mosca L (2010) *Chem Soc Rev* 39:3889–3915
55. Esteban Gómez D, Fabbri L, Licchelli M, Monzani E (2005) *Org Biomol Chem* 3:1495–1500
56. Sessler JL, Davis JM (2001) *Acc Chem Res* 34:989–997
57. Kang SO, Llinares JM, Day VW, Bowman-James K (2010) *Chem Soc Rev* 39:3980–4003
58. Sung OK, Kang SO, Powell D, Day VW, Bowman-James K (2006) *Angew Chem Int Ed* 45:1921–1925
59. Sacconi L (1968) *Pure Appl Chem* 17:95–127
60. Suh MP, Jeon JW, Moon HR, Min KS, Choi HJ (2005) *Comptes Rendus Chimie* 8:1543–1551
61. Liu H-B, Sun Y, Che Y-G (2009) *Synth React Inorg Met Chem* 39:236–242
62. Chen D, Martell AE (1991) *Tetrahedron* 47:6895–6902
63. Smith PH, Barr ME, Brainard JR, Ford DK, Freiser H, Muralidharan S, Reilly SD, Ryan RR, Silks LA, Yu W (1993) *J Org Chem* 58:7939–7941
64. Thompson JA, Barr ME, Ford DK, Silks LA, McCormick J, Smith PH (1996) *Inorg Chem* 35:2025–2031
65. De Santis G, Fabbri L, Perotti A, Sardone N, Taglietti A (1997) *Inorg Chem* 36:1998–2003
66. Coyle J, Downard AJ, Nelson J, McKee V, Harding CJ, Herbst-Irmer R (2004) *Dalton Trans* 2004:2357–2363
67. Barr ME, Smith PH, Antholine WE, Spencer B (1993) *Chem Commun* 1993:1649–1652
68. Lehn JM, Pine SH, Watanabe EI, Willard AK (1977) *J Am Chem Soc* 99:6766–6768
69. Lehn JM, Sonveaux E, Willard AK (1978) *J Am Chem Soc* 100:4914–4916
70. Dietrich B, Guilhem J, Lehn J-M, Pascard C, Sonveaux E (1984) *Helv Chim Acta* 67:91–104
71. Arnaud-Neu F, Fuangswasdi S, Maubert B, Nelson J, McKee V (2000) *Inorg Chem* 39:573–579
72. Harding CJ, Mabbs FE, MacInnes EJJ, McKee V, Nelson J (1996) *J Chem Soc Dalton Trans* 1996:3227–3230
73. Fabbri L, Pallavicini P, Perotti A, Parodi L, Taglietti A (1995) *Inorg Chim Acta* 238:5–8
74. Fabbri L, Leone A, Taglietti A (2001) *Angew Chem Int Ed* 40:3066–3069
75. Boiocchi M, Bonizzoni M, Fabbri L, Piovani G, Taglietti A (2004) *Angew Chem Int Ed* 116:3935–3940
76. Lehn J-M, Méric R, Vigneron J-P, Bkouché-Waksman I, Pascard C (1991) *Chem Commun* 1991:62–64
77. Dietrich B, Dilworth B, Lehn J-M, Souchez J-P, Cesario M, Guilhem J, Pascard C (1996) *Helv Chim Acta* 79:569–587
78. Arunachalam M, Suresh E, Ghosh P (2007) *Tetrahedron* 63:11371–11376
79. Hossain MA, Llinares JM, Miller CA, Seib L, Bowman-James K (2000) *Chem Commun* 2000:2269–2270
80. Zhang B, Cai P, Duan C, Miao R, Zhu L, Niitsu T, Inoue H (2004) *Chem Commun* 2004:2206–2207
81. Baker MV, Bosnich MJ, Williams CC, Skelton BW, White AH (1999) *Aust J Chem* 52:823–826



82. Yuan Y, Jiang Z-L, Yan J-M, Gao G, Chan ASC, Xie R-G (2000) *Synth Commun* 30:4555–4561
83. Willans CE, Anderson KM, Junk PC, Barbour LJ, Steed J (2007) *Chem Commun* 3634–3636
84. Amendola V, Boiocchi M, Fabbrizzi L, Fusco N (2011) *Eur J Org Chem* (in press: DOI: 10.1002/ejoc.201100902)
85. Xu Z, Singh NJ, Kim SK, Spring DR, Kim KS, Yoon J (2011) *Chem Eur J* 17:1163–1170
86. Watson JD, Milner-White EJ (2002) *J Mol Biol* 315:187–198
87. Watson JD, Milner-White EJ (2002) *J Mol Biol* 315:199–207
88. Pal D, Sühnel J, Weiss MS (2002) *Angew Chem Int Ed* 41:4663–4665
89. Kubik S (2010) *Chem Soc Rev* 39:3648–3663

# Index

## A

Acceptor–donor stacks, 107  
Allyl enammonium salts, 14  
Ammonia, 129  
Anion coordination, 127, 146  
Architectural beauty, 47  
ATP (adenosine triphosphate), 82  
Aza-Cope electrocyclization, 15

## B

Beauty, 1  
Binaphthocrown ether, 84  
Binaphthyl phosphate (BNP), 122  
Bistren cages, 150  
Bonnanes, 48, 54  
Borromean Rings, 25  
Brevetoxin A, 109  
Buckminsterfullerene, 22

## C

Cages, anions, 145  
Calixarenes, 77, 108  
Catalysis, 1  
Catenanes, 19, 22, 31, 73, 107  
    ring movements, 96  
Chemical topology, 19  
Chirality, 107  
    topological 107  
*o*-Chloranil, 97  
Clever molecules, 79  
Cobalt(III) hexamine, 135  
Cobalt(III) sepulchrate, 134  
Complexity, 54  
Concatenation, Leonardo da Vinci, 113

Copper complexes, 107  
Copper(I) knot triflate, 123  
Cp\*(pentamethylcyclopentadiene), 16  
Crown ethers, 140  
Cryptands, 127, 139  
Cryptates, 139  
Crystal field stabilisation energy (CFSE), 138  
Crystal structures, 37  
Cubane, 22, 108  
Cubic space division, Escher, 4  
Cucurbituril, 109  
Cyclam, 131  
Cyclobis(paraquat-*p*-phenylene) (CBPQT), 35  
Cyclobutadiene, 8  
Cyclophane, 56, 97

## D

Daisy chains, 49  
Dendrimers, 73, 87  
Dendron, 87  
Diaminobipyridine (DAB), 53  
Diammonium alkane, 145  
Dibenzo[24]crown-8, 85  
Diformylpyridine (DFP), 53  
Dimethoxybenzene (DOB), 96  
Dimethoxynaphthalene (DON), 96  
Discrete supramolecular assemblies, 1  
DNA, 23, 82, 115, 119  
    catenanes, 45  
Dodecahedrane, 22, 108  
Donor–acceptor [2]catenane, 42  
Double helices, 115  
Dynamic combinatorial chemistry (DCC), 55  
Dynamic combinatorial library (DCL), 55  
Dynamic covalent chemistry (DCC), 53

**E**

Electrical extension cable, mimick, 85  
Electrocyclization, 16  
Elegance, 19  
Emergence, 54  
Escher, M. C., 3, 28, 112  
Ethylenediamine, 131  
Extended coordination arrays, 1

**F**

Ferritin, symmetry, 7  
Ferrocene, 89  
Flasks, nanoscale/symmetrical, 9  
Fluoride encapsulation, 158  
Fullerene, 77, 108

**H**

Handcuff macrocycles, 49  
Hemicarcerand, 8  
HK97 capsid, 25  
Hofmann clathrate, 4  
Host–guest chemistry, 1  
Hydrogen bonds, 107

**I**

Imidazolidinium, 159  
Interlaced design, 107

**K**

Katapinand, 145  
Knotaxanes, 54  
Knots, 19, 107  
Kuratowski's graphs, 107

**L**

Language, 74  
Levi, P. 78, 83  
Ligands, 127  
Light-harvesting antennas, 87, 109

**M**

$M_4L_6$  assemblies, 11  
Maitotoxin, 109  
Mechanical bond, 23

Mechanically interlocked molecules (MIMs),  
19, 22

cartoons, 40

Mesoporous silica nanoparticles (MSNPs), 60

Metal coordination chemistry, 127

Metal–organic frameworks (MOFs), 1, 7, 39

Methylviologen, 136

Miniaturization, 22

Möbius strip, 33, 107, 110

Molecular batteries, 89

Molecular computational identification  
(MCID), 80

Molecular logic, 73, 82

Molecular machines, 82, 91

Molecular muscles, 58

Molecular necklace, 48

Molecular plug/socket, 83

Molecular recognition, 127

Molecular shuttle, 92

switchable, 57

Molecular switches, 56

Molecules as words, 73

Motor molecules, 57

Multicatenane, 49

Multidentate ligands, 132

**N**

Naphthalene, 9

Nazarov cyclization, 15

**O**

Olympiadane, 37

Orthoformates, 13

**P**

Palladium-vertexed octahedra, 12

Pentadienols, 16

Phenanthroline, 116

Phosphoric acid, 11

Phosphorus, P4, 11

Photosynthesis, artificial, 88

Platonic solids, 21

Polyethers, cyclic, 140

Polymeric “blue box” cyclophane, 56

Polyviologen, 90

Porous coordination polymers (PCP), 6

Post-synthesis modifications, 53

Pretzelane, 47, 54

Prime knots, 113

Pseudorotaxanes, 60, 85

## R

Random access memory (RAM) storage, 97

Rational design, 1

Receptors, 127

Redox metallo dendrimers, 89

Resorcarene-calixarene carcerand, 76

Rotacatenane, 47, 54

Rotation, controlled, 99

Rotaxanes, 19, 22, 31, 73

linear movements, 92

Ru(bpy), 79, 136

## S

Sarcophagines, 127, 129, 137

Sauvage's metal coordination template, 34

Schiff, Hugo, 162

Sepulchrand, 134

Sepulchrates, 135

Simplicity, 49

Size exclusion selectivity, 158

Snap-top rotaxane, 61

Solomon Knots, 26

Spontaneous assembly, 8

Suitane, 48

Supramolecular assemblies, 1, 8, 73

Symmetrical extended arrays, 4

Symmetry, 2

## T

T4 DNA polymerase, 25

Technomorphism, 43

Template-directed synthesis, 34

Tetrabutylammonium fluoride, 149

Tetrahydroxymethylethylene (THYME)  
polyethers, 32

Tetramine macrocycles, 131

Tetrathiafulvalene (TTF), 96

Topology, 107

Trefoil knot, 118

Triethylorthoformate, 159

Tris-benzimidazolium cage, 161

Tris-imidazolidinium cage, 159

## W

Writers, chemistry, 73

## X

X-ray diffraction, 162

## Z

ZIF-100, 6